Adapting Yeast to the Study of Higher Eukaryotes: 'Humanisation' of Histone H4

By Sally Rushton

Supervisor – Dr. S. Pennings

Submitted for the degree of PhD at the University of Edinburgh, August 2004

Declaration

This thesis is of my own composition and the work presented is entirely my own. Any contribution by others to any part of the thesis has been acknowledged.

Sally Rushton

Table of Contents

List of Figures

List of Tables

Acknowledgements

Firstly, I would like to thank my supervisor Sari Pennings for giving me the opportunity to undertake this PhD, and the Wellcome Trust for funding it.

Particular thanks to Sari and Ali Fleming for all they taught me about chromatin and yeast, and their patience with my tendency to get a wee bit over-excited sometimes! Big thanks to my co-PhD students Hazel and Claudette for their advice on matters scientific and otherwise, and just for being good company everyday.

Special thanks to Simon Plummer of CXR Biosciences in Dundee for letting me use their microarray scanner and associated software for nothing but biscuits. You saved me a lot of trouble.

All the fab friends I now have in Edinburgh I would also like to thank. Particularly Niki for being the best and most understanding house-mate I could ever wish to have, Nina without whom I could never have settled in so happily, and Herve for his Swiss charm. I will miss you all desperately. I'd also like to thank Black Bo's and its entourage for so many good laughs.

Thank you Markus for being here and not here in roughly the right proportions! Your patience has been greatly appreciated and will not be forgotten…

Last but most definitely not least, I would like to take the opportunity thank my mum and dad for the unending support they have given me during all my studies. Without you, Jen, Gareth and Tom I could not have gotten through the last three years, or indeed the previous twenty-seven. I love you all very much.

Abstract

Histone H4 is one of evolution's most highly conserved proteins. There are only eight amino acid differences between the protein sequences of *S. cerevisiae* and humans. My PhD thesis describes the construction and characterisation of *S. cerevisiae* histone H4 mutants that express forms of histone H4 more closely related to their human counterparts.

Seven of the eight differences between the yeast and human histone H4 amino acid sequences fall within the globular histone fold domain. The other is a conservative isoleucine to valine substitution in the more flexible N-terminal tail (I21V). A yeast mutant expressing a form of histone H4 with the seven globular mutations is unable to grow on non-fermentable carbon sources. Through Southern blotting and DAPI staining, this phenotype is shown to be due to loss of mitochondrial DNA (mtDNA). This leads to non-functional electron transport, and defines the strain as a '*petite*' mutant. This strain also shows a genome-wide reduction of histone H4 acetylation levels to 30% of WT.

Further incorporation of the I21V substitution generates a strain expressing human histone H4. This highly conservative mutation at an apparently distal site confers a partial rescue to its parent strain. MtDNA is not lost, and growth on non-fermentable media is restored. Histone H4 acetylation is at 60% of WT. The final histone H4 mutant of the set contains I21V in isolation. This strain exhibits heightened growth on non-fermentable media, and normal histone H4 acetylation levels.

Microarray experiments were designed to allow cross referencing between two complementary sets of genome wide expression data. This enabled changes in gene expression down-stream of mtDNA loss to be 'filtered out'. This analysis identifies genes which may have a novel, but indirect role in mtDNA maintenance. Additionally, these studies revealed that the I21V mutation has an overall activating effect on gene expression, which is partly tempered by the mutations in the globular domain.

From the genome-wide studies it is evident that metabolism is significantly altered in the mutant strains. The altered levels of histone H4 acetylation are shown to not be due to changes in transcript levels of enzymes conferring or removing these modifications, implying that the effect is a more direct consequence of the mutations.

These data provide insight into the role of the few residues that evolution has seen fit to change between yeast and human histone H4. It is clear that amino acid substitutions in these two distal regions of histone H4 interact in some way to restore balance to the partially altered protein. The strain described here that expresses human histone H4, represents the first step in construction of a more *practical model* of higher eukaryotic chromatin in yeast.

Chapter 1: Introduction

1.1 Chromatin: Structure and Consequences

1.1.1 The Nature of Chromatin

Eukaryotes accomplish the formidable task of fitting over a meter of DNA into a nucleus a micron in diameter, by packaging it into a hierarchical structure called chromatin. The fundamental unit of chromatin is a DNA-protein complex known as a nucleosome. Multiple levels of folding and compaction enforced upon long chains of nucleosomes eventually give rise to the chromosomes seen in a mitotic cell with a light microscope (figure 1.1).

The protein components of nucleosomes are five small, basic histone proteins with highly evolutionarily conserved amino acid sequences: H1, H2A, H2B, H3 and H4 (Johns, 1967). H2A, H2B, H3 and H4 are known as core histones, since it is around a hetero-octamer of these proteins that DNA is supercoiled to form a nucleosome core particle (Luger *et al.*, 1997). H1 is a 'linker' histone and member of a class with variants such as H5, which associate with the DNA connecting adjacent nucleosome cores (Allan *et al.*, 1980).

The 'beads on a string' arrangement of nucleosomes was observed by electron microscopy as early as 1975 (Oudet *et al.*, 1975). Similar arrays were observed in samples from transcriptionally active chicken liver cells, and transcriptionally inert chicken erythrocytes. With increasing ionic strength, reconstituted arrays of beads-

on-a-string are observed to compact into a fibre of 30nm in diameter (Thoma *et al.*, 1979). This structure is also visible in electron micrographs of thin sectioned nuclei, but its true nature remains unknown. Most models of the 30nm fibre are based on the solenoid model first proposed in 1976, whereby nucleosomes continuously coil about a central axis, with about 6 per helical turn (Finch and Klug, 1976).

Consistent with their fundamental role in genome organization, all four core histones are essential in yeast (Kim *et al.*, 1988). Their N-termini are required for condensation into the 30nm fibre and more compact structures (Carruthers and Hansen, 2000). Modification of these core-histone N-termini provides one way of regulating the dynamic structure of chromatin.

The 30nm fibre is stabilized by linker histones, but they are not essential for its formation (Schwarz and Hansen, 1994; Carruthers *et al.*, 1998). Yeast lacking their only linker histone homologue *HHO1* have only subtle phenotypes, and its role is still debatable (Patterton *et al.*, 1998). H1 is believed to bind linker DNA near its entry/exit point on the nucleosome, contacting 10-20bp of DNA (Simpson 1978; Allan *et al.*, 1980; Zhou *et al.*, 1998). Electron microscopy employing deuteriated H1 suggests that it lies at the interior of the 30nm fibre (Graziano *et al.*, 1994).

Even less is known regarding structures beyond the 30nm fibre, but DNA in chromatin is compacted over 10000-fold compared to its naked state. It is within this context that the processes of DNA replication, repair and transcription take place.

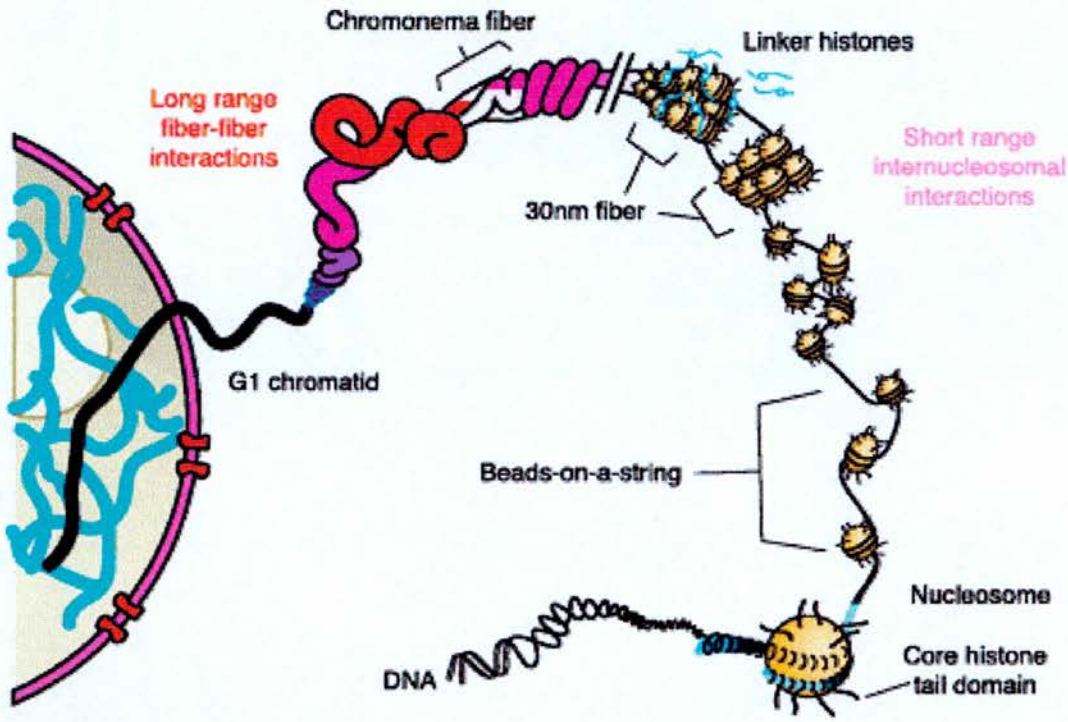

Figure 1.1 Hierarchical packaging of DNA into chromosomes (Horn and Peterson, 2002).

1.1.2 Overview of Transcription

Eukaryotic transcription is a highly regulated process, involving the orchestration of a multitude of general (GTF) and gene specific transcription factors. Additionally, there are three distinct RNA polymerases, which transcribe different classes of genes. RNA polymerase I (RNAPI) transcribes the large ribosomal DNA (rDNA) genes, and RNA polymerase III (RNAPIII) synthesizes tRNA's and 5SrRNA (reviewed by Paule and White, 2000). Together, RNAPI and RNAPIII account for over 80% of total cellular transcription. Despite this, it is synthesis of protein coding mRNA by RNA polymerase II (RNAPII) that has received by far the most attention.

The RNAPII transcription cycle begins with assembly of a pre-initiation complex (PIC) at the promoter of a gene. Traditionally this is divided into several steps: 1) Binding of activator(s) to their cognate sequences; 2) binding of TBP (usually as part of the TFIID complex) to the TATA box; 3) binding of TFIIB to aid identification of the transcriptional start site; 4) binding of RNAPII holoenzme (POLII) in concert with TFIIF, TFIIE and TFIIH (reviewed by Hampsey and Reinberg, 1999; Cosma, 2002). Transcription begins with melting of the DNA helix, catalyzed by the helicase activity of TFIIH. POLII clearance of the promoter is accompanied by TFIIH mediated phosphorylation of its C-terminal domain (CTD) and the enzyme proceeds into elongation.

The dynamic formation of this huge macromolecular complex has to contend with the chromatin environment. The intrinsic obstacle provided by incorporating regulatory DNA sequences into nucleosomes adds another level of complexity

(Knezetic and Luse, 1986). The modern view is that the chromatin of a gene promoter must be 'remodelled' prior to PIC assembly, and a variety of mechanisms have evolved to accomplish this. These include the activities of ATP-dependent chromatin remodelling complexes, and complexes that post-translationally modify histones. It is clear that the order of recruitment of complexes can vary from one gene to another (Neely and Workman, 2002), but cursory look at the types of activities required to accomplish remodelling of the yeast *HO* gene promoter will help to contextualize the following more detailed descriptions.

1.1.3 Chromatin modifying Events Preceding HO Gene Transcription

The order of events at the *HO* gene promoter that precede POLII and GTF recruitment were deduced by time resolved chromatin immunoprecipitation (CHIP) studies on synchronized yeast cells (Cosma *et al.*, 1999). *HO* encodes an endonuclease activity required for mating type switching (Strathern *et al.*, 1982). The ability of yeast to switch mating type is determined solely by *HO* expression, which is regulated developmentally and with the cell cycle (Nasmyth, 1982). The events leading to establishment of a chromatin structure permissible to *HO* gene transcription in G1 mother cells are illustrated in figure 1.2a. The cell-cycle regulated transcriptional activator (TA) Swi5p is first to bind at its upstream recognition site (URS1). This leads to recruitment of the ATP-dependent chromatin remodelling complex SWI/SNF in the region of URS1 and URS2. SWI/SNF in turn recruits the SAGA histone acetyltransferase complex, and Swi5p is lost around the same time. In the presence of SWI/SNF and SAGA, another cell-cycle regulated TA complex, SBF, binds to URS2. Although this study did not map arrival of the transcription

apparatus, only after this ordered remodelling of chromatin can *HO* gene transcripts be produced.

Chromatin remodelling in daughter cells where the *HO* gene is not transcribed is prevented by the binding of Ash1p to Swi5p. Ash1p is actively accumulated in daughter cells. Its interaction with Swi5p aborts SWI/SNF recruitment to give developmental control (figure 1.2b).

The first round of transcription is a rare event by definition, and subsequent rounds may be different. In the above study SWI/SNF and SAGA remain bound to the *HO* promoter, whilst Swi5p dissociates. This may represent a form of 'epigenetic memory' to facilitate subsequent rounds of transcription. Gene specific regulation of PIC formation at gene promoters can be achieved by the extreme combinatorial diversity existing within eukaryotic cells. Factors involved in the elongation and termination of nascent mRNAs are more general. However, these processes must also contend with chromatin and have recently become fields of intensive investigation (recently reviewed by Svejstrup, 2004).

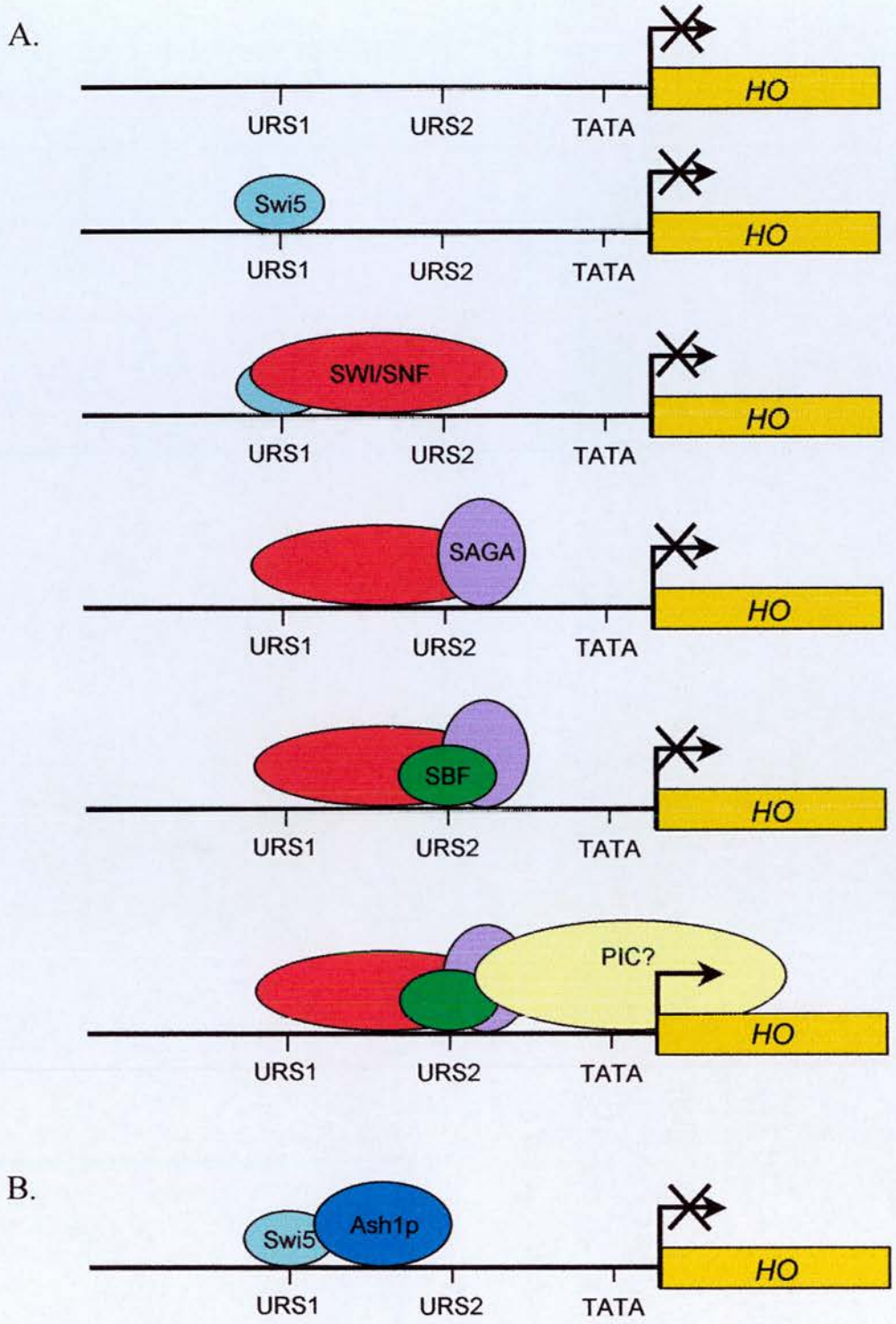

Figure 1.2 Events at the yeast *HO* gene promoter. A) Generation of a chromatin structure permissible to *HO* transcription in G1 mother cells The cell-cycle regulated transcriptional activator (TA) Swi5p binds first at its upstream recognition site (URS1). This recruits SWI/SNF in the region of URS1/URS2. SWI/SNF recruits SAGA, and Swi5p dissociates. In the presence of SWI/SNF and SAGA, another cell-cycle regulated TA, SBF, binds URS2. Only after this ordered remodelling of chromatin can *HO* be transcribed. B) Chromatin remodelling in daughter cells where the *HO* gene is not transcribed is prevented by Ash1p binding to Swi5p. Ash1p accumulates in daughter cells and its interaction with Swi5p aborts SWI/SNF recruitment.

1.1.4 The Two Types of Chromatin

In eukaryotes there exist two types of chromatin (reviewed by Grewal and Moazed, 2003). Euchromatin is less condensed and contains potentially active genes Heterochromatin is highly condensed and associated with transcriptionally silent regions. The two forms can also be distinguished by histone post-translational modification patterns. Heterochromatic regions are enriched in hypoacetylated, and in higher eukaryotes, hypermethylated histone H3 lysine 9. These epigenetic marks establish a scaffold of non-histone proteins that serves to repress transcription. Yeast heterochromatin is found at the silent mating loci, rDNA and telomeres, and requires the Sir proteins (see below). In an analogous situation in mammals and flies, HP1 (*h*eterochromatin *p*rotein 1) is associated with histone H3 methylated on lysine 9 (H3K9) (Lachner *et al.*, 2001).

A key feature of heterochromatin is its nucleation at specific sites, followed by spreading into adjacent regions. Spreading into adjacent euchromatin is prevented by barrier elements (Oki and Kamakaka, 2002). Once established, heterochromatin can be stably maintained over cell divisions. In higher eukaryotes, regional targeting of large domains is initiated by small, non-coding RNA's (Park and Kuroda, 2001). In female mammals, one X chromosome is shut down in somatic cells for dosage compensation. Initiation and maintenance of this requires Xist RNA (Plath *et al.*, 2002).

The following sections describe in more detail the structure of nucleosomes, the activities of complexes which act upon them, and the functional consequences.

1.2 The Nucleosome

1.2.1 Histone Genes

Yeast is well suited to the study of histone mutations because it has only two copies of each histone gene. These are organized in pairs of H3 and H4, and H2A and H2B genes, which are divergently transcribed from a shared promoter (Hereford *et al.*, 1979; Smith and Murray, 1983). Their expression is cell cycle-regulated, with transcripts accumulating just before S-phase (Osley *et al.*, 1986; Cross and Smith, 1988). Only one copy of each core histone gene is needed for viability (Kim *et al*, 1988).

Both copies of histone H3 and H4 genes (*HHT1* and *HHT2*, and *HHF1* and *HHF2*) encode identical proteins (Smith and Andresson, 1983). Whilst a deletion of locus I genes causes no discernable phenotype, deletion of locus II causes a slight increase in the rate of plasmid minichromosome loss (Smith and Stirling, 1988). Presumably this is due to a small difference in protein levels, since the homology does not extend to the promoter regions: in WT cells transcript levels from the locus II gene pair are 5- to 7-fold higher than from the locus I genes (Cross and Smith, 1988).

The sequences of proteins encoded by the two non-allelic sets of H2A and H2B genes (*HTA1* and *HTA2*, and *HTB1* and *HTB2*) are slightly different: they differ by two and four amino acids respectively (Choe *at al.*, 1982; Wallis *et al.*, 1980). In this case deletion of locus II (*TRT2*) has no effect, whereas deletion of locus I (*TRT1*) causes some local disruption of chromatin structure (Norris *et al.*, 1988). This is

presumably because the *TRT1* promoter is responsive to gene dosage, whereas the *TRT2* promoter is not (Moran *et al.*, 1988).

1.2.2 Histones

Histone proteins are amongst those most highly conserved throughout evolution. The amino acid sequence of histone H4 is almost perfectly conserved from pea to calf (DeLange *et al.*, 1969). The molecular masses of the core histones range from 10 to 14kDa, and histone H1 is 21kDa. Core histones can be divided into three structural domains: histone fold, histone-fold extensions, and N-terminal tails

The histone fold domain is a conserved protein-protein dimerisation motif, which governs the formation of the histone H3/H4 and H2A/H2B heterodimers (Kornberg and Thomas, 1974). The high sequence conservation of histones seems to serve preservation of this crescent-shaped motif. The histone-fold consists of a short α-helix (α1, 11 amino acids); a short loop, followed by a β-strand (L1); a long α-helix (α2, 27 amino acids); another loop and β-strand (L2), followed by a final short α-helix (α3, 11 amino acids) (Arents and Moudrianakis, 1995).

Histone fold extensions extend N-terminally from histones H3 and H2A, and C-terminally from H2A and H2B. They are less structured than the histone-fold itself, and pack against it or each other. The flexible histone N-terminal tails range from 16 (H2A), to 44 (H3) amino acids in length. They protrude from the nucleosome core, and are the sites of the numerous post-translational modifications discussed below.

1.2.3 From Histone Dimers to Nucleosome Core

Interactions between dimerising histones are mainly of the hydrophobic kind, and can be easily disrupted by alteration of environmental conditions (Baxevanis *et al.*, 1991). The exact conformation of histone-histone and histone-DNA interactions was revealed in 1997, when the high resolution (2.8Å) crystal structure of a Xenopus core nucleosome complexed with a 146bp palindromic segment of human α-satellite DNA was published (Luger *et al.*, 1997).

Histone dimers pair in an antiparallel fashion, offset by one helical turn with respect to their long α2 helices. In the nucleosome this organises 2.5 turns of DNA in a 140° arc. The head-to-tail arrangement of histones juxtaposes the L1 loop of one molecule and the L2 loop of the other. At this point they simultaneously contact the DNA backbone one end of the arc, and form one type of DNA-binding site (L1L2 site; two per dimer). The other interaction between histone-fold regions and DNA lies at the centre of the arc. Here, the α1 helices of the histone pair contact the DNA at neighbouring positions along its sugar-phosphate backbone (α1α1 sites).

At physiological ionic strength the preferred oligomeric states of core histones are $(H3/H4)_2$ tetramers and H2A/H2B dimers. The H3/H4 dimers interact via a 4-helix bundle formed from the α3, and C-terminal portion of α2 helices of H3 and H3'. The two H2A/H2B dimers are located on opposite sides of the assembled hetero-octamer. Tetramer-dimer interactions are mediated similarly via a four-helix bundle between H4 and H2B. Both 4-helix bundles are stabilised by hydrogen bonds and hydrophobic interactions, but the increase in the hydrophobic character of the

H4/H2A bundle in part explains the tendency of the dimer to dissociate. Additionally, a 'docking' domain formed by the H2A α3 helix and C-terminal extension interacts with the short C-terminal β-strand of histone H4. Mutations localising to the dimer-tetramer interfaces have both positive and negative effects on transcription (Santisteban *et al.*,1997). The H2A/H2B and H2A'/H2B' dimers interact via two hydrogen bonds and two salt bridges between the L1 loops of the H2A molecules.

The C-terminal extension of H2B (αC) is the most protruding part of the structured portion of the octamer. This may play a role in binding to non-histone proteins or chromatin condensation. This region contains the site of H2B ubiquitination (see below).

1.2.4 Histone-DNA Interactions

The L1L2 and α1α1 histone-DNA interactions account for the organisation of the central 121bp of DNA. The huge distortion of the DNA is accomplished by three types of interaction: 1) Direct or water mediated hydrogen bonds between ε-amino or guanidinium groups of lysine and arginine residues, and phosphate oxygen neutralizes the negative charge of DNA. Importantly, an arginine side chain penetrates the DNA minor groove at each L1L2 site, and also at the H3H4 α1α1 site. At the other 4 sites where the minor groove faces inwards, an arginine is inserted from another part of the structure. In most cases these ε-guanidinium groups mediate hydrogen bonds between adjacent threonine residues, and a water molecule linked to the N3 atom of the purine in the closest base pair. 2) Hydrophobic interactions

between proline, valine, threonine and isoleucine side chains, and deoxyribose moieties. 3) Frequent hydrogen bonds to main-chain amino groups from oxygens of the phosphodiester chain (Luger and Richmond, 1998).

The H3 N-terminal extension forms a short α-helix (αN), which organises the remaining 13bp at either end of the associated DNA. The C-terminal extension of H2A also plays a role, but even taken together the number of protein-DNA interactions here is small compared to the rest of the nucleosome. The weakness of interactions at the points at which DNA enters and leaves the nucleosome may have functional consequences relating to accessibility of nucleosomal DNA to other proteins, and higher order structure.

These interactions place the central base pair of DNA associated with the histone octamer upon the axis of symmetry, lending a pseudo 2-fold symmetry to the complete core particle.

1.2.5 Histone N-terminal Tails

These significantly less structured regions of the histones (in the context of crystal structure), protrude outwards from the core of the nucleosome. Those of H3 and H2B pass through channels made by the aligned minor grooves of the two turns of DNA. The H4 and H2A tails protrude from the flat faces of the nucleosome.

Although histones lacking their tails will form octamers that organise DNA, they will not condense into higher order arrays (Curruthers and Hansen 2000). On modelling

internucleosomal interactions, the highly basic histone H4 N-terminus fits well with an acidic patch on the H2A-H2B dimer of the neighbouring nucleosome (Luger and Richmond, 1998). Competition studies demonstrate that the N-terminus of histone H2B is particularly important for chromosome condensation, whereas that of H3 is dispensable (de la Barre *et al.*, 2001).

1.3 Nucleosome Positioning

Histones bind DNA by contacting the phosphodiester backbone, which explains their ability to package DNA regardless of sequence. However, certain properties of DNA make it more or less likely that a particular sequence will be centred on a nucleosome *in vitro* (Lowary and Widom, 1998). These parameters relate to the 'bendability' and 'twistability' of the sequence, since the curvature and twist of nucleosomal DNA is non-uniform (Luger and Richmond, 1998).

Nucleosomes possess a certain amount of intrinsic mobility that is affected by ionic strength, and restricted by linker histones (Meersseman *et al.*, 1992; Pennings *et al.*, 1994). Thus nucleosome positioning must be viewed as a statistical phenomenon. *In vivo* this equilibrium is further influenced by the presence of complexes that remodel chromatin. The original observations demonstrating increased susceptibility of chromatin to nucleases, and sometimes changes in nucleosome positions observed upon gene induction are reviewed by Gross and Garrard (1988).

1.4 ATP-Dependent Chromatin Remodelling Factors

Complexes that utilize the energy of ATP hydrolysis to remodel chromatin, have at their catalytic core a protein containing a conserved ATPase domain belonging to the DEAD/H superfamily of nucleic-acid stimulated ATPases (Eisen *et al.*, 1995). Interestingly, these ATPases also show similarity to known DNA helicases, but such an activity has never been demonstrated. Additional domain structures within these proteins permit further subdivision into four main classes, which have distinct properties and mechanisms of action (reviewed by Kamakaka, 2002). These classes are the SWI2/SNF2-, ISWI-, Mi-2/CHD-, and INO80-ATPases (figure 1.3).

Members of the SWI2/SNF2 class contain a bromodomain which is capable of binding to acetylated lysines (Winston and Allis, 1999), and an AT hook that may facilitate binding to DNA (Aravind and Landsman, 1998). ISWI homologues do not have a bromodomain, but contain a putative DNA binding SANT domain, towards the C-terminus (Aasland *et al.*, 1996). Many Mi-2/CHD-family members contain a chromodomain, which occurs in many proteins that repress transcription from chromatin templates (see below). The INO80 class is characterised by a split ATPase domain.

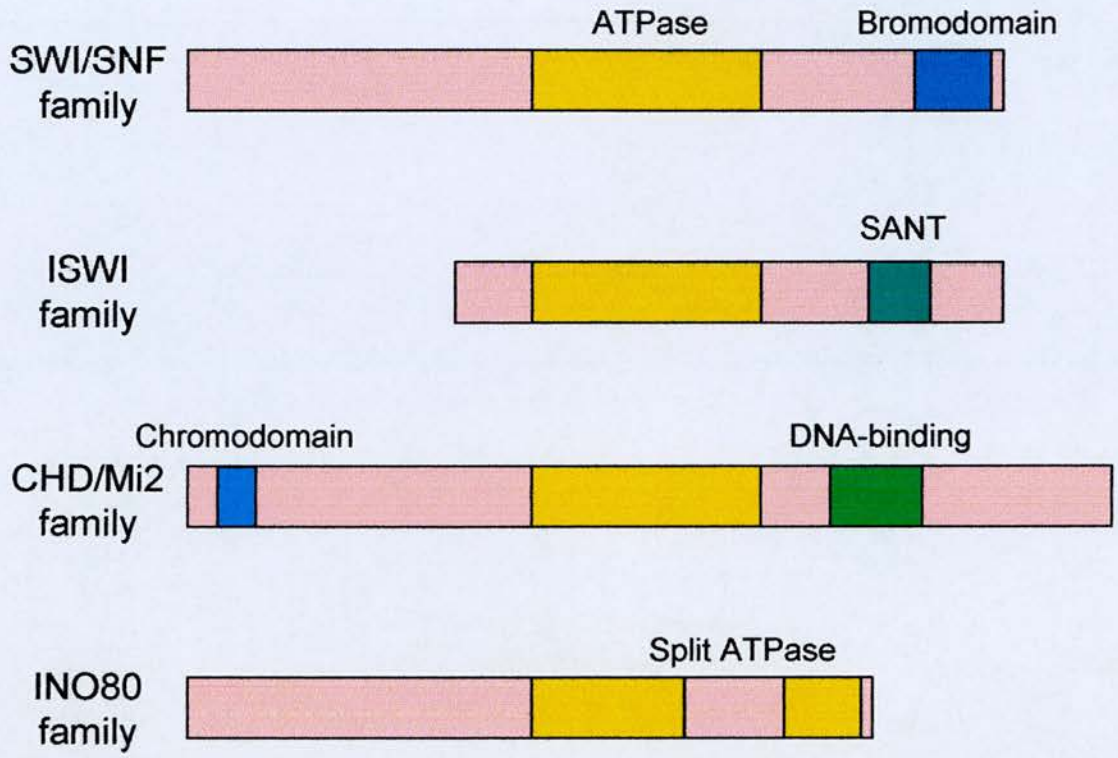

Figure 1.3 Classes of ATP-dependent chromatin remodelling complexes. SWI2/SNF2 class members contain a bromodomain, capable of binding to acetylated lysines and an AT hook that may facilitate DNA binding. ISWI homologues contain a putative DNA binding SANT domain towards the C-terminus. Many Mi-2/CHD-family members contain a chromodomain, which occurs in many proteins that repress transcription from chromatin templates. The INO80 class is characterised by a split ATPase domain.

*1.4.1 SWI2/SNF2 (mating type **swi**tch/**s**ucrose **n**on-**f**ermenting)*

Yeast SWI/SNF complex is the prototype of the SWI2/SNF2-ATPase containing family (Laurent *et al.*, 1991; Peterson and Herskowitz, 1992). Evidence that SWI/SNF promotes transcription by antagonising nucleosome mediated repression came first from studies on the *SUC2* gene (Hirschhorn *et al.*, 1992). *SUC2* encodes the enzyme invertase required for growth on sucrose. The gene is repressed by glucose, and strongly induced in its absence (Carlson *et al.*, 1981). The repressed state is associated with a nucleosome positioned directly over the TATA box. Upon gene activation, this nucleosome and another between the TATA box and upstream activation sequence (UAS) become 'remodelled', in the sense that the DNA of the region becomes more accessible to digestion by micrococcal nuclease (which cuts nucleosomal DNA in the linker). This remodelling was not observed in Snf2/Swi2 mutants. Since this study the role of SWI/SNF as a transcriptional co-activator that promotes access of DNA binding factors to their recognition motifs in nucleosomal templates has been well documented (reviewed by Carlson and Laurent, 1994; Peterson and Workman, 2000).

The traditional view of SWI/SNF as a general activator of transcription must be re-assessed in the light of more recent investigations. Genome wide analyses of Swi/Snf mutants generate a minimal estimate of 6% of the yeast genome being under some degree of SWI/SNF mediated control (Holstege *et al.*, 1998). The redundancy of SWI/SNF with other chromatin modifiers confounds a more accurate estimation. However, a proportion of the affected genes are induced upon SWI/SNF inactivation, implying a role in repression. This is in keeping with the demonstration that human

SWI/SNF can co-ordinate forward and reverse remodelling reactions *in vitro* (Schnitzler *et al.*, 1998). SWI/SNF has since been shown to be required for repression of the yeast *SER3* gene required for serine biosynthesis (Martens and Winston, 2002). This activity is specifically dependent on the Snf2 ATPase activity, which is required to maintain the positioning of a nucleosome over the TATA box.

A common theme of ATP-dependent remodelling activities is that they function as large, multisubunit complexes (Varga-Weisz and Becker, 1998). SWI/SNF is no exception, and exists as a stable complex of at least 11 subunits (Cairns *et al.*, 1994; Peterson *et al.*, 1994). Most of these subunits are required for activity *in vivo*, but until recently it has been the ATPase subunit that has received most attention. Roles for the additional subunits in the diverse functions of SWI/SNF are beginning to emerge.

SWI/SNF itself binds DNA and nucleosomes in a sequence non-specific manner (Quinn *et al.*, 1996). Sequence specific targeting of SWI/SNF to chromatin by the acidic activators Swi5p, Gcn4p, Gal4-VP16p and Hap4p has been observed (Neely *et al.*, 1999; Natarajan K *et al.*, 1999; Yudkovsky *et al.*, 1999). SWI/SNF has two activator-interaction domains. One maps to the Snf5p subunit, the other to the Swi1p subunit. Simultaneous deletion of these domains creates a mutant that is competent for complex formation, but which cannot be targeted in an activator dependent manner (Prochasson *et al.*, 2003). The Snf5p subunit of yeast SWI/SNF is conserved across species. Its distinct roles in assembly and targeting of the complex, and chromatin remodelling activities are essential to function (Geng *et al.*, 2001).

The bromodomains of SWI/SNF also play a role in its association with transcriptionally active chromatin, but whether they function mainly to facilitate initial targeting or continued association is debatable (Hassan *et al.*, 2002).

Yeast contains another SWI2/SNF2-related remodelling complex called RSC. RSC contains the ATPase subunit Sth1p, and other subunits similar to those of SWI/SNF. Unlike SWI/SNF this complex is essential for viability (Cairns *et al.*, 1996). Drosophila appears to employ only one SWI2/SNF2 complex (dSWI/SNF), of which Brahma (Brm) is the catalytic subunit (Dingwall *et al.*, 1995). Human cells have several similar complexes (hSWI/SNF), built around the ATPase activity of hBrm or Brg1 (Wang *et al.*, 1996).

1.4.2 ISWI (imitation switch) Complexes

Unlike SWI/SNF complexes, the ISWI family are more generally associated with repression of transcription. The founding member of the ISWI family (dISWI) was identified in Drosophila by its homology to Brahma within the ATPase domain (Elfring *et al.*, 1994). ISWI homologues are found from yeast to humans, and interact with multiple partners.

Biochemical studies employing Drosophila embryo extract identified three distinct ISWI-containing complexes. NURF (*nu*cleosome *r*emodeling *f*actor) was shown to be responsible for the alterations in DNAseI sensitivity at the *HSP70* promoter that occur on binding of the transcription factor GAGA. In addition to ISWI, NURF

contains the large p301 subunit, and two other smaller proteins (Tsukiyama and Wu, 1995).

ACF (*A*TP-dependent *c*hromatin–assembly and remodelling *f*actor) was identified by its abilities to form regularly spaced nucleosomal arrays, and mobilize nucleosomes to allow trans-acting factors access to DNA (Ito *et al.*, 1997). The large subunit of the ACF complex is ACF1, which contains a bromodomain and a PHD finger (Ito *et al.*, 1999).

CHRAC was discovered by its ability to cause global, energy dependent increases in the accessibility of chromatin to restriction enzymes, and its ability to form regularly spaced nucleosomal arrays. CHRAC also contains ACF1 as its large subunit, and two additional histone fold proteins CHRAC-14 and CHRAC-16 (Varga-Weisz *et al.*, 1997).

ISWI complexes can stimulate movement of a nucleosome positioned at the end of a DNA fragment to the centre, and appear to achieve this by a sliding mechanism (Längst *et al.*, 1999). Such a mechanism would not involve large disruptions in protein-DNA interactions, and can be thought of as 'bulging' or 'breathing' of the DNA across the nucleosome surface (Längst and Becker, 2001). Although ISWI alone can weakly stimulate nucleosome remodelling, its action is greatly enhanced and regulated by the large subunits of the complexes, such as ACF1 (Eberharter *et al.*, 2001).

In vivo evidence for the function of ISWI complexes in gene repression and DNA replication exists in mammalian cells. The ISWI complex NoRC (*n*ucle*o*lar *r*emodeling *c*omplex) is required for silencing of rDNA repeats, and an ACF1-ISWI complex is required for DNA replication through heterochromatin (Santoro *et al.*, 2002; Collins *et al.*, 2002). The histone fold proteins in the human homolog of CHRAC have been shown to facilitate DNA replication, perhaps by binding linker DNA (Kukimoto *et al.*, 2004). Whether this is to allow DNA polymerase access to the DNA to promote replication, or to re-position nucleosomes after the replication fork has passed is an open question.

Yeast has two ISWI homologues; ISW1 and ISW2. These assemble into complexes containing distinct subunits. Their roles *in vivo* are not well characterised, but both can be recruited to promoters by the DNA-binding repressor Ume6. ISW2 represses transcription of early meiotic genes, and shows widespread collaboration with the Sin3-Rpd3 complex (see below) (Goldmark *et al.*, 2000; Fazzio *et al.*, 2001)

1.4.3 CHD-Mi-2 Class

The best-known chromatin remodelling complex containing an Mi-2 family member is vertebrate NuRD (*nu*cleosome *r*emodelling and histone *d*eacetylation) (Xue *et al.*, 1999). The histone deacetylase and methylated DNA binding proteins within this complex help account for its role in repression (reviewed by Bowen *et al.*, 2004).

Yeast contain only one chromatin remodelling activity of this type of this class, Chd1p. In contrast to NuRD, Chd1p localises to transcriptionally active genes, and interacts with components of POLII elongation machinery (Simic *et al.*, 2003).

1.4.4 INO80 Class

INO80 is required for transcription of *INO1* and several other structural genes in yeast (Ebbert *et al.*, 1999). A novel member of this class is the yeast Swr1p. This functions in a complex which is required for the exchange of the histone variant H2A.Z (Krogan et al., 2003; Mizuguchi *et al.*, 2004)

1.4.5 Mechanisms of ATP-Dependent Chromatin Remodelling

The mechanisms underlying remodelling of nucleosomes remain unclear. There are discernable differences in the ways in which the different classes of remodellers function. For instance, Swi2p ATPase activity is fully stimulated by free DNA; ISWI is stimulated by free DNA, but only reaches maximal activity in the presence of nucleosomes; and Mi-2 absolutely requires nucleosomal DNA (Längst and Becker, 2001). Despite these differences and the fact that they can be persuaded to perform different reactions *in vitro*, it is possible that the fundamental mechanism is similar in all cases (Längst and Becker 2003).

What is clear *in vivo* is that all of these complexes are able to move nucleosomes with respect to DNA. This is termed 'sliding', and is most likely an enzymatic enhancement of native nucleosome mobility. The two currently most favoured models are 'twist defect diffusion' and 'bulge diffusion' (reviewed by Flaus and

Owen-Hughs, 2004). In the former model alterations in the twist of the DNA super-helix are envisioned to screw the DNA around the nucleosome. In the latter model, DNA unpeeling begins near the nucleosome entry/exit point. DNA can then re-bind to the histone contact sites at a slightly removed sequence. This would create a bulge which could propagate the translocations around the nucleosome surface.

Taken together these mechanisms provide possible explanations for the different types of mutation known to cause SIN (*S*WI/SNF *in*dependence) phenotypes (Kruger *et al.*, 1995). SIN mutations of histones H3 and H4 cluster upon the nucleosome surface, and three affect histone-DNA interactions (Luger *et al.*, 1997). These mutations may mimic the disruption of histone-DNA contacts usually performed by SWI/SNF. Interestingly, this SIN domain is also required for the *in vitro* folding of intramolecular nucleosomal arrays (Horn *et al.*, 2002).

Other SIN mutations in histones H2B and H4 compromise dimer-tetramer interactions, and in the case of H2B, dimer formation (Santisteban *et al.*, 1997; Recht and Osley, 1999). These mutations might promote the dimer exchange of removal postulated to be involved in SWI/SNF action (Hirschhorn *et al.*, 1992, Flaus *et al.*, 2003).

1.5 Epigenetics and the Histone Code

Epigenetics can be defined as heritable changes in gene expression that operate outside of changes in DNA sequence. The importance of chromatin in the regulation of gene expression lends histones a central role in this form of inheritance.

The N-terminal tails of histone proteins form the sites of numerous post-translational modifications (figure 1.4). These encompass acetylation of lysine residues, methylation of lysines and arginines and phosphorylation of serines. Additionally, larger moieties such as ADP-ribosyl groups, ubiquitin and sumo peptides may be covalently attached. The presence of so many modifiable residues lends extreme combinatorial potential to the nucleosome, and has been proposed to form a 'histone code'. This notion dictates that the 'meaning' of a particular mark is moderated within its context of other marks (Strahl and Allis, 2000).

The following sections discuss the different types of modification, and highlight some examples of 'cross-talk' between them (Fischle *et al.*, 2003).

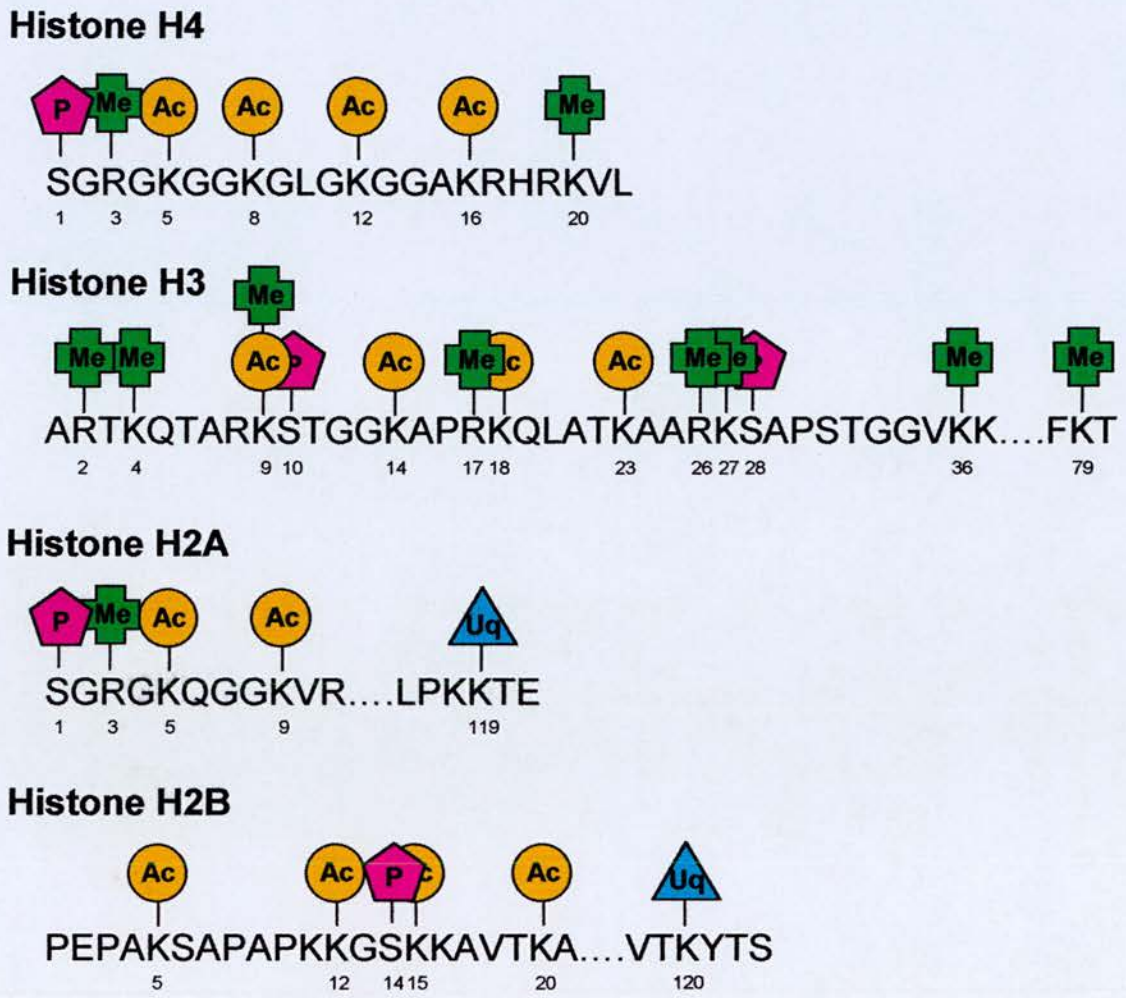

Figure 1.4 Histone post translational modifications. The protruding N-terminal tails of histone proteins form the sites of numerous post-translational modifications. These include acetylation of lysine residues (orange circles), methylation of lysines and arginines (green crosses), phosphorylation of serines (pink pentagons) and ubiquitination of lysines (blue triangles). The presence of so many modifiable residues lends extreme combinatorial potential to the nucleosome, and has been proposed to form a 'histone code'. Sequences here are mammalian: exact modification patterns and residue number vary between species.

1.6 Histone Lysine Acetylation

1.6.1 Role in Gene Activation

A positive correlation between histone hyperacetylation and transcription was first observed 40 years ago (Allfrey *et al.*, 1964). Since then it has been the best studied of the histone modifications, but even so, the exact mechanisms by which it promotes gene activation remain unclear.

Lysine acetylation reduces the positive charge carried by a histone, which could reduce the strength of histone-DNA interactions. Studies have demonstrated that histone-tail acetylation can increase the accessibility of DNA target sequences to transcriptional activators (Lee *et al.*, 1993). However if charge alone were important the effects of acetylated/deacetylated lysines should be mimicked by mutation to glycine or arginine respectively, and this is not the case (Thompson *et al.*, 1993).

A complementary notion is that acetylation disrupts higher order packing. The different hydrodynamic properties of acetylated versus non-acetylated nucleosomal arrays do indicate that acetylated arrays are less compact (Garcia-Ramirez *et al.*, 1995; Tse *et al.*, 1998).

Not mutually exclusive to the above ideas, and amassing considerable support is the notion that lysine acetylation opposes the binding of transcriptional co-repressors, whilst providing specific docking sites for co-activators. In yeast, transcriptionally repressive complexes of TUP1/SSN6 and SIR proteins bind preferentially to

hypoacetylated histones (Edmondson *et al.*, 1996; Hecht *et al.*, 1995) (see below). Consistent with this, many protein complexes associated with transcriptional activation contain bromodomains, which bind acetylated lysine residues of histones within a hydrophobic pocket (Owen *et al.*, 2000; Bottomley, 2004). FRET (*f*luorescence *r*esonance *e*nergy *t*ransfer) experiments using HeLa cells have demonstrated different *in vivo* specificities of bromodomain containing proteins. Whilst $TAF_{II}250$ will bind many acetylated histones, Brd2p requires acetylated lysine 12 of histone H4 (Kanno *et al.*, 2004). Given that many bromodomain-proteins contain two such domains, one can imagine how these help to read the histone code (Strahl and Allis, 2000).

1.6.2 Histone Acetyltransferases (HATs)

HATs catalyse the transfer of an acetyl group from acetyl-CoA, to the ε-amino group of lysine residues in the amino terminal tails of the core histones. Most HATs function within large, multi-protein complexes (see Roth *et al.*, 2001 for a detailed review). The activity and specificity of a HAT is modulated by the accessory subunits. For example, yGcn5p (the yeast homologue of the first verified HAT isolated from tetrahymena (Brownell *et al.*, 1996)), with accessory proteins Ada2 and Ada3 forms the catalytic core of both the ADA and SAGA HAT complexes. Whilst recombinant Gcn5p alone will not acetylate nucleosomes, it will acetylate free histone H3 on K14. The ADA complex will acetylate nucleosomal H3 on K9, K14 and K18, whereas SAGA will also acetylate H3K23 (Grant *et al.*, 1999; Balasubramanian *et al.*, 2002).

HATs genetically linked to histone function can be divided into the GNAT (Gcn5 related), and MYST (MOZ, Ybf2/Sas3, Sas2 and Tip60 related) families (Carrozza *et al.*, 2003). Many members of the GNAT class contain bromodomains, suggestive of a self-perpetuating action of histone acetylation. One subclass of MYST HATs contains chromodomains. These are able to bind methylated histones H3K9, providing another example of how a histone-code can be read.

Promoter proximal acetylation of histones can be achieved *in vitro* by activator-mediated targeting of HAT complexes (Utley *et al.*, 1998; Vignali *et al.*, 2000). NuA4 (*nu*cleosomal *a*cetyltransferase of histone H*4*) is a yeast HAT containing the essential acetyltransferase subunit Esa1p, which has specificity for histones H4 and H2A (Allard *et al.*, 1999). The complex contains at least 14 subunits, one of which is Tra1p, the yeast homologue of human TRRAP (McMahon *et al.*, 1998). Tra1p is the only subunit common to both NuA4 and SAGA, and an interaction between Tra1p and the acidic activation domains of Hap4p, Gcn4p, Gal4p and VP16p is essential for gene activation *in vitro* (Brown *et al.*, 2001).

Although NuA4 and SAGA are co-recruited to some gene promoters they are unlikely to have identical roles in transcription. Another subunit of NuA4, Yng2p, is required for p53 activated gene expression in a heterologous yeast system. This leads to increased levels of histone H4 acetylation, without affecting those of histone H3 (Nourani *et al.*, 2001). p33/ING, the human homologue of YNG, is essential for the tumour suppressor activity of p53 (Garkavtsev *et al.*, 1998). The closest human homologue of Esa1p is Tip60, which co-purifies with TRRAP amongst other

proteins (Ikura *et al.*, 2000). These facts suggest that p33/ING may mediate recruitment of a NuA4 related HAT to p53 regulated genes in human cells.

Given the link between histone acetylation and transcriptional activity, it is perhaps not surprising that some components of the general transcription machinery, $TAF_{II}250$ for example also possess HAT activity (Mizzen *et al.*, 1996).

1.6.3 Acetylation and Chromatin Assembly

Nucleosomes are rapidly reassembled after the passage of a replication fork in a two-step process: first new tetramers are added in a non-conservative manner, and then the dimers associate (Worcel *et al.*, 1978; Jackson, 1988). The three subunit complex CAF1 (*c*hromatin *a*ssembly *f*actor 1) isolated from human cell extracts is able to perform the first step in nucleosome assembly, the deposition of histone H3/H4 tetramers onto DNA *in vitro* (Smith and Stillman, 1991). CAF1 dependent nucleosome assembly is linked to DNA replication via a direct interaction with PCNA (*p*roliferating *c*ell *n*uclear *a*ntigen) (Shibahara and Stillman, 1999).

The pool of newly synthesized histones available for this process, are acetylated on histones H3 and H4. This is carried out by cytoplasmic (B-type) HATs that act on free histones. Histone H4 is K5- and K12-acetylated across species, whereas the pattern on histone H3 is less defined (Sobel *et al.*, 1995).

Observations made in yeast strains mutant/deleted for histones H3 and H4 have demonstrated the importance of acetylation in the assembly process. Although

removal of both histone H3 and H4 tails is a lethal, either tail alone will support cellular growth and nucleosome assembly. Additionally, acetylation of any one of lysines 5, 8 or 12 of histone H4 is sufficient for nucleosome assembly in the complete absence of a histone H3 tail (Ling *et al.*, 1996). Despite being the only known B-type HAT, yeast *Δhat1* mutants have no observable phenotype, suggesting the existence of redundant HATs or assembly processes (Kleff *et al.*, 1995).

Exactly why histone acetylation is important is not known. CAF1 stably binds tetramers lacking both histone H3 and H4 tails *in vitro*, and can even assemble them in an SV40 DNA replication system (Shibahara *et al.*, 2000). Very recent data show that the HAT1 complex has both cytoplasmic and nuclear localisation, and interacts with histones H3 and H4 in both compartments. Association of the newly identified histone chaperone and assembly factor Hif1p with acetylated histones H4 and histone H3 in the nucleus requires the HAT1 complex. This establishes a link between B-type HATs and chromatin assembly factors (Ai and Parthun, 2004).

1.6.4 Acetylation in Elongation

Biochemical links between transcriptional elongation and HAT activities are also emerging, suggesting that histone acetylation aids passage of POLII through chromatin. Yeast elongator complex contains a subunit Elp3p, with intrinsic HAT activity capable of acetylating all four core histones *in vitro* (Wittschieben *et al.*, 1999).

NuA3 (*nu*cleosomal *a*cetyltransferase of histone H*3*) is a Gcn5p independent histone H3 HAT, containing the Sas3p (*s*omething *a*bout *s*ilencing) catalytic subunit (John *et al.*, 2000). This complex does not exhibit the interactions with acidic activation domains characteristic of SAGA and NuA4, but instead interacts with components of the yeast CP complex. CP is homologous to human FACT (*f*acilitates *a*ctivation of *c*hromatin *t*emplates). FACT stimulates elongation of POLII through chromatin (reviewed by Belotserkovskaya et al., 2004), implying that the interaction between NuA3 and CP might have a similar role.

1.7 Histone Deacetylation

1.7.1 Histone Deacetylases (HDACs)

Removal of acetyl groups from histones is catalyzed by HDACs. Like HATs, these activities function within multi-protein complexes. HDACs are divided into three main families. Class I HDACs are similar to yeast Rpd3p and mammalian HDAC1. Class II HDACs are related to yeast Hda1p. This class includes yeast Hos1p, Hos2p and Hos3p, and mammalian HDAC4-7. These activities function in larger complexes than class I HDACs, but less is known about their *in vivo* interactions and roles (Verdin *et al.*, 2003). The third class is homologous to yeast Sir2p NAD^+-dependent HDAC. The dependence of enzymes in this class on NAD^+ creates a link between chromatin modifying activities and metabolic status, and even affects lifespan (reviewed by Denu, 2003). *SIR2* is required for all forms of silencing in yeast (see below), and mutations within *SIR2* have distinct effects at the different silent loci (Garcia and Pillus, 2002).

1.7.2 Differing Roles of Yeast HDACs

Histone acetylation microarray experiments have been used to define the genome-wide functions of different yeast HDACs (Robyr *et al.*, 2002). This group demonstrated that Rpd3p and Hda1p are the major activities, and that they generally target distinct promoters. *RPD3* deletion leads to an increase in histone H4 acetylation of diverse genes throughout the genome. The increased histone H4K5 and K12 acetylation correlates well with increased gene transcription. Increased histone H4K16 acetylation does not correlate well with increased transcription, consistent with this being a general euchromatic mark. Hda1p preferentially deacetylates histones H3 and H2B of gene promoters 10-25kb from telomeres, where many genes involved in regulation of carbohydrate utilization are housed. They propose that this constitutes a regional targeting of Hda1p activity under conditions of low stress.

Deletion of *HOS1* or *HOS3* affects rDNA genes, whereas deletion of *HOS2* affects ribosomal protein genes. *SIR2* deletion lead to increased histone H4 acetylation of regions normally transcriptionally silenced, such as telomeres and the silent mating loci (see below).

1.7.3 Global versus Targeted Acetylation and Deacetylation

HDAC action counteracts the activating functions of acetyl-lysines discussed in section 1.6 above, and promotes formation of repressive chromatin (see below). Rpd3p inhibits recruitment of the bromodomain containing activator complexes SWI/SNF and SAGA, and interferes with TBP binding. It does this without affecting

the binding of activator, and consistent with this Rpd3p mediated repression is most effective at promoters that employ weak activators (Deckert and Struhl, 2002).

Rpd3p is targeted to the yeast *INO1* gene promoter as part of a complex containing the Sin3p adaptor protein (Kadosh and Struhl, 1997). This is mediated by the DNA-binding repressor Ume6p, and results in deacetylation of histone H4K5 and K12 on two proximal nucleosomes (Rundlett *et al.*, 1998; Kadosh and Struhl, 1998). But this is not the only method of Rpd3p recruitment, as the promoters and coding regions of many genes not regulated by Ume6p are deacetylated by Rpd3p (Vogelauer *et al.*, 2000).

Genetic and biochemical evidence strongly indicate that Hda1p is recruited to promoters by a direct interaction with Tup1p, where it deacetylates histones H3 and H2B (Wu *et al.*, 2001). But again, this cannot explain all sites of Hda1 activity. Other studies suggest that Tup1p can also recruit Rpd3p (Watson *et al.*, 2000)

Extensive CHIP experiments have demonstrated that promoter-specific targeting of HATs and HDACs occurs within a global background of acetylation and deacetylation (Vogelauer *et al.*, 2000). This constant flux allows a rapid return to the basal levels of gene expression after dissociation of specific activator or repressor proteins (Katan-Khaykovich and Struhl, 2002).

1.7.4 Repression by TUP1/SSN6

The TUP1/SSN6 co-repressor complex down-regulates expression from as much as 2% of the yeast genome (DeRisi *et al.*, 1997). The complex is conserved across species, and comprises 4 Tup1p subunits, and one Ssn6p moiety (Varanassi *et al.*, 1996). The Tup1p domain is required for repressor function (Tzamaridis and Struhl, 1994).

TUP1/SSN6 possesses no intrinsic DNA binding capacity, and is recruited to gene promoters via interaction with DNA-bound repressors (Keleher *et al.*, 1992). At glucose repressed genes recruitment is by Mig1p, whereas α-cells use the α2/Mcm1p complex (Nehlin and Ronne, 1990; Keleher *et al.*, 1989). Ssn6p mediates the binding to structurally dissimilar, pathway specific DNA-binding proteins via subsets of its 10 TPR (tetratricopeptide) motifs (Tzamaridis and Struhl, 1995).

TUP1/SSN6 mediated repression is both promoted by histone hypoacetylation, and causative of it. The amino-terminal tails of histones H3 and H4 are necessary and sufficient for Tup1p binding. This interaction is disturbed by lysine acetylation (Edmondson *et al.*, 1996). Recruitment of TUP1/SSN6 is associated with localized histone hypoacetylation, consistent with its *in vivo* interaction with HDACs (Bone and Roth, 2001; Davie et al., 2003). Simultaneous deletion of *RPD3*, *HOS1* and *HOS2* abolishes TUP1/SSN6 mediated repression at all genes tested (Watson *et al.*, 2000). Whether or not this perpetuation of the hypoacetylated states causes 'spreading' of TUP1/SSN6 is debatable (Ducker and Simpson, 2000).

But HDAC recruitment is not the only method by which TUP1/SSN6 represses genes. TUP1/SSN6 is necessary for the establishment of repressive chromatin structures at the *SUC2* and *FLO1* genes (Gavin and Simpson, 1997; Fleming and Pennings, 2001). Activation of these genes requires the antagonistic action of SWI/SNF. A potential role of histone deacetylation in Tup1p dependent repressive, very regular nucleosome arrays cannot be excluded.

Furthermore, TUP1/SSN6 influences the core transcription apparatus. Genetic and biochemical interactions between *TUP1* and components of the POLII mediator complex have been reported (Gromoller and Lehming, 2000; Zaman *et al.*, 2001). These interactions might prevent formation of a functional PIC.

1.8 Methylation

1.8.1 Histone Lysine Methylation

In addition to acetylation, certain lysine residues in histone N-termini and core domains are subject to methylation. Lysines can be mono-, di- or tri-methylated. Unlike acetylation, this does not affect the overall charge on a histone.

The methylation pattern of histones is a prominent signature pertaining to the 'transcribability' of a genomic region (reviewed by Sims III *et al.*, 2003). Budding yeast lack the methylation systems of higher organisms that establish large, developmentally regulated domains of heterochromatin (Litt *et al.*, 2001). The importance of histone methylation in epigenetic inheritance is exemplified by the fact

that no enzymes have yet been discovered that are able to remove this covalent mark. Parent histone H3/H4 tetramers are randomly distributed between daughter strands following DNA replication. Consequently, each gene in the new DNA strand will have some memory of its transcriptional status in the previous generation.

Lysine methylation in *S. cerevisiae* occurs on histone H3 at positions 4, 36 and 79. Histone H3K4 methylation is by Set1p as part of COMPASS (*com*plex of *p*roteins *as*sociated with *S*et1) (Krogan *et al.*, 2002; Briggs *et al.*, 2001). This modification is absolutely dependent on the ubiquitination of histone H2BK123 by Rad6p (Sun and Allis 2002; Dover *et al.*, 2002). In fission yeast and higher eukaryotes, histone H3K9 is also subject to methylation, and this is mutually exclusive with histone H3K4 methylation (and H3K9 acetylation). Despite this additional level of complexity, Set1p dependence on Rad6p activity is conserved (Roguev *et al.*, 2003).

Set1p is tethered to the 5' end of genes by interacting with the CTD of RNAPII. This establishes a tri-methylated histone H3K4 'memory' of recent transcription throughout the coding sequence (Ng *et al.*, 2003). At the actively transcribed *MET16* gene in yeast, histone H3K4 di- and tri-methylation recruits Isw1p. This alters chromatin structure at the 5' end of the gene, and is required for proper distribution of RNAPII over the coding region and recruitment of cleavage and polyadenylation factors (Santos-Rosa *et al.*, 2003).

In mammals, fission yeast and flies, methylation of histone H3K9 by Su(var)39 initiates a major pathway of heterochromatin formation by providing an interaction

site for HP1 (see below). This is prevented by di-methylation of H3K4, a global euchromatic mark in higher organisms (Norma *et al.*, 2001). HP1 interaction is also prevented by tri-methylation of H3K4, a mark associated with active transcription (Santos-Rosa, 2002).

Histone H3K36 methylation by Set2p is associated with transcriptional elongation (Li *et al.*, 2002). Set2p interacts with RNAPII CTD in a manner influenced by the phosphorylation status of the CTD (Xiao *et al.*, 2003). Seemingly at odds with this, Set2p was first identified in yeast as a repressor of a heterologous promoter (Strahl *et al.*, 2001).

Dot1p methylates 90% of Histone H3 on K79 *in vivo*. The two groups simultaneously discovering this initially came to different conclusions regarding its role in silencing (Ng *et al.,* 2002; Leeuwen *et al.*, 2002). Silencing defects conferred by deletion and over-expression of *DOT1* are similar. It appears that histone H3K79 methylation in euchromatin opposes SIR protein binding, and counteracts the spread of heterochromatin.

Histone H3K9, H3K27 and histone H4K20 methylation occur in flies and mammals, but not budding yeast. These marks are all associated with repressive chromatin structures. Methyl H3K9 binds HP1, and methyl H4K20 prevents acetylation of H4K16, a mark associated with active chromatin (Nishioka *et al.*, 2002).

1.8.2 DNA Methylation

Although absent in budding yeast and flies, DNA methylation is an important epigenetic marker in higher eukaryotes. Methylation occurs at non-promoter CpG dinucleotides, and correlates with gene repression (reviewed by Bird and Wolffe, 1999). Propagation of this epigenetic mark within semi-conservative DNA replication is a relatively straightforward matter. A hemi-methylated site on a newly synthesized daughter strand is recognized by Dnmt1 (*DN*A *m*ethyl*t*ransferase 1). The same enzyme then modifies the opposite strand (Fatemi *et al*, 2001). The establishment of *de novo* DNA methylation is dependent on Dnmt3a and Dnmt3b.

DNA methylation contributes to gene repression by recruiting methyl-binding proteins, which are part of large complexes including HDACs. Experiments in Neurospora indicate an interface between DNA and histone methylation (Tamaru and Selker, 2001).

1.9 Other Histone Modifications

1.9.1 Phosphorylation

Addition of phosphate groups to serine and threonine residues of proteins is a common method of post-translational regulation in biology. Phosphorylation of histone H3 serine 10 is crucial for chromosome condensation during mitosis and meiosis in metazoans (Gurley et al, 1978). This is not the case in yeast, but phosphorylation of H2B may serve instead (Hsu *et al.*, 2000). In *Drosophila*, histone H3S10 phosphorylation correlates with transcriptional activation of heat shock

genes, but this correlation was not observed in yeast. A possible explanation for the difference is that histone H3S10 phosphorylation in *D. melanogaster* may promote the exchange for the H3.3 histone variant. Since H3.3 is equivalent to the only H3 in yeast, such modification may not be necessary (Nowak and Corces, 2004). However, there is some positive correlation between histone H3S10 phosphorylation and transcription in yeast. Histone H3S10 is linked to histone H3K14 acetylation by Gcn5p (Lo *et al.*, 2000). Correspondingly, the crystal structure of the Gcn5p bromodomain complexed with a synthetic histone H3 N-terminal peptide reveals a preference for a histone H3 tail which is both acetylated and phosphorylated (Bottomley, 2004).

1.9.2 Small Protein Groups and Sugars

The role of H2B ubiquitination is discussed in section 1.8.1 above. It is significant that less than 5% of H2B is ubiquitinated in yeast. However, histone H3K4 methylation that it effects is present on 35% of histone H3. Thus it is proposed that the bulky ubiquitin moiety acts a 'wedge', effecting regional histone H3K4 methylation (Sun and Allis, 2002).

Sumo is a ubiquitin-like moiety that has recently been discovered to modify some N-terminal tails of histone H4 in HeLa cells. The associated gene repression appears to be due to recruitment of HDAC's and HP1 (Shiio and Eisenman, 2003). Histones can also be glycosylated, ADP-ribosylated and methylated on arginine residues. These long-known modifications are not well characterised. Clearly there is a long way to go before the histone code is fully cracked and its importance ascertained.

1.10 Gene Silencing in Yeast

Three distinct forms of silencing exist in *S. cerevisiae*. These are at the silent mating loci, telomeres and rDNA repeats. Whilst the exact mechanisms employed at each region differs, all are associated with hypoacetylation of histones H3 and H4, and all require Sir2p (Braunstein *et al.*, 1993). Additionally, these regions contain histone H3 hypomethylated on K79.

1.10.1 Silent Mating Type Loci

The yeast mating mating-type locus is a tripartite assembly on chromosome III. Information at the central *MAT* locus is expressed. *HMLα* and *HMRa* (*HM* collectively) on either side are transcriptionally silent. *HMLα* contains genetic information specific to haploid cells of the α mating-type. *HMRa* contains genetic information specific to haploid cells of the a mating-type. The *MAT* locus houses an identical copy of either the *HMLα* or *HMRa* information, depending on mating type. The ability of yeast to switch mating type is conferred by a specific recombination pathway which is able to exchange the genetic information at the *MAT* locus for that held at one of the silent loci. Simultaneous expression of both α- and a-specific genes precludes mating, as in diploid cells or those with defective silencing mechanisms.

Silencing of *HM* requires Rap1p, ORC (*o*rigin *r*ecognition *c*omplex) and Abf1p. These proteins bind directly to DNA, and interact with products of the silencing information regulator (*SIR*) genes that mediate repression (Laurenson and Rine,

1992). Sir1p is important for the establishment of silencing. It remains localized at the E and I silencers that flank the *HM* loci and nucleate and limit the silenced domain. After nucleation, a complex of Sir2p, Sir3p and Sir4p is believed to spread outwards and establish a silent, heterochromatic domain (Hecht *et al.*, 1995; Rusche *et al.*, 2002).

HM silencing requires the amino-terminal tail of histone H4 (Kayne *et al.*, 1988). Specifically, efficient repression requires non-acetylated histone H4K16, and increased acetylation perturbs interaction with Sir3p (Johnson *et al.*, 1990; Carmen *et al.*, 2001). These observations fit well with the recent demonstration that the distal association of silencing proteins is dependent upon the HDAC activity of Sir2p (Rusche *et al.*, 2002; Hoppe *et al.*, 2002).

1.10.20 Telomeres

Telomeric silencing is similar to HM silencing (reviewed by Tham and Zakian, 2002). A model for establishment and propagation of telomeric heterochromatin is shown in figure 1.5. Sir4p is recruited by Rap1p, which binds to the multiple $C_{1\text{-}3}A$ repeats found at the very end of telomeres. Sir4p then recruits Sir3p, and Sir2p which deacetylates the tails of histones H3 and H4. This promotes Sir3p binding to histones and the concomitant recruitment of more Sir4p. Sir4p recruits more Sir2p, which deacetylates the next nucleosome along, and so on (Luo *et al.*, 2002). Elements that interrupt the perpetuation of Sir2p induced histone deacetylation limit the spread of heterochromatin. At yeast telomeres, this includes STAR (*sub*telomeric *a*nti-*s*ilencing region) elements, and the antagonistic effects of Sir2p and Sas2p on the

levels of histone H4K16 acetylation (Kimura *et al.*, 2002; Suka *et al.*, 2002). In higher eukaryotes, which do not possess Sir3p or Sir4p, it has been proposed that acetylation of histone H3K9 limits the spread of telomeric heterochromatin by preventing methylation of this same residue (Litt *et al.*, 2001).

1.10.3 rDNA

Yeast has up to 200 tandemly repeated rDNA genes, but only half of these are transcribed at any one time. Requirements for the silencing of rDNA are different, reflecting the different nature of these highly repetitive sequences (Smith and Boeke, 1997). Sir2p appears to be recruited by Net1p, but the other Sir proteins are not involved (Straight *et al.*, 1999). In Drosophila, a repressive chromatin structure is established at silent rDNA repeats by the NoRC ATP-dependent remodelling complex (Santoro *et al.*, 2002: Strohner *et al.*, 2004). Cross linking experiments in yeast indicate that a Sir2-dependent, specialized chromatin structure may also be involved in rDNA silencing (Fritze *et al.*, 1997).

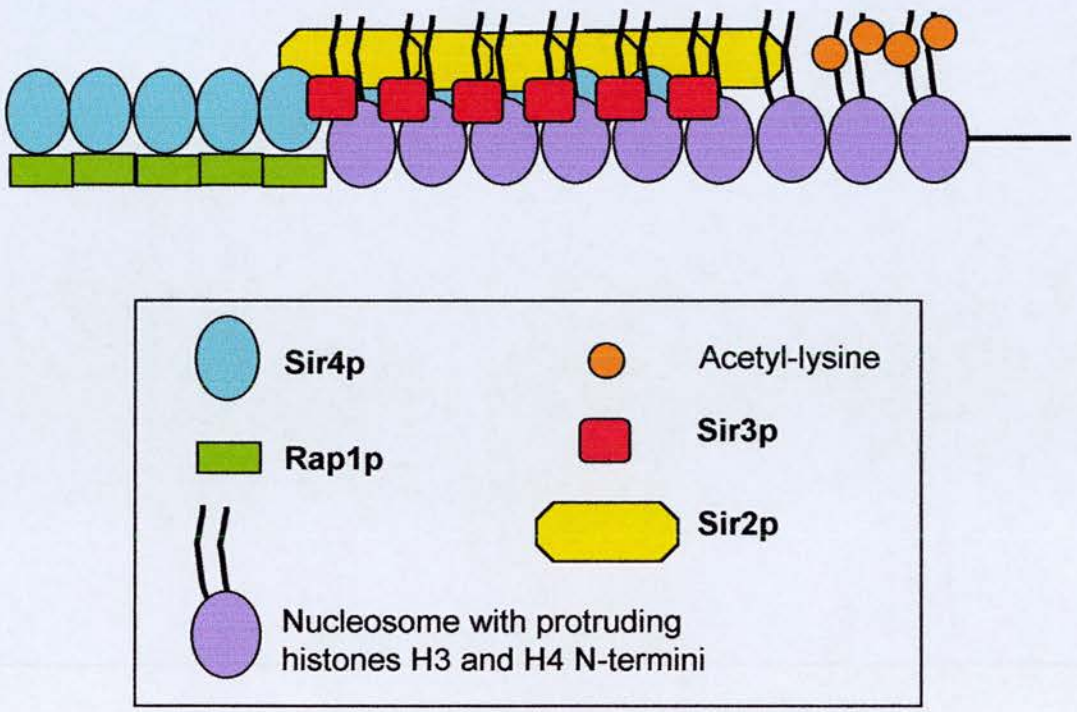

Figure 1.5 Model for formation of telomeric heterochromatin. Rap1p (green oblongs) binds the ends of telomeres and recruits Sir4p (blue ovals). Sir4p recruits Sir2p (yellow hexagons) and Sir3p (red squares). Sir2p deacetylates the tails of histones H3 and H4, allowing Sir3p to bind to nucleosomes (purple ovals). Sir3p recruits more Sir4p and the process is repeated.

1.11 Histone Variants

In addition to the canonical core histones, several variant forms exist. The specialist functions of histone variants and their importance in epigenetic inheritance are becoming clearer (reviewed by Henikoff *et al.*, 2004).

1.11.1 Histone H3 Variants

Eukaryotic centromeres control sister chromatid pairing, spindle microtubule attachment, and checkpoint regulation during cell division. The histone H3 variant, CENP-A is vital for these functions (reviewed by Smith, 2002). Centromeres appear to contain nucleosomes comprising CENP-A/H4 tetramers and H2A/H2B dimers. Their deposition is replication independent (RI) and yeast this might involve RSC mediated chromatin remodelling (Ahmad, Henikoff, 2001).

S. cerevisiae has small point centromeres, defined by the CEN DNA. Elements within this 125bp sequence somehow dictate use of Cse4p (the yeast CENP-A homologue). Higher eukaryotes have much larger centromeres. In flies, the assembly of centromeres requires the use of Cid (*drosophila* CENP-A homologue) and is reminiscent of the spreading of heterochromatin in silenced regions (Maggert and Karpen, 2001).

How CENP-A performs its specialist role remains unclear. Recalling the role of histone H3S10 phosphorylation in chromosome condensation, it is perhaps of

regulatory significance that S7 of CENP-A is subject to cell-cycle regulated phosphorylation (Zeitlin *et al.*, 2001).

Yeast histone H3 is actually most homologous to the H3.3 variant of higher eukaryotes. Although these isoforms differ only by four amino acids within the core domain, they have quite different properties (Ahmad and Henikoff, 2002). Importantly, H3.3 (and H3 in yeast) deposition is RI, and in contrast to CAF1 mediated RC deposition, this does not require the N-terminal tail. H3.3 is enriched at active rDNA loci, and other euchromatic regions. RI deposition of H3.3 provides a means to activate genes silenced by irreversible histone H3K9 methylation.

1.11.2 Histone H2A Variants

The best-studied histone variant is H2A.Z. In vertebrates it accounts for over 10% of H2A (West and Bonner, 1980). At present H2A.Z would appear to play several activating roles, which the current intensive investigation might succeed in uniting. At the yeast *GAL1* and *PHO5* genes, deletion of *HTZ1* (the gene encoding H2A.Z) causes increased dependence on SWI/SNF and SAGA (Santisteban *et al.*, 2000).

In vitro hydrodynamic studies comparing defined nucleosomal arrays with either H2A or H2A.Z dimers indicate effects on higher order structures (Fan *et al.*, 2002). H2A.Z dimers appear to promote interaction of adjacent nucleosomes within an array, but inhibit the oligomerisation necessary to form condensed structures. This is reminiscent of the effect of histone tail acetylation (Tse *et al.*, 1998)

H2A.Z is involved in limiting the spread of heterochromatin. Microarray analysis clustered H2A.Z activated genes near telomeres. High resolution CHIP demonstrates that H2A.Z is enriched in regions surrounding *HMR*, but underrepresented within it. Upon deletion of *HTZ1*, Sir2p and Sir3p, and post-translational marks associated with heterochromatin spread from *HMR*. This is rescued by *SIR2* deletion (Meneghini *et al.*, 2003). The authors note that the genes affected by *HTZ1* deletion do not significantly overlap with those affected by *DOT1* deletion, suggesting that these proteins play differing roles in limiting the spread of heterochromatin (note that *GAL1* and *PHO5* are not located near heterochromatin).

Incorporation of H2A.Z dimers requires the SWR1 chromatin remodelling complex (Mizuguchi *et al.*, 2004). The catalytic subunit, Swr1p contains an ATPase domain characteristic of the INO80 subfamily. Models for the reactions of SWI/SNF and ISWI complexes attempt to minimize disruption of protein-protein interactions, and focus mainly on energetically favourable mechanisms of disrupting protein-DNA interactions. Clearly this should not be the focus of models explaining dimer exchange, but unwrapping of nucleosomal DNA may promote the intrinsic tendency of a dimer to dissociate. The steric incompatibility of an H2A/H2B and an H2A.Z/H2B within a single nucleosome would lead to exchange of the other dimer (Suto *et al.*, 2000).

The crystal structure of an H2A.Z containing nucleosome reveals destabilization at the dimer/tetramer interface compared to a canonical nucleosome (Suto *et al.*, 2000). Additionally, the acidic patch of the H2A 'docking' site is enlarged in H2A.Z

dimers, which would be predicated to alter interactions with other histone and non-histone proteins.

It is not clear exactly how POLII transcribes through chromatin. *In vitro* evidence hints that it involves the loss of at least one H2A/H2B dimer, and that this requires ATP-dependent chromatin remodelling (Kireeva *et al.*, 2002, Bruno *et al.*, 2003). This might be facilitated directly or indirectly by H2A.Z containing dimers.

The mammalian H2A variant MacroH2A is associated with heterochromatin and is enriched on the inactive X chromosome (Chadwick and Willard, 2002).

1.12 Rationale for this Thesis

The preceding sections should make two points very plain. Firstly, regulation of chromatin structure is implicit to regulation of gene transcription. Secondly, a factor influencing chromatin must be considered in the context of all other factors that influence chromatin. Hard and fast rules cannot at present be determined, and each gene must be considered in its own right.

The relative simplicity of genetic studies in yeast makes this organism a powerful tool and useful model for higher eukaryotes. However, yeast is a non-terminally differentiating, single-cellular organism. It has a complement of about 6200 genes. Many of these express constitutively, and all of which it must be able to activate in response to appropriate external stimuli. Thus yeast are considered to retain their chromatin in a more 'open' conformation than that of higher eukaryotes.

Yeast nucleosomes are less stable than those of higher eukaryotes in high salt and at higher temperature (Lee *et al.*, 1982, Pineiro *et al.*, 1991). Nucleosomal arrays are more closely spaced, with an average repeat length of about 165bp compared to 175-240bp in metazoans (Horz and Zachau, 1980). Despite their high conservation across species, these differences must be at least in part due to changes in the amino acid sequences of histone proteins. In fact, yeast histones are among those most divergent from mammalian histones (Makalowska *et al.*, 1999).

The more 'open' structure of yeast chromatin compared to metazoan chromatin can be partially rationalised by comparing the crystal structures of *Xenopus* and yeast core nucleosomes (White *et al.*, 2001). The overall structures are very similar, and the amino acid differences that occur are scattered throughout the globular and tail regions (figure 3.15). The major apparent difference is the destabilisation of the interaction of the two histone H2A/H2B dimers via the L1 loop of the H2A molecules. In *Xenopus* this interaction has a surface area of 150Å^2, and is stabilised by two salt bridges, two hydrogen bonds, and numerous hydrophobic interactions. In yeast, amino acid changes and steric alterations abolish all of these stabilising interactions, and reduce the surface area to 90Å^2. The involvement of this region in holding together the two turns of nucleosomal DNA implies considerable functional importance for remodelling activities. The alterations buried within the octamer core may also have a combined de-stabilising effect.

Yeast chromatin structure can be said to be representative of the active chromatin fraction of higher eukaryotes but it is less well characterised than higher eukaryotic bulk chromatin. This lack prevents a thorough interpretation of the wealth of chromatin remodelling and modification data for this organism. In order to learn more about the different structures of active and bulk chromatin, yeast histone H4 was substituted with those from *Xenopus*/human and the effects on genome-wide expression recorded.

Given the importance of chromatin, it is not surprising that defects in systems by which it is regulated it can be deleterious. Mutations in proteins that establish or

manipulate chromatin structure stand out by their ability to potentially affect every gene in the cell. This often leads to highly pleiotropic effects of a single mutation, or a syndrome in the clinical terms of humans. Several clinical disorders are known to result from disruptions in ATP-dependent chromatin remodelling complexes, with symptoms that range from thalassemia to mental retardation (reviewed by Ausio *et al.*, 2003). In addition, aberrant gene expression can cause cancers. This might result from activation of oncogenes, of repression of tumour-suppressor genes (reviewed by Hake *et al.*, 2004)

A corollary of this is that drugs are being developed that target chromatin modifying complexes. SAHA, a compound that inhibits HDAC's is in clinical trials at this moment.

An *S. cerevisiae* strain expressing human histones in place of its own might be a better model for higher eukaryotic chromatin. If such a strain were viable it could provide a simple framework in which to investigate the action of heterologous human chromatin modifying complexes. It could also be used to test the effectiveness of new drugs. Before results of these hypothetical experiments could be interpreted, the yeast strain would need to be well characterised with respect to wild type. This thesis describes the construction of yeast strains expressing forms of histone H4 more closely related to the human protein. Somewhat unexpectedly, much of the discussion revolves around metabolic changes induced by the mutations. The relevant concepts are appropriately introduced in the results chapters. This thesis represents the first step in construction of an *S. cerevisiae* strain that contains

'humanised' nucleosomes, and provides insight into the role of amino-acids that evolution has seen fit to change.

Chapter 2: Materials and Methods

Many of the standard protocols and solutions outlined in this section are derived from: Current Protocols in Molecular Biology; series 3 (edited by Ausubel *et al.*)

2.1 Reagents and Stock Solutions

All solutions were made using distilled water.

Agarose Gel Loading Buffer at 5X concentration consisted of 0.208% orange G, 12.5% ficoll-400, and 100mM EDTA.

Ampicillin was dissolved in distilled water to give a stock solution of 100 mg/ml.

Buffered Phenol was prepared as follows: 250g of solid phenol were dissolved in 127ml of 2M Tris-HCl pH 7.5, and the phases left to settle. The aqueous phase was removed and discarded. To the organic phase, 55ml 2M Tris-HCl pH8, 13.75ml m-cresol, 550µl β-mercaptoethanol and 275mg 8-hydroxyquinoline were added. The solution was mixed well and left to settle. The phenol layer was retained, aliquoted, and stored at -20°C.

Chloroform:Isoamyl alcohol (IAA) consisted of chloroform and iso-amyl alcohol (IAA) mixed at a ratio of 24:1.

Coomassie blue stain comprises 0.025% [w/v] coomassie blue G-250, in 10% [v/v] acetic acid.

Diethyl pyrocarbonate (DEPC)-water was prepared by diluting diethyl pyrocarbonate to 0.1% in distilled water, followed by incubation at 37°C for 1 hour/room temperature (RT) overnight. The solution was then autoclaved to deactivate the DEPC.

Dithiothreitol (DTT) was prepared by dissolving solid dithiothreitol to 1M in distilled water, and was stored at 4°C.

Ethylene diamine-tetraacetic acid (EDTA) (disodium salt) was dissolved in distilled water and adjusted to pH 8.0 with NaOH. The volume was adjusted to give a final concentration of 0.5M.

Ethidium bromide stock solution was prepared by dissolving ethidium bromide to 10mg/ml in distilled water, and stored at RT in a light proof bottle.

MOPS solution was prepared as a 10X solution by dissolving 20.93g MOPS and 2.05g sodium acetate in DEPC-water. 25ml of 0.1M DEPC-EDTA pH8 was added. The volume was adjusted to 250ml, to give final concentrations of 0.4M MOPS, 0.1M sodium acetate, 0.01M EDTA.

Phenol:Chloroform:IAA consisted of a 25:24:1 ratio of buffered phenol, chloroform, and IAA.

Phenyl-methyl-sulphonyl-fluoride (PMSF) was dissolved in isopropanol to a final concentration of 250mM, and stored at 4°C.

RNaseA was dissolved in water to 1mg/ml and boiled for 30 minutes to an hour to inactivate DNase. Aliquots were stored at -20°C.

Salmon sperm DNA at 2, or 10mg/ml in TE (pH 8) was dissolved by stirring slowly overnight at 4°C. Aliquots were stored at -20°C, and denatured before use by boiling for 5 minutes.

SDS sample buffer at 2X concentration contained 25ml 4X Tris-Cl/SDS pH6.8 (0.5M Tris-Cl pH6.8, 0.4% SDS), 20ml glycerol, 4g SDS, 1mg bromo-phenol-blue and 55ml water. This was stored at 4°C, and 20µl β-mercaptoethanol was added per ml prior to use.

SDS electrophoresis buffer was prepared as a 5X stock by dissolving 15.1g Tris, 72g glycine and 5g SDS in 1l of water.

Sodium acetate was dissolved in water, and the pH adjusted to 5.2 with glacial acetic acid. The volume was adjusted to give a final concentration of 3M.

Sodium dodecyl-sulphate (SDS) stock was prepared at 10% (w/v) in distilled water.

SSC was prepared as a 20X stock by dissolving 175g (3 moles) NaCl, and 88g (0.3 moles) tri-sodium citrate in 1l of distilled water.

TBE (Tris-borate-EDTA) buffer for agarose gel electrophoresis was prepared as a 10X stock by dissolving 108g Tris (0.89 moles) and 55g (0.89 moles) boric acid in 960ml distilled water, and adding 40ml of 0.5M EDTA pH8.

TBST buffer comprises 20mM Tris-Cl pH7.5, 150mM NaCl and 0.05% [v/v] Tween 20.

Transfer Buffer (TB) comprises 25mM Tris, 192mM glycine, and 20% methanol. SDS was added to 0.1% after mixing, to prevent bubbles.

Tris(hydroxymethyl)aminomethane (Tris)-HCl) was dissolved in distilled water and adjusted to the appropriate pH with concentrated HCl. The volume was adjusted to give a final concentration of 1M.

Tris/EDTA (TE) buffer is10mM Tris-HCl pH 8, 1mM EDTA pH8.

2.2 Culture and Manipulation of *Escherichia coli*

2.2.1 Media

All media were made using distilled water, and were autoclaved at 15lb/in^2 for 15 minutes prior to addition of supplements.

Liquid cultures of *E. coli* cells were grown in Luria-Bertani (LB) broth:

1% tryptone

0.5% yeast extract

0.5% NaCl

1mM NaOH

For plates, agar was added to LB broth at 1.5%.

For plasmid selection after transformation, ampicillin was added to broth or solid media to a final concentration of 100μg/ml.

2.2.2 Bacterial Strains

Bacterial cultures were grown overnight at 37°C, unless otherwise stipulated.

E. coli strain DH5α (F'/*endA1 hsdR17*($r^K m^K_+$) *supE44 thi-1 recA1 gyrA* (Nal^r) *relA1 Δ(lacIZYA-argF) U169 deoR* (*Φ80dlacΔ(lacZ)M15*)) was used for routine cloning.

2.2.3 Bacterial Glycerol Stocks

1ml of a saturated culture was added to an equal volume of sterile glycerol solution (65% glycerol, 0.1M $MgSO_4$, and 0.025M Tris.HCl pH8), mixed well by vortexing and stored at -70°C.

2.2.4 High Efficiency Transformation of E. coli by Electroporation

Electro-competent cells were prepared as follows: 2ml of an *E. coli* overnight starter culture was used to inoculate 500ml of fresh LB. This was shaken at 300rpm at 37°C, until cells had grown to an OD_{600} of 0.6. The culture was chilled in ice/water for 15 minutes, and all subsequent steps were performed at 4°C. Cells were harvested by centrifugation at 4000rpm for 20 minutes, using a JA-14 rotor in a Beckman centrifuge. Cells were then washed twice in ice-cold sterile water and centrifuged as before. For final harvesting, centrifugation was performed using a JA-20 rotor at 5000rpm. Electro-competent cells were resuspended in an equal volume of ice-cold, 10% glycerol. Aliquots of 50µl were either used immediately or stored at -70°C.

Electro-competent cells were transformed as follows: 0.1-0.5µg of plasmid DNA was added to 50µl of competent cells, and transferred to a pre-chilled 2mm electroporation cuvette. The cuvette was then placed in the electroporation chamber and pulsed briefly at 240V. 1ml of LB was immediately added, and the cell suspension removed to a 50ml falcon tube. Cells were allowed to recover for 30 minutes at 37°C with gentle agitation. Transformants were selected by spreading aliquots onto LB plates supplemented with ampicillin.

2.3 Culture and Manipulation of *Saccharomyces cerevisiae*

2.3.1 Media

All media were made using distilled water, and were autoclaved at 15lb/in^2 for 15 minutes prior to addition of supplements.

Yeast cells were cultured routinely in YPD medium:

1% yeast extract

2% peptone

2% glucose

For plates, agar was added to YPD broth at 2%.

Rich media containing alternative carbon sources were made as for YPD but omitting glucose. Carbon source was added after autoclaving by filter sterilization, to a final concentration of 2%, except in the case of EtLac media. Supplements were added in disruption phenotype experiments as indicated in table 3.1.

EtLac media contains 2% ethanol, 2% lactate, and 0.1% glucose. A 5X stock of this carbon source was prepared by titrating lactic acid with an equimolar amount of NaOH. Ethanol, glucose and water were added to appropriate concentrations.

For selection or maintenance of plasmids, and selection of integrants, synthetic-complete medium was used. This contains:

0.67% yeast nitrogen base

2% glucose/galactose

1% casamino acids

This was appropriately supplemented with:

40μg/ml adenine

30μg/ml lysine

40μg/ml tryptophan (10μg/ml for low-trp media)

30μg/ml tyrosine

20μg/ml arginine

200μg/ml threonine

For plates, agar was added to 2%.

For curing yeast of plasmids bearing the *TRP1* marker allele, 5-flouroanthranilic acid (FAA), which counterselects for *TRP1* (Toyn *et al.*, 2000), was added to low-trp media to a final concentration of 1g/l FAA.

2.3.2 Saccharomyces cerevisiae Strains

The parental strain used in these experiments is UKY403 (Johnson *et al.*, 1990): *(MATa, ade2-101, his3-Δ200, leu2-3, 112 lys-801, trp1Δ901, ura3-52, GAL+, thr, tyr, arg4-1 Δh4-1[HIS3+],Δh4-2 [LEU2+], pUK421 (CEN, TRP+, GAL-H4-2+)*). In this nomenclature *H4-1* is equivalent to *HHF1*, and *H4-2* is equivalent to *HHF2*. UKY412 (WT) is isogenic with UKY403 except that plasmid pUK421 is replaced by

pUK499 (*CEN, URA3+, H4-2+*). UKY500, UKY501 and UKY502 are isogenic with UKY412, except that plasmid pUK499 is replaced by pUK500, pUK501 and pUK502 respectively. These plasmids are identical to pUK499 except for site-directed mutations within *H4-2* (*HHF2*).

The strain used in mating assays was D587-11c (*MATα, his1*)

Except where stipulated, yeast cultures were incubated at 30°C, with good aeration.

2.3.3 Yeast Glycerol Stocks

1ml of a late-logarithmic culture was mixed well with an equal volume of 30% glycerol and stored at -70°C.

2.3.4 High Efficiency Transformation of Saccharomyces cerevisiae

Yeast were transformed by the lithium acetate/single-stranded carrier DNA/polyethylene glycol (LiAc/ss-DNA/PEG) protocol (Agatep *et al.*, 1998). Briefly, the cell density of an overnight culture was ascertained by counting cells on a heamocytometer. An appropriate volume was used to inoculate 50ml of fresh media to a density of 5×10^6 cells/ml. This culture was shaken at 200rpm at 30°C until a density of 2×10^7 cells/ml had been reached. Cells were harvested by centrifugation at 5000 rpm for 5 minutes at room temperature, washed in sterile water and re-centrifuged as before. Cells were resuspended in 1ml of 100mM lithium acetate, then harvested in a microcentrifuge and resuspended in 400µl of 100mM lithium acetate. 50µl aliquots of cells were harvested, and the lithium acetate was

removed. Cells were resuspended in 326µl transformation mix (240µl 50% polyethylene glycol, 36µl 1M lithium acetate, 50µl 2mg/ml denatured salmon sperm DNA), and the desired plasmid was added within a volume of 36µl sterile water. Cells were incubated at 30°C for 30 minutes, and then heat shocked 30 minutes at 42°C. Cells were gently harvested at 6000 rpm for 1 minute, and resuspended in 1ml sterile water. Appropriate volumes were spread onto selection plates, and incubated at 30°C.

2.3.5 Mating

Strains to be mated were grown to mid-logarithmic phase (4 x 10^7 cells/ml) in YPD. A *MAT-a* test strain/*MAT-α* standard strain ratio of 2:1 was used. Mating was performed at 30°C for 4 hours without shaking. Dilutions were plated onto unsupplemented minimal media to determine the number of successful conjugations. Total cell number was estimated by plating dilutions of unmated test-strain onto YPD.

2.3.6 Fluorescence Microscopy

Cells were grown to mid-logarithmic phase in YPD. 200µl aliquots were harvested by microcentrifugation, and washed twice in water. Cells were resuspended in 10µl of water, and fixed by rapidly drying on a hot-plate. 10µl moiwi oil mounting medium (a kind gift from L. Wilson) containing 50ng/ml 4', 6'-diamidino-2-phenylindole (DAPI) was put on the slide, and a coverslip placed on top. Slides were sealed with nail varnish and stored overnight at 4°C. An Olympus BX61 fluorescence microscope was used to observe and photograph the slides.

2.4 Cloning and Manipulation of DNA

2.4.1 Plasmid DNA Preparation from E. coli

Processing 5ml overnight bacterial cultures with a QIAprep spin mini-prep kit (Qiagen) yielded approximately 10μg of DNA. For larger amounts, 100ml overnight cultures were processed with a QIA filter Plasmid Midi Kit (25) (Qiagen). The steps in these kits remove genomic DNA and RNA. The plasmid DNA isolated is dissolved in an appropriate volume of water and is ready to use.

2.4.2 Phenol/Chloroform Extraction and Ethanol Precipitation

100-200μl of phenol/chloroform/IAA was added to an equal volume of aqueous DNA solution, and the immersion mixed well by vortexing. Phases were separated by microcentrifugation at 13000 rpm for 10 minutes. The aqueous phase was removed to a clean tube, and extraction repeated until the interface was clean. Re-extraction with an equal volume of chloroform/IAA to remove any residual phenol from the sample was sometimes performed.

DNA was precipitated at -20°C for 30 minutes, to 16 hours by 1/10 volume 3M sodium acetate (pH 5.2) or 4MLiCl, and 2.5 volumes 100% ethanol. DNA was collected by centrifugation at 13000 rpm for 10 minutes. The pellet was washed in 0.5ml of 70% ethanol (at -20°C) to remove any residual salt. The DNA pellet was dried under vacuum, and resuspended in an appropriate volume of water.

2.4.3 Agarose Gel Electrophoresis

DNA fragments were separated according to size by agarose gel electrophoresis. Depending on the size of fragments to be resolved, gels were between 1 and 1.5% agarose, in 1X TBE. DNA samples were loaded in 1X agarose gel loading buffer. Gels were run in 1X TBE, at 80 to 110 volts for an appropriate time. Gels were then stained in 3mg/ml ethidium bromide solution for 10 minutes, to visualize DNA. De-staining was achieved by washing twice for 10 minutes in distilled water. Images of stained gels were obtained by scanning in a Fujifilm FLA-2000 in fluorescent mode.

2.4.4 Gel Extraction

DNA fragments were resolved on an agarose gel and stained with ethidium bromide. The band of interest excised with a razor blade. The DNA was eluted using the Qiaex II gel extraction kit (Qiagen). Dilute preparations were re-concentrated by ethanol precipitation.

2.4.5 DNA Concentration

This can be determined spectrophotometrically by measuring the absorbance of dilutions at 260nm, and using the conversion:

1 A_{260} absorbance unit = 50μg DNA/ml.

2.4.5 Restriction Enzyme Digestion

Except where stipulated, DNA was digested with restriction enzymes as specified by the relevant manufacturer. Digestion products were resolved by agarose gel

electrophoresis. For use in cloning the relevant fragments were excised and gel purified.

2.4.6 Dephosphorylation of Vector DNA

To an overnight restriction digest of 10µl, 1µl of calf intestinal alkaline phosphatase (NEB) was added and incubated for 1 hour at 37°C. Vector DNA was then separated from other digestion products and purified as in section 2.4.4.

2.4.7 DNA Ligation

Ligation reactions were carried out overnight at 16°C in a final volume of 10-20µl. 100ng of dephosphorylated vector DNA was incubated with insert DNA at a 1:3 molar ratio, in the presence of 400U T4 DNA ligase and buffer containing ATP (NEB). 5µl of the ligation mix was used directly to transform electro-competent *E. coli* cells.

2.4.8 Polymerase Chain Reaction (PCR)

For amplification of DNA fragments to be used for cloning or as probes, PCR reactions were normally performed in a volume of 100µl as follows: 10-500ng template DNA; 1X Taq buffer; 1.5mM $MgCl_2$; 0.2mM deoxy-nucleotide triphosphates (dNTPs); two primers at 0.5µM; 1U Taq polymerase (Promega). In some instances Vent polymerase (NEB) was used. In this case, 1X Vent buffer was used, and 1.5mM $MgSO_4$ was substituted for 1.5mM $MgCl_2$. A standard PCR program comprised 5 minutes at 95°C, followed by 30 cycles of: denaturation at 95°C for 1 minute; annealing at an appropriate temperature for 1 minute; extension at

72°C for 45 seconds or more (approximately 1 minute per kilobase of DNA to be amplified). A final elongation at 72°C for 10 minutes ensures amplified fragments are of the same length. Reaction products were separated in an agarose gel and purified as described.

2.4.9 Splicing by Overlap Extension (SOE)

The procedure described by Horton *et al.,* (1993) enables two overlapping DNA fragments to be joined together in a PCR reaction. The reaction mix is as described above, and the following amplification program was used: 4 minutes at 95°C, followed by 5 cycles of; denaturation at 95°C for 1 minute; annealing at 40°C for 2 minutes; extension at 72°C for 1.5 minutes; then 25 cycles of denaturation at 95°C for 1 minute; annealing at 53°C for 1 minute; extension at 72°C for 1.5 minutes. A final elongation for 5 minutes at 72°C ensures amplified fragments are of the same length.

2.5 Radio-labelling of DNA fragments

2.5.1 Marker DNA

300ng of 1kb ladder (Promega) was labelled on the 5'-end by incubating with 1X polynucleotide kinase buffer, 5U polynucleotide kinase (NEB) and 4 picomoles of [γ-^{32}P]ATP at 37°C for 1 hour. The enzyme was deactivated by heating to 68°C for 20 minutes. Unincorporated label was removed by passing the sample through a MicroSpin™ G-25 Column (Amersham Biosciences).

2.5.2 Probe DNA

DNA fragments to be used as probes were labelled by random priming.1-2μg of DNA were combined with 5μg hexanucleotide of mix in a volume of 14μl. This was boiled for 5 minutes to denature the DNA and then put on ice. To this the following was added: 1X Klenow polymerase buffer; 0.5mM 3dNTP's (-dCTP); 12.5U Klenow polymerase (NEB); and 8 picomoles [α-^{32}P]dCTP. The reaction was allowed to proceed for four hours at RT, and was then halted by adding 1μl 0.5M EDTA. 24μl of TE were added, and the sample passed through a MicroSpin™ G-25 Column (Amersham Biosciences) to remove unincorporated label. Another 75μl of TE were added, and the probe denatured before use by boiling for 5 minutes.

2.6 Preparations from *S. cerevisiae*

2.6.1 Genomic DNA

Yeast from a 10ml overnight culture were harvested at 5000rpm for 5 minutes and washed in 0.5ml sterile water. Cells were resuspended in 200μl of breaking buffer (2% triton X-100, 1% SDS, 100mM NaCl, 10mM Tris.HCl pH8, 1mM EDTA pH8). 200μl glass beads and 200μl phenol/chloroform/IAA were added, and the cells lysed by vortexing for 1 minute. Samples were cooled on ice before another minute of vortexing, and this was repeated up to a total of 4 minutes. 200μl of TE buffer was added, and the sample briefly vortexed again before microcentrifugation at 13000 rpm for 10 minutes. 1ml of ethanol was added to the aqueous phase to precipitate the DNA. DNA was harvested by microcentrifugation as before, and resuspended in 400μl of TE buffer and 30μl of RNaseA (1mg/ml). This was incubated at 37°C for 30

minutes. DNA was precipitated at RT with 10µl of 4M ammonium acetate and 1ml ethanol. DNA was harvested by microcentrifugation and resuspended in TE. This DNA was further purified by repeated phenol/chloroform/IAA extractions, and ethanol precipitated again once the interface was clean. This procedure yields approximately 20µg of DNA. For larger amounts, DNA was extracted from a 100ml yeast culture, with the treatments scaled up appropriately.

2.6.2 Plasmid DNA

1.5ml of an overnight yeast culture was harvested in a microcentriguge, and washed in water. Cells were resuspended in 200µl of breaking buffer. 200µl glass beads and 200µl phenol/chloroform/IAA were added, and sample vortexed for 2 minutes. Phases were separated by microcentrigation at 13000 for 5 minutes, and the aqueous phase removed. The DNA was further purified by phenol/chloroform/IAA extraction and ethanol precipitation. The pellet was resuspended in 10µl of water, and the DNA used to transform competent *E. coli* cells.

2.6.3 Total RNA

For preparation and manipulation of RNA, all glass and plastic ware was soaked for 20 minutes in 3% hydrogen peroxide, and then rinsed with DEPC-water. Solutions were either DEPC treated themselves, or made using DEPC-water.

When comparisons between YPD and EtLac grown cells were being made, 10ml yeast cultures were grown to 2–2.25 x 10^7 cells/ml. Cells were then harvested by centrifugation at 6000rpm for 5 minutes. YPD cells were washed in YPD, harvested

as before, and resuspended in fresh YPD. EtLac cells were washed in YP, harvested as before, and resuspended in fresh EtLac. Cells were then grown to mid-logarithmic phase (4-4.5 x 10^7 cells/ml), although UKY500 could not complete a doubling in this media. When only YPD grown RNA was needed, 10ml yeast cultures were grown in YPD to mid-logarithmic phase (4-4.5 x 10^7 cells/ml).

RNA was prepared as follows: a 10ml culture was grown to mid-logarithmic phase (4-4.5 x 10^7 cells/ml) and harvested by centrifugation at 6000rpm for 3 minutes. Cells were resuspended in 400µl AE buffer (50mM sodium acetate pH5.3, 10mM EDTA pH8) and transferred to a 1.5µl Eppendorf tube. 40µl 10% SDS was added and the sample vortexed. 440µl of AE equilibrated buffered phenol was added, and the mixture vortexed before heating at 65°C for 5 minutes. Tubes were then transferred to dry ice for 15 minutes to precipitate protein and DNA. Phases were separated by microcentrifugation at 13000rpm for 15 minutes. The aqueous phase was re-extracted with phenol/chloroform/IAA and ethanol precipitated. Pellets were resuspended in 50µl DEPC-water, and stored at -70°C. This method was adapted from Schmitt *et al.*, 1990.

2.6.4 RNA Concentration

This can be determined spectrophotometrically by measuring the absorbance of dilutions at 260nm, and using the conversion:

1 A_{260} absorbance unit = 42µg RNA/ml.

2.6.5 Nuclei

When comparisons between YPD and EtLac grown cells were being made, two 1l yeast cultures were grown to 2–2.25 x 10^7 cells/ml. Cells were then harvested by centrifugation at 4000rpm for 20 minutes. YPD cells were washed in YPD then harvested as before and resuspended in fresh YPD. EtLac cells were washed in YP then harvested as before and resuspended in fresh EtLac. Cells were then grown to mid-logarithmic phase (4-4.5 x 10^7 cells/ml), although UKY500 could not complete a doubling in this media. When only YPD nuclei were needed, two 1l yeast cultures were grown in YPD to mid-logarithmic phase (4-4.5 x 10^7 cells/ml). When preparing YPD nuclei, 2% glucose was added to all buffers mentioned below.

Cells were harvested by centrifugation at 4000rpm for 20 minutes at 4°C. The weight of the cell pellet was determined and designated as 1 volume. Cells were washed in 3 volumes of water and then harvested in a JA14 rotor in a Beckman centrifuge, at 5000rpm for 5 minutes at 4°C. The supernatant was decanted and cells resuspended in 1 volume zymolase buffer (50mM Tris-Cl pH7.5, 10mM $MgCl_2$, 1M sorbitol, 14mM β-mercaptoethanol) containing 30mM DTT. The suspension was incubated at RT for 15 minutes to break disulphide bonds, and then cells harvested at 5000rpm for 5 minutes at 4°C. Cells were resuspended in 3 volumes zymolase buffer containing 1mM DTT. 100mg of yeast lytic enzyme were added per 5g of cells. Cells were incubated for 1 hour at 30°C with gentle agitation to form spheroplasts. Spheroplasts were harvested by centrifuging as before, and washed 3 times in 2 volumes ice-cold zymolase buffer containing 1mM DTT. All subsequent steps were performed at 4°C. Spheroplasts were lysed by stirring vigorously for 20 minutes in 15 volumes ficoll

buffer (18% Ficoll-400, 10mM Tris-HCl pH7.5, 20mM KCl, 5mM $MgCl_2$, 1mM EDTA, 3mM DTT, 1mM PMSF). The suspension was centrifuged at 5000 rpm for 5 minutes to pellet cell debris and unlysed spheroplasts. This step was repeated once more, and the supernatant removed and centrifuged at in a JA20 rotor at 13000rpm for 20 minutes. The pellet volume was estimated and resuspended in an equal volume of storage buffer (20mM Tris-HCl pH7.5, 0.1mM EDTA pH8, 10% glycerol, 100mM KCl, 1mM DTT, 1mM PMSF, 14mM β-mercaptoethanol). Aliquots were stored at -70°C.

2.6.6 Protein Extracts

200ml cultures of yeast were grown to mid-logarithmic phase (4-4.5 x 10^7 cells/ml). Cells were harvested by centrifugation at 5000rpm for 5 minutes at 4°C, and all subsequent steps were performed at 4°C. The weight of the cell pellet was determined and designated as 1 volume. Cells were washed in 2 volumes of water, and harvested as before. Cells were resuspended in 3 volumes of glass bead disruption buffer (20mM Tris-Cl pH7.9, 10mM $MgCl_2$, 1mM EDTA, 5% glycerol, 0.3M ammonium sulphate, 1mM DTT, 1mM PMSF). To this, 4 volumes of chilled glass beads were added. Samples were vortexed for 45 seconds then chilled on ice. This was repeated 5 times. The glass beads were allowed to settle, and the supernatant removed to a clean tube. The beads were rinsed again in 2 volumes of glass bead disruption buffer. Supernatants were centrifuged in a JA20 rotor in a Beckman centrifuge at 10000rpm for 60 minutes to pellet cell debris. The supernatant containing soluble protein extract was removed to a clean tube.

To enrich for basic proteins, a method was adapted from that used in Rundlett *et al.*, 1996. Crude preparations were acid extracted by adding concentrated HCl to 0.25M. Samples were incubated on ice for 2 hours, and then centrifuged at 9500rpm for 15 minutes. The supernatant was removed to a clean tube, to which an equivalent volume of 50% trichloroacetic acid (TCA) was added. This incubated on ice for 1 hour, and then centrifuged at 12000rpm for 15 minutes. The supernatant was discarded, and the pellet washed in 99:1 acetone/5M HCl, and then in acetone. Pellets were resuspended in 8M UREA, and aliquots stored at -70°C.

2.7 DNA Analysis

2.7.1 Southern Blotting

Prior to Southern blotting (Southern, 1975), DNA fragments resulting from a restriction digest of approximately 10µg genomic DNA were separated in an agarose gel. 50 counts of radiolabelled 1kb marker were also included on the gel. DNA was denatured in-situ by washing for 2 x 20 minutes in 1.5M NaCl, 0.5M NaOH. The gel was neutralized for 2 x 25 minutes in 1mM ammonium acetate, 20mM NaOH. DNA was transferred overnight to nitrocellulose membrane (Zeta-Probe GT, BIO-RAD), by upward capillary transfer in 20X SSC.

The membrane was washed in 2X SSC and air-dried for 20 minutes. The DNA was immobilized by baking on a vacuum dryer at 80°C for 1 hour. The membrane was then incubated at 65°C in pre-hybridization buffer (3X SSC, 10mM EDTA pH8, 0.2% PVP, 0.2% Ficoll-400, 0.2% BSA, 0.1% SDS, 0.1mg/ml denatured salmon

sperm DNA, 0.5mg/ml heparin), for 2-3 hours in a rotating oven. The denatured probe was added to 25ml of hybridization buffer (pre-hybridization buffer supplemented with 2.25g of dextran sulphate) at 65°C. Hybridization was performed overnight at 65°C. The membrane was washed at 65°C for 4 x 15 minutes in 2X SSC/0.1% SDS, and for 2 x 20 minutes in 0.1X SSC/0.1% SDS. Finally, the membrane was rinsed in 2X SSC at RT, and exposed to a phosphorescent screen (Fuji).

2.8 RNA Analysis

2.8.1 Agarose Gel Electrophoresis

RNA fragments were size separated in a denaturing gel containing 1.5% agarose, 1X MOPS and 7.2% formaldehyde. 10-20µg samples of RNA were prepared in 15µl of MMF solution (500µl formamide, 162µl 40% formaldehyde, 100µl 10X MOPS). Ethidium bromide was added to a final concentration of 0.1mg/ml, and samples were heated at 60°C for 15 minutes. Samples were loaded in 1X loading buffer (1mM EDTA, 0.25% bromo-phenol-blue, 0.25% xylene-cycol, 50% glycerol), and gels were run in 1X MOPS. Images of stained gels were obtained by scanning in a Fujifilm FLA-2000 in fluorescent mode.

2.8.2 Northern Blotting

Prior to Northern blotting, RNA was separated in a denaturing agarose gel. Gels were washed for 2 x 20 minutes in DEPC-water to remove formaldehyde. RNA was then

transferred to nitrocellulose membrane, and hybridized to a cDNA probe as for a Southern blot.

2.8.3 Microarrays

10μg of RNA was labelled with Cyanine 3-dCTP (Cy3) or Cyanine 5-dCTP (Cy5) with an Agilent Fluorescent Direct Label kit, as per the manufacturer's instructions. Briefly, RNA was denatured in the presence of oligo-dT primer by heating to 70°C for 10 minutes. Samples with incubated in a buffered reaction mixture containing Cy3 or Cy5 and reverse transcriptase (MMLV-RT) for an hour at 42°C. MMLV-RT was deactivated by heating to 70°C for 10 minutes and then RNA was degraded by RNAse1A. The Cy3- and Cy-5 labelled cDNA to be co-hybridized on a single array were combined, and the cDNA purified with a QIAquick PCR purification kit (Quiagen). Samples were now ready to be hybridized to the array.

Labelled cDNA samples were hybridized to Agilent 11K Microarrays using an Agilent Microarray Hybridization kit, according to the manufacturer's instructions. Briefly, cDNA samples were denatured for 3 minutes at 98°C and then allowed to cool to RT. They were then combined with control targets (which allow orientation of the array when scanning) in a buffered mixture, and loaded into the array chamber set-up. Hybridization proceeded for 17 hours at 60°C, in a rotating oven. Post hybridization, the chambers were submerged in wash solution 1 (6X SSC, 0.005% Triton X-102), and disassembled. Slides were removed to a slide rack and washed for 10 minutes with stirring. The slide rack was then transferred to a dish containing ice-

cold wash solution 2 (0.1X SSC, 0.005% Triton X-102), and washed for 5 minutes with stirring. Slides were dried with a nitrogen source, and stored under vacuum.

Cy3 and Cy5 fluorescent intensities were measured in an Agilent dual-laser Microarray Scanner, with the kind permission of Simon Plummer, CXR Biosciences, Dundee. Data were extracted using Agilent's Feature Extraction software, using the Rank Consistency Filter method of dye normalization to remove dye bias. 'Dye bias' refers to both the differential rates of incorporation of Cy3- or Cy5- labelled nucleotides into a cDNA chain, and the differences in intrinsic fluorescence between the two dyes. The Rank Consistency Filter normalization method assumes that the central tendency of the data is unregulated, i.e. these genes are not differentially expressed between strains, and the log ratio equals zero. All non-control features that fall within this central tendency and have not been flagged as saturated or non-uniform, are used to normalize the data set. Microarray data was analyzed in the by importing the text file generated by Feature Extraction into Microsoft Excel.

2.9 Chromatin Analysis

2.9.1 Digestion of Nuclei with Micrococcal Nuclease (MNase)

Nuclei were washed 3 times in 1ml of micrococcal nuclease digestion buffer (1M sorbitol, 15mM Tris-HCl pH8, 1mM $MgCl_2$, 50mM NaCl, 0.5mM PMSF) and harvested by microcentrifugation at 11000rpm for 2 minutes. Nuclei were resuspended in 400µl digestion buffer and pre-incubated for 2 minutes at 37°C. 1-3U of micrococcal nuclease was added, and the reaction initiated by addition of 5µl

$CaCl_2$. Digestion proceeded at 37°C. A 90µl aliquot was removed to 10µl of termination solution (250mM EDTA pH8, 5% SDS, 50mM Tris-Cl pH8) at 30 seconds, 1 minute, 2 minutes and 4 minutes. Protein was degraded by 5µl of 20mg/ml proteinase K at 50°C for 45 minutes. DNA was extracted with phenol/chloroform/IAA, and residual phenol removed with chloroform/IAA. After ethanol precipitation the samples were resuspended in 90µl 1mg/ml RNaseA and incubated at 37°C for 45 minutes. DNA was extracted from the RNaseA, and precipitated as above. Pellets were resuspended in water.

When preparing YPD grown nuclei, all buffers mentioned above were supplemented with 2% glucose.

2.9.2 Indirect End Labelling

MNase digested DNA was restricted overnight with an appropriate enzyme. Prior to Southern blotting, DNA was ethanol precipitated and separated slowly on an agarose gel.

2.10 Analysis of Proteins

2.10.1 Poly-acrylamide Gel Electrophoresis

Protein extracts were separated according to size in a 15% poly-acrylamide mini-gel (788µl water, 3.75ml 30% acrylamide/0.8% bisacrylamide, 2.81ml Tris-Cl pH8.8, 75µl 10% SDS, 75µl 10% ammonium persulphate, 4µl TEMED), with a 5% poly-acrylamide stacking gel (2.75ml water, 675µl 30% acrylamide/0.8% bisacrylamide,

500µl Tris-Cl pH6.8, 40µl 10% SDS, 40µl 10% ammonium persulphate, 4µl TEMED).

Protein samples were mixed with an equal volume of 2X SDS sample buffer, and heated to 95°C for 5 minutes prior to loading into the gel. Standard size markers were similarly treated. Gels were run at 120 volts for 2 hours and 20 minutes. Gels were then either stained with coomassie blue for 20 minutes and destained in ethanol/methanol, or used in a western blot.

2.10.2 Western Blot

Freshly run protein gels were equilibrated in TB for 15 minutes. The gel was then sandwiched with nitrocellulose membrane in a Mini Trans-Blot electrophoretic transfer cell (BIO-RAD). Proteins were transferred at 100 volts for an hour. The membrane was then blocked in TBST containing 3% Marvel for 2 hours at RT. The membrane was rinsed for 6 x 10 minutes in TBST at RT. Primary antibody was diluted 1000-fold in 10ml TBST containing 3% Marvel, and the membrane was incubated overnight at 4°C with agitation. After washing as before, the membrane was incubated with a 10000-fold dilution of secondary antibody in TBST containing 3% Marvel for an hour at RT. The membrane was washed again and secondary antibody detected by treating with 5ml Lumiphos (BIO-RAD) for 3 minutes. After waiting 30 minutes for the background to die down, the membrane was exposed to film for 30 seconds to 2 minutes. Results were quantified by scanning the film in a UMAX PowerLook 1000 and importing the TIF file into AIDA software.

Chapter 3: Expression of a Human/Yeast Chimeric Histone H4 in *S. cerevisiae*

3.1 Summary

This chapter describes the construction and characterisation of a yeast mutant expressing a form of histone H4 closely related to its human counterpart. This mutant exhibits a severe growth impairment phenotype on non-fermentable carbon sources, in addition to displaying mild temperature sensitivity. We hypothesise that this results from the altered expression of nuclear genes involved in respiration. The expression levels of such a gene, *CYC1* were quantitated under fermentative and respiratory conditions, and the chromatin of this region examined. The results show subtle differences in chromatin organisation between WT and mutant strains that are consistent with mRNA expression levels.

3.2 Introduction

Saccharomyces cerevisiae is a facultative anaerobe, capable of meeting all its energy requirements with the ATP generated from fermentation (figure 3.1). Glucose (or fructose) is the preferred carbon source, and expression levels of many genes change in response to varying glucose concentration (DeRisi *et al.*, 1997). In particular, a large set of genes involved in the metabolism of alternative carbon sources, gluconeogenesis and respiration are repressed in the presence of glucose. This regulation occurs at the level of transcription, and involves both activation of negative regulators and interference with positive regulators of affected genes. The

mechanisms encompassed are collectively termed *glucose repression* (reviewed by Gancedo, 1998; Scheuller, 2003).

Central to glucose repression is the zinc finger protein Mig1, which can bind to the promoters of many glucose repressible genes (Lundin *et al.*, 1994), including the *GAL* locus and *SUC2* gene (Klein *et al.*, 1998). Mig1p exerts its repressive effect by recruitment of the transcriptional co-repressor complex TUP1/SSN6 (Treitel *et al.*, 1995; Tzamarias and Struhl, 1995), and is coordinated with glucose concentration through the Snf1 protein kinase: evidence suggests that in conditions of low glucose concentration, Mig1p is phosphorylated by Snf1p, resulting in its export from the nucleus and concomitant release of repression (De Vit *et al.*, 1997).

Upon transition from fermentable to non-fermentable carbon sources, not only is glucose repression relieved, but genes encoding elements of the respiratory and gluconeogenic pathways have their expression levels raised above basal. The changes in metabolism occurring upon the transition from fermentation to respiration are collectively called the diauxic shift. In some instances this involves co-regulation of a small group of closely related genes involved in a specific pathway, as for the *GAL* genes required for catabolism of galactose (Johnston and Davies, 1984; Johnston and Carlson, 1992). Protein products of the HAP (*h*aem *a*ctivator *p*rotein) genes on the other hand form a complex that serves to regulate a diverse range of genes involved in mitochondrial function (de Winde and Grivell, 1993). Transcriptional activation by the HAP proteins is haem dependent (Pfeifer *et al.*, 1989), and so is responsive to levels of molecular oxygen, the terminal acceptor of

mitochondrial electron transport (figure 3.2). The HAP2/3/4/5 complex only activates genes when yeast is grown on a non-fermentable carbon source. Sensitivity of the HAP2/3/4/5 complex to glucose concentration is largely due to glucose repression of the *HAP4* gene (Forsburg and Guarente, 1989; DeRisi *et al.*, 1997), which encodes the primary transcriptional activation domain (Olesen and Guarente, 1990).

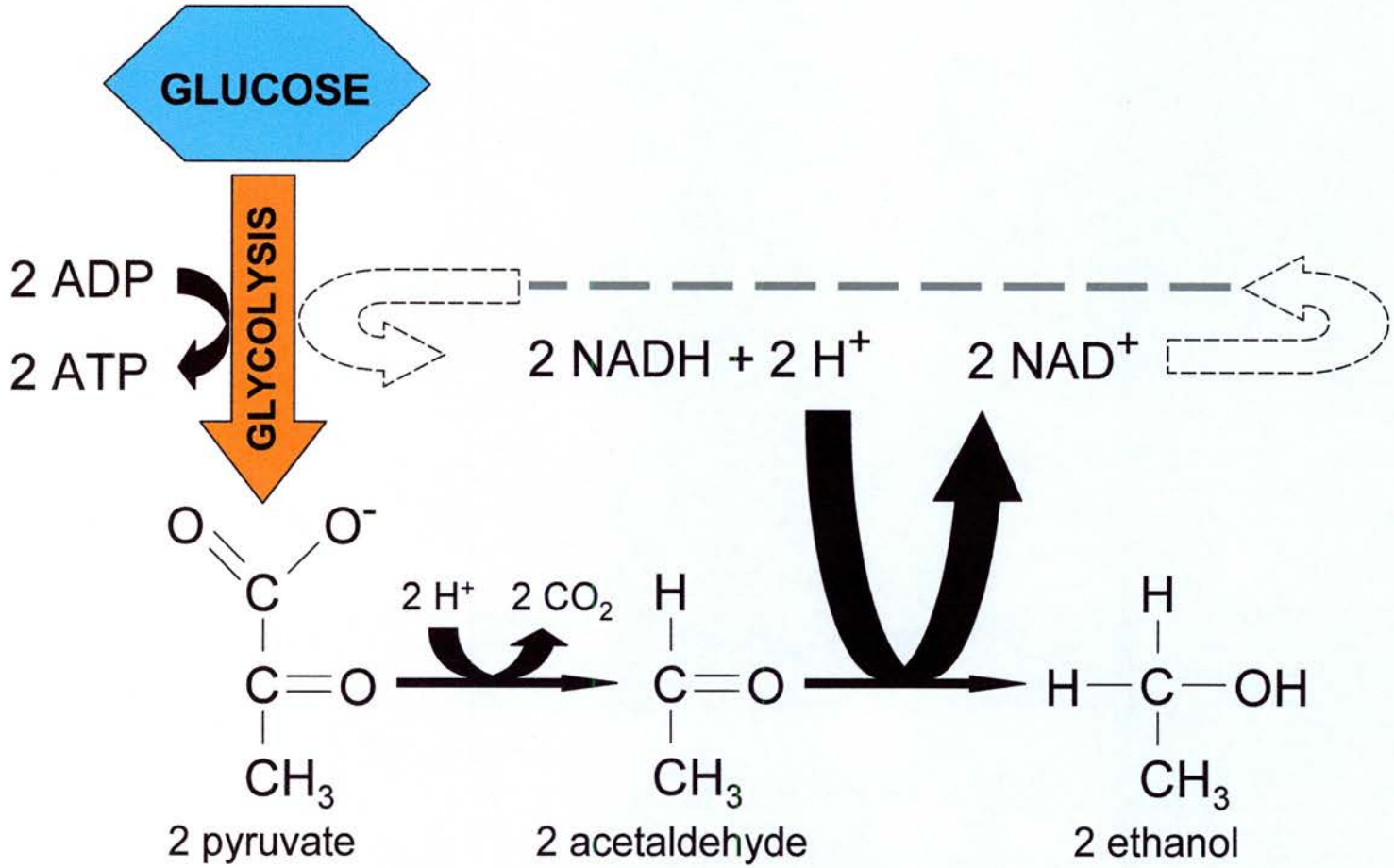

Figure 3.1 Fermentation of glucose by *S. cerevisiae* occurs in the cytosol. Two molecules of ATP are generated by substrate level phosphorylation per molecule of glucose entering the pathway. Yeast is able to meet all of its energy requirements with ATP generated in this way, but under aerobic conditions, respiratory competent strains are able to further metabolise the ethanol produced in their mitochondria.

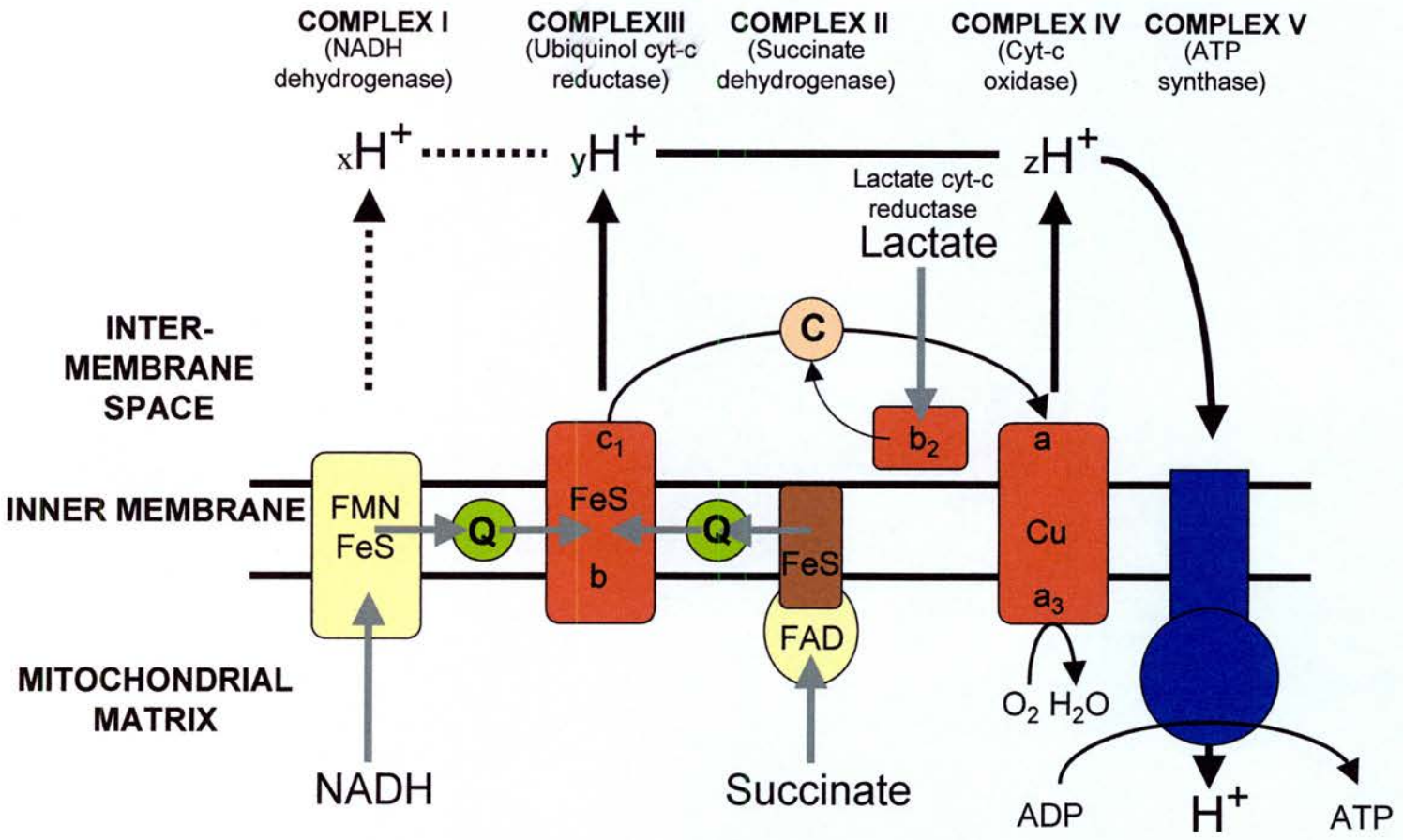

Figure 3.2 The mitochondrial electron transport chain resides within the inner mitochondrial membrane. Electrons from NADH are passed down a chain of iron or copper containing redox-active complexes, and protons are translocated across the membrane to generate a proton gradient. Electrons are terminally accepted by molecular oxygen to generate water, in a reaction facilitated by cytochrome-c oxidase (cyt-c oxidase). Potential energy stored in the proton gradient is converted to ATP by ATP-synthase: protons pass through the membrane in a channel formed by the stalk region of the complex, and the free energy liberated is used to phosphorylate ADP in a reaction catalysed by the head region of the complex.

Because yeast is a facultative anaerobe, strains harboring mutations in elements of the respiratory pathway are still able to grow well on fermentable substrates. On glucose, such mutants form smaller colonies than WT due to their inability to metabolize the ethanol produced through fermentation, once glucose is exhausted. For this reason they are said to have a '*petite*' phenotype. Some elements of mitochondrial electron transport and oxidative phosphorylation are encoded by the mitochondrial genome, and due to the relative instability of this DNA, most yeast strains grown on glucose media will 'throw *petites*' at a rate that can be as high as 1-2% (for further discussion of *petite* mutations see chapter 4).

In addition, lesions in nuclear genes can generate a petite phenotype. These are termed '*PET*' mutations, and often occur in genes encoding components of mitochondrial systems (Sherman, 1963; Tzagoloff and Dieckmann, 1990). These are distinct from '*cytoplasmic petite*' mutants (that lack mitochondrial DNA) and '*mit*' mutants (which have point mutations in the mitochondrial genome).

This chapter describes the construction and preliminary characterization of an *S. cerevisiae* mutant that expresses a partially 'humanised' histone H4 protein.

3.3 Results

3.3.1 Construction of pUK500

Haploid *S. cerevisiae* has two gene copies for each core histone. Yeast strain UKY403 has had both of its genomic copies of histone H4 genes knocked out by replacement with the marker genes *HIS3* and *LEU2* (Kim *et al.*, 1988). An episomal copy of the histone H4 copy 2 gene (*HHF2*), under control of the inducible GAL promoter on centromeric plasmid pUK421 ensures survival of this strain on galactose-containing media. UKY403 will not grow on glucose media due to shut-down of the GAL promoter by glucose repression (Johnston and Davies, 1984) (figure 3.3). Yeast strain UKY412 (WT) is isogenic to UKY403, except that instead of pUK421, it harbours centromeric plasmid pUK499, which carries a copy of *HHF2* under control of its WT promoter (Kayne *et al.*, 1989) (figure 3.4).

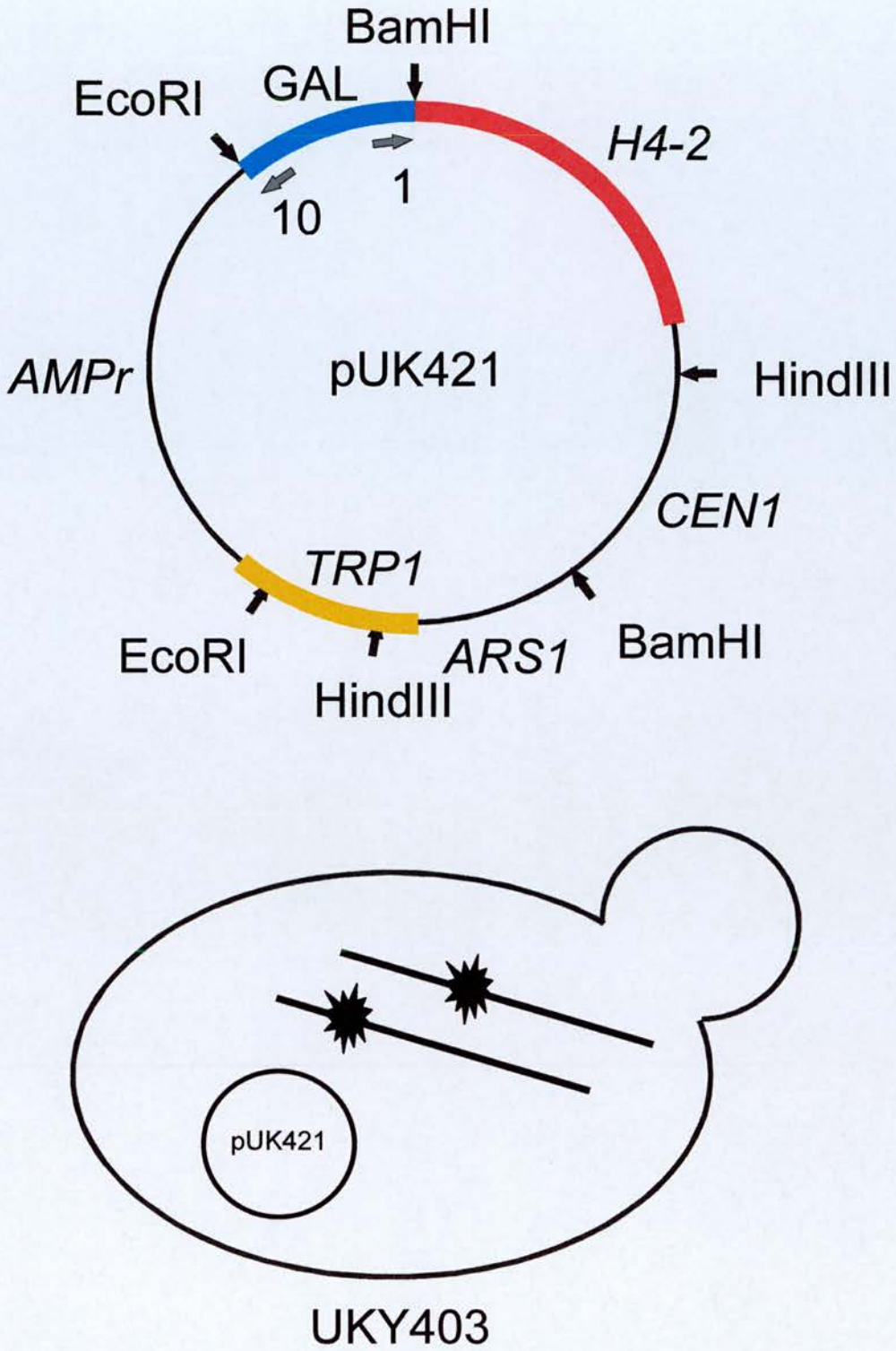

Figure 3.3 ***S. cerevisiae*** **strain UKY403** has had both its genomic copies of histone H4 genes knocked out and replaced *HIS3* and *LEU2* markers. An episomal copy of the histone H4 gene *HHF2* (*H4-2*) under control of the inducible GAL promoter on centromeric plasmid pUK421 allows survival of this strain on galactose-containing media. UKY403 will not on glucose media due to shut-down of the GAL promoter by glucose repression.

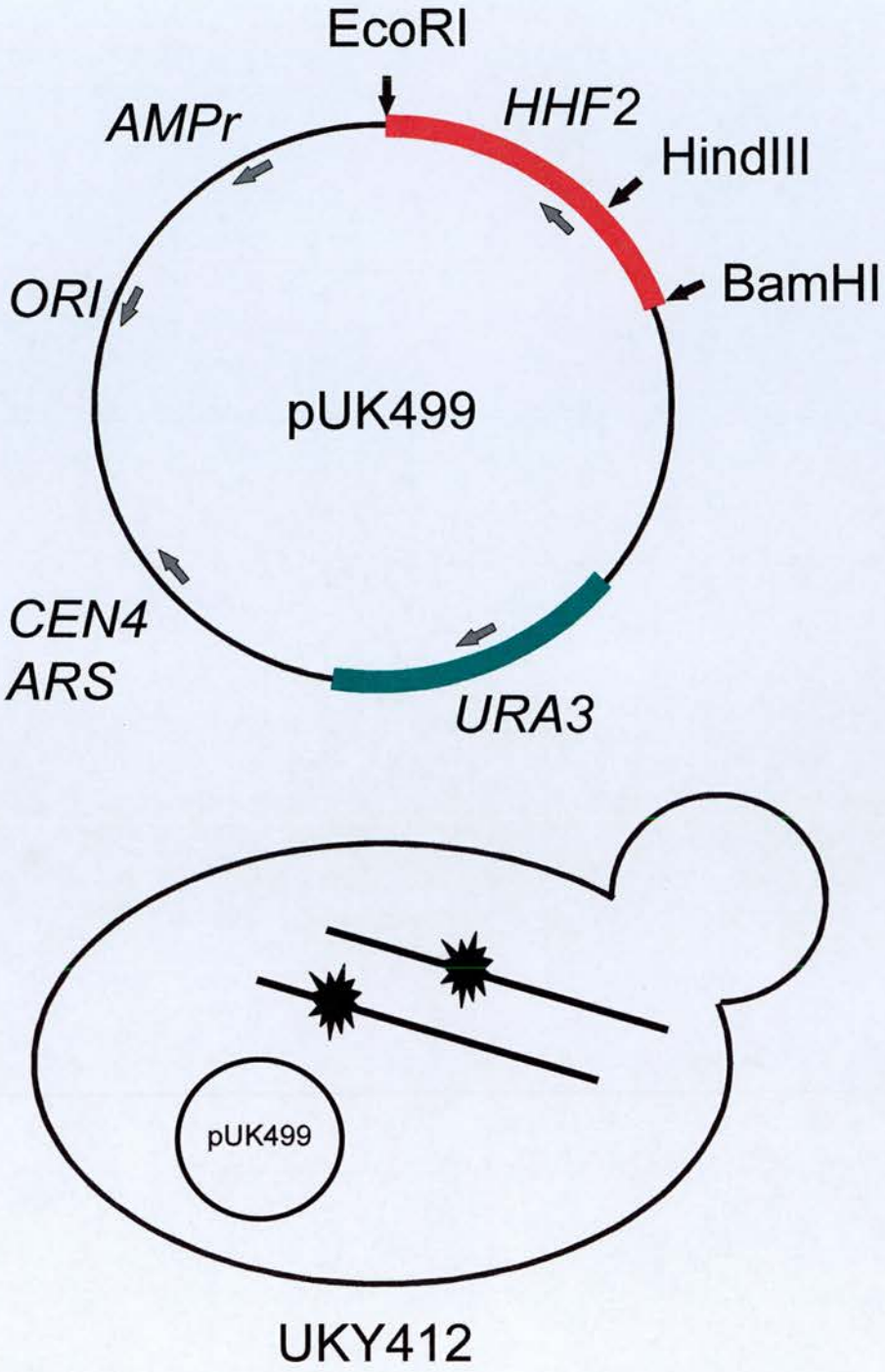

Figure 3.4 ***S. cerevisiae*** **strain UKY412** is the wild type (WT) strain employed in these experiments. The strain is isogenic to UKY403, except that instead of pUK421, it harbours centromeric plasmid pUK499, which carries a copy of histone H4 gene *HHF2* under control of its WT promoter.

As shown in the sequence alignments in figure 3.5a, there are only eight amino acid differences between the protein sequences of *S. cerevisiae* and human histone H4. Seven of these fall within the globular 'histone fold' domain (Arents and Moudrianakis, 1995): five in the α2 helix, one in the α3 helix, and one in the L2 loop just preceding α3 (White *et al.*, 2001). With respect to DNA sequence, the codons supplying the amino acid changes fall within two clusters, and could thus be easily introduced into pUK499 using the multi-step PCR procedure detailed in figure 3.5b. This strategy amplifies the two clusters of nucleotides to be mutated separately from the pUK499 *HHF2* gene, using two types of PCR primer: short (20 base pair), conventional primers that nest just outside the *HindIII* and *EcoRI* restriction enzyme sites, and longer (30-65bp) primers containing regions of homology to the *HHF2* gene, and mismatched sections encoding the mutations to be introduced. A subsequent reamplification of the longer fragment introduces a 16bp region of complementary overlap between the *HindIII* and *EcoRI* fragments. These can then be joined together in a splicing by overlap extension (SOE) reaction as detailed in materials and methods (Horton *et al.*, 1993). The mutations introduced are depicted in figure 3.6a. Substitution of this fragment into pUK499 by conventional cloning generates pUK500 (figure 3.6b). This plasmid was sequenced in forward and reverse directions, and shown to be correct.

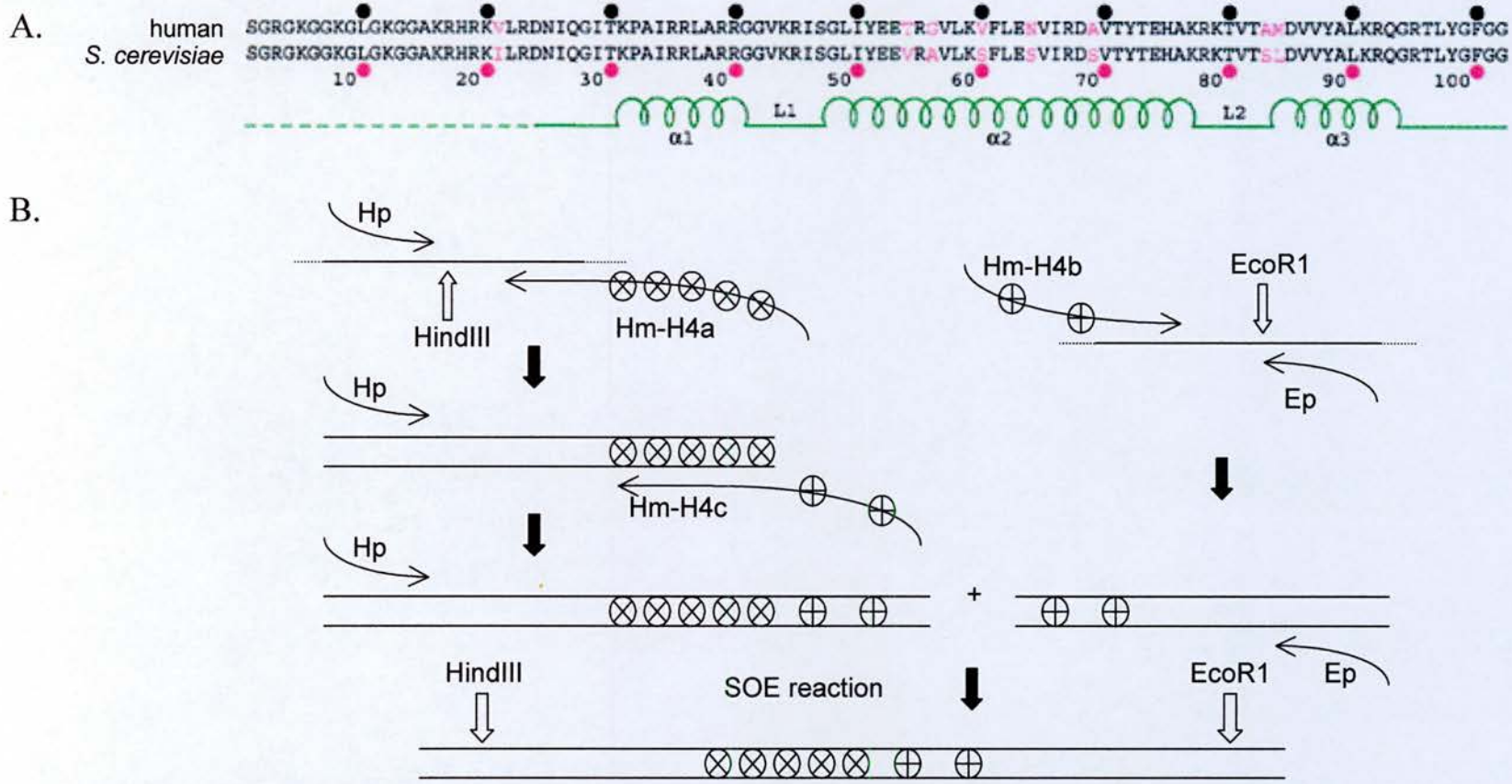

Figure 3.5 Site directed mutagenesis of the *HHF2* gene in plasmid pUK499. A) 7 of the 8 amino acid differences between yeast and human histone H4 proteins are within the globular histone fold domain (solid green line). The other is in the more flexible N-terminal region (dashed green line) (White *et al*., 2003). B) Mutations were introduced into pUK499 using a multi-step PCR procedure. The two clusters of nucleotides to be mutated were amplified separately using two types of PCR primer: short primers that nest just outside the *HindIII* (Hp) and *EcoRI* (Ep) restriction enzyme sites, and longer primers containing homology to the *HHF2* gene, and extra sections encoding the mutations to be introduced (Hm-H4a, Hm-H4b, Hm-H4c). Reamplification of the longer fragment introduces a 16bp region of complementary overlap between the *HindIII* and *EcoRI* fragments. These are joined in a splicing by overlap extension (SOE) reaction.

A.

Position	21	54	56	60	64	69	83	84
Yeast	I	V	A	S	S	S	S	L
human	V	T	G	V	N	A	A	M

B.

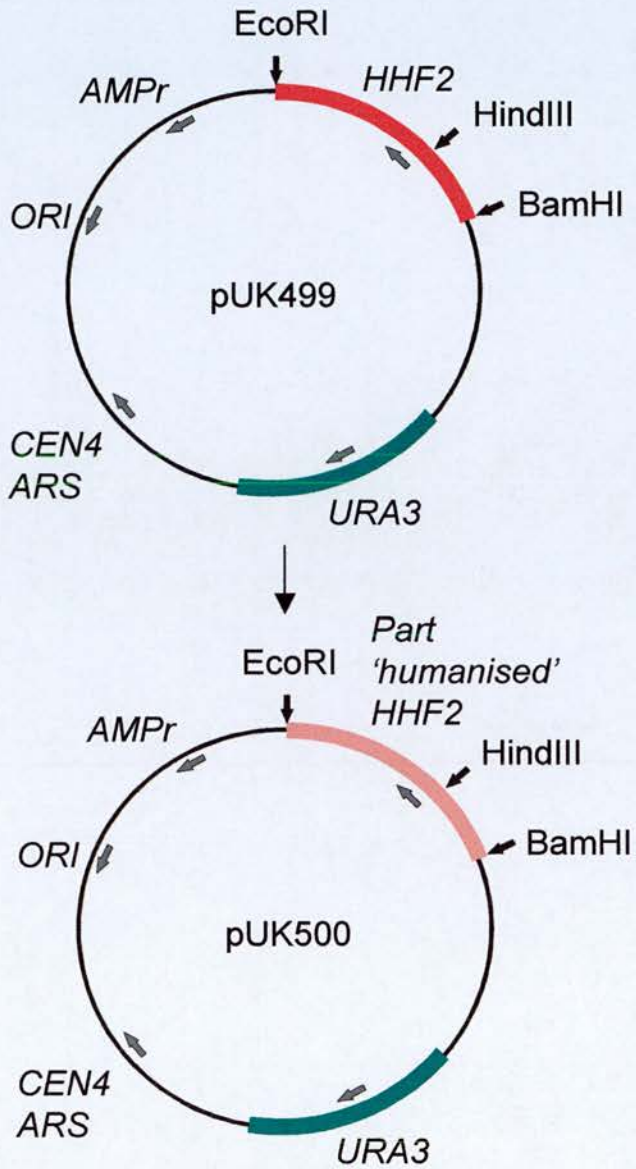

Figure 3.6 Position of mutations introduced into histone H4. A) Position of amino acid substitutions between pUK499 and pUK500 in the primary sequence of histone H4 protein. B) The part 'humanised' *HHF2* gene was cloned back into the parental pUK499 plasmid between the *HindIII* and *EcoRI* restriction enzyme sites.

3.3.2 Generation of UKY500

A simple test to determine whether the mutant histone H4 encoded by pUK500 can maintain yeast survival is provided by the glucose shift viability test (Kayne *et al.*, 1988) (fig 3.7a). Transformation of pUK500 into UKY403, and selection on GAL-trp-ura plates generates a strain bearing a GAL promoter-regulated WT copy of *HHF2*, and a mutant *HHF2* with a WT promoter.

Eight of the resultant transformants were re-streaked onto GAL-trp-ura plates, and also onto GLC-trp-ura plates to shut down WT H4 expression from pUK421. As shown in figure 3.7b, all transformants grew on glucose media, demonstrating that the partially humanised histone H4 encoded by pUK500 can be incorporated into nucleosomes and maintain yeast survival.

This strain was then cured of pUK421, and named UKY500.

A.

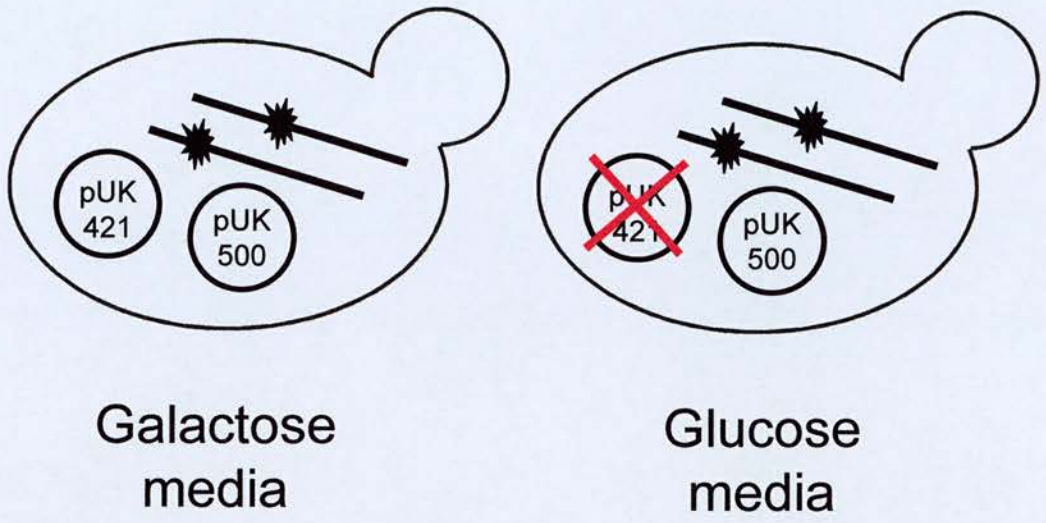

B.

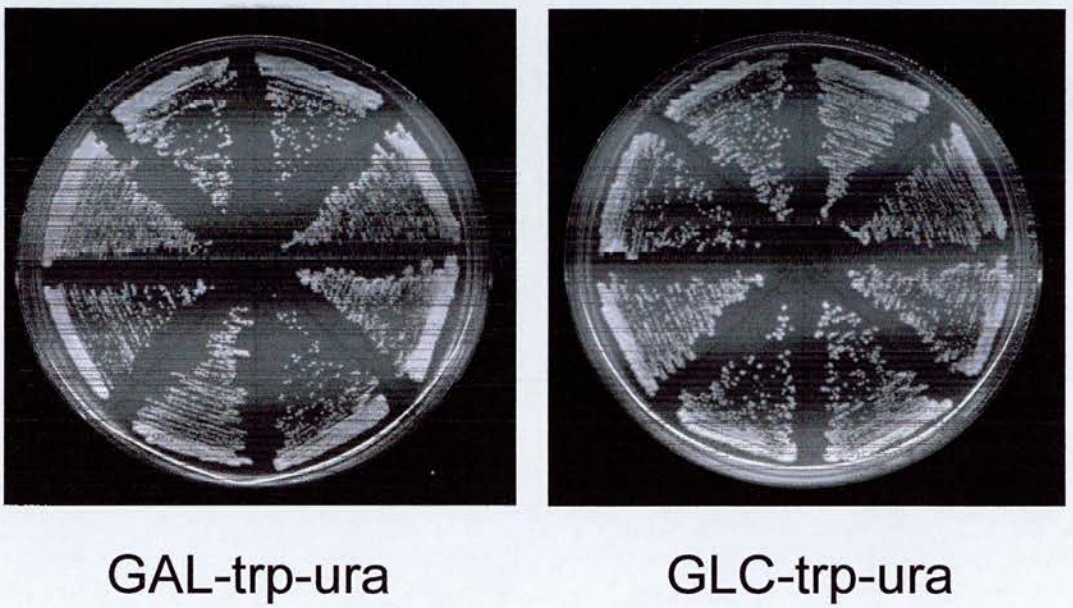

Figure 3.7 The glucose shift viability test. A) Expression of the WT *HHF2* gene is shut down by glucose repression when yeast are transferred from galactose media to glucose media, and cells surviving the transition express only the mutant histone H4 encoded by pUK500. B) Transformants containing pUK421 and pUK500 were selected for on galactose media lacking trptophan and uracil (GAL-trp-ura). All transformants survive the transition to glucose media (GLC-trp-ura), indicating that the mutant histone H4 encoded by pUK500 can maintain yeast viability.

3.3.3 UKY500 is Temperature and Carbon Source Sensitive

UKY500 grows at a similar rate to UKY412 (WT) on rich glucose media (YPD) at 30°C, but at a slightly reduced rate on YPD at 37°C (figure 3.8). Temperature sensitivity is often seen in yeast mutants, and presumably results from the greater instability of the protein and/or protein-protein interactions at the higher temperature.

In an effort to find additional phenotypic differences between UKY412 (WT) and UKY500, yeast were grown in media containing one each of the chemicals listed in table 3.1 (Ross-Macdonald *et al.*, 1999). Resistance or hypersensitivity to these substances can be indicative of altered gene expression in certain areas of cellular metabolism and homeostasis. The results shown in figure 3.9 reveal no difference between growth of UKY412 (WT) and UKY500 on glucose media containing 2mM 2EGTA or 0.9M NaCl (which indicate cation or salt sensitivity respectively), but they do show poor growth of UKY500 on media containing glycerol as the carbon source. This could indicate altered expression of genes involved in cellular respiration. Qualitative data were obtained for the other growth conditions listed in table 3.1, but little difference was observed between WT and mutant (data not shown).

To investigate whether this phenotype is specific for glycerol, for example if expression of glycerol transporter genes is affected, growth of UKY500 was compared to UKY412 (WT) on a variety of carbon sources, as shown in figure 3.10 and summarised in table 3.2. On the non-fermentable carbon sources lactate, ethanol

and glycerol, growth of UKY500 is negligible, but is better on the di- and tri-saccharides galactose and raffinose (these are fermentable, but net ATP yield per molecule entering the glycolytic pathway is half that for glucose).

These data indicate that incorporation of the mutant histone H4 expressed in UKY500 has indeed led to an alteration of expression in the genes involved in cellular respiration. They also define UKY500 as a *PET* mutant: it contains nuclear mutations that lead to impaired growth on non-fermentable carbon sources.

A.

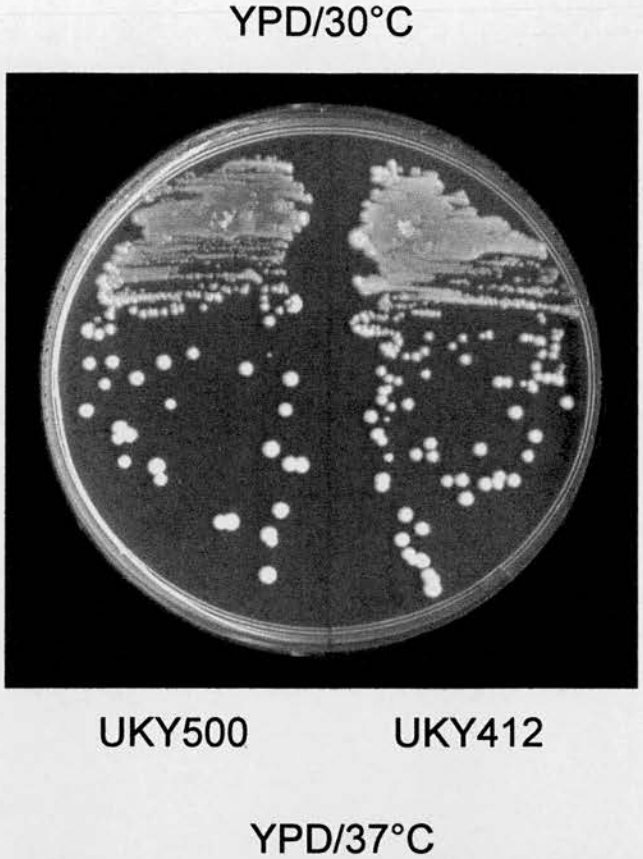

B.

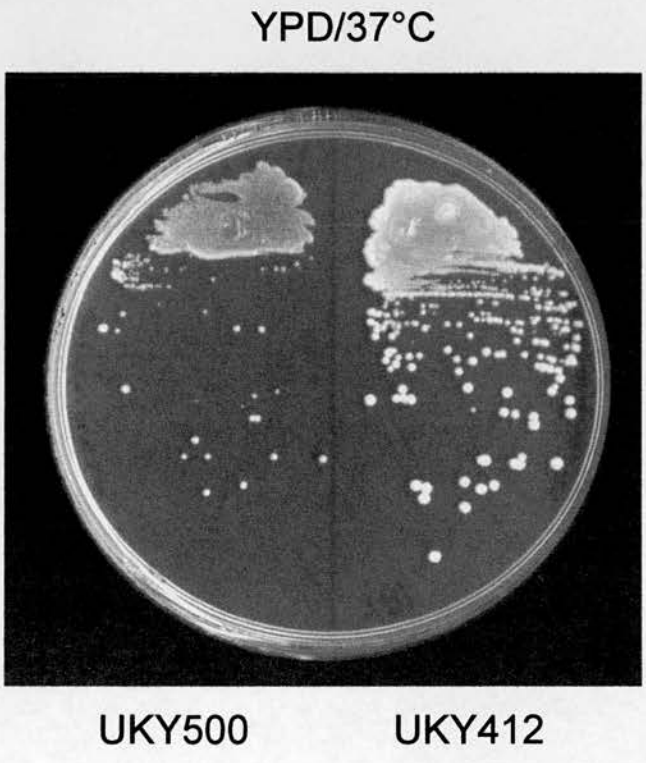

Figure 3.8 Temperature sensitivity. A) UKY412 (WT) and UKY500 grow at similar rates on rich glucose media (YPD) at the optimum temperature of 30 °C. B) UKY500 displays slow growth on YPD at 37°C.

Growth Conditions:	Identify genes potentially functioning in:
YPD + 10μg/ml benomyl	microtubule dynamics
YPD + 20μg/ml benomyl	
YPD + 0.008% MMS	DNA metabolism
YPD + 75mM hydroxyurea	DNA metabolism
YPD + 12 μg/ml calcoflour	cell wall maintenance/biogenesis
YPD + 67 μg/ml calcoflour	
YPD + 46 μg/ml hygromycin	cell wall maintenance/biogenesis
YPD + 0.003% SDS	cell wall maintenance/biogenesis
YPD + 2mM EGTA	cation sensitive mutants
YPD + 0.08 μg/ml cycloheximide	protein synthesis
YPD + 0.3 μg/ml cycloheximide	
YPD + 0.9M NaCl	salt sensitive mutants
YPGlycerol (2%)	cellular respiration

Table 3.1 Disruption phenotype data. Hypersensitivity or resistance to the presence of certain chemicals in the growth medium can be indicative of altered expression of genes involved in particular areas of metabolism (Ross-MacDonald *et al.*, 1999)

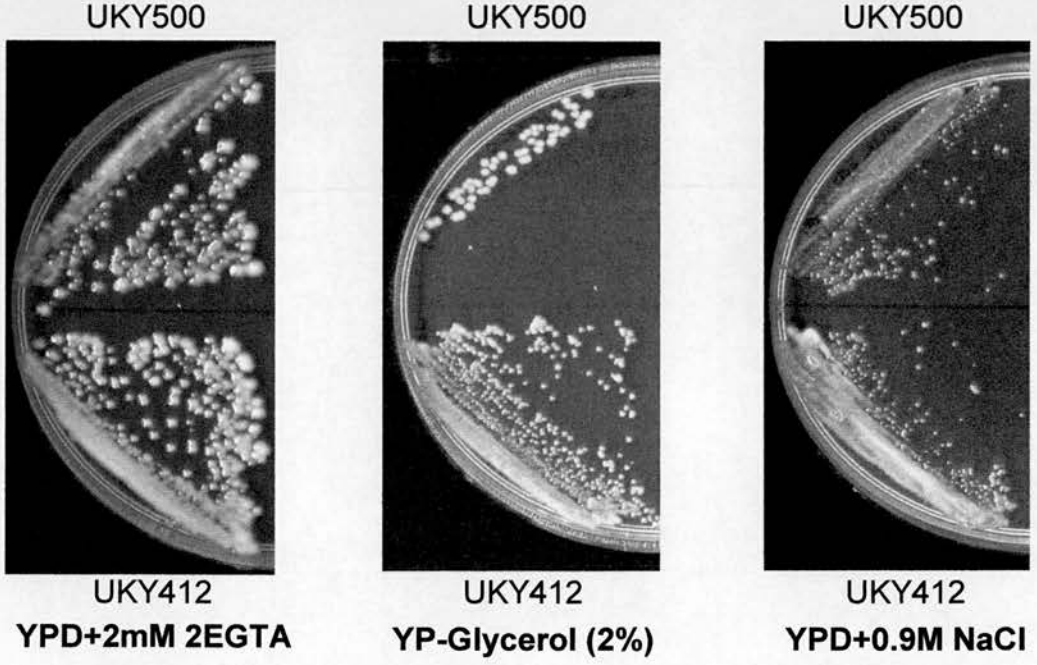

Figure 3.9 Altered expression of genes involved in cellular respiration is implied by the poor growth of UKY500 on media containing glycerol as the sole carbon source. No difference in growth was observed on media containing EGTA or NaCl.

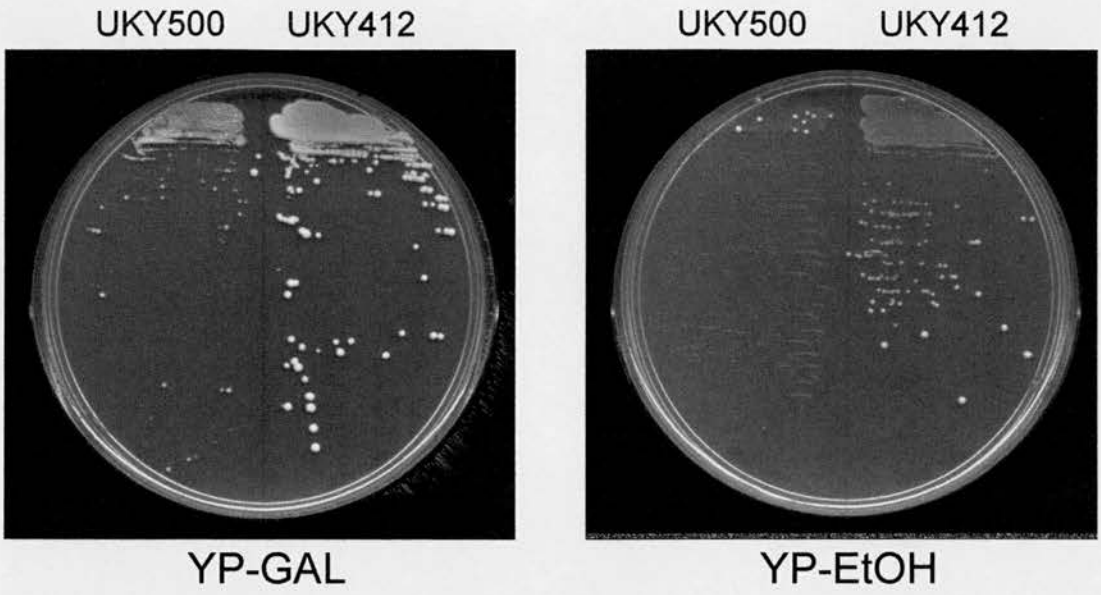

Figure 3.10 Carbon source sensitivity is not restricted to glycerol. UKY500 grows at reduced rates on media containing galactose (YP-GAL) or ethanol (EtOH) as the sole carbon source.

Carbon Source	UKY412	UKY500
YPD	++++	++++
YP-Gal	+++	++
YP-Raffinose	+++	++
YP-Glycerol	++	+/-
YP-Ethanol	++	+/-
YP-Lactate	++	+/-

Table 3.2 Carbon source sensitivity is displayed by UKY500 on all secondary carbon sources tested.

3.4 Investigation of a HAP-Regulated Gene

One hypothesis to explain the inability of UKY500 to use non-fermentable carbon sources would be that the altered nucleosomal context has interfered with transcription of genes that are normally up-regulated under such conditions. In many cases this up-regulation is mediated by the HAP2/3/4/5 complex, and mutations in *HAP3* have been shown to cause a *petite* phenotype (Tzagoloff and Dieckmann, 1990).

The importance of chromatin remodelling in the activation of respiratory genes by HAP proteins is highlighted by two lines of research. Firstly, activation by the HAP2/3/4/5 complex is mediated through interaction of the Hap4p activation domain with the Tra1p subunit of the SAGA and NuA4 histone acetyltransferase complexes (Brown *et al.*, 2001). Secondly, Hap4p contacts Swi1, Snf1 and Snf5 of the SWI/SNF complex (Neely *et al.*, 2002). These interactions have been shown to be necessary for transcriptional activation by the HAP2/3/4/5 complex, as has the histone acetyltransferase activity of Gcn5p that is present in the SAGA complex (Georgakopoulos and Thireos, 1992).

It is possible that the mutant histone H4 expressed by UKY500 has altered the nucleosome in such way as to impair the function of the HAP2/3/4/5 complex. The mutations may have directly affected binding of the complex to it DNA target site, or influenced its down-stream interaction with chromatin remodelling activities.

To investigate these possibilities the expression level and chromatin structure of a HAP-regulated gene, *CYC1* were examined.

3.4.1 CYC1

CYC1 encodes iso-1-cytochrome c of the mitochondrial electron transport chain. Transcription of *CYC1* is sensitive to chromatin structure, as is evident from the fact that histone H4 depletion, resulting in loss of approximately half of the nucleosomes, leads to gene activation (Han and Grunstein, 1988).

Expression of *CYC1* in response to oxygen is mediated via Hap1p binding to its up-stream activation sequence (UAS1) in the *CYC1* promoter, and leads to a 200-fold increase in expression (Guarente and Mason, 1983). Under hypoxic conditions, Hap1p preferentially activates transcription from the minor cytochrome c gene, *CYC7*. During logarithmic aerobic growth, however, 95% of cytochrome c is isoform 1 (Dumont *et al.*, 1991). Transcription from *CYC1* is increased a further 5-10-fold in the presence of a non-fermentable carbon source (Zitomer *et al.*, 1979). This is mediated by the HAP2/3/4/5 complex binding to UAS2 of the *CYC1* promoter (Forsburg and Guarente, 1989; McNabb *et al.*, 1995).

3.4.2 CYC1 Expression Levels

RNA prepared from WT and mutant cells grown under both repressive (YPD) and de-repressive (EtLac) conditions, was subjected to Northern blotting, and simultaneously hybridised to *CYC1* and *ACT1* cDNA probes (figure 3.11). Signals were normalised to 28s rRNA as summarised in table 3.3, and the gene expression levels from UKY412 (WT) were arbitrarily set to 100%. Although there is a formal possibility that mRNA stability is affected, the data indicate that whilst UKY412 (WT) up-regulates *CYC1* transcription more than 7-fold upon the transition from glucose to EtLac media, UKY500 shows only a very modest increase of about 1.5-fold. That this is specific, and not due to a general effect on RNAPII transcribed genes is indicated by the transcript levels from the *ACT1* gene, which are similar between wild type and mutants under both conditions.

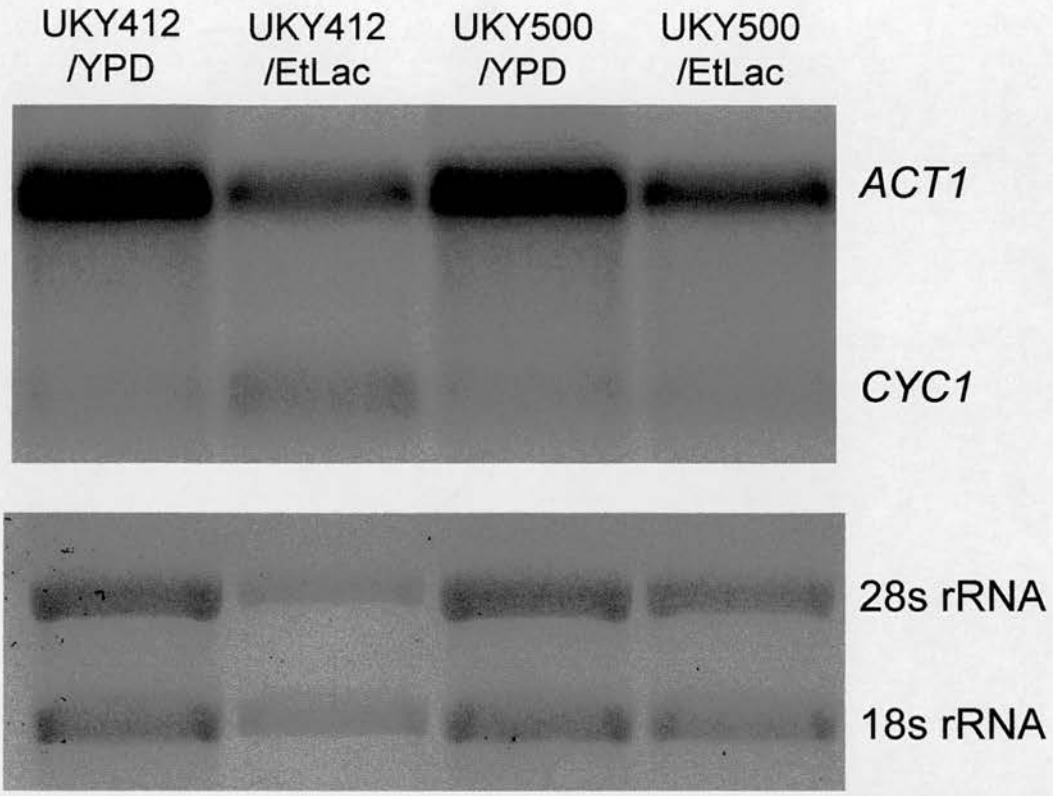

Figure 3.11 Northern blot analysis of *CYC1* and *ACT1*. Transcript levels of *CYC1* and *ACT1* in strains grown under repressive (YPD) and de-repressive (EtLac) conditions were visualised by co-hybridising to radiolabelled cDNA probes specific for these genes. Ribosomal RNAs (rRNA) were visualised by ethidium bromide staining.

	Expresssion levels on YPD		Expression levels on EtLac		YPD to EtLac fold up-regulation	
Strain	***ACT1***	***CYC1***	***ACT1***	***CYC1***	***ACT1***	***CYC1***
UKY412	100%	100%	100%	100%	0.56	7.3
UKY500	101%	138%	76%	28%	0.42	1.46

Table 3.3 *CYC1* and *ACT1* mRNA expression levels were normalised to 28s rRNA. The gene expression levels from UKY412 (WT) were arbitrarily set to 100%. The fold up-regulation of the genes upon the transition from YPD to respiratory (EtLac) media is indicated. This demonstrates that UKY500 does not up-regulate the *CYC1* gene to as great an extent as UKY412 (WT) on transfer form fermentable YPD media, to respiratory EtLac media. This is not a general effect on RNAPII gene expression, as the change in levels of *ACT1* transcripts is similar between strains.

3.4.3 Nucleosome Positioning at the CYC1 Gene

Changes in expression of genes regulated at the chromatin level often correlate with alterations of nucleosome positions at the promoter region. Indirect end labelling methodology provides a way of mapping nucleosome positions relative to a restriction site, and observing any changes that occur upon gene activation (Wu, 1980). Nuclei are subjected to partial digestion by micrococcal nuclease (MNase), an enzyme that cuts the linker DNA between adjacent nucleosomes with little sequence specificity. This generates a population of polynucleosomal particles of varying lengths. The DNA fragments associated with these particles are then deproteinised and purified, and digested with a restriction enzyme that cuts about 1kb away from the region of interest. Digestion products are separated by agarose gel electrophoresis, and Southern blotted onto nitrocellulose membrane. The blot is then hybridised with a radiolabelled oligonucleotide probe complementary to sequences from just inside the restriction enzyme cut site. The distance between this reference point and the cuts made by MNase allows determination of nucleosome positions.

The results of indirect end labelling experiments on the *CYC1* gene are presented in figures 3.12 to 3.14. Two different restriction enzyme digests were used to look at the promoter region. Looking downstream toward the coding region as well as in the upstream direction, gives a clear picture of nucleosome positions. DNA from MNase digested nuclei prepared from yeast grown as for the RNA prep, was restricted with *XbaI*, as depicted in figure 3.12a, or *HindIII* as in figure 3.13a. The purified fragments were separated in a 1.25% agarose gel and Southern blotted onto

nitrocellulose. Probing the membrane with a specific radiolabelled cDNA generates a clear pattern of cutting and protection when this membrane is exposed to a phosphorescent screen (figure 3.12b and 3.13b). Figure 3.14 shows intensity traces of these data. Examination of these and the raw data in figures 3.12b and 3.13b highlights several features.

As has been reported previously for this gene (Martens *et al.*, 2001), the coding region is organised into a closely spaced nucleosomal array. Analysing figure 3.12b, it appears that when grown in glucose, the coding region of *CYC1* contains three regions of protection from digestion by MNase, each of about 160bp, which are susceptible in naked DNA. This is consistent with three closely spaced, positioned nucleosomes. Upon transfer to EtLac media, the cleavage sites between these nucleosomes become less distinct; reflecting more randomised positioning of nucleosomes, accompanying an increase in transcription. The effect is particularly pronounced in UKY500 where the region of protection effectively merges into one. It is difficult to speculate on the significance of this, but it may be that there is some degree of instability in the positioning of the nucleosomes on the apparently miss-regulated gene.

UAS2 of the *CYC1* promoter comprises two binding sits for the HAP2/3/4/5 complex; one between -273 and -286, the other from -280 to -299. UAS1 further upstream is bound by Hap1p in aerobic conditions. On examination of figures 3.12b, 3.13b and 3.14, it can be seen that UAS2 and UAS1 both lie within a protected region from -240 to -400, the size of which corresponds to a positioned nucleosome.

Protection here was also seen by Martens et al, but in contrast to my results, they saw no cleavage of naked DNA in this region either (3.13a). In light of my results I have allocated a nucleosome position here, and four more further upstream.

The *CYC1* gene promoter contains two functional TATA elements. These are termed TATA2α and TATA1β, and are located at -115,-123 and -169,-177 respectively (Li and Sherman, 1991). From the *XbaI* restricted indirect end labelling experiment (3.12b and 3.14) it appears that there is protection from MNase digestion in this area between –70 and –190. Although approximating to the size of a nucleosome, the protection observed here is not due to a nucleosome, as can be clearly seen by examination of the corresponding region in the *HindIII* digested blot (figure 3.13b). Better resolution in this region of the gel shows five clear cut sites within about 250 base pairs; the distance between these cut sites is far to small to accommodate a nucleosome.

It is in the region between 0 and -240 that there are subtle differences between the digestion patterns of UKY412 (WT) and UKY500. Both the *XbaI* and *HindIII* digests reveal a highly sensitive site centred 50bp upstream of the *CYC1* gene start codon (defined +1) that is accessible to MNase digestion under all conditions. This encompasses the RNA start sites (Li and Sherman, 1991) and hypersensitivity here is consistent with transcription of the gene. On transfer from YPD to EtLac, the peak of digestion shifts slightly upstream in the WT pattern, an effect not seen in the mutant. It is also apparent that the chromatin of UKY500 nuclei grown in EtLac is the most susceptible to digestion in this region.

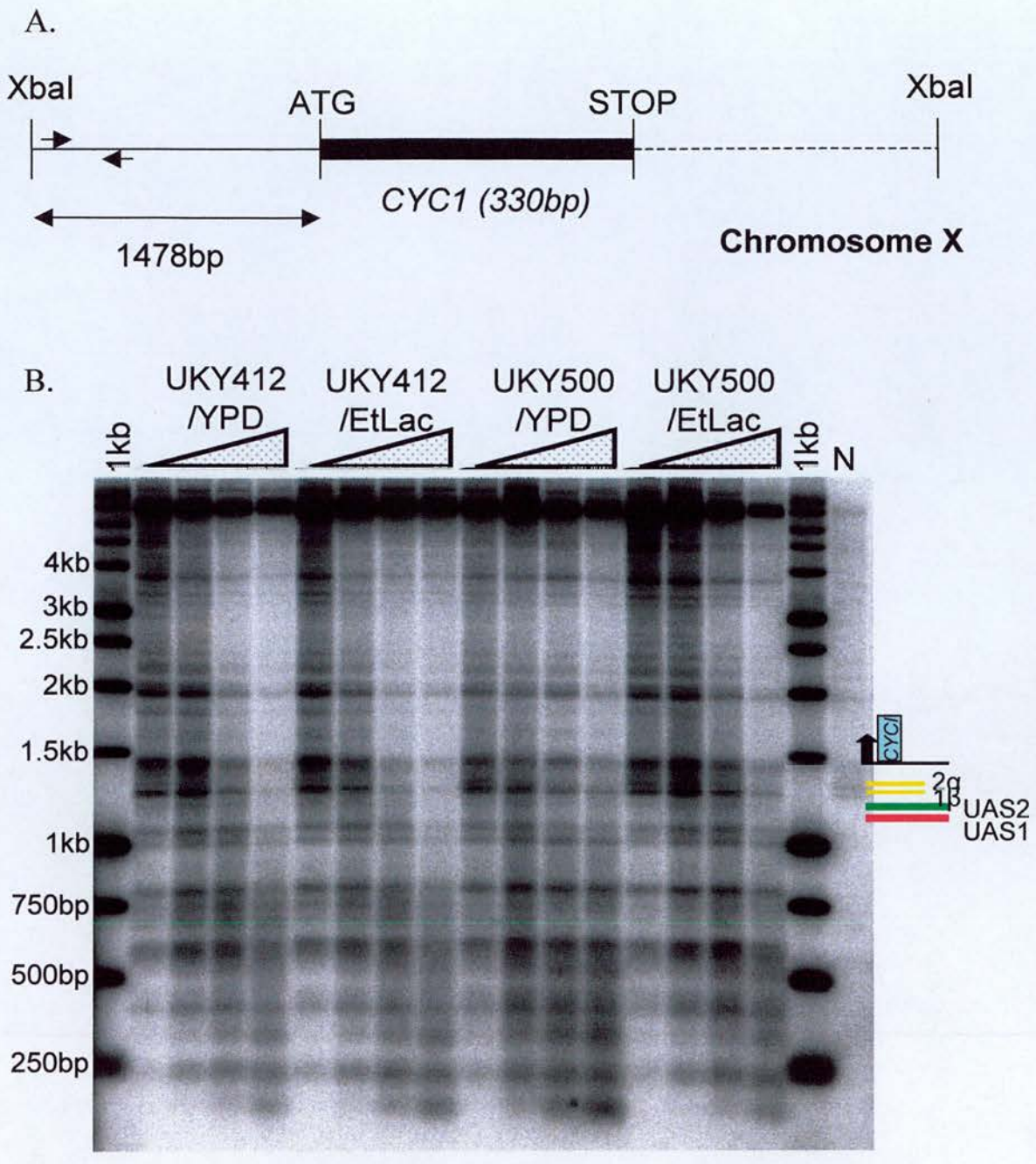

Figure 3.12 Nuclease mapping at the *CYC1* gene A) Schematic representation of the position of the *XbaI* restriction enzyme sites relative to the *CYCI* coding sequence, and the position of the probe PCR amplified using primers IDEl1 and IDEL2. B) Nuclei prepared from strains grown under repressive (YPD) and de-repressive (EtLac) conditions were subjected to a time-course of partial digestion by micrococcal nuclease. Purified DNA was subsequently digested to completion by *XbaI.* The fragments were separated by agarose gel electrophoresis and transferred to nitrocellulose. Naked DNA control (N) was treated similarly, and a radiolabelled 1kb size marker was included on the gel. The blot was probed with a 249bp radiolabelled cDNA probe complementary to sequences just inside the upstream *XbaI* restriction enzyme site. Exposure of the blot to a phosphorescent screen generated the image shown. The positions of the *CYC1* coding sequence, as well as upstream activation sequences 1 and 2 (UAS1 and UAS2) and TATA boxes 1β and 2α (1β and 2α) are indicated.

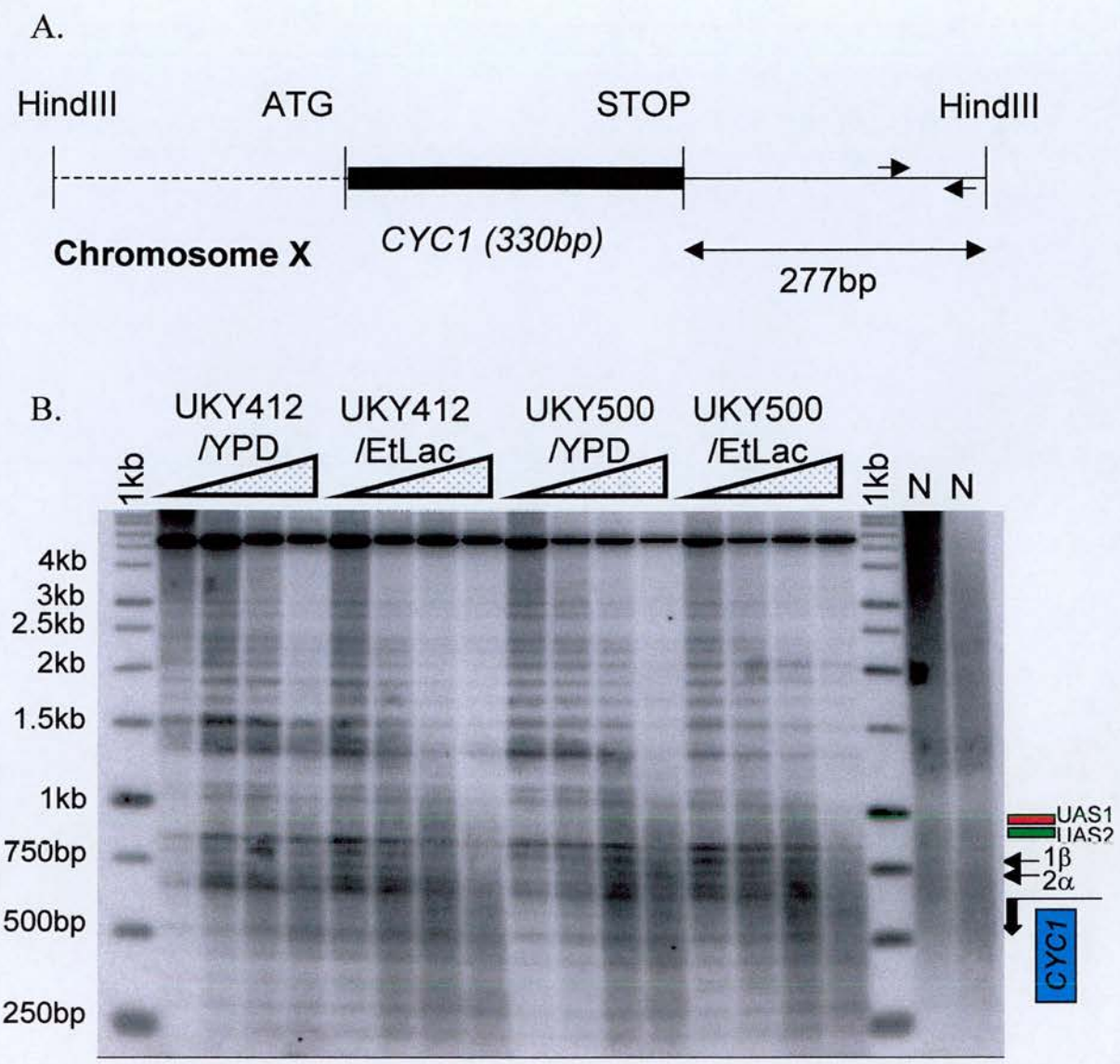

Figure 3.13 Nuclease mapping at the *CYC1* gene A) Schematic representation of the position of the *HindIII* restriction enzyme sites relative to the *CYC1* coding sequence, and the position of the probe PCR amplified using primers CYC1Ha and CYC1Hb. B) Nuclei prepared from strains grown under repressive (YPD) and de-repressive (EtLac) conditions were subjected to a time-course of partial digestion by micrococcal nuclease. Purified DNA was subsequently digested to completion by *HindIII.* The fragments were separated by agarose gel electrophoresis and transferred to nitrocellulose. Naked DNA controls (N) were treated similarly and a radiolabelled 1kb size marker was included on the gel. The blot was probed with a 226bp radiolabelled cDNA probe complementary to sequences just inside the downstream *HindIII* restriction enzyme site. Exposure of the blot to a phosphorescent screen generated the image shown. The positions of the *CYC1* coding sequence, as well as upstream activation sequences 1 and 2 (UAS1 and UAS2) and TATA boxes 1β and 2α (1β and 2α) are indicated.

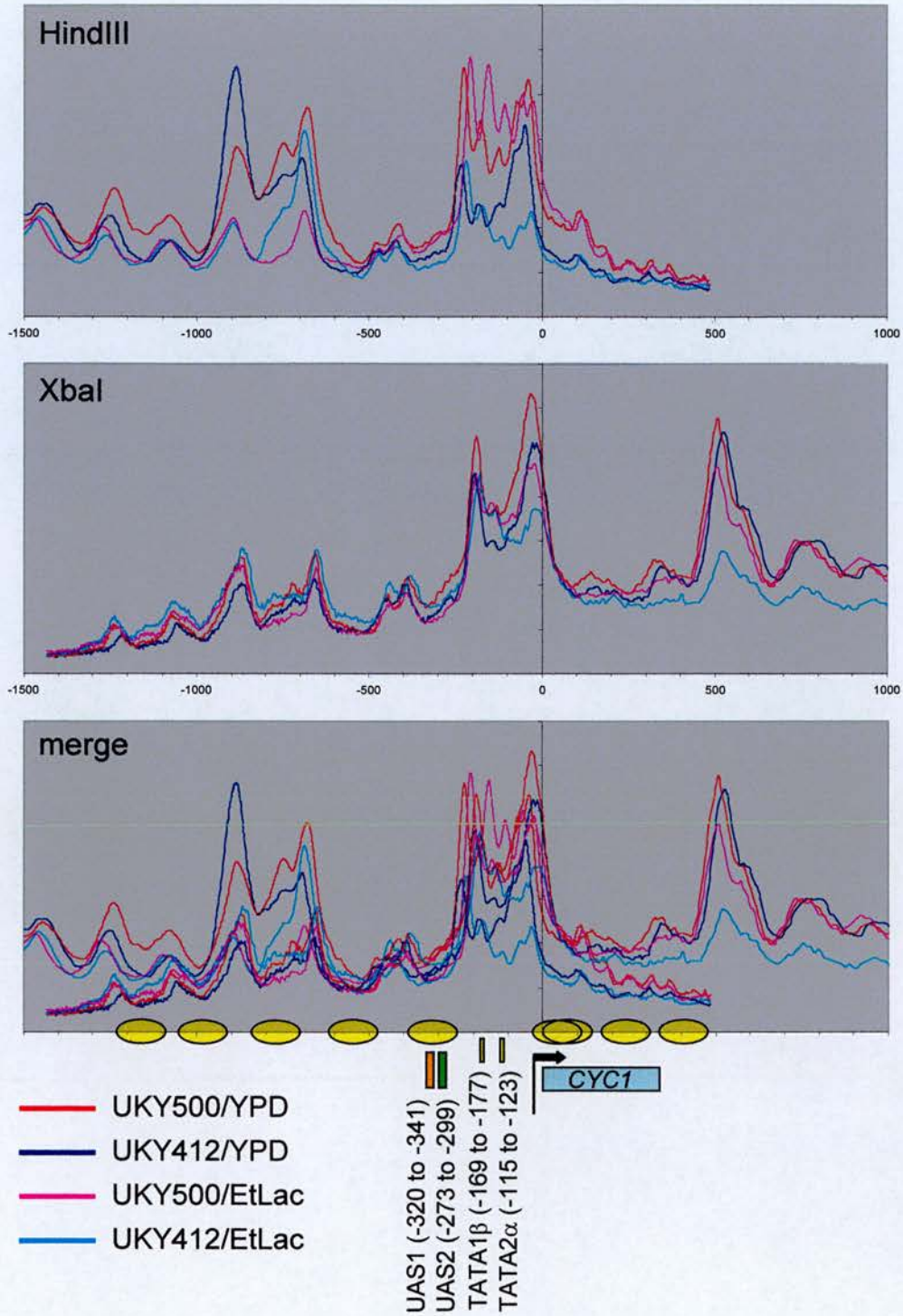

Figure 3.14 Nuclease positions at the *CYC1* gene. Intensity traces generated by quantitation of the *XbaI* and *HindIII* indirect end labelling experiments shown separately and merged. Base pairs are plotted on the x-axis and intensity is plotted on the y-axis. Assigned nucleosome positions are indicated by gold ovals. The positions of the *CYC1* coding sequence, as well as upstream activation sequences 1 and 2 (UAS1 and UAS2) and TATA boxes 1β and 2α (1β and 2α) are indicated. The bold arrow upstream of the *CYC1* coding sequence represents the approximate region of transcriptional start.

3.5 Discussion

The results presented in this chapter demonstrate that the high level of histone H4 sequence conservation throughout evolution means that an *S. cerevisiae* strain solely expressing a partially humanised form of this essential protein is not only viable but grows almost as well as WT under optimal conditions.

The differences between yeast and *Xenopus* histones are highlighted in figure 3.15 (White *et al.*, 2001). In the case of histone H4, these differences are the same as those between yeast and human (human and *Xenopus* histone H4 proteins being identical). The residues I have altered to create UKY500 lie mainly within the globular domain of the assembled hetero-octamer. Importantly, none of the amino acids substituted are directly involved in DNA binding (White *et al.*, 2001).

From the near WT growth rate of UKY500 under optimal conditions, I would predict that the interactions between mutant histone H4 and WT histones H3, H2A and H2B are not greatly different from those in the WT nucleosome core, and have not caused large distortions of nucleosome structure. Tetramer/dimer interaction is partly mediated via 4-helix bundle formed by the α3 helices, and C-terminal portion of the α2 helices of histones H4 and H2A. Histone dimerisation involves hydrophobic interactions between amino acids along the entire molecules (Luger *et al.*, 1997). Examination of the position of the mutations within the crystal structure (figure 3.15) suggests that histone H4/H3 dimerisation might be most affected in UKY500. It may

be significant that the mutations at positions 60, 69 and 83 represent substitution of a serine residue for a less hydrophilic amino acid.

At higher temperature, the changes in histone-histone interactions that must exist in the mutant will be more manifest due to increased molecular motion, and this may partly account for the temperature sensitivity of UKY500. Even so, this effect is only slight, and yeast is well able to tolerate the mutant histone H4 under such stress.

Although tolerable the mutations are not innocuous, as is evident when UKY500 is grown on non-fermentable carbon sources. Under these conditions growth of UKY500 is severely impaired. This classifies UKY500 has a '*PET*' mutant, defined as a strain bearing a mutation(s) in a nuclear gene that leads to a growth impairment on non-fermentable carbon sources.

In the absence of a fermentable substrate, yeast must meet all of its cellular energy requirements with ATP generated from mitochondrial oxidative phosphorylation. Under such conditions, glucose repression is lifted and the transcription of genes involved in cellular respiration is up-regulated. In many cases this occurs via the HAP2/3/4/5 transcriptional activator complex. Activation by the HAP2/3/4/5 complex requires relief of chromatin-mediated repression, as is implied by the recruitment of histone acetyltransferase activities and SWI/SNF (Georgakopoulos and Thireos, 1992; Neely *et al.*, 2002).

The distortion of DNA that occurs when it is wrapped around a nucleosome is maintained by tight interactions between the structured regions of the histones and the minor groove of DNA. There are 14 such contact sites per nucleosome, which are found in the L1L2 loops and α1α1 DNA-binding motifs (Luger and Richmond, 1998). The S83A mutation is on the border between the histone H4 L2 loop and the α3 helix, the neighbouring L84M mutation is at the beginning of the α3 helix. It is thus possible that these mutations have slightly altered the path of the DNA on the nucleosome, which could have affected interactions with regulatory proteins.

The *CYC1* gene was chosen to test the hypothesis that gene activation by the HAP2/3/4/5 complex is impaired in UKY500. In keeping with previous studies (Zitomer *et al.*, 1979), I have found that under aerobic conditions WT cells up-regulate *CYC1* transcription approximately 7-fold in non-fermentable media (EtLac) as compared to glucose media (YPD). In contrast, UKY500 increases *CYC1* transcript levels only 1.5-fold when transferred to EtLac media (figure 3.11 and table 3.3).

To investigate whether these changes in expression levels are accompanied by an alteration in nucleosome positions, indirect end labelling was used to visualise the positions of nucleosomes on the *CYC1* gene and promoter region. By mapping nucleosome positions of each strain under repressive and de-repressive conditions, it is possible to tell if changes occur in the WT on media switch and if so, whether they also occur in UKY500 (figures 3.12 – 3.14).

There are two upstream activation sites (UAS) in the *CYC1* promoter. UAS1 is bound by the Hap1p transcriptional activator when it is activated by haem in response to oxygen. This leads to a 200-fold increase in *CYC1* expression as compared to anaerobic conditions. Since aerobic conditions prevailed for the experiments presented here, Hap1p is presumably bound to UAS1 and directing gene expression on glucose. Hence, although glucose repression exerts a negative regulatory effect under these conditions, the *CYC1* gene is not fully repressed. The study by Martens *et al.* employed a yeast strain deficient in the haem biosynthesis pathway to achieve full repression, such that *CYC1* mRNA is undetectable when cells are grown on glucose (Martens *et al.*, 2001).

In WT yeast on transfer from YPD to EtLac, the peak of digestion centred at -50bp shifts slightly upstream. The mRNA initiation sites of the de-repressed *CYC1* gene are at -70, -62, -57, -46 and -38; transcript initiation from the first three sites is directed from TATA1β, and from the second two by TATA2α (Li and Sherman, 1990). Although indirect end labelling is not a high resolution mapping method, it is conceivable that the shift seen in WT reflects the first nucleosome of the coding region being repositioned slightly further downstream, thus exposing the initiation sites at -46 and -38. Under de-repressed conditions, over 50% of mRNA transcripts originate at these sites (Li and Sherman, 1990). This shift in the digestion pattern is not observed in UKY500, which could in part account for the reduced levels of *CYC1* mRNA if use of these alternative transcriptional start sites is prevented by the presence of a nucleosome.

It is also apparent that the chromatin of UKY500 grown in EtLac media is the most susceptible to cleavage between -50 and -250 (this is best seen by looking at figure 3.14). The peculiarity is perhaps not in this, but rather in the partial protection seen under the other conditions. MNase is a small enzyme that cuts DNA with little sequence specificity, but with a preference for the linker DNA. It cannot cut DNA wrapped on a nucleosome, hence its use in mapping nucleosome positions: large areas of protection usually correspond to a positioned nucleosome. Mapping also requires that MNase will not normally be prevented from cutting when protein complexes that have a less static interaction with DNA than nucleosomes are bound to DNA. In fact, quite the reverse can be true; a highly sensitive site seen in amongst positioned nucleosomes in an MNase generated map may indicate a recognition site for a protein complex, the binding of which is mutually exclusive with a nucleosome. MNase does not normally footprint major groove binding proteins. There are instances however when an appreciable degree of protection is conferred by other proteins. The fully repressed *CYC1* promoter is protected between -50 and -240, but not by a nucleosome: high resolution primer extension demonstrates that the area of protection is too small. Chromatin immunoprecipitation (CHIP) demonstrates that protection is conferred by TBP and RNAPII being permanently bound at the repressed promoter (Martens *et al.*, 2001). Martens *et al.* theorise that the loss of protection they observe in the region upon gene activation is consistent with an activated POLII elongating off the promoter. Perhaps the presence of two functional TATA elements and multiple mRNA initiation sites causes enough hindrance in the activated *CYC1* core promoter to confer some protection to MNase digestion not afforded to UKY500, despite the kinetic nature of these interactions.

Although revealing subtle differences between strains, the results of *CYC1* chromatin analysis provide no evidence to support the hypothesis that incorporation of a partially humanised form of histone H4 into the UKY500 nucleosomes has disrupted binding of the HAP2/3/4/5 complex. The predicted localisation of a nucleosome over UAS2 is consistent with the interaction between HAP2/3/4/5 and chromatin modifying activities, but there is no difference between WT and mutant in this region. Certainly the results do not disprove the hypothesis that HAP2/3/4/5 action is compromised either. I have observed no difference in the position of the UAS2 nucleosome in WT cells upon the diauxic shift, although the necessity of Gcn5p activity for the activation of *CYC1* by HAP2/3/4/5 would suggest that nucleosomes in the promoter are modified by acetylation (Georgakopoulos and Thireos, 1992.) This does not necessarily mean the modified nucleosome will move, but it may direct changes in chromatin conformation that are reflected by the movement of the susceptible region seen in UKY412 (WT). It could perhaps have an effect on the nucleosomes in the coding region too, since these appear perturbed in the mutant.

It is noteworthy that the S82A mutation lies next to a cluster of residues in histones H4 and H3 identified as forming a domain on the surface of the nucleosome important for silencing. This includes histone H3K79, the target of Dot1 methylation (Park *et al.*, 2002). Considering this and the crystal structure, there is evidence that mutations in this area are 'visible' on the nucleosome.

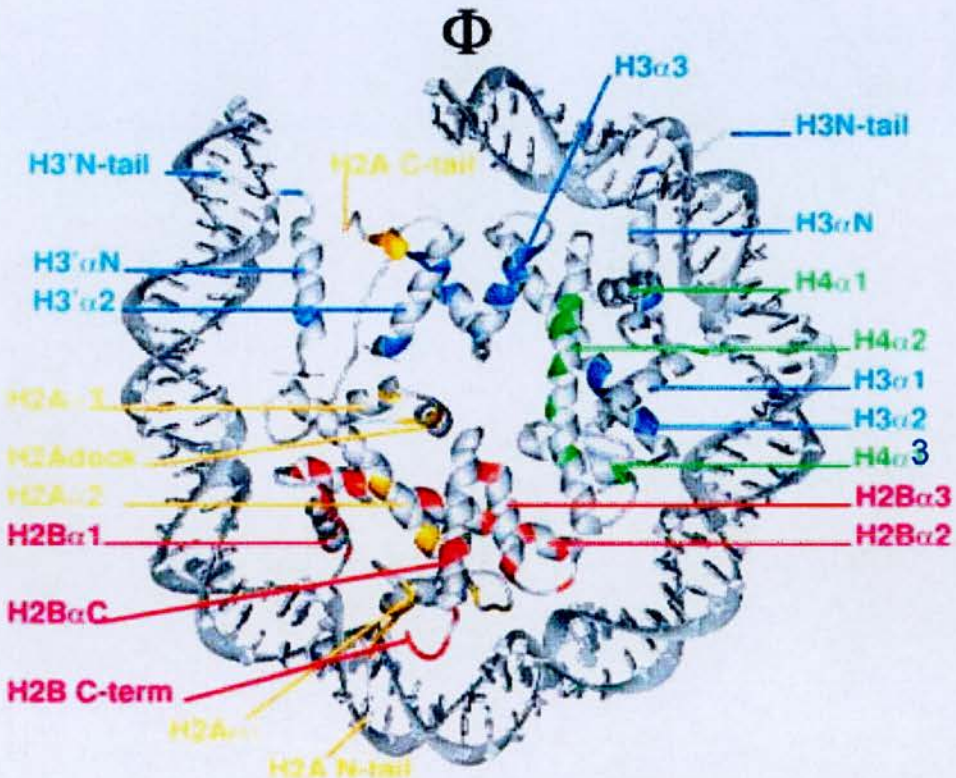

Figure 3.15 Position of amino acid differences between *S. cerevisiae* and *Xenopus* core histones within the quaternary structure of the nucleosome. Histones H3, H4, H2A and H2B are shown in blue, green, yellow and red, respectively. The axis of 2-fold pseudo-symmetry is indicted by Φ (White *et al.*, 2001).

Chapter 4: Expression of Human and 'Humanised' Histone H4 in *S. cerevisiae*

4.1 Summary

This chapter describes construction of two further histone H4 mutants, which completes the set of four characterised in this PhD. To generate a fully 'humanised' mutant an isoleucine to valine change (I21V) was introduced into the UKY500 mutant background. This was discovered to partially-rescue with respect to growth on non-fermentable carbon sources. A second mutant was constructed containing the I21V mutation in isolation in a WT background. This strain was found to grow more quickly than WT on respiratory media. In this chapter it is also demonstrated that there appears to be no genome-wide alteration of chromatin structure in the mutants, as assessed by micrococcal nuclease sensitivity. In contrast, some strains show distinct phenotypes with regards to bulk levels of histone H4 acetylation.

4.2 Introduction

The respiratory defect of UKY500 points to a mitochondrial defect, which was an unanticipated result of a chromatin mutation on a non-chromatin containing environment. The mitochondrion is an essential organelle in all but the most primitive of eukaryotes. Even in facultative anaerobes like *S. cerevisiae*, their functions in haem, lipid, amino acid and nucleotide synthesis, as well as intracellular iron homeostasis are vital (Tzagoloff, 1982). The cellular complement of mitochondria is termed the chondriome, and its form and volume change depending

on growth rate and physiological conditions. A rapidly growing, respiring cell will usually contain less than ten mitochondria (sometimes just one giant mitochondrion), but the chondriome may represent 10-12% of the volume of the cell. Within these mitochondria are housed 20-50 copies of the AT-rich mitochondrial genome (mtDNA) (Stevens, 1977). The 86kb *S. cerevisiae* mtDNA (Foury *et al.*, 1998 for the full sequence) exists in mitochondria as discrete 'clumps', visible by DAPI staining, that comprise one or more copies of mtDNA (Williamson, 1976).

An estimated 13% of the yeast proteome is localised to mitochondria (Kumar *et al.*, 2002). The vast majority of these proteins are encoded in the nucleus, translated in the cytosol, and then either inserted into, or transported across the mitochondrial membranes and into the matrix (Attardi and Schatz, 1988). Only about a dozen proteins corresponding to elements of oxidative phosphorylation are encoded by mtDNA, and made within the mitochondrion (Schatz, 1995).

Cytoplasmic petite mutants (termed *petite* hereafter) lack mitochondria that are functional in oxidative phosphorylation, due to complete loss (ρ^0), or large deletions (ρ^-) of mtDNA (cells with a WT mitochondrial genome are termed ρ^+). Such cells cannot grow on non-fermentable carbon sources, and form small (petite) colonies on glucose media because of their inability to metabolise the ethanol generated by fermentation.

Biogenesis and maintenance of mtDNA is a complex process dependent upon expression of many diverse genes, and influenced by the prevailing physiological

conditions (reviewed comprehensively by Contamine and Picard, 2002). Mitochondria contain their own DNA polymerases for replication, recombinases, helicases and other elements of DNA damage repair and recombination systems, all of which are obviously necessary for mtDNA maintenance (Contamine and Picard, 2002). Components of protein, amino acid, and various metabolite import systems must be intact, and mitochondrial protein synthesis has long been known to be necessary for maintenance of ρ^+ genomes (Myers *et al.*, 1985). Protein degradation systems that complete processing of signal sequence-containing pre-proteins imported from the cytosol, and those that mediate mitochondrial protein turnover are also necessary (reviewed by Rep and Grivvel, 1996). Additionally, the phospholipid membranes of mitochondria have a unique composition, and alteration of this can lead to mtDNA instability (Contamine and Picard, 2002 and references therein). The situation is even further confounded since factors affecting maintenance of ρ^+ genomes are not always the same as those required for ρ^- genome maintenance (Piskur, 1997).

As stated in the previous chapter, all WT yeast strains 'throw *petites*' when grown on glucose media. Overall it is clear that many genetic and environmental factors affect maintenance of the inherently unstable mtDNA.

Our mutations of the yeast histone H4 sequence lead us to verify whether this affected acetylation of lysine residues in its N-terminal tail. Acetylation of yeast nucleosomal histone H4 is mediated predominantly by the NuA4 histone acetyltransferase complex, which can be targeted to stimulate transcription from

chromatin templates (Ikeda *et al.*, 1999). This and the co-localisation of acetylated histone H4 and transcriptionally active chromatin, strongly suggest a role for NuA4 in transcriptional regulation. NuA4 contains the Esa1p catalytic subunit, which is a member of the MYST family of histone acetyltransferases. NuA4 is capable of acetylating histone H4 on each of the lysine residues in its N-terminal tail, and *ESA1* is required for yeast cell cycle progression (Allard *et al.*, 1999, Clarke *et al.*, 1999). The essential nature of *ESA1* suggests it may be involved in the regulation of many genes, or an essential subset required for cell cycle progression (Smith *et al.*, 1998).

SAS2 encodes another histone acetyltransferase activity with a preference for histone H4, and a positive role in transcriptional silencing. Whilst Esa1p will acetylate all four lysines in the histone H4 N-terminal tail (Suka *et al.*, 2001), Sas2p has a preference for K16. Sas2p action prevents interaction of the silencing protein Sir3p with hypoacetylated histone H4K16 by opposing the action of the Sir2p histone deacetylase (Suka *et al.*, 2002). Disruption of *SAS2* leads to spreading of telomeric heterochromatin by altering the gradient of histone H4K16 acetylation and localisation of Sir proteins (Kimura *et al.*, 2002).

This chapter describes further characterisation of UKY500, in addition to two more *S. cerevisiae* mutant strains that survive by expressing mutated forms of histone H4 that substitute to varying degrees the human amino acid sequence.

4.3 Results

4.3.1 Construction of pUK501 and pUK502 Plasmids

The I21V substitution in the histone H4 amino acid sequence was introduced into the pUK500 plasmid backbone using a strategy similar to that shown in figure 3.5b. *HHF2* already substituted with seven out of eight human amino acid differences was PCR amplified from pUK500 in two separate sections, using two sets of primers: Ep and Hp primers that nest just outside the *EcoRI* and *HindIII* restriction enzyme sites, and 20bp primers (I-Vfw and I-Vbk) complementary to the region of the I21V mutation, except that they contain the single base pair alteration encoding the substitution (figure 4.1). These fragments were then joined in an SOE reaction, and substituted into pUK499 to generate pUK501, which carries an *HHF2* gene encoding a fully 'humanised' histone H4 protein.

The I21V single mutation plasmid, pUK502, was created using the same primers and strategy as detailed above, except that pUK499 WT *HHF2* sequence instead of pUK500 was used as the template (figure 4.2).

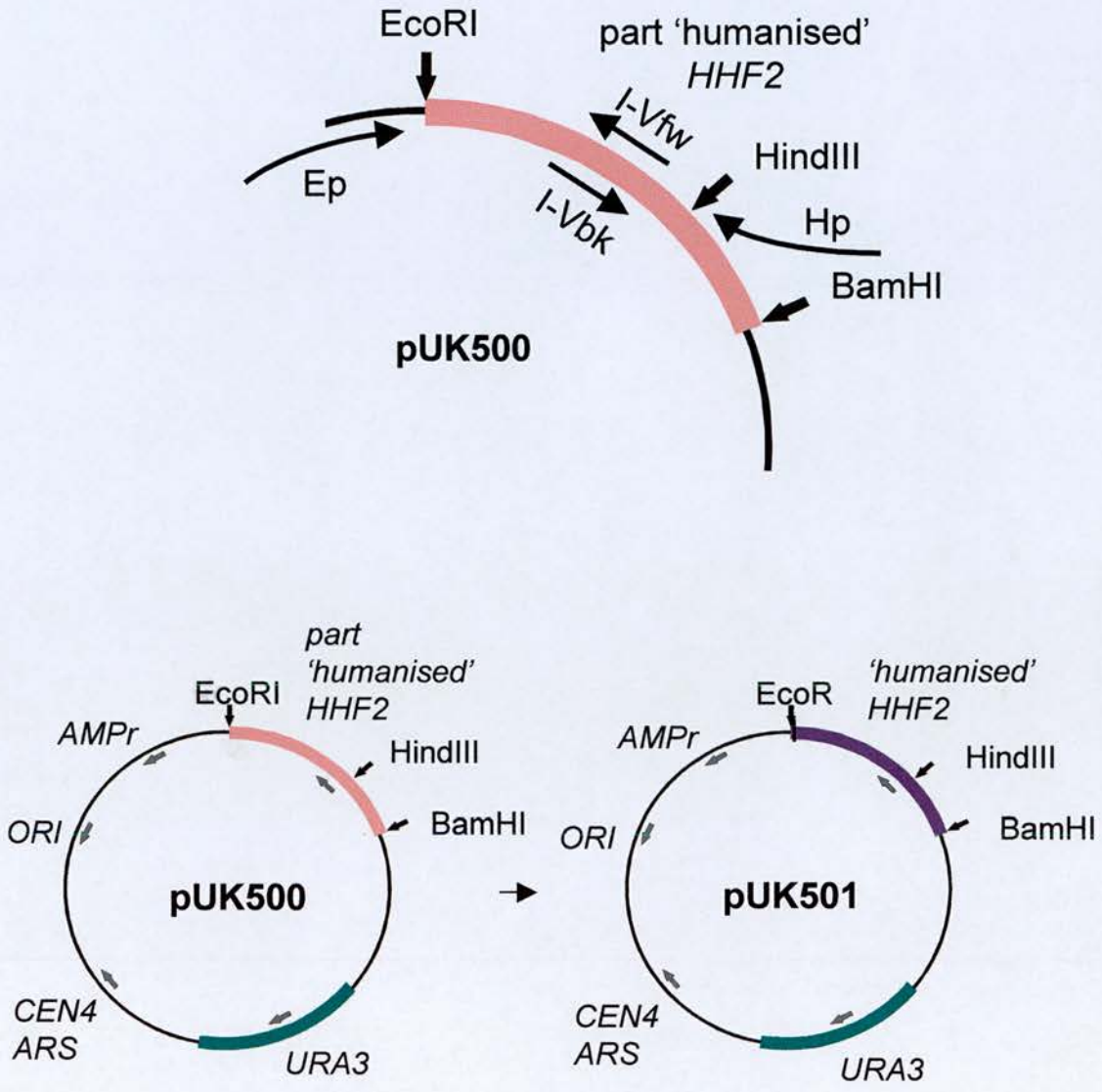

Figure 4.1 Human histone H4 protein is encoded by pUK501. I-Vfw and I-Vbk primers were used to introduce the I21V mutation into the pUK500 backbone to create pUK501 which encodes a histone H4 protein identical to that of humans.

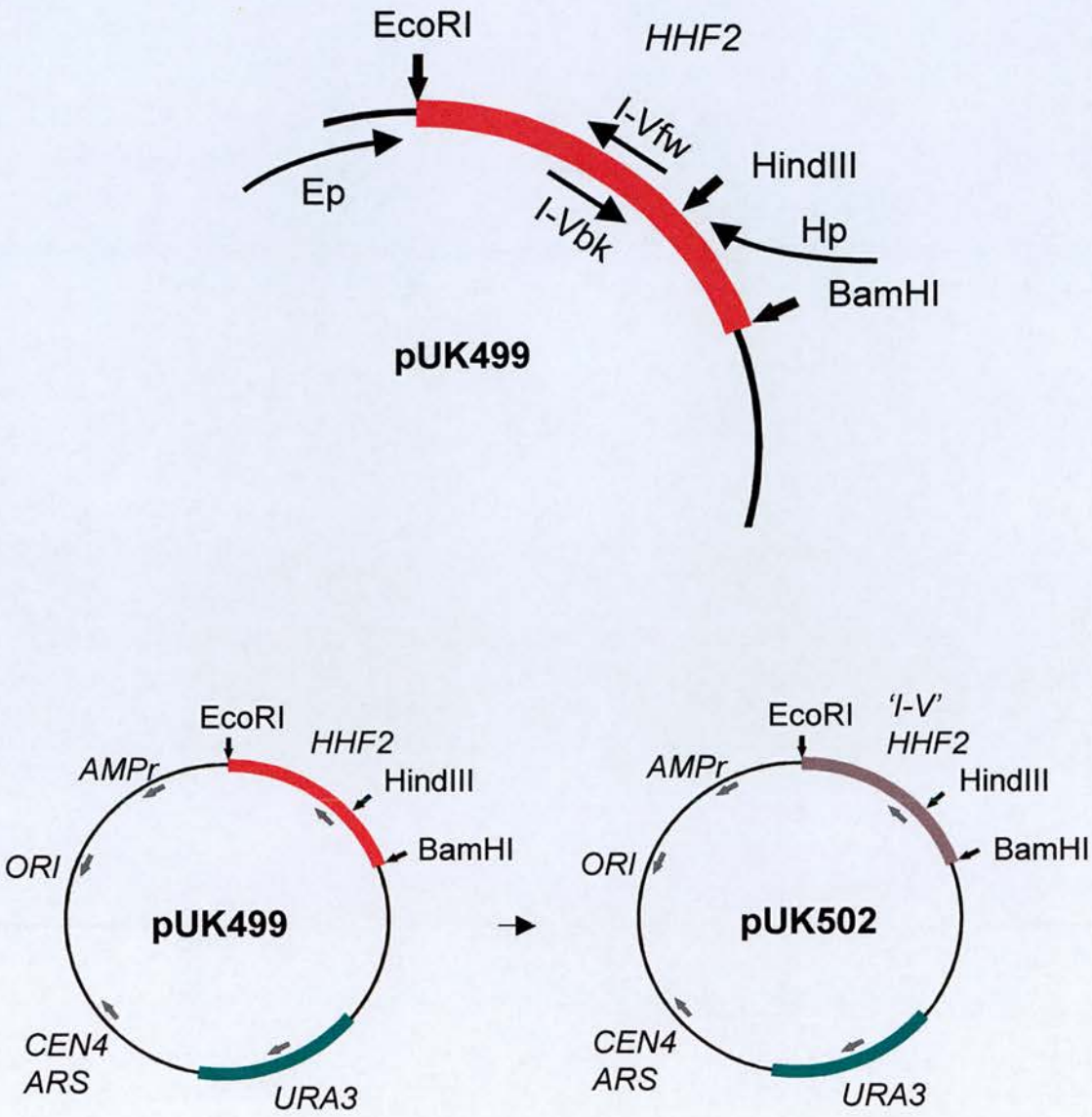

Figure 4.2 I21V histone H4 protein is encoded by pUK502. I-Vfw and I-Vbk primers were used to introduce the I21V mutation into the pUK499 backbone to create pUK502, which encodes a histone H4 protein with the I21V substitution in the N-terminal region.

4.3.2 Generation of UKY501 and UKY502 Strains

pUK501 and pUK502 were transformed separately into UKY403, and transformants selected on GAL-trp-ura plates. Resultant colonies were then replica-plated onto GLC-trp-ura plates, to test for glucose shift viability. All colonies survived the transition, indicating that the human form of histone H4, and I21V histone H4 encoded by pUK501 and pUK502 respectively, can be incorporated into nucleosomes and maintain yeast survival.

pUK421 was then cured from these strains to generate UKY501 and UKY502. Figure 4.3 has diagrammatic representations of the positions of mutations introduced into histone H4 in the three mutants compared to WT. To eliminate the possibility that the mutant episomal *HHF2* genes had undergone recombination with the pUK421 wild type *HHF2* gene prior to curing, the plasmids were re-extracted from yeast, and transformed into *E. coli* DH5α cells for amplification. Resultant plasmid preparations were restriction enzyme digested to check their size (figure 4.4), sequenced in both forward and reverse directions, and all shown to be correct.

Figure 4.5 demonstrates that all four yeast strains grow well and at comparable rates on YPD at the optimum temperature of 30°C.

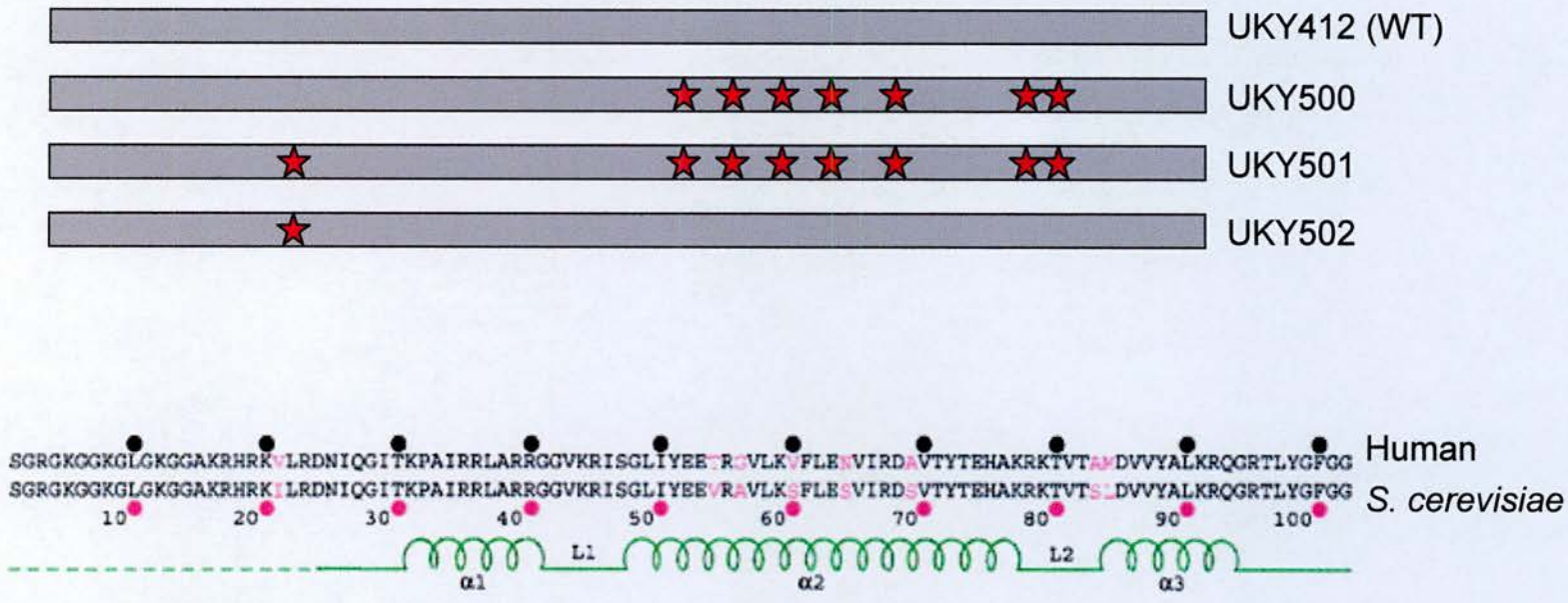

Figure 4.3 Schematic representation of amino acid substitutions introduced into the *S. cerevisiae* histone H4 sequence (top) to make it more closely related to the human protein (bottom; White *et al*., 2001).

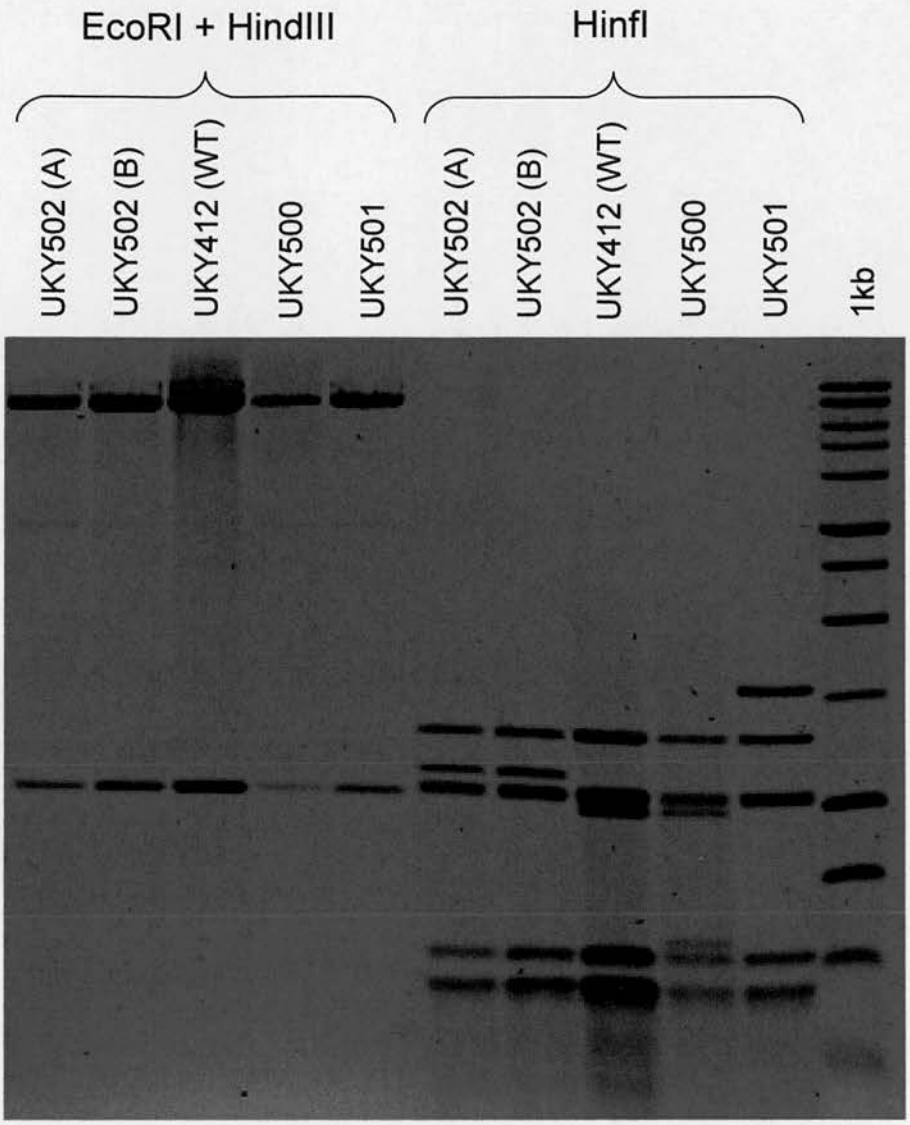

Figure 4.4 Restriction enzyme digestion of plasmids extracted from yeast demonstrated that all pUK plasmids are of the expected size of 9.22kb. Digestion with *EcoRI* and *HindIII* excises only the fragment containing the introduced mutations, and is the same in all strains. Introduction of the I21V mutation destroys a *HinfI* restriction site, thus mutants with this substitution have a different pattern to WT. A 1kb ladder was used as a size marker, and two independent UKY502 strains were being used at this time, whilst awaiting sequencing results.

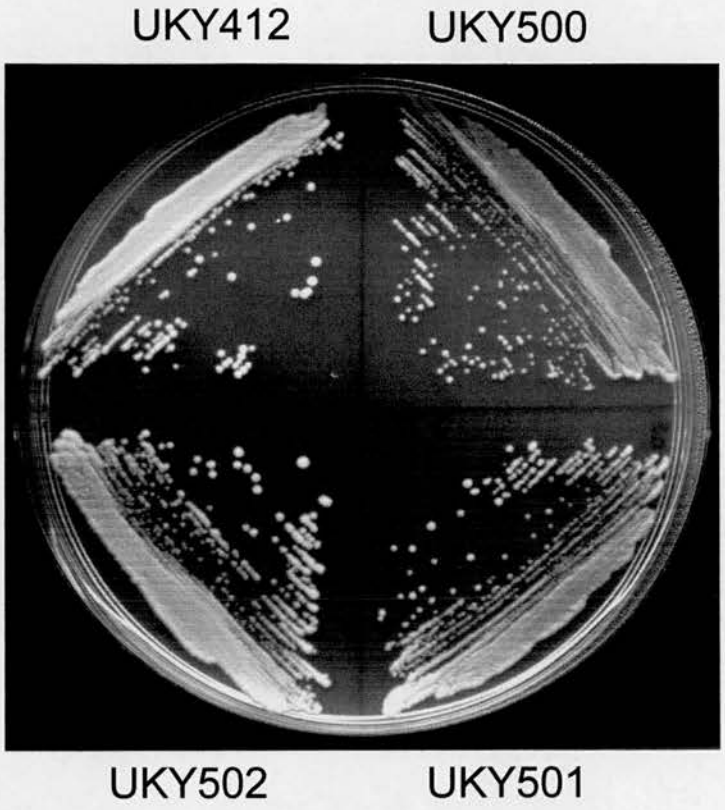

Figure 4.5 Strains grow at comparable rates under optimal conditions of rich glucose media (YPD) at 30°C.

4.3.4 HHF2 mRNA Expression

To confirm that the levels of *HHF2* mRNA expressed from the four pUK plasmids are comparable, RNA was prepared from duplicate cultures in mid-logarithmic growth. These RNAs were separated by agarose gel electrophoresis and transferred to nitrocellulose. For Northern blot the membrane was hybridised with the *NotI-BamHI* fragment excised from plasmid pRS414.GAL.H4 containing the full length WT *HHF2* sequence. Figure 4.6 and table 4.1 show the results of this experiment with *HHF2* mRNA levels normalised to both 28S rRNA and *ACTI* mRNA (WT *HHF2* mRNA levels in UKY412 are arbitrarily set to 100%).

Although the probe is a perfect match to the *HHF2* mRNA expressed in UKY412 (WT), the small number of base pair differences from the mutant *HHF2* sequences of the other strains (at a maximum of 16 mismatches per 331 base pairs for the histone H4 mRNA expressed by UKY501), were not expected to cause large differences in hybridisation efficiency. Histone H4 mRNA levels from the three mutants are consistently slightly lower than WT, particularly when normalised to 28S rRNA. This may result from either decreased expression, or increased instability of *HHF2* mRNA, less efficient hybridisation of the WT cDNA probe to the mutated *HHF2* sequences, or it could be that the mutations have an effect on rDNA transcription which is known to have a strong chromatin element to its regulation (Conconi *et al.*, 1989). Either way, the differences do not seem large enough to have significant effect on viability.

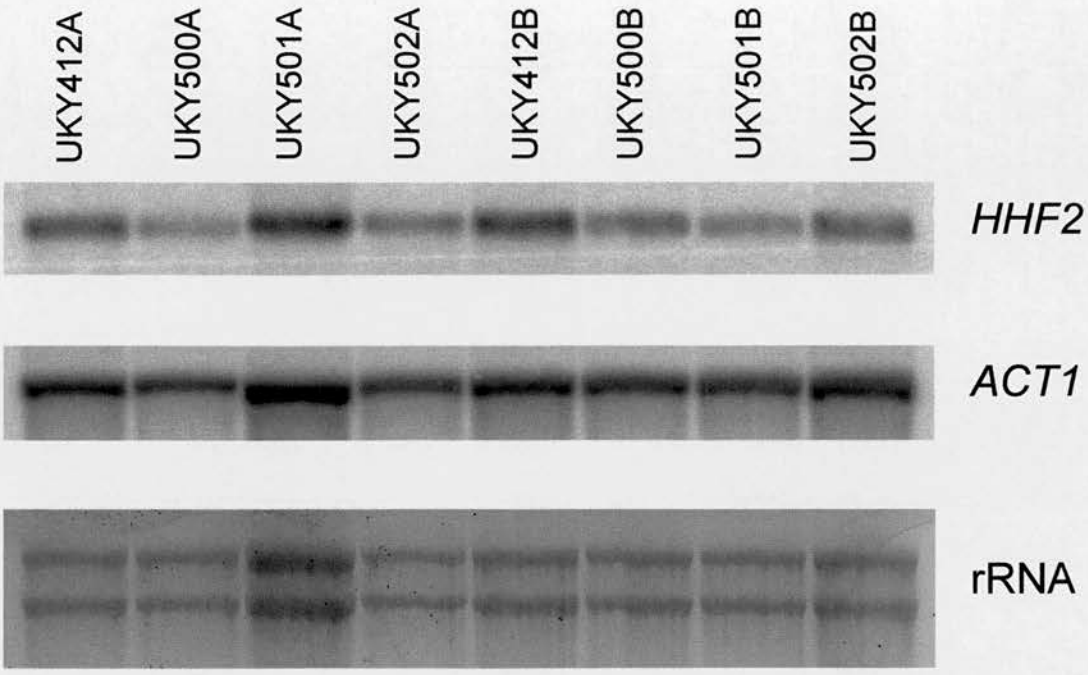

Figure 4.6 Northern blot of *HHF2* demonstrates that all strains express similar amounts *HHF2* mRNA. Transcript levels of *HHF2* and *ACTI* from duplicate cultures of each yeast strain were visualised in a Northern blot by hybridising to specific radiolabelled cDNA probes. Ribosomal RNAs (rRNA) were visualised by ethidium bromide staining.

	UKY412	UKY500	UKY501	UKY502
***ACT1* normalised**	100%	83%	83%	94%
28s rRNA normalised	100%	75%	85%	79%

Table 4.1 *HHF2* mRNA expression levels were normalised to 28s rRNA and *ACTI* signals, and averaged for each strain across the duplicates. The gene expression levels from UKY412 (WT) were arbitrarily set to 100%.

4.3.4 Bulk Chromatin

Partial digestion of bulk chromatin with MNase generates a population of mono-, di-, tri-, tetra-, etc nucleosomal particles. De-proteinised, purified DNA run on an agarose gel separates into size fractions associated with one, two, three, four etc nucleosomes. MNase has exonucleolytic as well as endonucleolytic activities. The 'nibbling' away of nucleosomal DNA ends by MNase, visualised by the gradual lowering of bands, can be addressed by performing time course experiments. This allows an estimate of nucleosomal repeat length in bulk chromatin to be calculated.

Results of such an experiment are shown in figure 4.7. The ethidium bromide stained gel in figure 4.7a shows a nucleosomal ladder with DNA fragments corresponding to mono- to hexa-nucleosomal particles clearly visible by eye. By performing linear regression on the size of the DNA fragments at each time point, the graph in figure 4.7b can be drawn with a slope representing the number of base pairs per nucleosome. The downward trends of the curves of the graphs highlight the effect of MNase exonuclease activity at the ends of nucleosomal DNA at longer digestion times. Extrapolation back to a time point approaching zero, where MNase is assumed to have cut on average in the centre of the linker DNA, allows an estimation of nucleosomal repeat length.

From the graphs in figure 4.7b, a repeat length of 170-175bp can be assigned to all four strains, which is fairly typical of yeast bulk chromatin. The differences between WT and the three mutants expressing 'humanised' forms of histone H4 do not appear

to be significant, as they are within error of this experiment. The shapes of the curves in figure 4.7b are also very similar, indicating little difference in the kinetics of MNase digestion. This implies that there is no gross difference in the accessibility of nucleosomal DNA to MNase digestion between strains. Together the results of this experiment suggest no changes in nucleosomal array conformation occur as a result of the human amino acid substitutions in the histone H4 sequence.

4.3.5 Chromatin Organisation in the Region of a Housekeeping Gene

In addition to assessing the effect of the mutations on MNase digestion sensitivity on a genomic scale, chromatin was examined in the region of the constitutively active *ACT1* gene (which, as can be seen in figure 4.1, is similarly expressed in all strains). Time course digestions performed as above were Southern blotted and hybridised to a probe corresponding to the *ACT1* coding sequence, to visualise chromatin structure over about a kilo base either side of this gene (figure 4.8a).

Again, a clear nucleosomal ladder is visible, and there is also a strong band at about 1.5kb in all strains. This possibly corresponds to the distance between two putative hypersensitive sites. From the graphs in figure 4.8b it appears again that there is little difference between strains, and a nucleosomal repeat length of approximately 165bp can be assigned to each. This is shorter than the average repeat length of bulk chromatin, as is often observed in transcriptionally active regions due to their less condensed nature.

A.

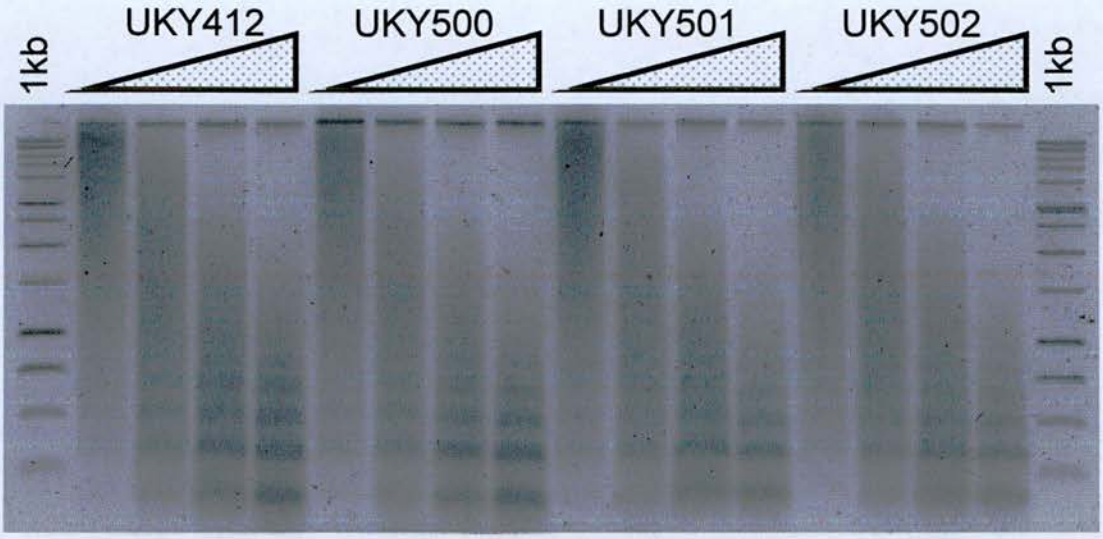

B.

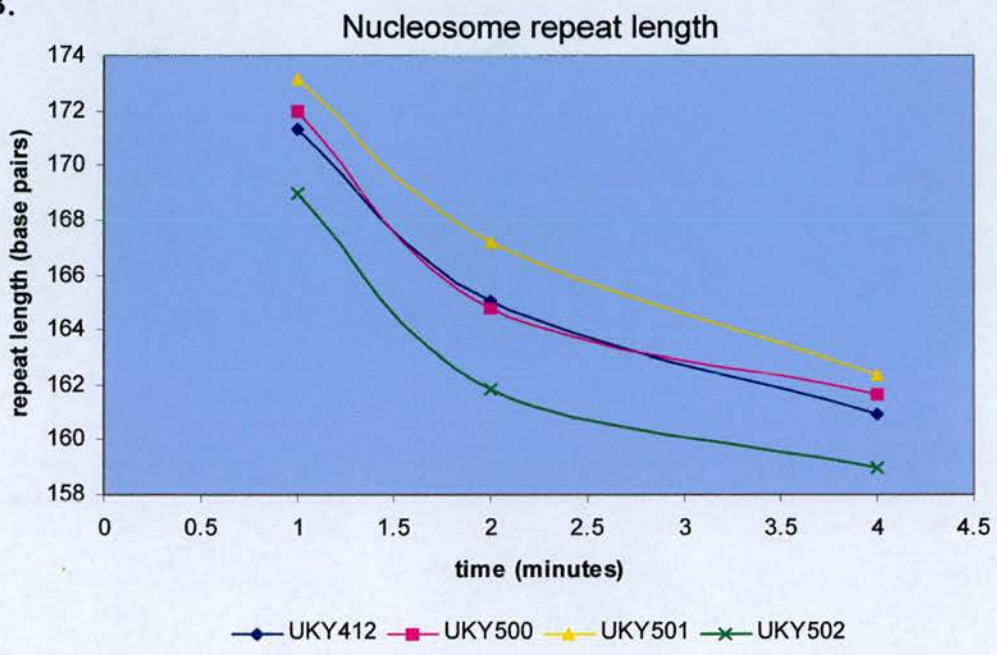

Figure 4.7 Nucleosomal repeat length of bulk chromatin is unchanged between strains as assessed by micrococcal nuclease digestion. A) DNA purified from nuclei digested by micrococcal nuclease was separated in an agarose gel along side 1kb size markers. Staining with ethidium bromide reveals a clear ladder of mono- and poly-nucleosomal fragments. B) Linear regression on the intensity and position of bands in the gel enables this graph to be drawn. Extrapolation back to a time point approaching zero give an estimate of average nucleosome repeat length of 170-175bp for each strain. The similar shapes of the curves imply that the reaction kinetics are also unaffected.

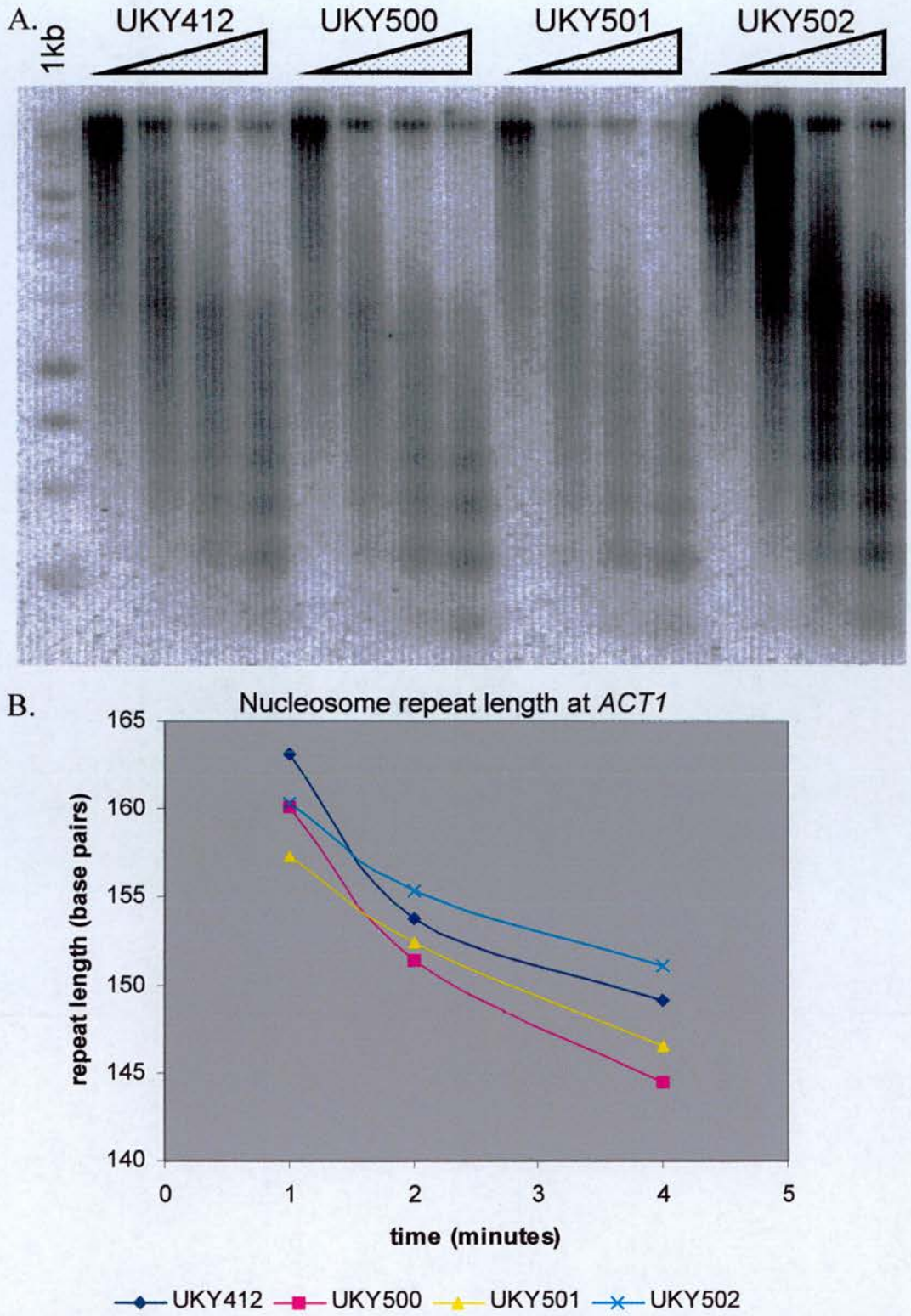

Figure 4.8 Nucleosomal repeat length at *ACT1* is unchanged between strains as assessed by micrococcal nuclease digestion. A) DNA purified from nuclei digested by micrococcal nuclease was separated in an agarose gel along side 1kb size markers, blotted onto nitrocellulose and hybridised to a radiolabelled cDNA probe specific for the *ACT1* coding sequence. B) Linear regression on the intensity and position of bands gives an estimate of average nucleosome repeat length of 165bp for each strain.

4.3.6 Carbon Source and Temperature Sensitivity

In the previous chapter it was demonstrated that UKY500 is unable to grow on non-fermentable carbon sources, and also that it is slightly temperature sensitive. Thus, on construction of UKY501 and UKY502, growth of the four strains was compared on respiratory (EtLac) media at 30°C, and on YPD at 37°C (figure 4.9). The results of these plate assays reveal a surprising partial-rescue conferred by the introduction of the I21V mutation into the UKY500 mutations background.

The effect is most pronounced when cells are grown on EtLac media, as shown in figure 4.9a. Under these conditions, UKY412 expressing WT histone H4 grows well, but UKY500 shows only a tiny amount of residual growth, which is presumably halted once the 0.1% glucose present in the media is exhausted. However, in UKY501 growth on EtLac is restored, albeit not to the full extent of WT. Interestingly, and in keeping with the UKY501 partial-rescue phenotype, UKY502 appears to grow even more readily than UKY412 (WT) under these conditions.

The phenotypic pattern observed on EtLac media is mirrored, although less pronounced, on YPD at 37°C (figure 4.9b). These results suggest, intriguingly, that the I21V mutation in the N-terminal tail region of histone H4 in some way interacts with the mutations, or a subset thereof, introduced into the globular domain of histone H4.

A.

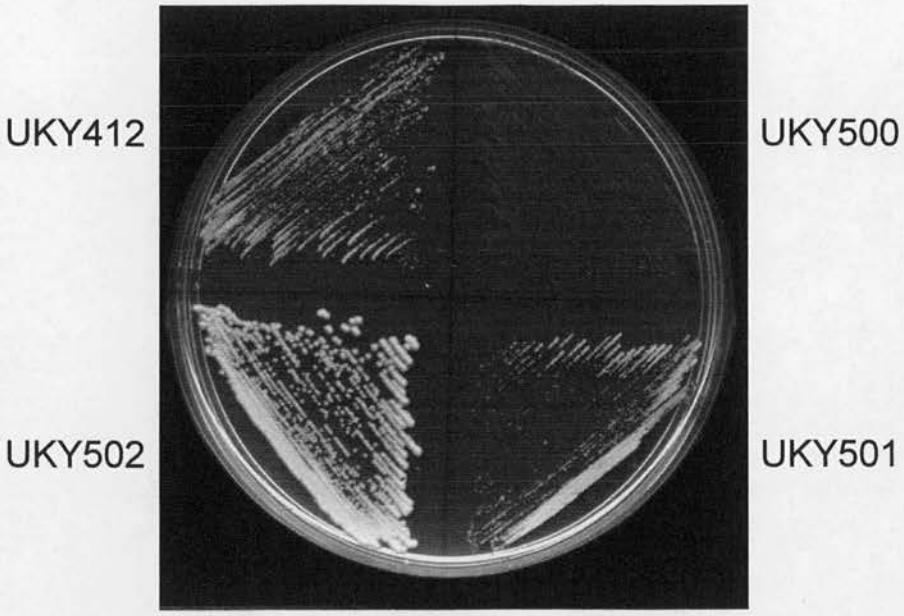

B.

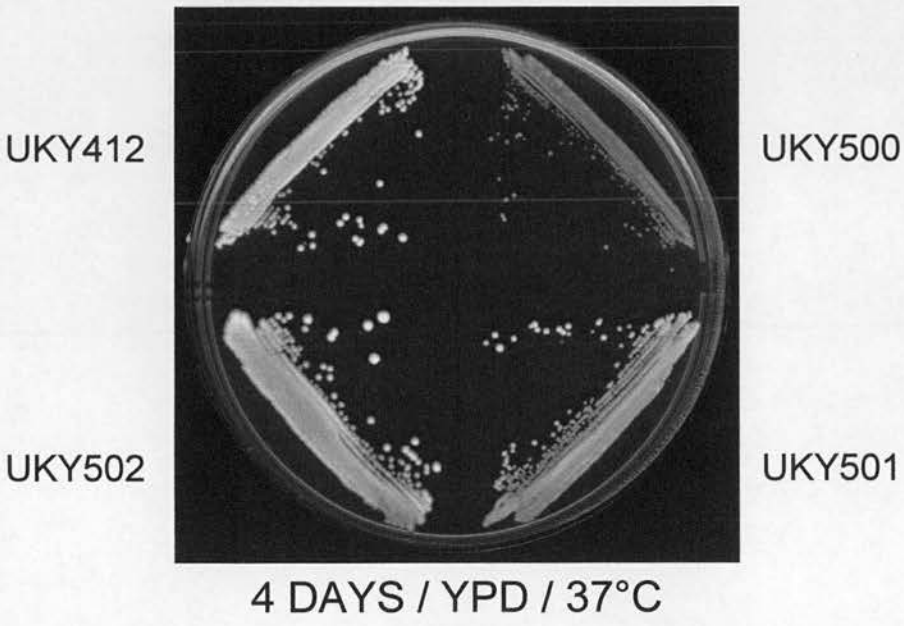

Figure 4.9 Carbon source and temperature sensitivity. A) Relative growth rates of strains on respiratory (EtLac) media at 30°C. UKY500 will not grow on this media once the 0.1% glucose is depleted. UKY501 grows more slowly than UKY412 (WT), but UKY502 grows more quickly than WT. B) Relative growth rates of strains on rich glucose media (YPD) at 37 °C. The pattern of growth rates on EtLac is mirrored, albeit to a lesser extent.

4.4 *SUC2* Gene Analysis

The *SUC2* gene of *S. cerevisiae* encodes the enzyme invertase that is required for growth on sucrose and related di- and trisaccharides such as raffinose. Invertase catalyses hydrolysis of the glycosidic bond that links the glucose and fructose moieties that comprise sucrose. The *SUC2* gene has no known activator. Expression is controlled solely by glucose repression, and is induced up to 100-fold in low glucose (Johnston and Carlson, 1992).

SUC2 is well studied with regards to its chromatin structure. Upon gene activation, nucleosomes in the promoter, coding region, 3' untranslated region (UTR), and several kb upstream are remodelled (Perez-Ortin *et al.*, 1987, Fleming and Pennings, in preparation). Particularly, four nucleosomes that are positioned over the TATA box and UAS regions become remodelled by the interplay between the SWI/SNF and TUP1/SSN6 complexes when glucose repression is relieved, resulting in a chromatin structure compatible with elevated expression levels (Hirschhorn *et al.*, 1997).

Since growth of UKY500 is impaired on raffinose (table 3.2), expression of *SUC2* in the series of histone H4 mutants was checked, to see whether it is reduced in UKY500, as *CYC1* expression is. Any differences in expression of this gene reflected at the chromatin level might be simpler to understand in a well characterised context.

4.4.1 Expression of SUC2 mRNA

Figure 4.10 shows a Northern blot analysis of RNA prepared from mid-logarithmic cultures of the four strains grown under repressing (YPD) and de-repressing (EtLac) conditions, probed for the *SUC2* coding sequence. The appreciable *SUC2* transcript levels on YPD, and modest 3.4-fold up-regulation on transfer to EtLac imply that the gene is not fully repressed under the conditions employed here. The concentration of glucose remaining in the media when the cells were harvested (at a density of 4-4.5 x 10^7 cells/ml; see materials and methods) must not have been high enough to elicit full repression of *SUC2*. This is despite being the same conditions as used for *CYC1* analysis, where the expected degree of up-regulation was observed. UKY501 and UKY502 also show modest increases in *SUC2* mRNA levels of 1.9- and 3.0-fold respectively upon de-repression. However, contrary to what might be expected from the growth observed on raffinose plates, UKY500 up-regulates *SUC2* expression over 45 fold; thirteen times more than WT.

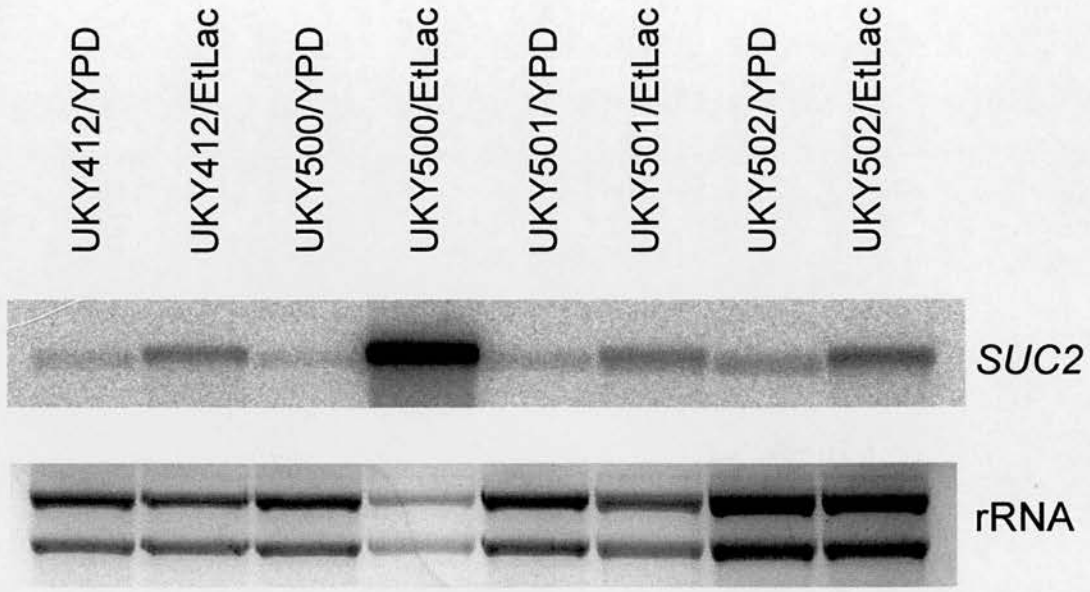

Figure 4.10 Northern blot analysis of *SUC2* expression shows that UKY500 hyper-expresses *SUC2* mRNA. Transcript levels of *SUC2* mRNA in strains grown under repressive (YPD) and de-repressive (EtLac) conditions were visualised in a Northern blot by hybridising to a radiolabelled cDNA probe specific for *SUC2*. Ribosomal RNAs (rRNA) were visualised by ethidium bromide staining.

Fold up-regulation on YPD to EtLac transition

UKY412	UKY500	UKY501	UKY502
3.4	45.7	1.9	3.0

Table 4.2 *SUC2* mRNA expression levels were normalised to 28s rRNA signals. The fold up-regulation of the *SUC2* upon the transition from YPD to respiratory (EtLac) media is indicated. This demonstrates that all strains increase *SUC2* expression when glucose repression is lifted, but UKY500 shows a huge induction of over 45-fold.

4.4.2 Mapping of Nucleosomal Organisation at the SUC2 Gene

The scheme for indirect end labelling analysis of the *SUC2* gene is detailed in figure 4.11. Nuclei prepared from mid-logarithmic cultures of all four strains were subjected to partial MNase digestion, and the DNA purified prior to restriction with *HinfI*. This DNA was separated on an agarose gel and blotted onto nitrocellulose. Figure 4.12 shows the results of hybridising a radiolabelled probe corresponding to the first 285bp of the *SUC2* coding region to this blot, and illustrates the position of the coding sequence, and TATA and UAS promoter elements.

Lane intensity quantitation and calibration of the blot shown in figure 4.12 allows the traces shown in figures 4.13 and 4.14 to be drawn. By looking at these traces eight nucleosome positions can be assigned upstream of the *SUC2* gene under repressing conditions. The first of these is centred over the TATA box situated between -128 and -133. In all four strains, an increase in susceptibility to digestion by MNase upon transfer to EtLac media implies remodelling of this nucleosome. This is fairly subtle, and weaker peaks of digestion over the TATA box and transcriptional start site at -39 exist in YPD grown cultures, further implying that the conditions employed here were not fully repressive. The next nucleosome upstream, centred around -280bp, also appears to be remodelled as glucose repression is lifted.

The two positioned nucleosomes centred at -410 and -610 encompass the *SUC2* UAS. Mig1p mediates the glucose repression of *SUC2,* and the UAS contains two Mig1p binding sites (from -431 to -445, and -488 to -499). The distal site appears

accessible under all conditions, whereas the proximal site appears to become slightly more accessible upon strong de-repression in UKY500. The nucleosome sitting on the Sko1p activator binding site (from -618 to -627) looks to be remodelled in all strains on transfer to EtLac media, but the effect is greatest in the most highly expressing UKY500 as the DNA becomes more accessible to MNase digestion.

Comparison of the cutting pattern of repressed nuclei with that of naked DNA, implies four more nucleosomes are positioned between -700 and -1300. These all appear to be remodelled upon gene activation in UKY500, but not in the other strains. The positions of nucleosomes and the increase in DNA accessibility on gene activation are consistent with previous observations on this gene (Hirschhorn *et al.*, 1992, Wu and Winston, 1997, Gavin and Simpson, 1997), and reveal little about the effects of incorporating mutant histone H4 into nucleosomes. On the contrary, they would imply that the UKY500 mutant is behaving normally at this gene, perhaps responding to an upstream signal that differs between this mutant and the other three strains (see discussion in section 4.8).

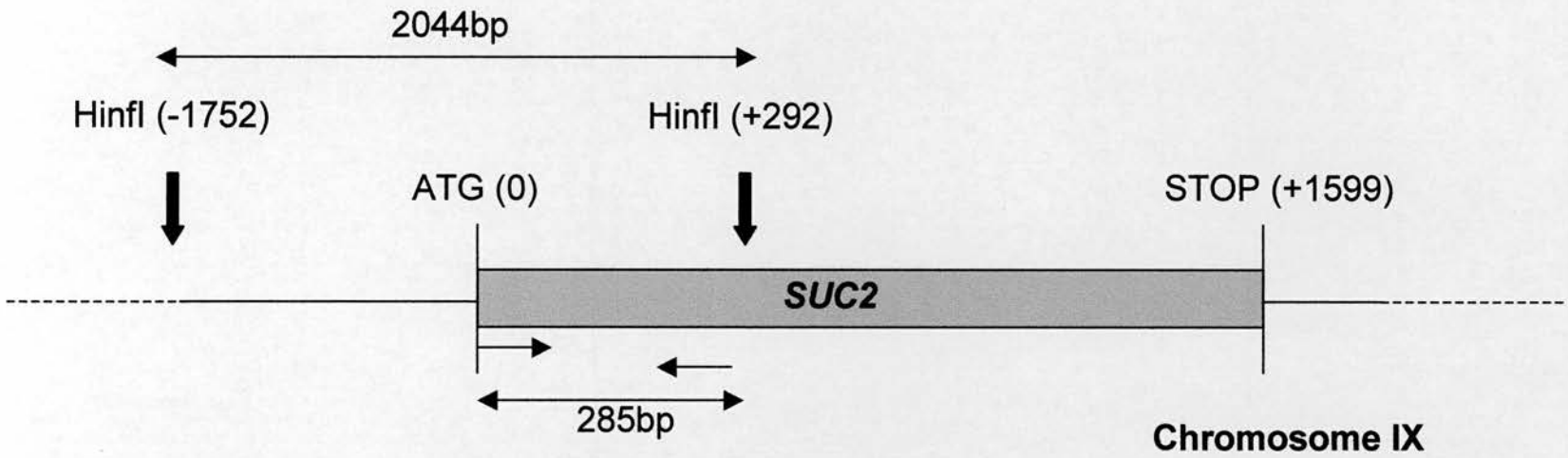

Figure 4.11 Indirect end labelling at *SUC2*. Schematic representation of the position of the *HinfI* restriction enzyme sites relative to the *SUC2* coding sequence on chromosome IX, and the position of the 285bp radiolabelled probe which was PCR amplified from genomic DNA using primers SUC2-ielC and SUC2-ielD

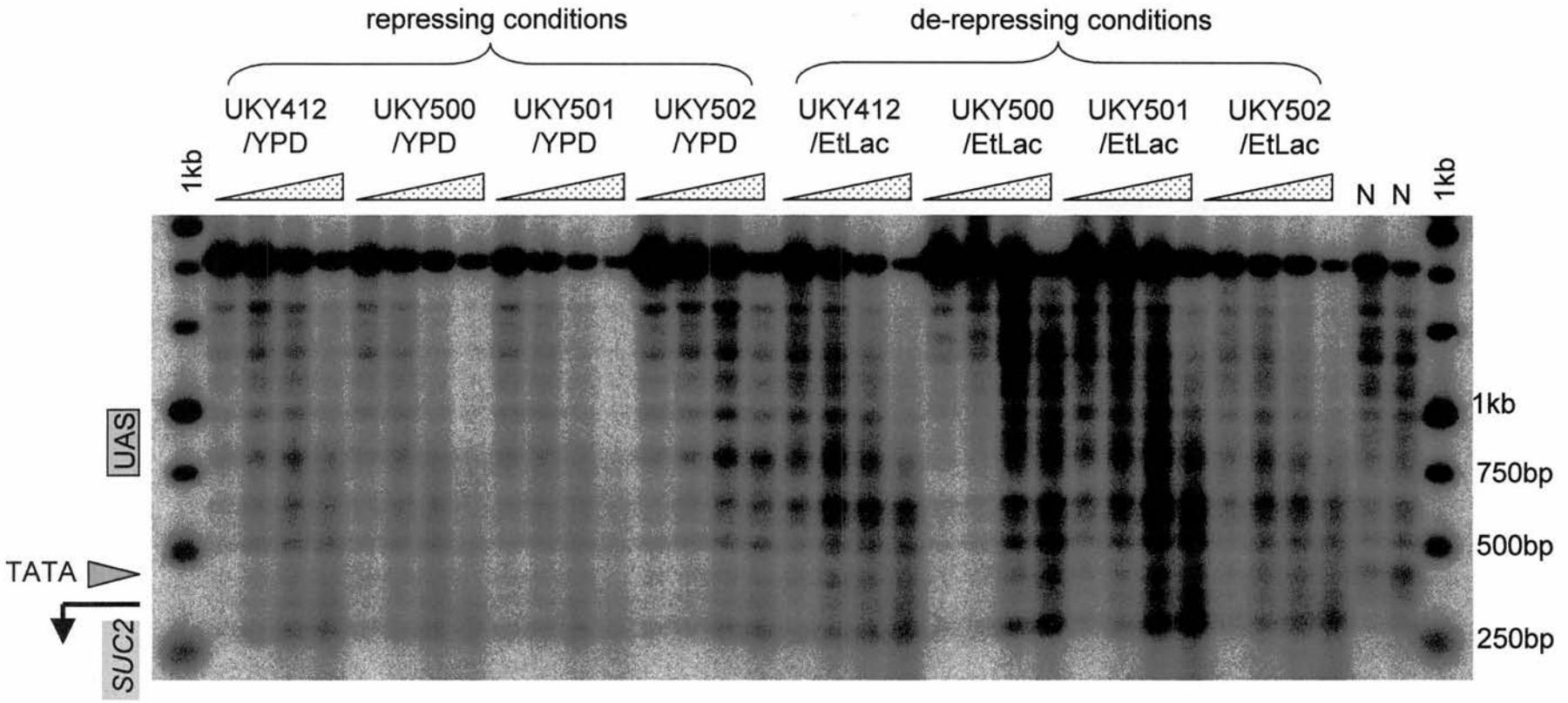

Figure 4.12 Nuclease mapping at the *SUC2* gene. Nuclei prepared from strains grown under repressing (YPD) and de-repressing (EtLac) conditions were subjected to a time-course of partial digestion by micrococcal nuclease. Purified DNA was subsequently digested to completion by *HinfI*. The fragments were separated by agarose gel electrophoresis and transferred to nitrocellulose. Naked DNA controls (N) were treated similarly and a radiolabelled 1kb size marker was included on the gel. The blot was probed with a 285bp radiolabelled cDNA probe complementary to sequences just inside the downstream *HinfI* restriction enzyme site. Exposure of the blot to a phosphorescent screen generated the image shown. The positions of the *SUC2* coding sequence, as well as upstream activation sequence (UAS) and TATA box are indicated.

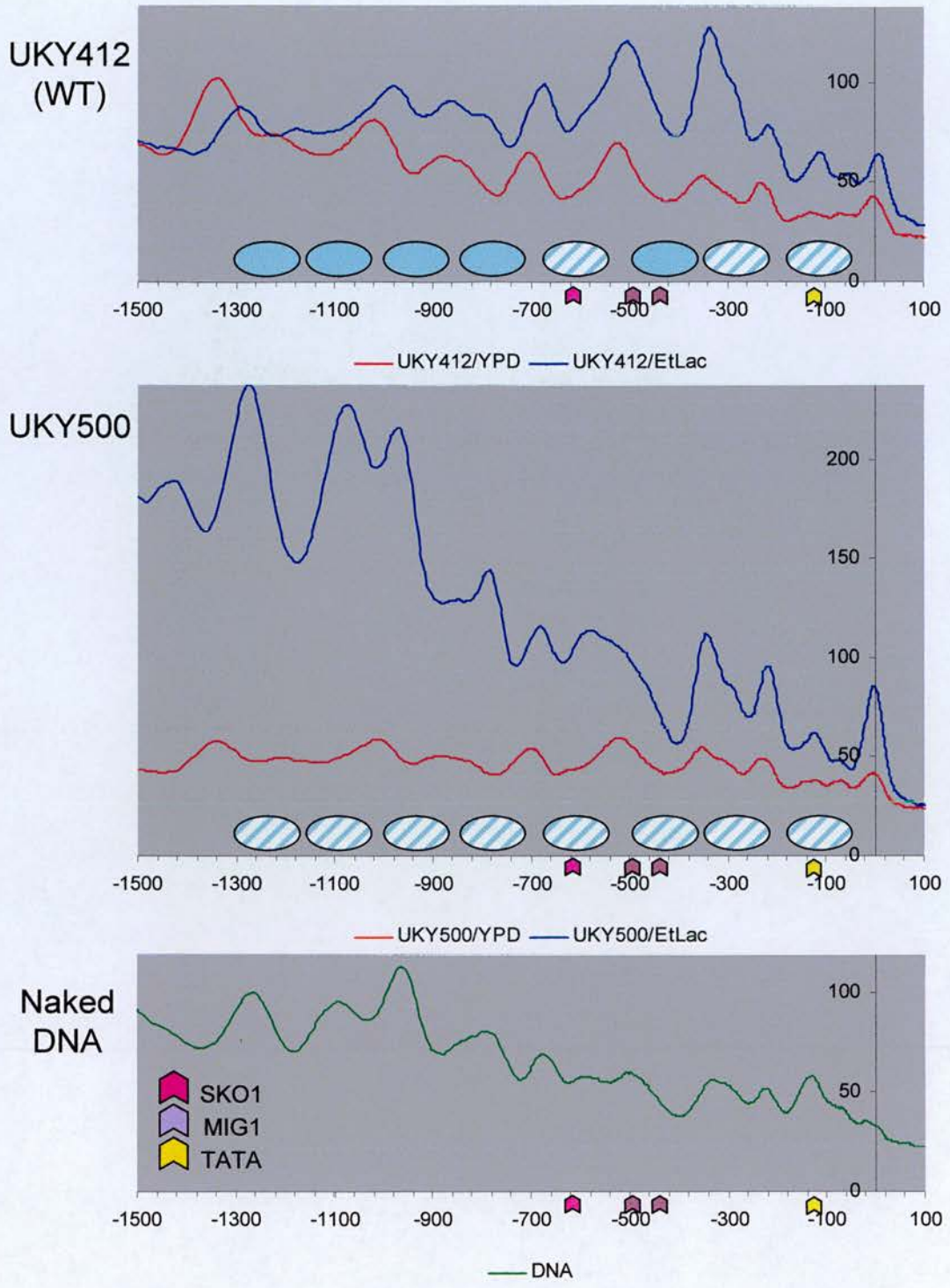

Figure 4.13 Nuclease positions at the *SUC2* gene. Intensity traces generated by quantitation of the UKY412 (WT) and UKY500 indirect end labelling experiments, with base pairs plotted on the x-axis and intensity plotted on the y-axis. Red traces represent repressive (YPD) conditions; blue traces represent de-repressive (EtLac) conditions. Assigned nucleosome positions on YPD are indicated by ovals. Those that do not appear to undergo remodelling on media switch are represented by solid blue ovals and those that do are represented by striped blue ovals. Naked DNA is shown in green. The positions of Mig1 and Sko1 binding sites and TATA box are indicated by pink, purple and yellow arrows, respectively. Position zero on the x-axis corresponds to the beginning of the *SUC2* coding sequence.

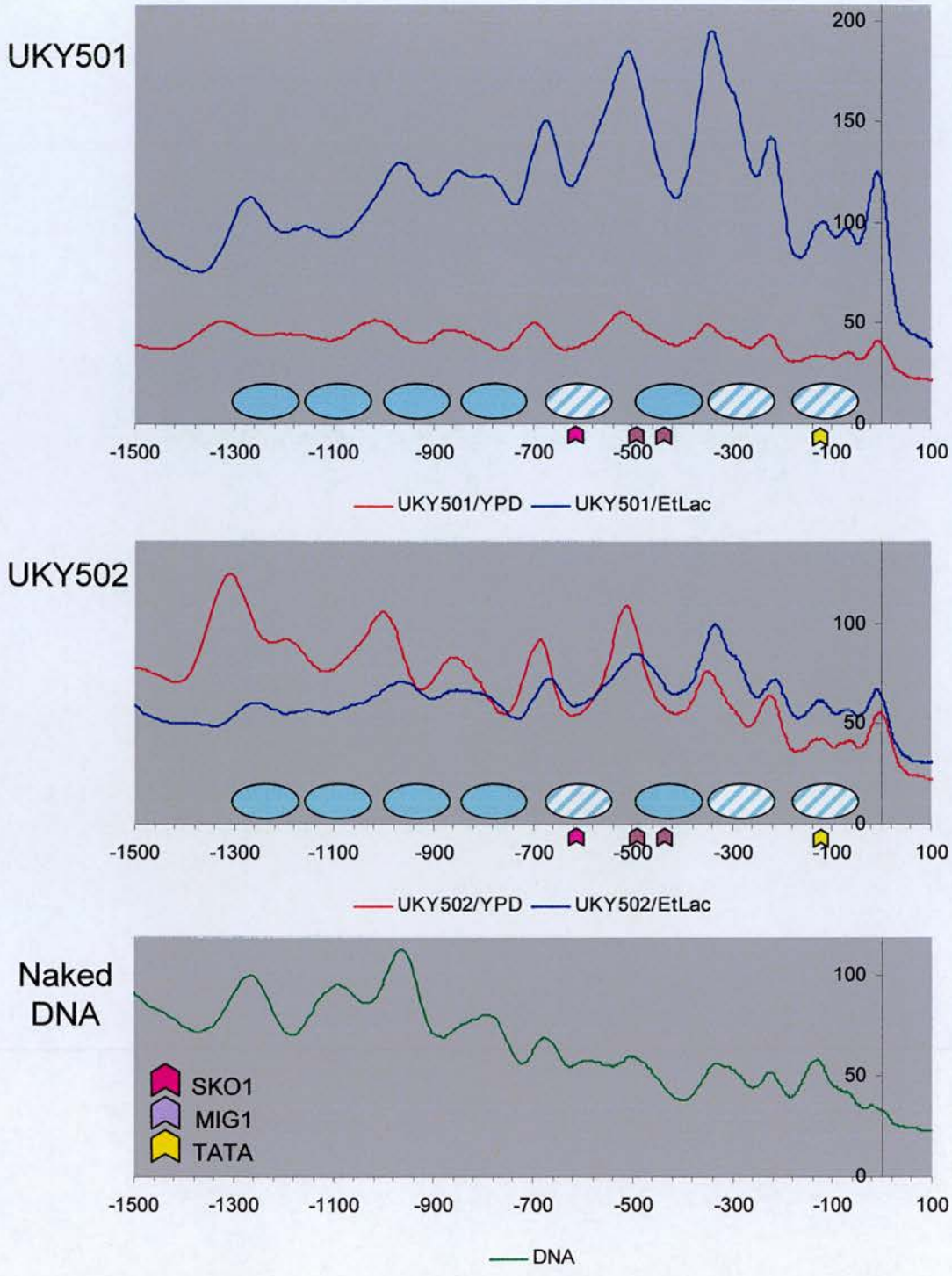

Figure 4.14 Nuclease positions at the *SUC2* gene. Intensity traces generated by quantitation of the UKY501 and UKY502 indirect end labelling experiments, with base pairs plotted on the x-axis and intensity plotted on the y-axis. Red traces represent repressive (YPD) conditions; blue traces represent de-repressive (EtLac) conditions. Assigned nucleosome positions on YPD are indicated by ovals. Those that do not appear to undergo remodelling on media switch are represented by solid blue ovals and those that do are represented by striped blue ovals. Naked DNA is shown in green. The positions of Mig1 and Sko1 binding sites and TATA box are indicated by pink, purple and yellow arrows, respectively. Position zero on the x-axis corresponds to the beginning of the *SUC2* coding sequence.

4.4.3 Restriction Fragment Length Polymorphisms Induced by UKY500 Mutations

Digestion of purified DNA with a restriction enzyme during an indirect end labelling experiment involves digestion of total genomic DNA, usually with an infrequently cutting restriction enzyme. Consequently, ethidium bromide staining of the agarose gel usually reveals a smear of relatively long digestion products, with the MNase generated nucleosomal ladder still visible at the bottom. *HinfI*, however, cuts fairly frequently as it recognises a 5bp palindrome with no preference for the middle position. This produces a more distinct banding pattern, as in the ethidium stained gel in figure 4.15.

Interestingly, the restriction fragment pattern generated by UKY500 is different from that of the other strains. There are several possible reasons for this: a) gross rearrangement of the genome; b) a direct effect on sequence recognition by *HinfI*; c) alteration of the relative proportions of DNA sub-populations.

The robustness of UKY500 makes the first possibility seem unlikely, and that the difference does not result from the methylation sensitivity of *HinfI* is demonstrated in figure 4.16. *HpaII* and *MspI* are isoschizomers, but cleavage of mammalian genomic DNA by *HpaII* is blocked by CpG methylation (figure 4.16a). Yeast is not known to methylate its DNA, and the possibility that the partially 'humanised' histone H4 expressed by UKY500 might have created a target site for a latent/evolving methylase activity was dismissed using *HpaII* and *MspI*: the restriction patterns generated by the isoschizomers are the same, and thus discount a vertebrate-type

DNA methylation. The *HpaII/MspI* digests do however re-affirm what was seen using *HinfI*, as the patterns generated by digestion of UKY500 DNA are yet again different from the other three strains (figure 4.16b).

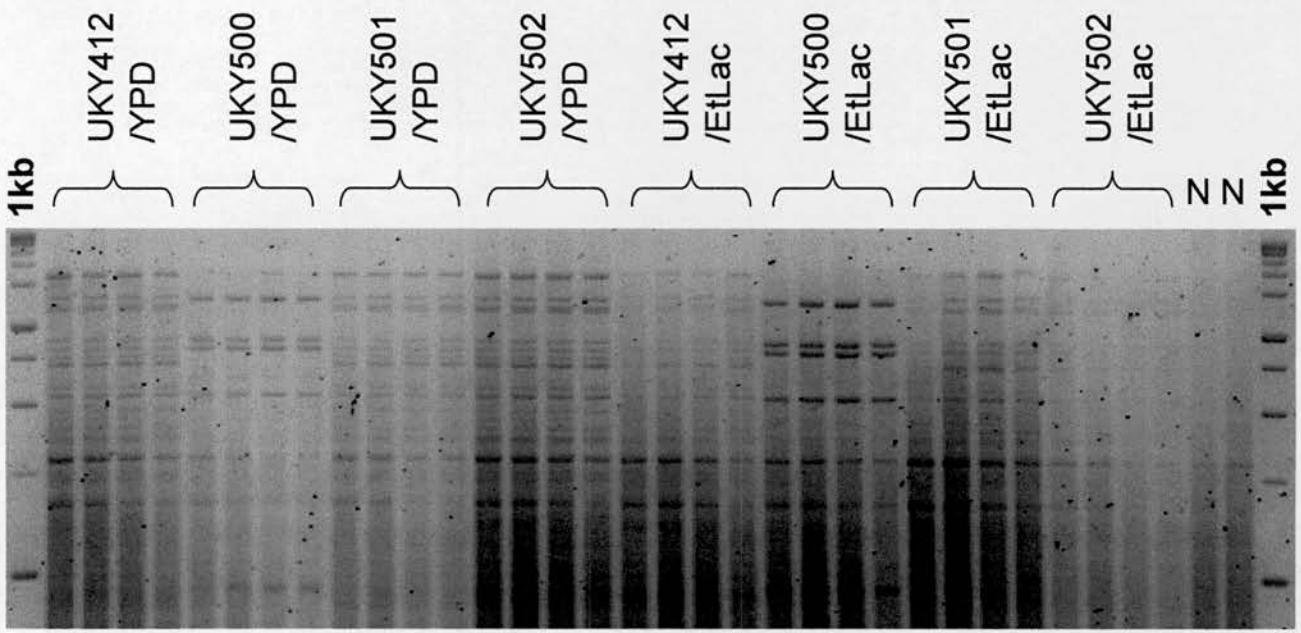

Figure 4.15 Different restriction fragment pattern in UKY500 DNA was revealed during nuclease mapping at the *SUC2* gene. Nuclei prepared from strains grown under repressive (YPD) and de-repressive (EtLac) conditions were subjected to a time-course of partial digestion by micrococcal nuclease. Purified DNA was subsequently digested to completion by *HinfI*. Naked DNA (N) was treated similarly. The fragments were separated by agarose gel electrophoresis along side a 1kb size marker and stained with ethidium bromide. The pattern from digestion of UKY500 DNA is different from that of the other strains under both conditions.

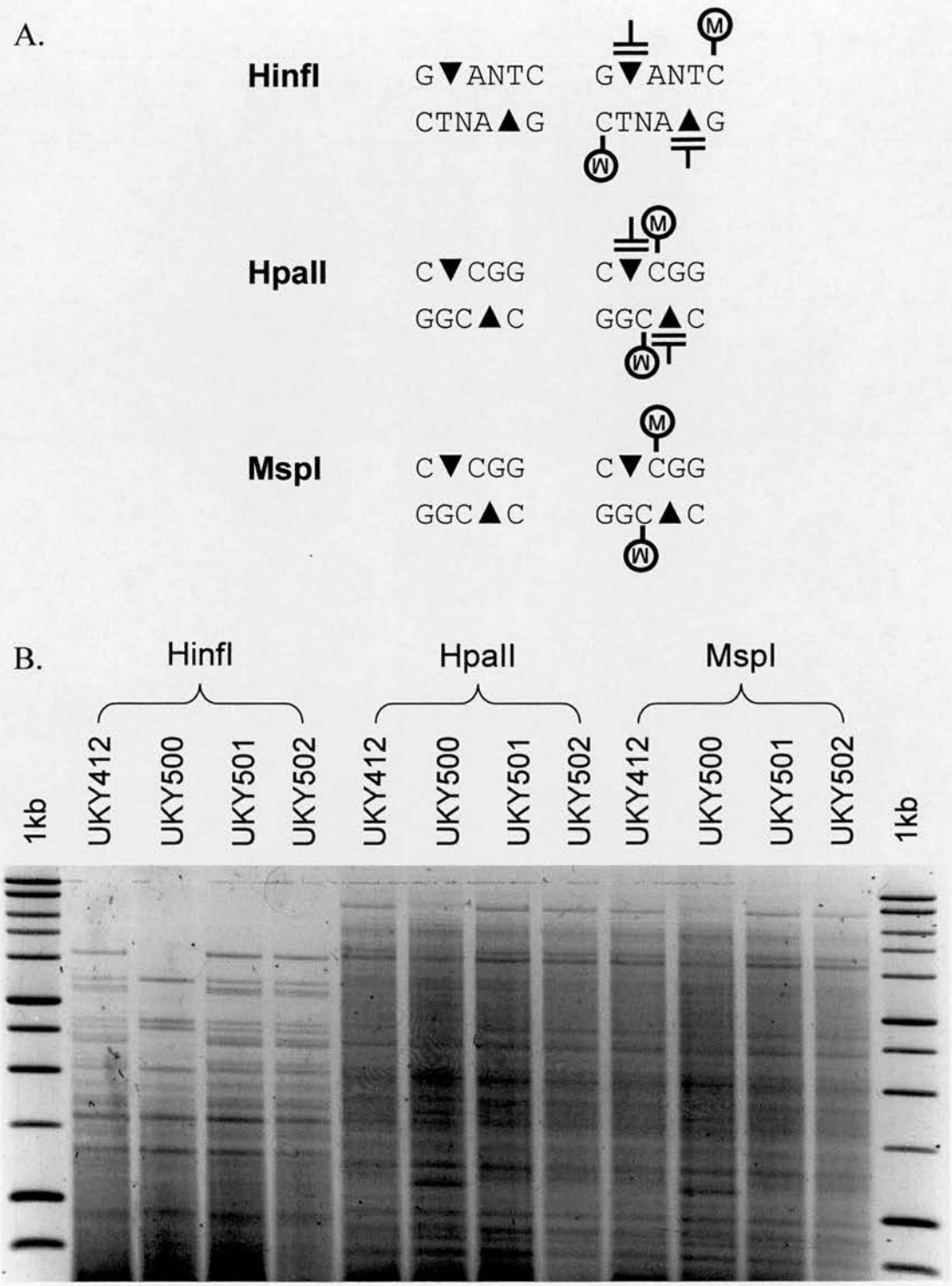

Figure 4.16 Digestion with isoschizomers *HpaII* and *MspI* A) DNA cleavage by *HinfI* and *HpaII* restriction enzymes is blocked by methylation of cytosine bases in CpG dinucleotides. *MspI* recognises the same DNA sequence as *HpaII* but is unaffected by methylation. B) Digestion with isoschizomers *HpaII* and *MspI* confirms the different restriction digest pattern seen in UKY500-*HinfI* digests, and demonstrates that it is not due to methylation of DNA.

4.5 UKY500 is Missing Mitochondrial DNA

4.5.1 Southern Blot Analysis

Although indirect end labelling experiments use nuclei as the substrate, the method of nuclei preparation described in materials and methods is relatively crude, and the preparation is not pure. Therefore, the respiratory deficient phenotype of UKY500 made the mitochondrial genome an obvious candidate for having generated the different restriction pattern seen in figures 4.15 and 4.16b. Figure 4.17 shows Southern blot of the gel in figure 4.16b, co-hybridised to the *SUC2* indirect end labelling and Northern blot probe, and a 257bp probe corresponding to the mitochondrial *COXII* gene encoding cytochrome-c-oxidase. The *COXII* probe was PCR amplified from a non-commercial genomic DNA preparation (as this contained sufficient mtDNA). The results clearly show that UKY500 is missing the mtDNA corresponding to the *COXII* gene.

Even after overexposure, no bands corresponding to *COXII* are visible in the Southern blotted UKY500 DNA digests (data not shown). This indicates that there are no copies of this particular gene in the cell (as opposed to an effect of fewer mitochondria). However, use of a single probe does not determine whether UKY500 is missing all mitochondrial DNA (ρ^0), or contains large deletions (ρ^-).

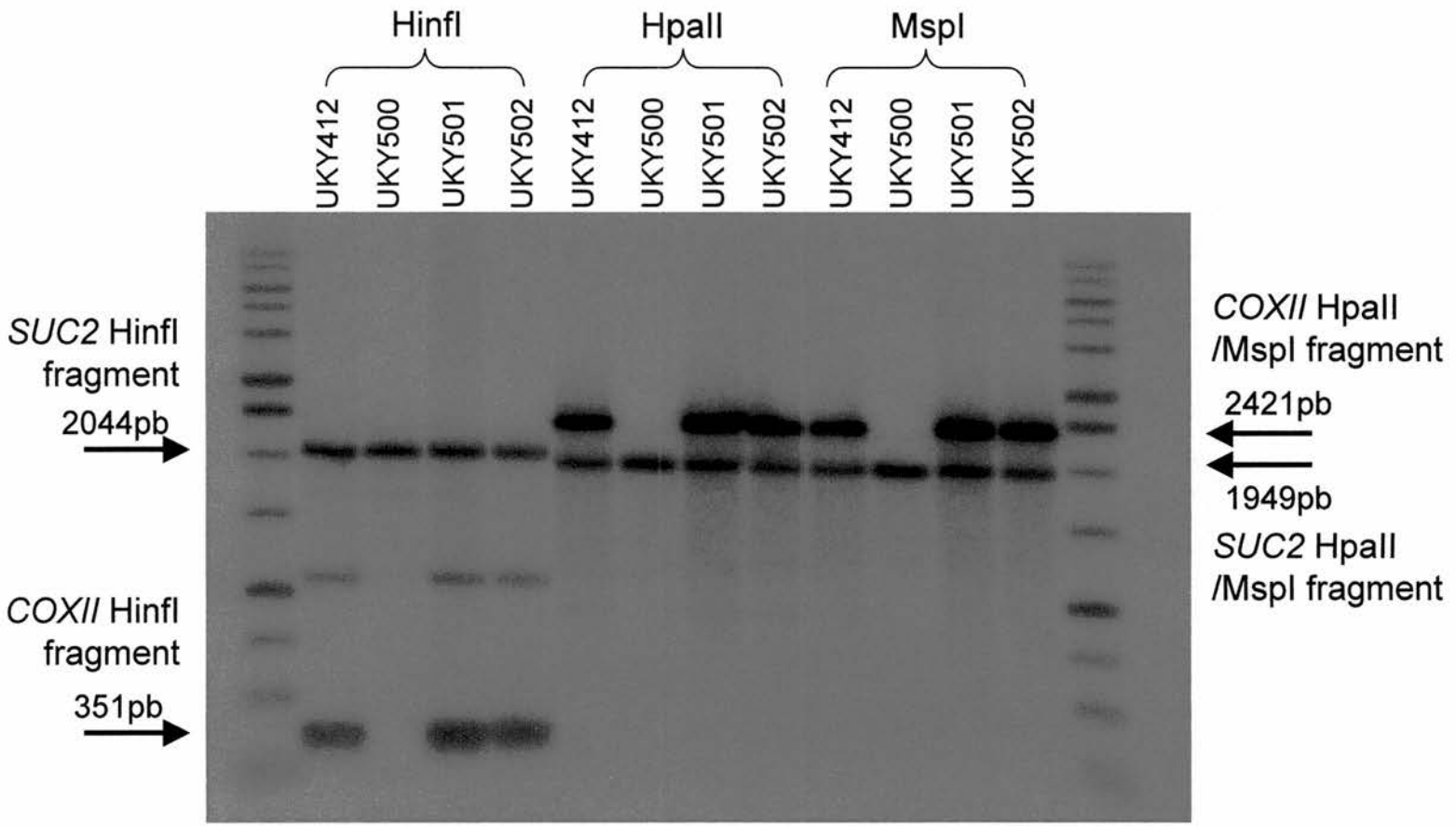

Figure 4.17 Southern blot of *SUC2* and *COXII* demonstrates that UKY500 is missing mitochondrial DNA. DNA prepared from each of the four strains was digested with *HinfI*, *HpaII* and *MspI*. Fragments were separated in an agarose gel alongside a radiolabelled 1kb size marker. DNA was transferred to nitrocellulose in a Southern blot, and co-hybridised to the 285bp *SUC2* indirect end labelling probe, and a 257bp probe corresponding to the mitochondrial *COXII* gene. Even after over exposure, no band hybridising to *COXII* can be detected in any of the UKY500 digests, indicating that the mutant has lost the mitochondrial DNA corresponding to this gene. The intermediate band apparent in the *HinfI* digests is presumed to be a partial digestion product.

4.5.2 Fluorescence Microscopy

DAPI (4', 6'-diamidino-2-phenylindole) is a water soluble fluorochrome that binds specifically to double stranded DNA, exhibiting enhanced fluorescence in the association. Low concentrations of DAPI allow visualisation of nuclear and mitochondrial DNA, thus providing a way of distinguishing between ρ^0 and ρ^- genotypes. Figure 4.18 shows the results of DAPI staining fixed UKY412 (WT), UKY500, UKY501 and UKY512 cells. The large, bright spots are nuclei, and the smaller cytoplasmic speckles correspond to mtDNA. UKY500 clearly does contain some mtDNA, and as such must be of the ρ^- genotype.

There is less fluorescence associated with mtDNA in UKY500 than in the other strains. However it cannot be determined from DAPI staining alone if this is due solely to large deletions within the mitochondrial genome, or whether there is also a reduction in the number of mitochondria. Attempts were made to address the question of mitochondrial number, but this is was made difficult by the fact that mitochondria specific stains rely on the presence of a membrane potential, which does not exist in dysfunctional mitochondria.

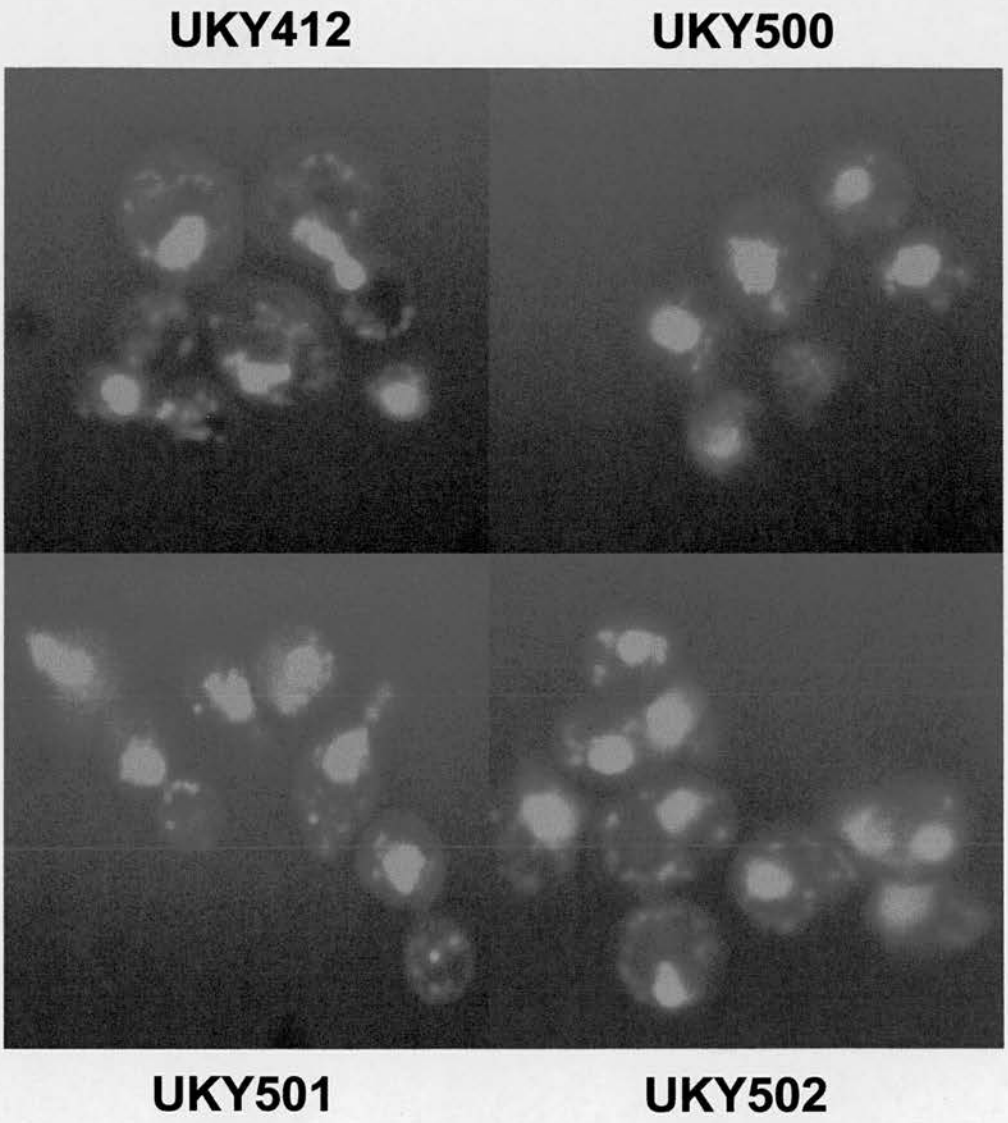

Figure 4.18 DAPI staining of fixed cells reveals that UKY500 is a *ρ- petite.* DAPI staining shows nuclear DNA as a large, bright spot, and mitochondrial DNA as small 'speckles' of cytosolic fluorescence. This demonstrates that UKY500 has not lost all mitochondrial DNA, thus defining it as a *ρ- petite* mutant.

4.6 Histone H4 Acetylation Levels

Figure 4.6 demonstrates that histone H4 mRNA is transcribed in all mutants, and the Western blot analyses presented in figure 4.19b show that the mutant histone H4 proteins are expressed. Yeast cell extracts were prepared and acid extracted to enrich for basic proteins, and separated on a 15% SDS-PAGE gel. Histone H4 is not distinguishable on the coomassie blue stained gel (figure 4.19a), but blotting with rabbit α-histone H4 polyclonal antibody lights up a band at the same position as the purified chicken octamer and calf histone H4 controls, in all lanes (figure 4.19b). On comparison of the histone H4 signals with the total protein extracts visualised on the coomassie blue stained gel, it appears that there are similar levels of histone H4 in all strains.

Duplicate gels were Western blotted with a rabbit polyclonal antibody raised against a peptide corresponding to amino acids 2-19 of *Tetrahymena* histone H4, acetylated on each of the four acetylatable lysine residues (K5, K8, K12, K16). Normalisation of these results to calf histone H4 (1μg was loaded per gel) and total histone H4 reveals reproducibly much lower levels of acetylated histone H4 in UKY500; an acetylated H4:H4 ratio of only 29% of WT (table 4.3). In UKY501 this value is up to 64%, and UKY502 has 95% of the acetylated H4:H4 ratio of WT.

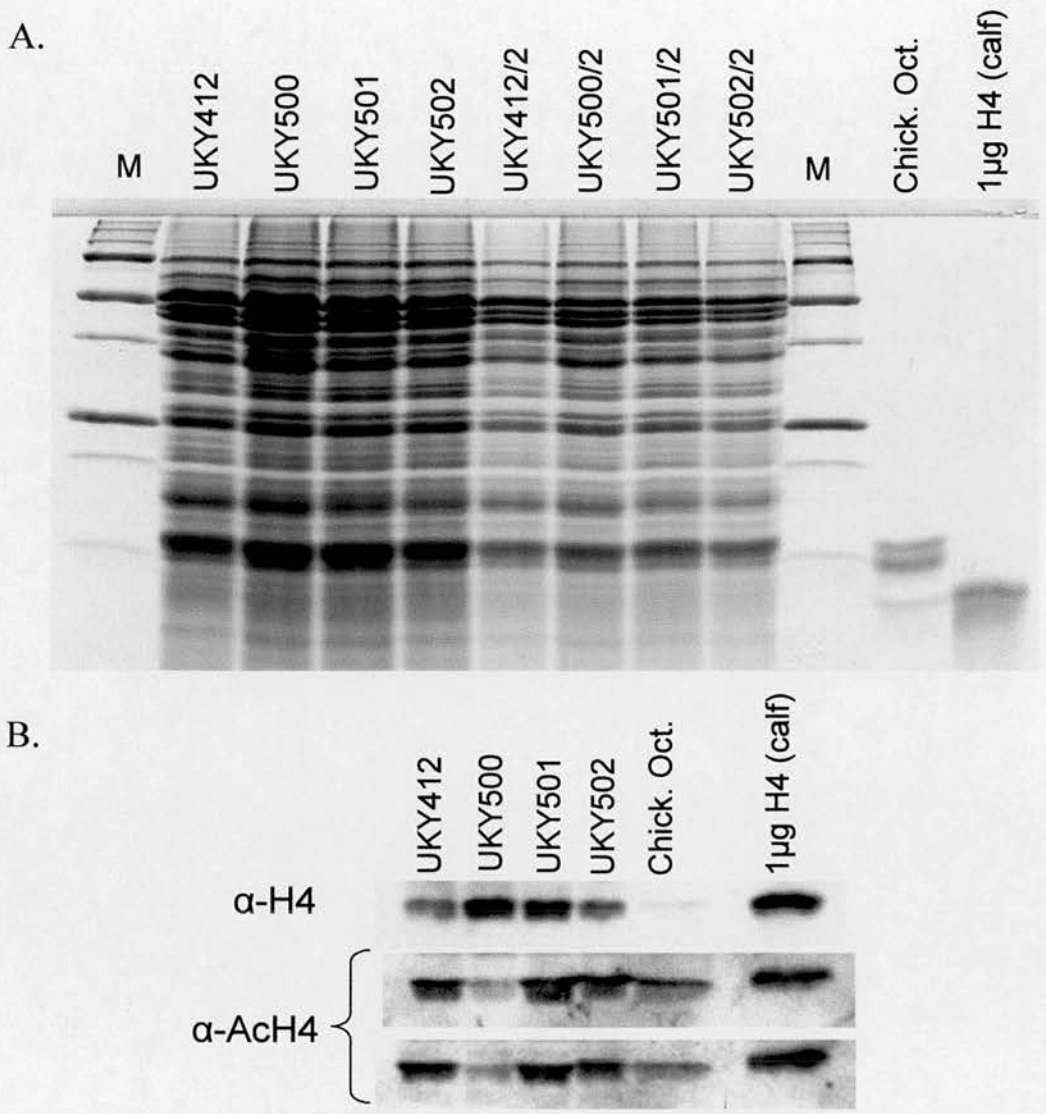

Figure 4.19 Western blot of histone H4 and acetylated histone H4. A) Yeast whole-cell extracts were prepared and acid extracted to enrich for basic proteins. Dilutions were separated on a 15% SDS-PAGE gel along side markers (M) and controls of purified chicken histone octamer (chick oct.) and calf histone H4, then transferred to nitrocellulose. B). Western blotting with poly-clonal antibodies specific for histone H4 (α-H4) or total acetylated histone H4 (α-AcH4) demonstrates that all strains have similar levels of histone H4 protein, but differ in the degree of total histone H4 acetylation.

	UKY412	UKY500	UKY501	UKY502
AcH4:H4	100%	29%	64%	95%

Table 4.3 Relative levels of histone H4 acetylation. Western blot signals were normalised to calf histone H4 and total histone H4, and averaged across the duplicates. The ratio of acetylated histone H4 to histone H4 (AcH4:H4) in UKY412(WT) were arbitrarily set to 100%.

4.7 Mating

Positions 21 to 29 in the histone H4 amino acid sequence have been shown to be important for repression of the silent mating loci (Johnson *et al.*, 1992). Mutation of residue 21 to proline, serine or alanine reduces mating efficiency in a *MATa* background by 5 to 7 orders of magnitude (the strains are isogenic to those used in this work).

In order to investigate whether the I21V mutation also leads to a reduction in mating efficiency, UKY412 (WT), UKY500, UKY501 and UKY502 were mated with a *MATα* tester strain as described in section 2.3.5.

Mating efficiency in the laboratory is critically dependent upon three factors as defined by Dutcher and Hartwell: growth phase, cell ratio/density, and time (Dutcher and Hartwell, 1983). Some methods are also better than others: mating cells on a filter is more efficient than mixing cells in liquid culture (Hartwell, 1973), and pre-synchronising cells with the opposite mating pheromone also increases mating efficiency (Reid and Hartwell, 1977). Thus the same strains can mate with very different efficiencies depending on the conditions and methods employed. Whilst a crude experiment will distinguish between mating competent and sterile strains, careful optimisation is needed to identify more subtle phenotypes.

Results from the mating experiment are shown in table 4.4. These imply that all strains are mating competent, and that the I21V mutation does not confer a sterile

phenotype. This is said with caution however, as the mating efficiencies are rather low, and I was not able to reproduce the results, due to failed mating of the controls.

If I21V has a negligible effect on mating efficiency, then this is consistent with the model put forward by Kayne *et al.* They proposed that the relatively uncharged amino acids between 21 and 29 in the tail of histone H4, and the basic domain from 16 to 19 also important for repression (Kayne *et al.*, 1988), from an amphipathic α-helix in the presence of DNA or an acidic protein. Whilst the proline, serine and alanine mutants isolated in their work would disrupt the structure or nature of this helix, the very conservative I21V mutation would most likely not.

Strain	Mating efficiency	Relative to WT
UKY412	4.6	1
UKY500	8.5	1.8
UKY501	5.1	1.1
UKY502	6.7	1.5

Table 4.4 Mating efficiency is expressed in number of successful conjugations per thousand cells, and relative to the mating efficiency of UKY412 (WT), which is arbitrarily set to 1.

4.8 Discussion

Construction of an *S. cerevisiae* mutant expressing a fully 'humanised' version of histone H4, and another strain bearing only the I21V substitution in the N-terminal tail completes the set of mutants analysed in this study. The new strains survive the glucose shift viability test and show growth rates similar to WT under optimal conditions, demonstrating that the mutant histone H4 proteins can be incorporated into nucleosomes and support yeast survival. Any phenotypic differences displayed by the mutants are not due to differences in levels of histone H4, as demonstrated by Northern and Western blotting.

As discussed in the general introduction, much of the yeast genome is poised for activation. As such, yeast chromatin has a more open structure than that of higher eukaryotes, which renders it more sensitive to nuclease digestion. Analysis of bulk chromatin from UKY412 (WT), UKY500, UKY501 and UKY502 reveals no gross differences between strains in MNase digestion sensitivity, or in the nucleosomal repeat length. This suggests that the incorporation of mutant forms of histone H4 related to their human counterpart into yeast nucleosomes containing WT yeast histones H3, H2A and H2B, does not 'tighten' chromatin structure on a genome wide scale. In its strictest terms, MNase digestion only provides information about the accessibility of the linker DNA between nucleosomes, and it would be interesting to see if any of the mutants have an effect on sensitivity to DNAseI (which makes single stranded cuts in the DNA minor groove), or restriction enzyme accessibility.

The partial-rescue of growth on non-fermentable carbon sources conferred by introduction of the I21V mutation into the UKY500 background is a surprising result, but the reason for this phenotypic rescue becomes obvious on examination of the state of the mitochondrial genome. UKY501 regains respiratory competence because it does not experience the mtDNA loss observed in UKY500. A possible explanation for this is that the expression of some genes involved in mitochondrial function and mtDNA maintenance is affected to a greater degree by introduction of the 'humanising' mutations in the histone H4 globular domain alone, than by the full complement of mutations. In UKY500 expression of these genes might be below the threshold for retention of mtDNA. The I21V mutation introduced into UKY501 could somehow restore expression of these genes to a level above the threshold necessary for mtDNA maintenance, albeit not to WT levels, hence its growth on non-fermentable carbon sources is still slightly impaired. This idea is supported by the enhanced growth of UKY502 compared to UKY412 (WT) on EtLac.

The phenotypic pattern apparent on a non-fermentable carbon sources is also observed on growth on YPD at 37°C. Temperature sensitivity of UKY500 and UKY501 could result from greater instability of interactions between mutant and WT histones within the nucleosome core at higher temperature, as discussed in the previous chapter. The enhanced growth of UKY502 compared to UKY412 (WT) at 37°C is more difficult to explain in such general terms. This may suggest that the sensitivity to temperature results from a similar effect on genes required for growth under temperature stress, as it does for those required for respiration (see general discussion).

Examination of events at the *SUC2* gene upon relief of glucose repression reveals hyper-induction of the gene in UKY500, even though this mutant grows poorly on media containing raffinose as the carbon source. From indirect end labelling experiments it appears that the remodelling of nucleosomes in the *SUC2* promoter is consistent with normal regulation of this gene; they do not necessarily imply that hyper-induction of gene expression is a direct result of mutant histone H4 expression.

Events at the *SUC2* and *CYCI* genes must be re-assessed in light of the discovery that UKY500 is a ρ^- *petite* mutant missing mtDNA. The retrograde pathway of eukaryotes is a signal transduction cascade mediating information transfer from the mitochondrion to the nucleus (reviewed by Butow and Avadhani, 2004). In yeast with dysfunctional mitochondria, the retrograde response serves to initiate changes in gene expression patterns relating to carbohydrate metabolism. The classes of genes affected are discussed in more detail in the next chapter; suffice to say here that the results of genome wide analyses comparing ρ^0 and ρ^+ strains differ depending on carbon source and strain (Traven *et al.*, 2001; Epstein *et al.*, 2001).

Traven *et al.* observe a two-fold increase in *CYCI* expression in glucose grown ρ^0 cells compared to ρ^+. Epstein *et al.* observe an increase in *SUC2* expression of raffinose grown cells ρ^0 cells (compared to raffinose grown ρ^+ cells), that is abrogated by deletion of the Rtg1/2/3 proteins central to the retrograde response. Although not directly comparable to the experiments described here, these results demonstrate that *CYCI* and *SUC2* are among the many genes affected by the

retrograde response. The differences observed between ρ^- UKY500 and the other ρ^+ strains at these genes may thus be a normal response to differing upstream signals, and not a direct consequence of the histone H4 mutations.

Why does UKY500 lose mtDNA? As stated in the introduction, mtDNA is inherently unstable and its maintenance is influenced by many different factors. Comparison of UKY500 growth on glycerol plates streaked soon after its generation (figure 3.8b), and the EtLac plate in figure 4.9a streaked many months later, would imply that the mtDNA was lost over a number of generations. This would explain the breakthrough colonies on the glycerol plates, which no longer emerge on EtLac.

The reduction in genome-wide levels of histone H4 acetylation in UKY500 is striking. Again this phenotype is partially corrected by introduction of the I21V mutation in UKY501, and UKY502 has WT histone H4 acetylation levels. The polyclonal antibody used in the Western blots detects acetylation on any of the histone H4 acetylatable lysines, so does not determine which residue(s) is affected Western blotting with more specific antibodies would determine this. However, if acetylation by Esa1p or Sas2p is reduced in UKY500 and UKY501 as a consequence of the introduced mutations, it is likely that histone H4K16 would be affected since both proteins have an affinity for this site. That said, their redundant affinities for this site could perhaps mean that this position is less likely to show reduced acetylation.

The reduced histone H4 acetylation in UKY500 might be either a cause or effect mtDNA loss, but the former would perhaps seem more likely. If the altered histone

H4 acetylation levels were downstream of mtDNA loss, one would expect to see loss of mtDNA in UKY501, which does not appear to be the case (figures 4.17-18 and section 5.5.3).

One plausible hypothesis to link the observations made in this chapter is that histone H4 acetylation has been affected directly by the 'humanising' mutations, and that this leads to an altered expression of genes involved in mitochondrial function. Interestingly, genome-wide analyses of expression patterns in *Drosophila* cell lines in which the SIN3 complex has been inactivated by RNAi, show increased expression of a substantial number of genes involved in mitochondrial and cytosolic energy generation, and mitochondrial protein translation (Pile *et al.*, 2003). The SIN3 complex functions as a transcriptional repressor in eukaryotes by virtue of its Rpd3p histone deacetylase component, establishing link between acetylation levels and regulation of expression of genes involved in mitochondrial function.

But why does the I21V substitution rescue the acetylation, and carbon source and temperature sensitivity phenotypes? The N-terminal tails of histone proteins extrude from the core nucleosome particle, where they are involved in the formation of higher order structures, and also form interaction sites for macromolecular complexes that confer and recognise post-translational modifications (see general introduction). Considering this, and the structure of the yeast core nucleosome (figure 3.15), the mutations introduced into the globular domain of histone H4, and I21V are not expected to be particularly close in space in the context of a single nucleosome. In addition, the substitutions at positions 54, 56, 60, 64 and 69 are

buried within the quaternary structure of the nucleosome. However, the regions obviously interact on some level.

The simplistic interpretation would be that action of a histone H4 acetyltransferase has been disrupted by the 'humanising' mutations in the histone fold domain, and that a functional interaction is restored by introduction of the I21V substitution. This could be due to a general distortion of protein-protein or protein-DNA interactions within the nucleosome particle, or alteration of specific residues at interaction points between histone H4 and an acetyltransferase complex at the site of mutation. This could be due to the two regions of mutation having an influence on one particular activity, or they could affect related activities. More western blots and CHIP experiments on specifically affected genes could shed some light on this.

Whether the rescue results from intra- or inter-nucleosomal interactions is open to discussion. Notably, the X-ray crystal structure of the nucleosome core particle reveals that residues 16-25 of histone H4 interact with a negatively charged pocket of the H2A-H2B dimer in the adjacent nucleosome in the lattice. This interaction could conceivably be weakened by acetylation of histone H4K16 (Luger *et al.*, 1997). It is possible that the I21V mutation is interacting with the globular domain mutations in the neighbouring nucleosome.

Results of the mating experiments indicate that silencing at *HML* and *HMR* is intact. Not only does silencing in this region depend on interactions between SIR proteins and the hypoacetylated histone H4 N-terminal tail, it also requires the non basic

domain between residues 21 and 29 (Johnson *et al.*, 1992). The I21V mutation introduced into UKY502 does not lead to sterility as less conservative mutations at this position have been found to.

In fact, a recurring theme in the literature relevant to the positions of the mutations described here is mutations is silencing: position 21 is implicated in repression of the silent mating loci (Johnson *et al.*, 1992), and the S83A and L84M mutations reside next to a nucleosomal surface vital to transcriptional silencing as highlighted in the previous chapter (Park *et al.*, 2002). It may prove that the 'humanising' mutations are interacting at the level of establishment of facultative heterochromatin.

Chapter 5: Genome-wide Expression Analyses

5.1 Summary

This chapter describes genome-wide expression analyses performed on each of the four strains employed in this thesis. The data imply an overall activation function of the I21V mutation in the histone H4 N-terminal tail, which is tempered by the globular domain mutations. Comparison of WT and *petite* mutant UKY500 transcriptomes reveals only small differences when grown in rich glucose media, a condition under which many inducible genes have low expression levels. Cross referencing of two complementary data sets allows identification of genes whose altered expression might have lead ultimately to loss of mtDNA in UKY500.

5.2 Introduction

When a fermentable carbon source such as glucose is present, expression of genes involved in mitochondrial biogenesis and respiratory activity is down-regulated (whether or not oxygen is present). Upon exhaustion of glucose, transcription is induced of nuclear genes encoding proteins of the mitochondrial transcription and translation apparatus, as well as components of electron transport and oxidative phosphorylation. This is mediated by HAP2/3/4/5 and HAP1 activity in response to glucose and oxygen concentrations, respectively. The alteration of gene expression patterns in response to these environmental changes represents a flow of information from the nucleus to the mitochondrion. But in *petite* cells, increasing expression of

nuclear components of mitochondrial pathways will still leave these pathways incomplete and non-functional, if critical mtDNA encoded proteins are missing. A similar situation arises in ρ^+ cells that are compromised for mitochondrial function due to lesions in nuclear genes of respiratory pathways. Thus a signal response pathway, called the retrograde response, exists in all organisms from yeast to mammals, which allows mitochondria to pass information to the nucleus (reviewed by Butow and Avadhani, 2004).

Retrograde signalling provides an interface between carbon and nitrogen metabolism. Glutamate, a good nitrogen source and precursor to nucleotide and other amino acid biosyntheses, is derived directly from the TCA cycle intermediate α-ketoglutarate (figure 5.1). A key function of retrograde signalling in WT and respiratory deficient cells is to maintain glutamate supplies, and glutamate is a powerful inhibitor of the pathway (Liu *et al.*, 1999). When glutamate concentrations are low, the retrograde response up-regulates the early steps of the TCA cycle that generate α-ketoglutarate, without affecting subsequent steps (Liu and Butow, 1999). This forces the deamination reaction catalysed by glutamate dehydrogenase (*GDH1*) in the direction of ammonium assimilation and glutamate synthesis. However, this siphoning off of TCA cycle intermediates for use in anabolic pathways reduces the levels of TCA cycle substrates. These are replaced by retrograde signalling-dependent activation of other metabolite restoration (anaplerotic) pathways. Increased expression of *CIT2*, the peroxisomal citrate synthase isoform functioning in the first step of the glyoxylate cycle, is characteristic of the retrograde response (Liao *et al.*, 1991). The glyoxylate cycle can convert two carbon compounds

generated from fatty acid oxidation into TCA cycle intermediates such as succinate. Increased Cit2p activity thus facilitates efficient utilization of carbon via the transport of metabolites from the glyoxylate cycle to latter steps of the TCA cycle (as it bypasses the steps of the TCA cycle at which CO_2 is released).

Despite its role in WT cells, much of the available information regarding the mechanism of retrograde signalling has come from comparison of ρ^+ and ρ^0 *S. cerevisiae* strains (for examples: Liu *et al.*, 1999; Traven *et al.*, 2001, Epstein *et al.*, 2001). It is important to note that the ρ^0 state of these mutants was a result of ethidium bromide treatment and not lesions in nuclear genes, which would have complicated the analysis. In respiratory-deficient strains, the retrograde response is constitutively active. This maintains glutamate supplies and homeotic balance, as well as preventing futile gene expression. In this case the TCA cycle is incomplete because succinate cannot be oxidized to fumarate (because the $FADH_2$ generated by oxidation of succinate remains covalently bound to succinate dehydrogenase, until the electrons are passed directly into the electron transport chain (figure 3.2)). The retrograde response induces expression of anaplerotic and peroxisomal pathways, as well as related transporters, to re-supply mitochondria with the TCA cycle substrates oxaloacetic acid (OAA) and acetyl-CoA (Butow and Avadhani, 2004 and references therein). Increased *CIT2* expression is also characteristic of retrograde signalling in respiratory deficient strains. However, the balance of metabolites in this instance means that the peroxisomal glyoxylate cycle donates its TCA cycle intermediate at the level of citrate, not succinate, which cannot be used by respiratory deficient cells. This highlights the importance of metabolite balance in determining the

directionality of reversible enzymatic reactions: systems are not only altered at the level of gene expression.

Increased *CIT2* expression is dependent on the proteins Rtg1p, Rtg2p and Rtg3p (Liao *et al.*, 1991; Liao *et al.*, 1993). Although they are not the sole regulators, *RTG1*, *RTG2* and *RTG3* are central players in the retrograde response. Rtg1p and Rtg3p are basic helix-loop-helix (bHLH) leucine zipper transcription factors, which bind to the consensus GTCAC 'R-box' as a heterodimer (Jia *et al.*, 1997). Rtg3p contains N- and C-terminal activation domains, including a motif at the extreme N-terminus that interacts with the SAGA histone acetyltransferase complex (Massari *et al.*, 1999). Rtg2p is the proximal sensor of mitochondrial dysfunction. Its exact mode of action is unknown, but it is required for dephosphorylation of Rtg3p, which results in translocation of the Rtg1p/Rtg3p heterodimer from the cytoplasm to the nucleus (Sekito *et al.*, 2000, Komeili *et al.*, 2000).

RTG1, RTG2 and *RTG3* are non-essential in yeast, but they play a role in respiratory deficient and respiratory competent strains. For example, TCA cycle genes under HAP2/3/4/5 control in respiratory competent yeast become increasingly RTG-dependent as respiratory competence declines (Liu and Butow, 1999).

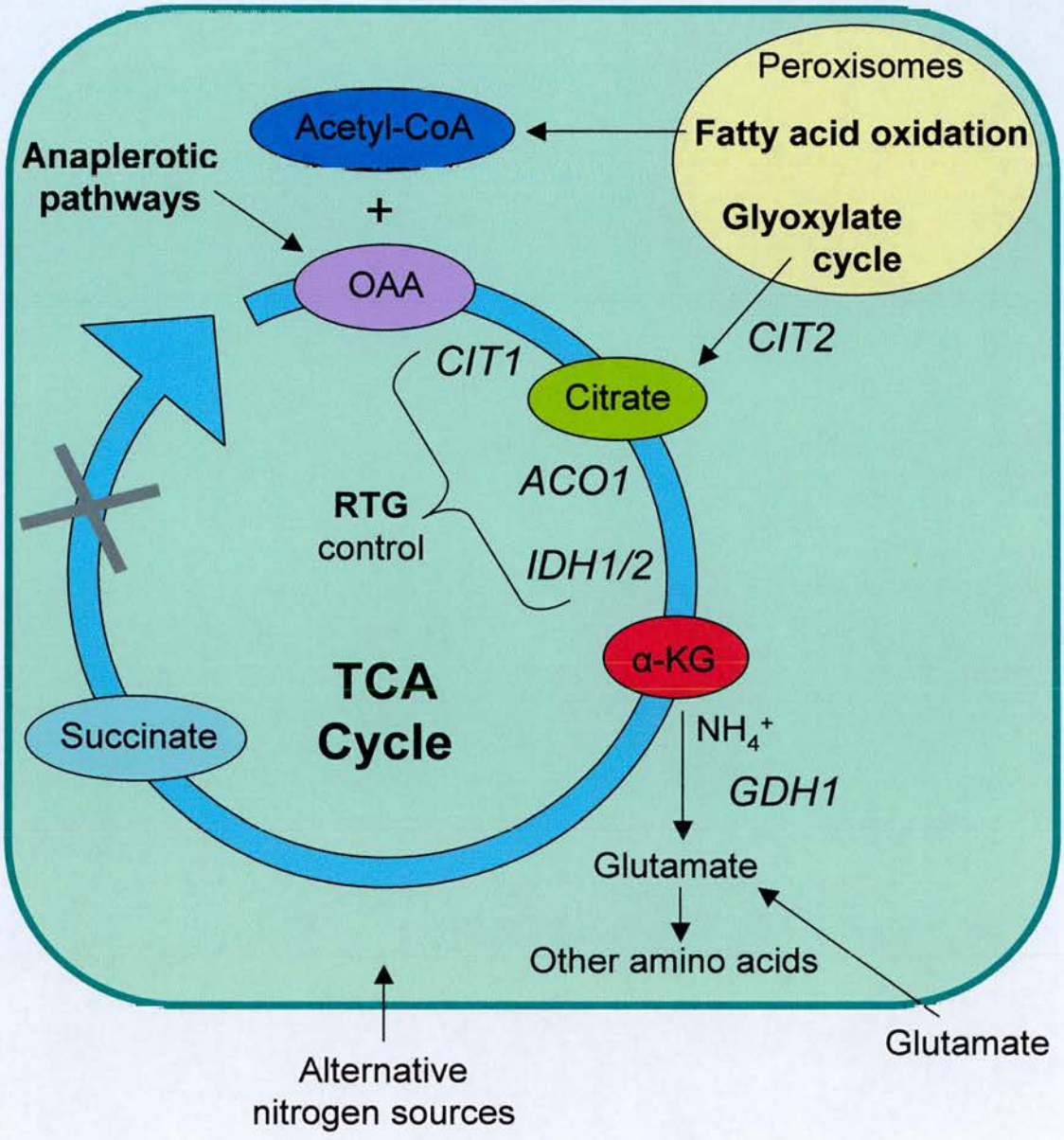

Figure 5.1 Induction of metabolic pathways by retrograde signaling in respiratory-deficient cells. The retrograde response (RTG control) enables respiratory-deficient cells to maintain glutamate supplies by providing substrates for α-ketoglutarate synthesis through anaplerotic pathways, and increasing transport into cells of glutamate and alternative nitrogen sources.

5.3 Aims and Methodology

Genome-wide expression analysis and microarray technology are powerful tools in the present genomics age. They provide a huge amount of gene expression information for a relatively small amount of experimental work. Apart from the intensive data processing, they have other limitations such as cost, and unless one has access to an unlimited number of array slides, experiments must be designed carefully, with specific questions in mind.

A major aim of these microarray experiments was to determine why UKY500 loses mtDNA, and the strategy described below was designed to this aim. Since mtDNA loss triggers alterations in gene expression patterns via the retrograde response, a genome-wide expression analysis comparing UKY500 to (WT) was expected to reveal many downstream effects, as well as more directly affected genes. In addition, despite the lack of phenotypic differences detected in 'disruption phenotype' experiments, it was predicted that the genome wide reduction of histone H4 acetylation levels in UKY500, would nevertheless lead to altered expression of a considerable number of genes.

The range of phenotypes displayed by the 'humanised' mutants on non-fermentable media (and YPD at 37°C), and their relative levels of histone H4 acetylation, are summarized in figures 5.2a and 5.2b, respectively. These patterns suggest that the seven 'humanising' mutations in the globular domain of histone H4 have similar effects whether in the WT or I21V background: relative to these strains they lead to

impaired growth under conditions of non-fermentable carbon source or temperature stress; and they lead to reduced levels of histone H4 acetylation under optimal conditions. This could be due to an effect of the globular domain mutations at the molecular level, which alters gene expression enough to ultimately cause loss of mtDNA in YPD grown UKY500, but not in UKY501 that has the I21V rescuing mutation. Working on this hypothesis, the four strains were compared in the pair wise manner depicted in figure 5.2c.

The list of genes whose expression is decreased in UKY500 compared to UKY412 (WT) should contain genes that somehow play a role in biogenesis/maintenance of mtDNA. If the above hypothesis stands, these genes will also be down regulated in UKY501 compared to UKY502, but not to a level low enough to cause mtDNA loss. Cross referencing of these gene lists is predicted to eliminate downstream effects of mtDNA loss, as well as any effects solely involving I21V. From this 'filtered' list, it should be possible to identify candidate genes responsible for the loss of mtDNA in UKY500.

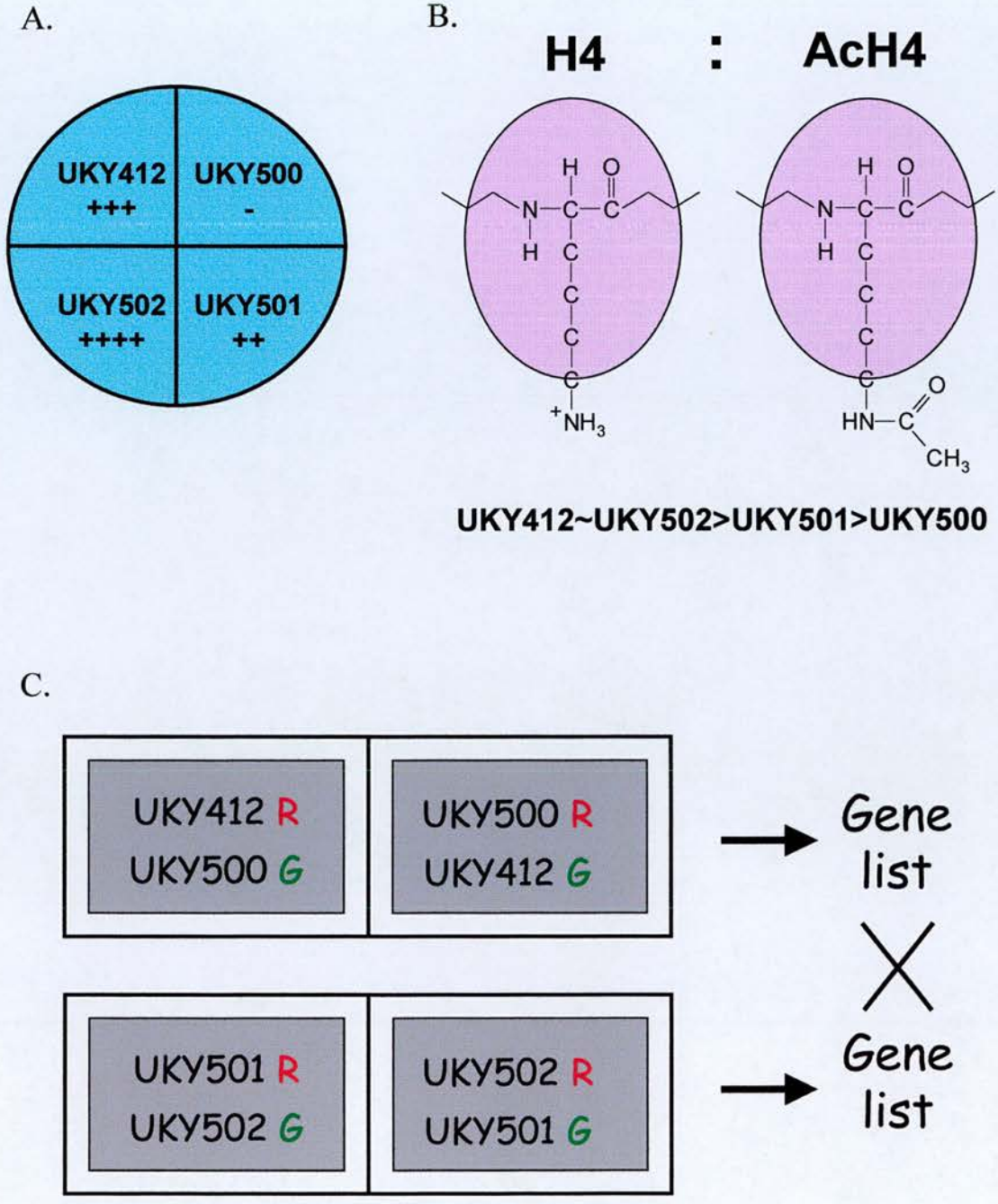

Figure 5.2 Mutant Phenotypes and array comparisons A) Summary of growth rates on respiratory EtLac media. B) Summary of relative levels of histone H4 acetylation. C) Pair wise comparisons of strains were made on the hypothesis that the globular domain mutations in histone H4 have similar effects in either the WT (UKY412) or I21V (UKY502) backgrounds. Gene lists could then be cross referenced to eliminate effects of I21V and those downstream of mtDNA loss.

The details of sample preparation and microarray hybridization are described in section 2.8.3. Figure 5.3 provides an overview of the procedure. RNA prepared from the two strains to be compared on a single array, is reverse transcribed in the presence of either Cy3- or Cy5-deoxy-cytosine-triphosphate (dCTP) by reverse transcriptase (MMLV-RT). The RNA templates are then degraded by RNase treatment, to leave a population of Cy3 (which is red by eye, but fluoresces green) or Cy5 (which is blue by eye, but fluoresces red) labelled cDNA complementary to the cellular transcriptome.

Arrays were performed in duplicate, using independent RNA preparations. Dyes swapped arrays using the same RNA preparations, but with cDNAs conversely labelled with Cy3 and Cy5 were performed simultaneously on the same two-array slide (figure 5.3). Dye swap experiments should theoretically generate identical lists of up and down regulated genes, although the absolute values may differ due to dye bias (see below and section 2.8.3). Combined, these generate four sets of data for each pair wise comparison.

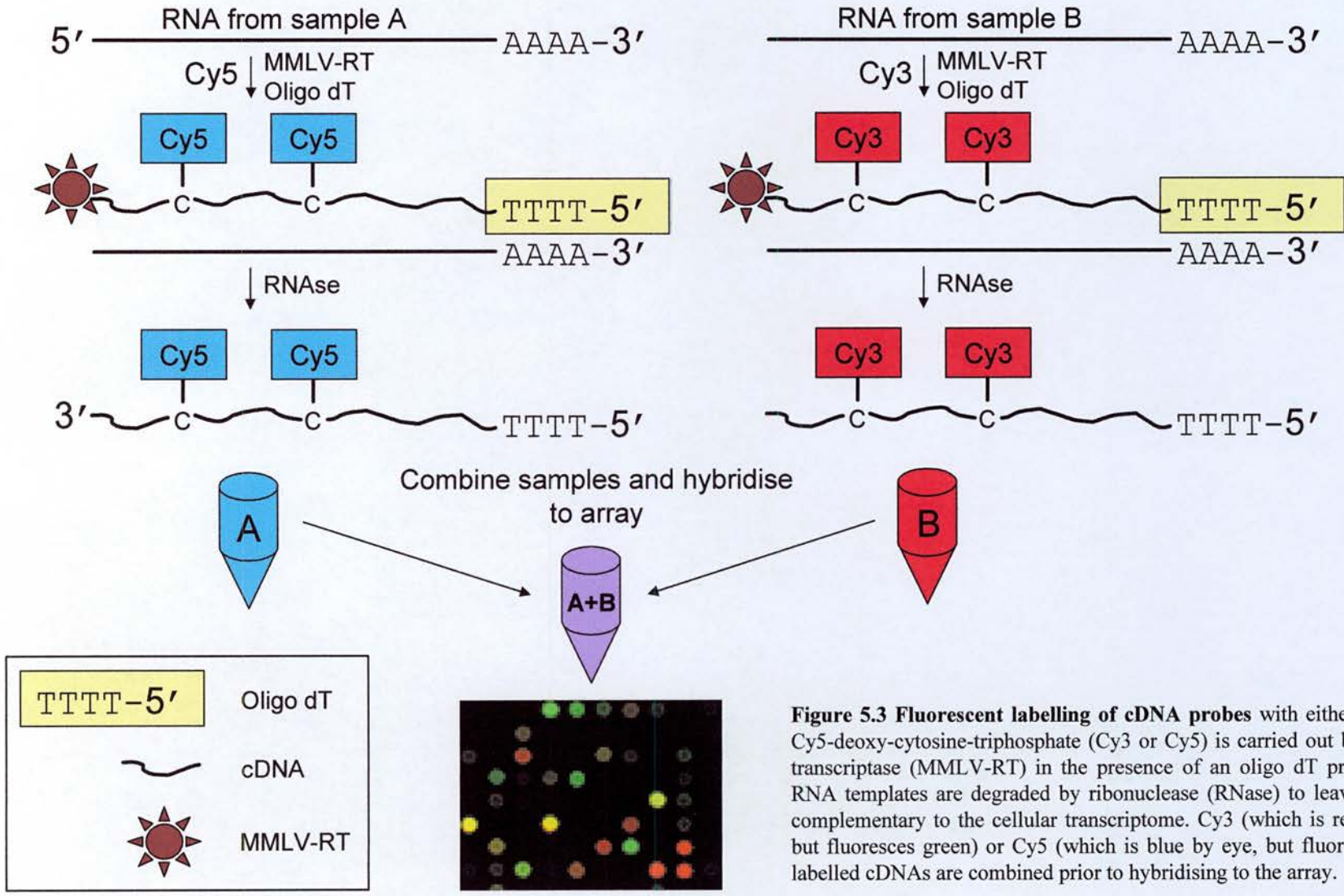

Figure 5.3 Fluorescent labelling of cDNA probes with either Cy3- or Cy5-deoxy-cytosine-triphosphate (Cy3 or Cy5) is carried out by reverse transcriptase (MMLV-RT) in the presence of an oligo dT primer. The RNA templates are degraded by ribonuclease (RNase) to leave cDNAs complementary to the cellular transcriptome. Cy3 (which is red by eye, but fluoresces green) or Cy5 (which is blue by eye, but fluoresces red) labelled cDNAs are combined prior to hybridising to the array.

5.4 Results # 1

5.4.1 UKY412 versus UKY500 Microarray

Figure 5.4a-d plots the hybridised cDNA emission intensities for each array comparing UKY412 (WT) and UKY500. In each case, green processed signal plotted on the x-axis corresponds to the normalized Cy3 emissions, and red processed signal plotted on the y-axis corresponds to the normalized Cy5 emissions. Normalisation was as described in section 2.8.3. Positive and negative control spots have been removed. The red line represents no change in gene expression (a red/green ratio of 1); the dark and light green lines represent two- and 10-fold changes in gene expression levels, respectively. Dye-normalization assumes that the central tendency of the data is 1, and the majority of the data set should sit evenly around this line. The correlation coefficients (c) of the two data sets are indicated for each array.

From the scatter plots in figure 5.4, several points are immediately obvious. Firstly, the data sits neatly around the length of the red line, with no tendency to slump towards the lower values, which can indicate RNA degradation. Secondly, the duplicate experiments (a and c, and b and d) correlate very well (correlation coefficients of 0.89 and 0.87 for A01 and A02 respectively), and the dye swap experiments (a and b, and c and d) show inverse patterns (see the circled *OLI1* and *IHN1* genes for reference). This demonstrates that the data are of good quality, and highly reproducible. Thirdly, the bulk of the data points fall between the two dark green lines that indicate two-fold changes in gene expression. Two-fold changes are

often taken as the bench-mark for biological significance; thus, it appears that most genes are similarly expressed by the two strains. Fourthly, there is a small set of genes that are clearly expressed to a greater level in UKY412 (WT) than UKY500.

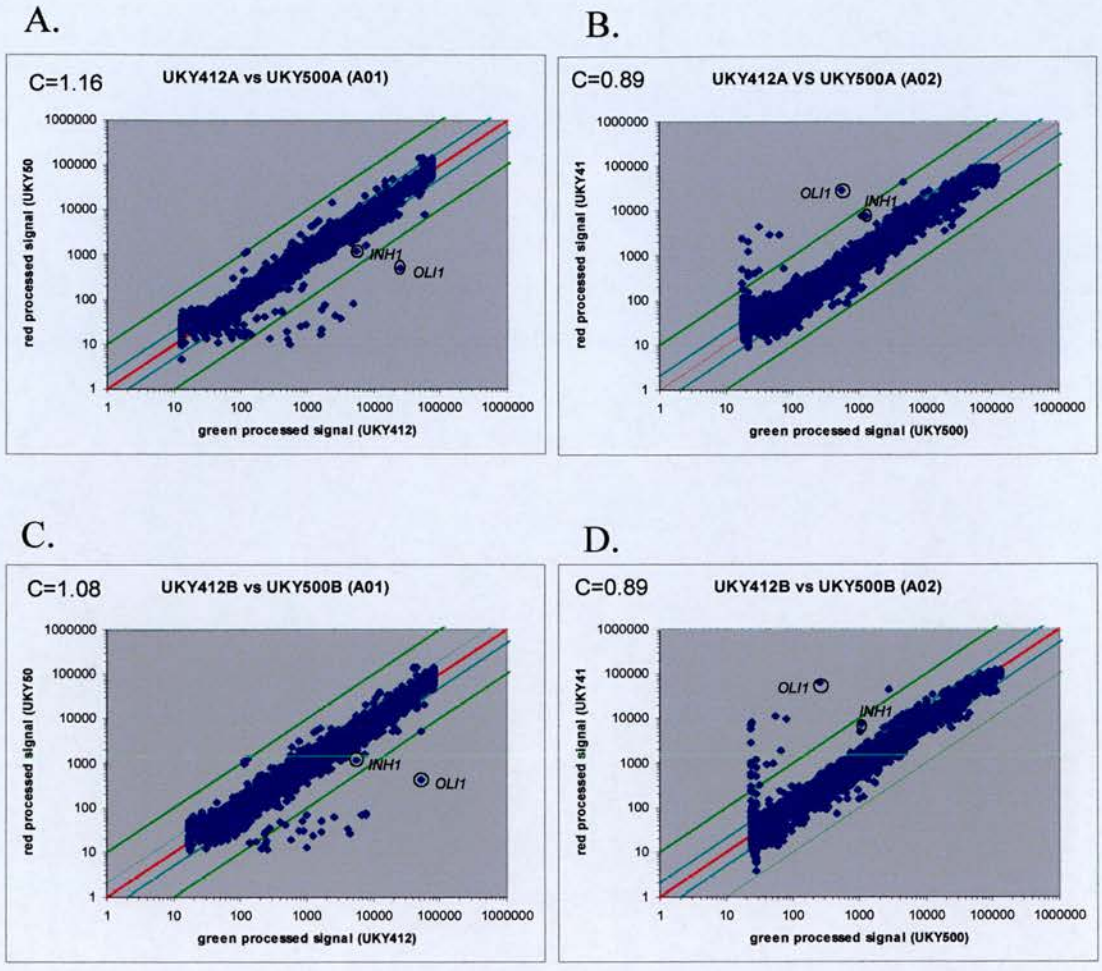

Figure 5.4 Hybridised cDNA emission intensities for each array comparing UKY412 (WT) and UKY500. A and C represent Cy3 labelled UKY412 and Cy5 labelled UKY500. B and D represent Cy3 labelled UKY500 and Cy5 labelled UKY412. Points are plotted on a logarithmic scale. Green processed signal plotted on the x-axis corresponds to the normalized Cy3 emissions. Red processed signal plotted on the y-axis corresponds to the normalized Cy5 emissions. Normalisation was as described in materials and methods. Positive and negative control spots have been removed. The red line represents no change in gene expression; the dark and light green lines represent two- and 10-fold changes in gene expression levels, respectively. The correlation coefficients (c) of the red and green data sets are indicated for each array.

5.4.2 Microarray versus Northern Blot

To confirm that the data from the genome-wide microarray analyses correlate with data obtained from single gene assays, the expression levels of fifteen representative genes were tested individually in Northern blots (figure 5.5 and table 5.1). Three large gels were run using the same RNA preparations as used in the microarrays. Each gel was then cut into eight duplicate mini-gels, which were then Northern blotted separately and hybridised to a PCR amplified probe specific for each of the genes indicated (figure 5.5 and table 5.1, column a). Local background was subtracted, and expression levels were normalized to the relevant value of 28S rRNA (table 5.1, column b) averaged across the duplicate mini-gels. The ratio of mRNA levels between UKY500 and UKY412 (WT) was then calculated (table 5.1, column c).

Values for the ratio of mRNA levels between UKY500 and UKY412 (WT) observed in the microarrays are mean averages taken from all four arrays. Figure 5.6 is a bar graph depicting the UKY500:UKY412 (WT) ratio across these fifteen genes as calculated from Northern blots and microarrays. Examination of this graph shows that the data sets correlate very well.

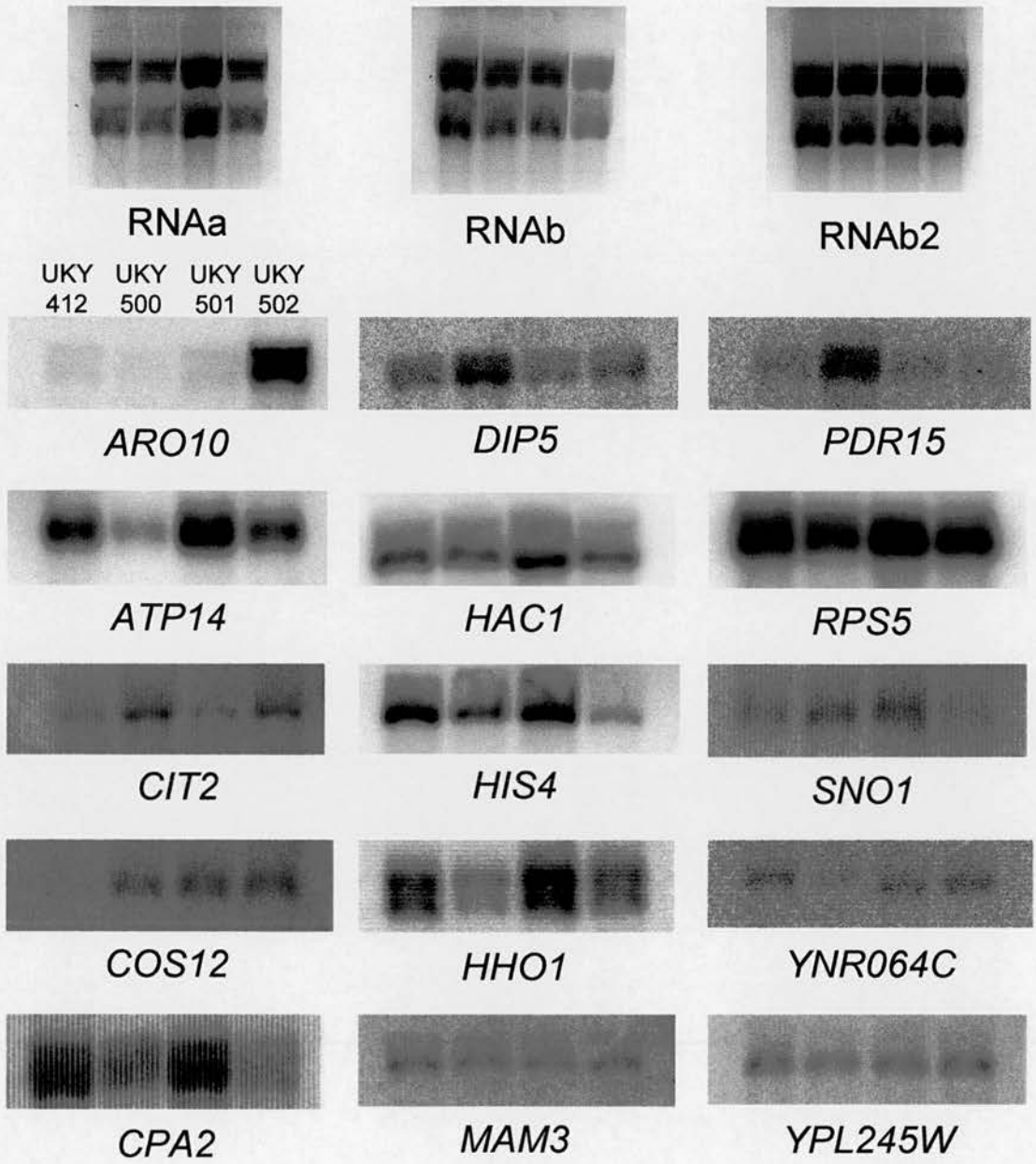

Figure 5.5 Northern blots to validate microarray data were performed at 15 independent genes. Three large gels were run using the same RNA preparations as used in the microarrays. Each gel was then cut into eight, representatives of which are shown in the top 3 ethidium bromide stained gels. These were Northern blotted separately, and hybridized to a PCR amplified probe specific to each of the genes indicated in the lower 15 panels. In each case the strains are loaded in the same order as indicated for *ARO10*.

GENE	GEL	UKY500 /UKY412	UKY502 /UKY501
PDR15	RNAb	3.50	1.04
CIT2	RNAb	2.62	4.19
COS12	RNAb	7.42	1.62
DIP5	RNAb	2.14	1.55
SNO1	RNAb	1.89	0.34
ATP14	RNAa	0.44	0.80
RPS5	RNAa	0.85	0.88
YNR064C	RNAa	0.45	1.70
HHO1	RNAa	0.60	0.83
ARO10	RNAa	0.70	12.27
HAC1	RNAa	1.12	0.75
HIS4	RNAb2	0.74	0.28
CPA2	RNAb2	0.71	0.32
YPL245W	RNAb2	0.88	1.07
MAM3	RNAb2	0.82	0.95
a	b	c	d

Table 5.1 Northern blots to validate microarray data were performed at 15 independent genes. Three large gels were run using the same RNA preparations as used in the microarrays. Each gel was then cut into eight, Northern blotted separately, and hybridized to a PCR amplified probe specific to each of the genes indicated in column a. Local background was subtracted, and expression levels were normalized to the relevant value of 28S rRNA column b averaged across the duplicate mini-gels. The ratios of mRNA levels between UKY500 and UKY412 (WT), and UKY501 and UKY502 were then calculated for each gene columns c and d, respectively.

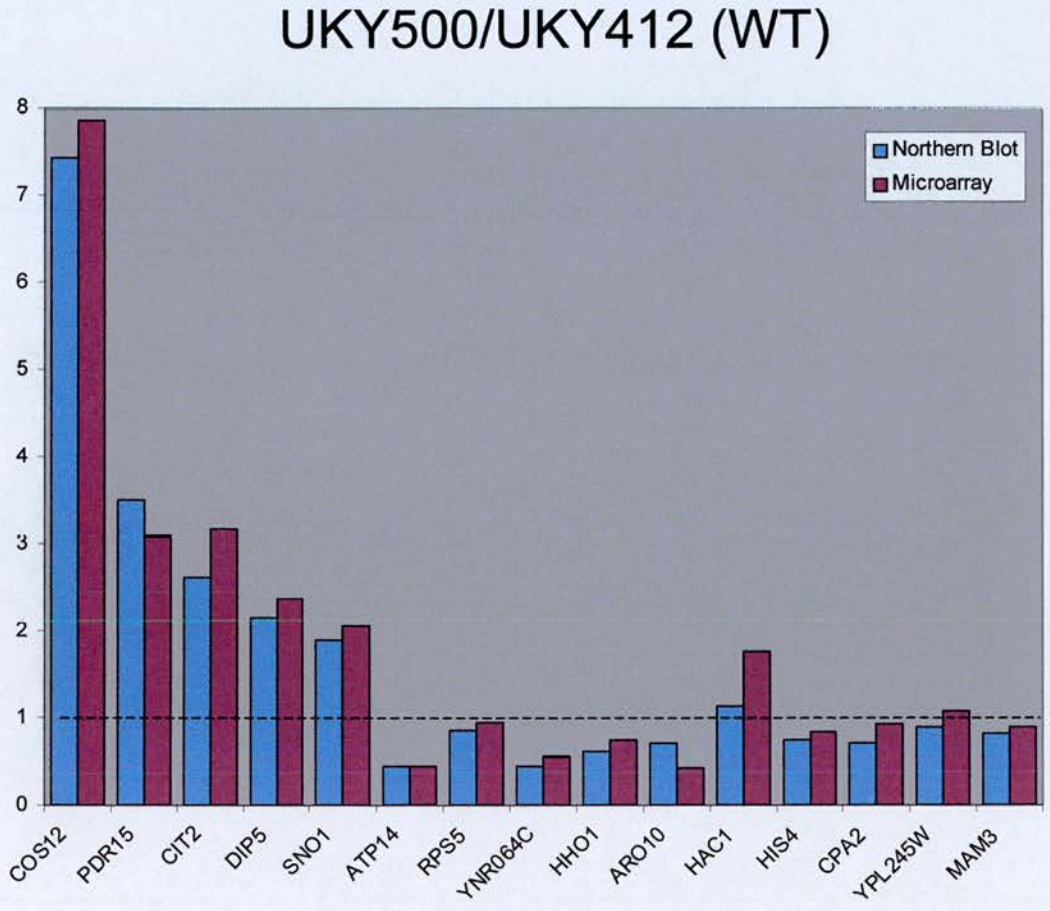

Figure 5.6 Northern blots and microarray data comparison. Bar graph depicting the UKY500:UKY412 (WT) mRNA expression ratio (x-axis) at the 15 genes subjected to Northern blot (y-axis). Ratios calculated from Northern blot data are blue, and those from microarrays are plum. The dashed line represents an expression ration of 1, i.e., no difference between strains. This demonstrates that the Northern blot and microarray data correlate well.

5.4.3 Gene Lists

As mentioned above, two-fold changes in gene expression levels are often considered significant, although this is likely to generate conservative estimates of the effects of a mutation. To generate a list of two-fold differentially regulated genes, mean averages were again taken across the four data sets, for each spot in which the *p*-value of the log ratio is less than 0.01 in each comparison. This *p*-value not only relates to the significance of the measured difference in green and red emissions, but also to the error associated with these measurements. *P*-value filtering thus removes data of low confidence and reduces the changes of spurious significance.

Table 5.2 contains a list of all genes that are expressed to at least two-fold lower level in UKY500 than UKY412, and the degree of down-regulation. Of the 41 genes in this list, 13 are contained within the mitochondrial genome (QOXXX). These are the genes that show the greatest-fold decrease in expression in UKY500 as compared to WT, and some/all of these presumably correspond to the mtDNA that is missing in this mutant. It is difficult to imagine that expression of any of these genes has been directly affected by mutant histone H4, as mtDNA is not complexed with histones. 39 of the genes encode proteins that localize to the mitochondrion (shown in purple). Putting this gene list through 'FunSpec' - a web-based cluster analysis tool for yeast (Robinson *et al.*, 2002) unsurprisingly indicates a massive enrichment of genes involved in cellular energy generation, respiration and mitochondrial function, as well as proteins localised to the mitochondrion ($p<1e^{-14}$). What is striking is the number of affected genes that encode structural components of electron transport

chain complexes: 24 represented genes out of a total of 44 members of the group ($p<1e^{-14}$). Specifically, these affect the mitochondrial F0/F1ATP synthase (complex V of the respiratory chain):14 represented genes from a total of 18 ($p<1e^{-14}$), cytochome-c-oxidase (complex IV of the respiratory chain): 6 represented genes from a total of 11 ($p=2.1x10^{-11}$), and the cytochrome- bc1 complex (ubiquinol-cytochrome c reductase, complex III of the respiratory chain): 4 represented genes from a total of 10 ($p=2.9x10^{-7}$).

The other genes represented in this list are: *ARO10*, which encodes phenylpyruvate decarboxylase (Vuralhan *et al.*, 2003); *HSP12* encoding a heat shock protein; *MLS1*, which is a cytoplasmic/peroxisomal, carbon-catabolite sensitive malate synthase gene; the mitochondrial elongation factor gene *MEF2*, and *PUT4* which encodes a proline specific plasma membrane permease.

It is highly plausible that the decreased expression of mitochondrial proteins observed here is due to retrograde signalling. Genes marked with '*', are down regulated in ρ^0 as compared to ρ^+ *S. cerevisiae* strains in the study by Traven *et al*, and those marked with '^' are down regulated in ρ^0 as compared to ρ^+ in the study by Epstein *et al.* Down-regulation of *MLS1* and *PUT4* is also consistent with the function of the retrograde response to divert metabolites away from futile pathways, and slow cellular growth rate.

Gene	ORF	Molecular function	Cell. Loc.	Fold dn-reg	Diauxic shift	TATA	H4 Δ2-29	rpd3Δ	sin3Δ	hda1Δ
AAP1	Q0080	hydrogen-transporting ATP synthase activity, rotational mechanism	Mito.	99 / 93	N/A	N/A	N/A	N/A	N/A	N/A
AI5_ALPHA	Q0070	Endonuclease I-SceIV	Mito.	89	N/A	N/A	N/A	N/A	N/A	N/A
COB	Q0105	Cytochrome b	Mito.	79 / 79	N/A	N/A	N/A	N/A	N/A	N/A
OLI1	Q0130	F0-ATP synthase subunit 9	Mito.	72	N/A	N/A	N/A	N/A	N/A	N/A
AI4	Q0065	Endonuclease I-SceII	Mito.	49 / 35	N/A	N/A	N/A	N/A	N/A	N/A
AI5_BETA	Q0075	unknown function	Mito.	40	N/A	N/A	N/A	N/A	N/A	N/A
AI2	Q0055	Reverse transcriptase	Mito.	27 / 39	N/A	N/A	N/A	N/A	N/A	N/A
AI1	Q0050	Reverse transcriptase	Mito.	35 / 26	N/A	N/A	N/A	N/A	N/A	N/A
BI2	Q0110	mRNA maturase	Mito.	17	N/A	N/A	N/A	N/A	N/A	N/A
COX1	Q0045	Subunit I, cytochrome c oxidase	Mito.	14 / 12	N/A	N/A	N/A	N/A	N/A	N/A
ATP6	Q0085	subunit 6, F0 sector mitochondrial F1F0 ATP synthase	Mito.	11 / 11	N/A	N/A	N/A	N/A	N/A	N/A
VAR1	Q0140	Mitochondrial ribosomal protein	Mito.	9.5 / 5.6	N/A	N/A	N/A	N/A	N/A	N/A
SCEI	Q0160	I-SceI DNA endonuclease	Mito.	8.4	N/A	N/A	N/A	N/A	N/A	N/A
INH1*	YDL181W	Inhibitor, mitochondrial ATPase	Mito.	5.8 / 5.6	I (3.3)	N	I/D/D/I	N/A	N/A	N/A
ATP7	YKL016C	F0-ATP synthase subunit 7	Mito.	2.6	I (2.3)	Y	D/D/D/D	N/C	N/C	N/C
COX4^	YGL187C	cytochrome-c oxidase chain IV	Mito.	2.6 / 2.6	I (4.6)	Y	D/D/D/D	N/C	N/C	N/C
ARO10*	YDR380W	Phenylpyruvate decarboxylase	Cyto.	2.5	N/C	Y	D/D/D/D	I (3.8)	I (8.6)	N/C
ATP3^	YBR039W	Gamma subunit, F1 sector mitochondrial F1F0 ATP synthase	Mito.	2.5	I (3.3)	N	NC/NC/NC/NC	N/C	N/C	N/C
COX5A^	YNL052W	Subunit Va of cytochrome c oxidase	Mito.	2.4	I (5.0)	Y	D/D/D/D	N/C	N/C	N/C
HSP12	YFL014W	heat shock protein	Cyto/Nuc	2.4 / 2.3	I (11)	Y	I/I/I/I	N/A	N/A	N/A
MDH1^	YKL085W	mitochondrial malate dehydrogenase	Mito.	2.4 / 2.4	I (5.9)	Y	NC/I/NC/I	N/C	N/C	N/C
QCR2*	YPR191W	ubiquinol--cytochrome-c reductase 40K chain II	Mito.	2.3	N/C	Y	NC/I/D/NC	N/C	N/C	N/C
ATP14	YLR295C	Subunit h, F0 sector mitochondrial F1F0 ATP synthase	Mito.	2.3	I (2.6)	N	D/NC/D/D	N/C	N/C	N/C
ATP1	YBL099W	Alpha subunit , F1 sector of mitochondrial F1F0 ATP synthase	Mito.	2.2	I (4.6)	N	NC/I/NC/NC	N/C	N/C	N/C
ATP17	YDR377W	Subunit f, F0 sector mitochondrial F1F0 ATP synthase	Mito.	2.2 / 2.2	N/A	Y	D/D/D/D	N/A	N/A	N/A
MEF2	YJL102W	translation elongation factor	Mito.	2.2	I (2.5)	N	D/NC/D/D	N/C	N/C	N/C
ATP4	YPL078C	Subunit b, stator stalk mitochondrial F1F0 ATP synthase	Mito.	2.2	I (2.6)	N	D/NC/D/D	N/C	N/C	N/C
ATP5*	YDR298C	Subunit 5, stator stalk of mitochondrial F1F0 ATP synthase	Mito.	2.2 / 2.2	I (2.1)	N	D/D/D/D	N/C	N/C	N/C
QCR7^	YDR529C	ubiquinol cytochrome-c reductase subunit 7	Mito.	2.2 / 2.2	I (5.9)	Y	D/NC/D/D	N/C	N/C	N/C
ATP2	YJR121W	Beta subunit, F1 sector mitochondrial F1F0 ATP synthase	Mito.	2.2	I (4.4)	Y	NC/I/NC/NC	N/C	N/C	N/C
ATP20^	YPR020W	Subunit g, mitochondrial F1F0 ATP synthase	Mito.	2.2 / 2.1	I (3.7)	Y	D/D/D/D	N/C	N/C	N/C
MLS1	YNL117W	carbon-catabolite sensitive malate synthase	Cyto/Perox	2.2	I (9.1)	Y	NC/NC/NC/MI	N/C	I (2.3)	N/C
YLR294C	YLR294C	unknown function, invoulved in cellular respiration	U.K.	2.2 / 2.2	I (2.1)	N/A	D/NC/D/NC	N/A	N/A	N/A
COR1^	YBL045C	ubiquinol--cytochrome-c reductase 44K core protein	Mito.	2.2	I (5.6)	N	I/NC/NC/D	N/C	N/C	N/C
ATP19	YOL077W-A	Subunit k, mitochondrial F1F0 ATP synthase	Mito.	2.2	N/A	N	D/D/D/D	N/C	N/C	N/C
COX8^	YLR395C	Subunit VIII, cytochrome c oxidase	Mito.	2.1	I (3.1)	N	D/D/D/D	N/A	N/A	N/A
ATP16	YDL004W	Delta subunit, central stalk of mitochondrial F1F0 ATP synthase	Mito.	2.1 / 2.1	I (2.3)	N	D/D/D/D	N/C	N/C	N/C
PUT4	YOR348C	Proline-specific permease	P.M.	2.1	N/C	N	NC/D/D/D	D (4)	D (11)	N/C
MIR1	YJR077C	Mitochondrial phosphate carrier, imports inorganic phosphate into mitochondria	Mito.	2.1 / 2.0	I (2.0)	N	D/D/D/D	N/C	N/C	N/C
COX12	YLR038C	Subunit VIb, cytochrome c oxidase	Mito.	2.0 / 2.0	I (2.5)	N	D/D/D/D	N/A	N/A	N/A
COX7	YMR256C	Subunit VII, cytochrome c oxidase	Mito.	2.0	N/A	N	D/D/D/D	N/A	N/A	N/A

Table 5.2 Genes expressed to at least two-fold lower level in UKY500 than UKY412. Includes: Common and systematic names (ORF); molecular function; subcellular location (Cell. Loc), i.e. cytoplasm (Cyto), nucleus (Nuc), plasma membrane (P.M.), peroxisome (Perox), mitochondria (Mito, purple), unknown (UK); degree of down-regulation (Fold dn-reg) as measured for both array determinants where relevant. Comparisons to other genome-wide analyses are made for genes induced on the diauxic shift, genes containing a TATA box (Y indicates a TATA box; N indicates no TATA box) and genes induced upon histone H4 tail truncation (H4 Δ2-25), *RPD3* deletion (Δrpd3), *SIN3* deletion (Δsin3) and *HDA1* deletion (Δhda1). Genes down-regulated under the conditions stipulated have the degree of down-regulation indicated in blue, those induced have values in red, and those showing no change (N/C) are indicated in green. Numerical values were not available for the histone H4 tail truncation mutant. In this case the results of the 4 duplicate experiments are given where D is a decrease, I an increase and N/C no change. The colour coding is as above and represents an approximate average.

Examination of table 5.3, which contains a list of genes whose expression is up-regulated by UKY500 as compared to UKY412 (WT), is also supportive of an active retrograde response. Genes identified in the studies by Traven *et al.* and Epstein *et al.* are indicated as above. The characteristic retrograde response gene *CIT2* is present, and there is enrichment of genes involved in transport facilitation (p=0.0004), and cell rescue, defence and virulence (p=0.007). Two genes encoded within mtDNA are also represented. Since the function of these genes is not known, it is not possible to comment on the significance of this, or whether theses genes are up-regulated or even amplified.

As discussed above, many transporters are induced during the retrograde response to deal with the metabolites generated by anaplerotic pathways. Induction of genes conferring pleotropic drug resistance may represent some way of cells trying to compensate for dysfunctional mitochondria (Traven *et al.*, 2001) It would appear here that an increase in *PDR3* transcript levels has led to increases in transcription of the responsive genes *PDR5*, *PDR15* and *YOR049C*.

The exact function of Sno1p is unknown, but it is involved in pyridoxine metabolism, and forms a putative glutamine amidotransferase complex with Snz1p, which could catalyse conversion of glutamine to glutamate. *SNO1* and *SNZ1* are induced in response to nutrient limitation (Padilla *et al.*, 1998), thus induction of *SNO1* by retrograde signalling would perhaps not be surprising.

PHO5 encodes the major secreted acid phosphatase of *S. cerevisiae,* and the different chromatin structures associated with the active and repressed states of the promoter are well characterised (reviewed by Svaren and Horz, 1997). Under high-phosphate conditions, *PHO5* is inactive and its promoter is protected by four positioned nucleosomes. When phosphate is depleted, Pho4p, a bHLH transcription factor, and Pho2p, a homeodomain protein, act cooperatively to bind the *PHO5* promoter and activate *PHO5* transcription. The increase in *PHO5* observed here might represent retrograde signalling, or be directly affected by the histone H4 mutation.

The most strongly up-regulated gene is *COS12*. Again, the molecular function of the protein is unknown, but it is a member of a highly conserved family of sub-telomerically encoded, co-regulated genes (Spode *et al.*, 2002). Increased expression of this gene has not been observed in other studies comparing ρ^0 and ρ^+ strains, and the large degree of up-regulation and sub-telomeric location of this gene make it a definite candidate to have been directly affected by incorporation of mutant histone H4 into nucleosomes.

Gene	ORF	Molecular Function	Loc.	Fold up-reg	Diauxic shift	TATA	H4 Δ2-29	rpd3Δ	sin3Δ	hda1Δ
COS12	YGL263W	function unknown, similarity to other subtelomeric encoded proteins	UK	7.9 / 7.8	N/C	N	MD/NC/NC/NC	D (9.7)	D (5.9)	N/C
ORF:Q0010	Q0010	function unknown	Mito.	5.9	N/A	N/A	N/A	N/A	N/A	N/A
ORF:Q0017	Q0017	function unknown	Mito.	3.8 / 3.3	N/A	N/A	N/A	N/A	N/A	N/A
CIT2^	YCR005C	Peroxisomal citrate-synthase	Perox.	3.2 / 3.1	I (4.8)	Y	I/I/I/I	N/C	N/C	N/C
PDR15	YDR406W	member of ATP-binding cassette (ABC) protein family	Memb.	3.1 / 3.1	N/C	N	I/I/I/I	N/A	N/A	N/A
PDR5*	YOR153W	pleiotropic drug resistance protein	P.M.	2.9 / 2.8	D (3.9)	Y	NC/NC/NC/I	N/A	N/A	N/A
ORF:YOR049C*	YOR049C	phospholipid-translocating ATPase activity	P.M.	2.8	I (3.1)	N	I/I/I/I	N/C	N/C	N/C
HXT3*	YDR345C	low-affinity hexose transporter	P.M.	2.6 / 2.5	N/C	Y	I/NC/I/I	N/C	N/C	N/C
DIP5^	YPL265W	dicarboxylic amino acid permease	P.M.	2.4 / 2.3	I (2.5)	N	NC/D/I/NC	N/C	N/C	N/C
DLD3	YEL071W	D-lactate dehydrogenase	Cyto.	2.4	N/C	N	I/I/I/I	D (2.4)	D (2.9)	N/C
ORF:YKL071W	YKL071W	function unknown	Cyto.	2.4 / 2.4	N/C	Y	NC/I/I/I	N/C	N/C	N/C
ORF:YMR158C-B	YMR158C-B	function unknown	UK	2.3	N/A	N/A	NC/NC/NC/NC	N/A	N/A	N/A
ORF:YKR075C	YKR075C	function unknown, expression regulated by glucose and Rgt1p	Cyto./Nuc.	2.3	N/C	N	I/I/NC/NC	N/C	N/C	N/C
ATO3	YDR384C	member of TC family of putative transporters (ammonia export?)	P.M.	2.2	D (4.5)	N	NC/D/NC/D	N/C	N/C	N/C
PDR3	YBL005W	Zinc-finger transcription factor related to Pdr1p	Cyto./Nuc.	2.2	D (2.3)	Y	I/I/I/I	N/C	N/C	N/C
SIT1	YEL065W	siderochrome-iron (ferrioxamine) uptake transporter activity	Cyto./Endo	2.2 / 2.1	N/C	Y	I/NC/I/I	N/C	N/C	I (2.3)
SNO1	YMR095C	Function unknown, involved in pyridoxine metabolism	Cyto.	2.1	N/C	N	I/I/I/I	N/C	D (3.1)	I (2.5)
PHO5	YBR093C	acid phosphatase activity	CW / P.P.	2.0 / 2.0	D (2.7)	Y	D/I/D/I	N/C	N/C	N/C

Table 5.3 Genes expressed to at least two-fold higher level in UKY500 than UKY412. Includes: Common and systematic (ORF) names; molecular function; subcellular location (Cell. Loc) i.e. cytoplasm (Cyto), nucleus (Nuc), peroxisome (Perox), plasma membrane (P.M.), membrane (Memb.), endoplasmic reticulum (Endo), cell wall (C.W.), periplasm (P.P.), unknown (UK); degree of up-regulation (Fold up-reg) as measured for both array determinants where relevant. Comparisons to other genome-wide analyses are made for genes induced on the diauxic shift, genes containing a TATA box (Y indicates a TATA box; N indicates no TATA box) and genes induced upon histone H4 tail truncation (H4 Δ2-25), *RPD3* deletion (Δrpd3), *SIN3* deletion (Δsin3) and *HDA1* deletion (Δhda1). Genes down-regulated under the conditions stipulated have the degree of down-regulation indicated in blue, those induced have values in red, and those showing no change (N/C) are indicated in green. Numerical values were not available for the histone H4 tail truncation mutant. In this case the results of the 4 duplicate experiments are given where D is a decrease, I an increase and N/C no change. The colour coding is as above and represents an approximate average.

5.4.4 Comparisons to other Microarray Data Sets

Although the presence of most of the genes in the above lists is explicable by retrograde signalling, it is also possible that their altered expression is the cause of mtDNA loss. Lesions in many of the genes encoding subunits of the mitochondrial ATP synthase have been shown to have an influence on *petite* production (table 5.4, compiled from Contamine and Picard, 2000). Additionally, mutations that impair mitochondrial protein synthesis have led to an increase in *petite* production in every instance studied (Myers *et al.*, 1985; Contamine and Picard, 2000), and the mitochondrial translational elongation factor gene *MEF2* is represented in the gene list.

UKY500 might lose mtDNA because of altered expression of a 'master regulator' of mtDNA stability. Alternatively, it could result from a combined effect at a subset of nuclear genes involved in mitochondrial function. The promoters of genes involved in mitochondrial function that are represented in table 5.2 were examined for shared features and/or peculiarities. None of the genes stand out as being unique in their regulatory mechanisms, but most do share putative activator recognition sites. However, these are binding sites for activators mediating inducible gene expression such as Adr1p and Pho4p. The genes for these activators are not up or down-regulated. Their binding sites on mitochondrial gene promoters are furthermore not expected to be occupied on YPD (although this would need to be confirmed); it is therefore hard to see how an effect of mutant histone H4 at these sites could lead to mtDNA loss under such conditions.

Gene	Sector	Mutation	% petite
ATP6 (mt)	F_O	Point	20-80
ATP9 (mt)	F_O	Point	35-49
ATP8 (mt)	F_O	Point	50-70
ATP4 (n)	F_O	Disruption	70
ATP5 (n)	F_O	Disruption	40-80
ATP7 (n)	F_O	Deletion	high
ATP14 (n)	F_O	Deletion	90
ATP17 (n)	F_O	Disruption	60
ATP18 (n)	F_O	Disruption	high
ATP1 (n)	F_1	Uncharacterised	1
ATP1 (n)	F_1	Deletion	<1
ATP2 (n)	F_1	Uncharacterised	1
ATP2 (n)	F_1	Deletion	<1
ATP3 (n)	F_1	Disruption	20
ATP3 (n)	F_1	Deletion	100
ATP16 (n)	F_1	Deletion	near 100
ATP16 (n)	F_1	Deletion	100
ATP15 (n)	F_1	Deletion	25-50
ATP15 (n)	F_1	Deletion	60

Table 5.4 Mutations in components of mitochondrial ATP-synthase which affect *petite* production. Table indicates whether the genes is nuclear (n) , or mitochondrially (m) encoded, and whether the protein is part of the F0 proton cannel, or F1 catalytic head section. Adapted from Contamin and Picard, 2000.

An effect on constitutive transcription of the genes down-regulated in UKY500 seems most unlikely given the relatively small number of affected genes. However, if the genes do share uncharacterised elements that promote their expression in glucose repressed conditions, they may have been previously identified as a co-regulated group. On the basis of the physiological relevance of the phenotype and relative levels of histone H4 acetylation of the mutants, the effects on expression of the genes identified here were compared to several other data sets, as shown in tables 5.2 and 5.3.

5.4.1.1 Diauxic Shift

The genes identified as being expressed to a higher level in UKY412 (WT) cells than the ρ^- strain UKY500 are generally induced during the diauxic shift (deRisi *et al.*, 1997). This is not surprising as the majority of these genes are required for respiration. *QCR2* induction slipped just below the threshold of significance set in this study, and the other non-induced genes, *PUT4* and *ARO10* are concerned with nitrogen metabolism rather than respiration.

The genes expressed more highly in UKY500 than UKY412 (WT) do not show a correlation with genes affected during the diauxic transition.

5.4.1.2 TATA Box Genes

Although half of the genes encoding mitochondrial proteins have no discernable bacterial origins (Karlberg *et al.*, 2000), the endosymbiotic theory of mitochondrial origin (reviewed most recently by Gray, 1992) raises the possibility that genes encoding mitochondrial proteins share some of the most fundamental regulatory elements. Recent studies have pointed towards a bipolar nature of the eukaryotic genome, which correlates with the either TATA-containing, or TATA-less nature of promoters (Basehoar *et al.*, 2004, Huisinga *et al.*, 2004). Briefly, the authors conclude that about 90% of the genome is involved in housekeeping functions, and that these genes tend towards being TATA-less, and TFIID regulated. The remaining 10% is biased towards general stress responsive genes, which tend to be more stringently regulated by the SAGA complex and contain a TATA box. There is naturally considerable overlap between the classes, as evidenced by the fact that ~20% of the genome is said to have a true TATA-box (Basehoar *et al.*, 2004).

The nuclear genes expressed to a higher level in UKY412 (WT) compared to UKY500, as well as those expressed to a lower level, show enrichment of TATA containing promoters compared to the genome as a whole, consistent with the inducible nature of these genes: 43% and 44%, respectively, compared to 20% of the genome. It cannot be said that most of the genes fall into the TATA box containing class however, so the genes affected by the mutations in UKY500 are not specific to this class.

5.4.1.3 Histone H4 Tail Deletion

Yeast expressing an N-terminally truncated form of histone H4 (Δ2-29) do not show the genome wide increase in transcription observed with a histone H3 tail deletion mutant (Sabet *et al.*, 2003). If anything there is a slight decrease in overall transcription, implying that on a genome-wide scale, the histone H4 tail positively regulates gene transcription (under optimal growth conditions). Consistent with this, table 5.2 shows that the genes with reduced mRNA expression in UKY500 mostly correlate with those down-regulated upon histone H4 tail truncation. *HSP12* transcript levels in the histone H4 globular domain mutant do not agree with those in the histone H4 tail-truncation mutant, however. The pleiotropic roles of molecular chaperones confound classification of particular effects of these proteins.

Equally, there is some agreement between the lists of genes with increased expression in UKY500 and those negatively regulated by the N-terminal tail of histone H4, although the most highly up-regulated gene in this study, *COS12*, is unaffected by the histone H4 (Δ2-29) truncation. This lends more credence to the idea that the expression of this gene may have been directly affected by the mutations introduced into the globular domain of histone H4.

In general, the full extent of the correlation between these two data sets could not be established since no numerical expression values were published for the histone H4 (Δ2-29) truncation study. The apparent agreement between the results suggests a connection between the histone H4 tail and the globular domain, since mutations in

either domain appear to affect histone H4 function on gene expression in similar ways. The decrease/abolishment of histone H4 acetylation in the two studies may be at the basis for this agreement between gene lists. However, this does not into account the effect of retrograde signalling on these genes.

5.4.1.4 Histone Deacetylase Mutants

Due the lack of genome-wide studies employing histone H4 acetyltransferase (HAT) mutants, the data are compared here to studies employing histone deacetylase (HDAC) mutants. In HDAC mutants, histone acetylation levels are increased, with possibly opposite effects on gene expression compared to UKY500, which has reduced histone H4 acetylation levels. In keeping with this hypothesis, in *Drosophila* inactivation of the SIN3 deacetylase complex (by RNAi methodology) induces transcription of mitochondrial protein genes (Pile *et al.*, 2003). SIN3 contains the histone deacetylase activity of *RPD3*, which deacetylates histones H3 and H4. Thus, the effect of *SIN3* and *RPD3* deletion on gene expression in *S. cerevisiae* was checked (Bernstein *et al.*, 2000).

With the exception of *ARO10*, the genes down-regulated by the mutations in the histone H4 globular domain are not induced by *SIN3* or *RPD3* deletion. In addition, Bernstein *et al.* do not find enrichment of genes involved in energy processes among those affected by *SIN3* and *RPD3* deletions, implying that the situation is different from that in *Drosophila*, at least at this subset of genes. On the contrary, they find deletion of *HDA1* has most effect, but again, there is no correlation between the

genes affected by the mutations described here, and those affected by *HDA1* deletion.

5.4.1.5 Chromosomal Location

Figures 5.7 and 5.8 show the chromosomal positions of genes differentially expressed between UKY412 (WT) and UKY500. Apart from the concentration of affected genes within the mitochondrial genome (chromosome XVII), and sub-telomerically located *COS12*, the genes are scattered throughout euchromatin. *ATP14* (*YLR295C*) and *YLR294C* on chromosome XII (highlighted by the pink box) are adjacent ORF's that are similarly affected. Both are encoded on the Crick strand, discounting the possibility that they are divergently transcribed from a shared promoter. *YLR294C* is classified as a dubious ORF with a possible role in cellular respiration (Steinmetz *et al.*, 2002), and is perhaps not separable from *ATP14*.

Finally, the affected genes do not fall within domains deacetylated on histone H4K12 by Hos1p or Hos3p, or in the regions where H4K16 is deacetylated by Sir2p (Robyr *et al.*, 2002). Additionally they do not correlate with chromosomal domains deacetylated by Hda1p or Rpd3p (Robyr *et al.*, 2002).

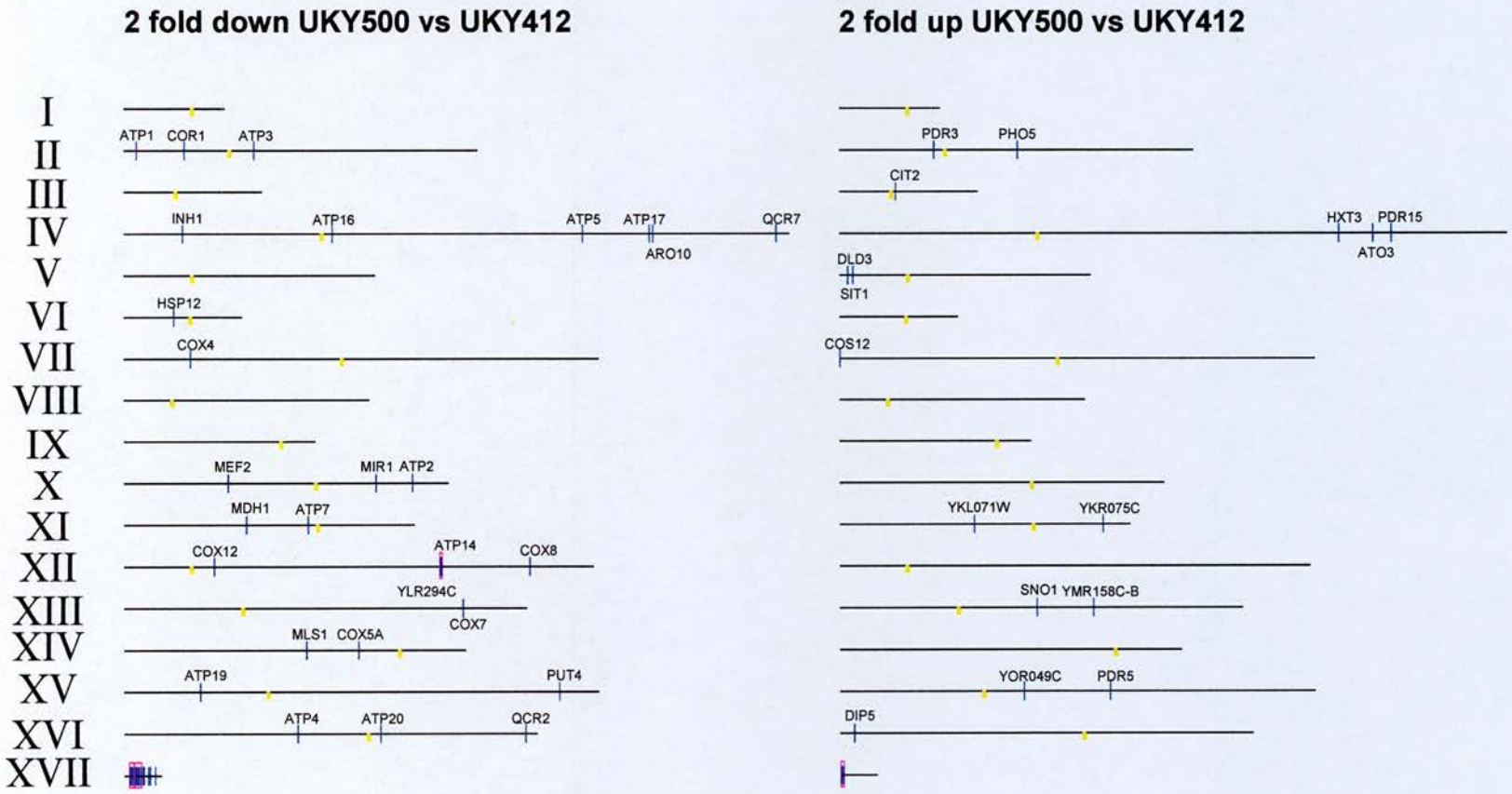

Figure 5.7 Chromosomal locations of genes differentially expressed between UKY412 (WT) and UKY500. The left hand panel represents genes expressed to at least a 2-fold higher level in UKY412(WT) than UKY500, and the right hand panel represents genes expressed to at least a 2-fold higher level in UKY500 than UKY412(WT). Roman numerals represent chromosome number. Centromeres are shown in yellow, and gene names are indicated. Pink boxes are drawn around neighbouring genes. The concentration of affected genes within chromosome XVII reflects deletions within the mitochondrial genome.

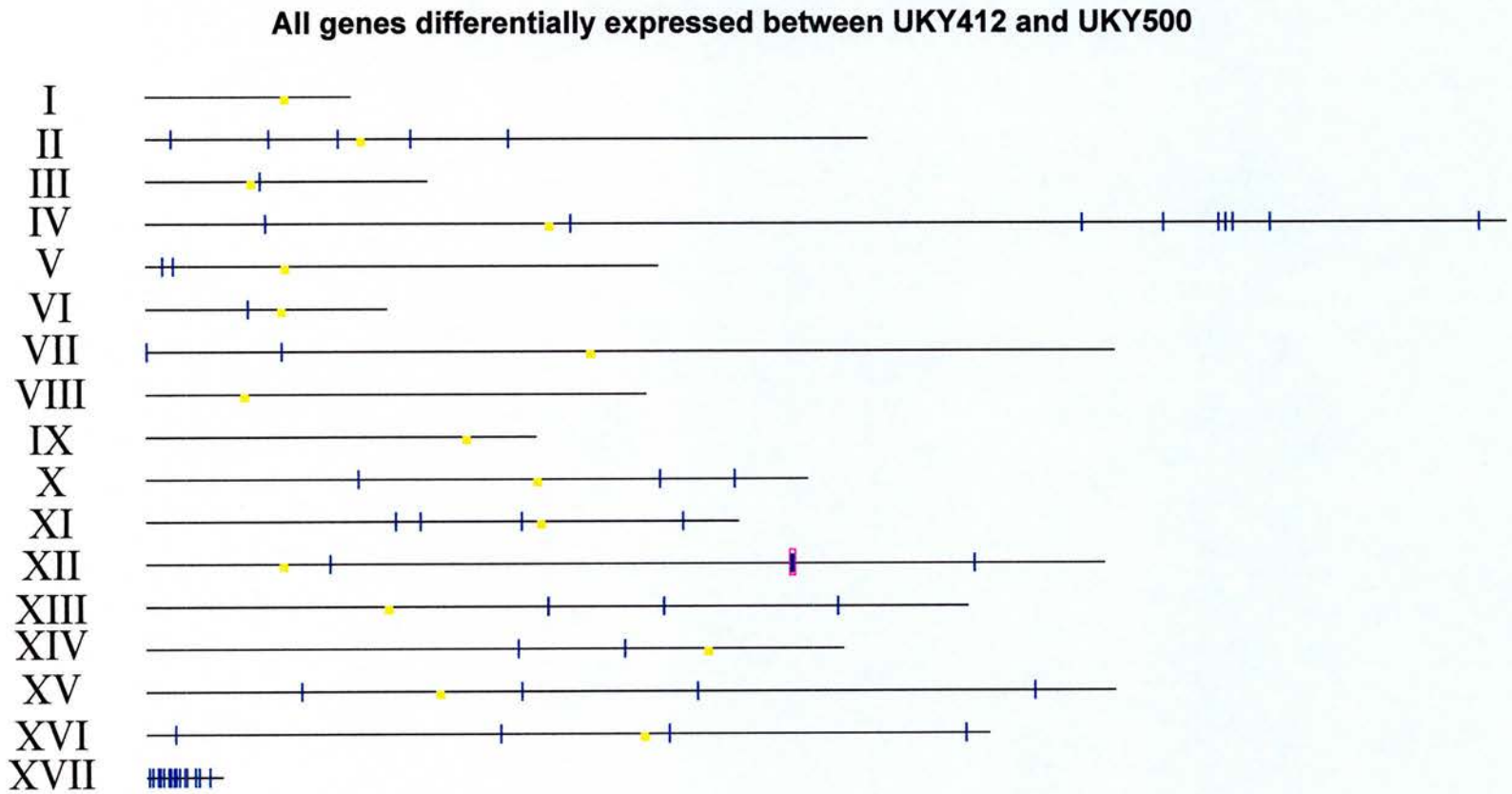

Figure 5.8 Disperse chromosomal positions of genes differentially expressed between UKY412 (WT) and UKY500. All genes differentially expressed by at least a factor of 2 between UKY412(WT) and UKY500. Roman numerals represent chromosome number. Centromeres are shown in yellow, and gene names are indicated. Pink boxes are drawn around neighbouring genes. Other than the concentration of genes within mitochondrial genome (chromosome XVII), genes are scattered throughout the genome.

5.5 Results # 2

5.5.1 UKY501 versus UKY502 Microarray

If the hypothesis that the humanising mutations in the histone H4 globular domain have similar effects in both the WT and I21V background is correct, then the most direct indication that the effect on mitochondrial protein genes is downstream of mtDNA loss comes from the comparison of UKY501 and UKY502. The list of genes expressed to a higher level in UKY502 (I21V) as compared to UKY501 does not contain these mitochondrial proteins.

Figure 5.9a-d shows the raw data of hybridised cDNA signal for each array comparing UKY501 and UKY502. As in figure 5.4, green processed signal (Cy3) is plotted on the x-axis, and red processed signal (Cy5) is plotted on the y-axis. Positive and negative control spots have been left out. The red, dark green and light green lines represent no change, two- and 10-fold changes in gene expression respectively.

As mentioned above, data are expected to form a uniform cloud around the length of the line representing no change in gene expression, and this does not appear to be the case for the arrays comparing UKY501A and UKY502A. The correlation coefficients (c) of the two Cy3 and Cy5 labelled cDNA populations are indicated on the graphs. These are very good at 1.01 and 1.15 for the UKY501B and UKY502B comparisons, but poorer for UKY501A and UKY502A comparisons at 1.27 and 0.51. Additionally, the data from the comparisons of UKY501A and UKY502A, and

UKY501B and UKY502B are not nearly as reproducible as those for the UKY412 and UKY500 comparisons. The correlation coefficients for the duplicate arrays are rather low; 0.42 and 0.28 for A01 and A02 respectively.

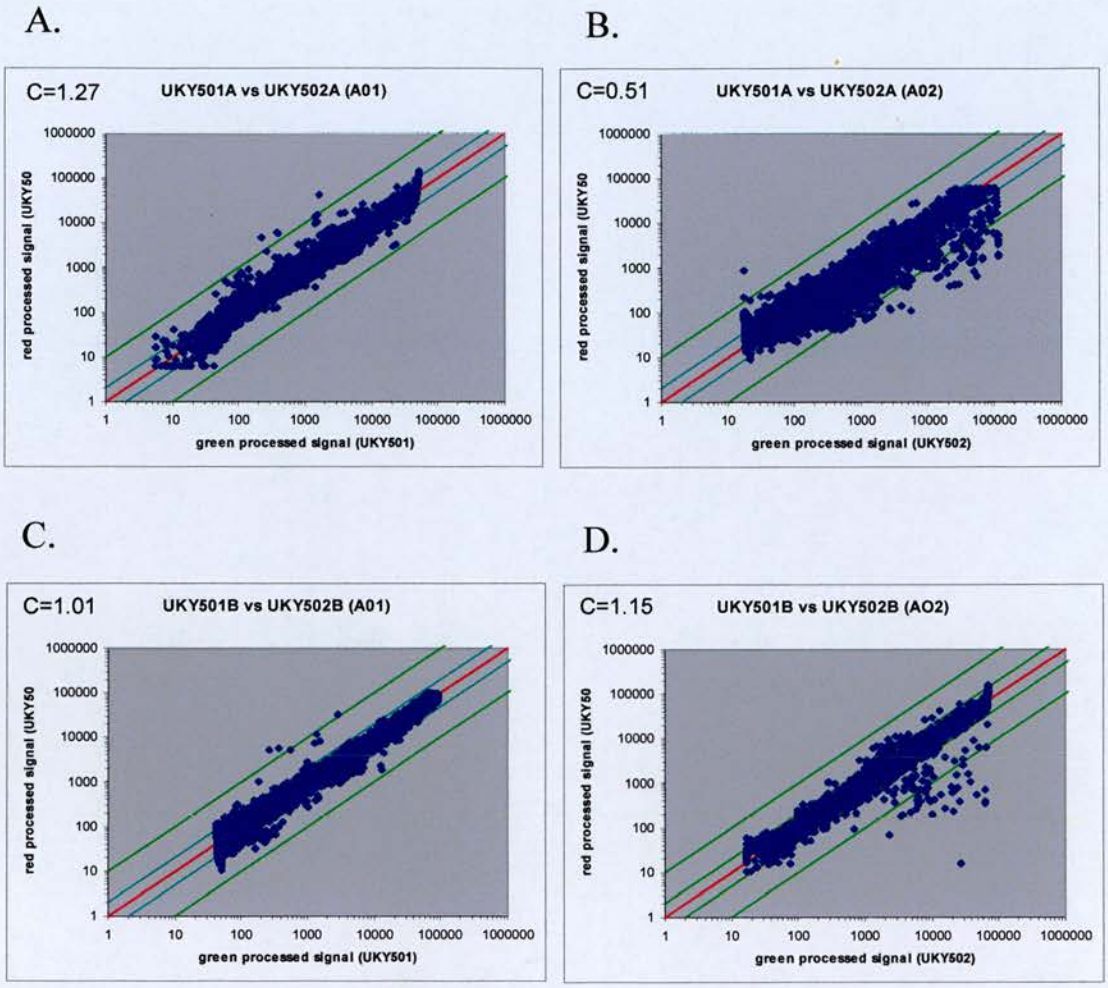

Figure 5.9 Hybridised cDNA emission intensities for each array comparing UKY501 and UKY502. A and C represent Cy3 labelled UKY501 and Cy5 labelled UKY502. B and D represent Cy3 labelled UKY502 and Cy5 labelled UKY501. Points are plotted on a logarithmic scale. Green processed signal plotted on the x-axis corresponds to the normalized Cy3 emissions. Red processed signal plotted on the y-axis corresponds to the normalized Cy5 emissions. Normalisation was as described in materials and methods. Positive and negative control spots have been removed. The red line represents no change in gene expression; the dark and light green lines represent two- and 10-fold changes in gene expression levels, respectively. The correlation coefficients (c) of the red and green data sets are indicated for each array.

5.5.2 Microarray versus Northern Blot

The irregularity of both of the UKY501A/UKY502A data sets (A01 and A02) implies that there may have been a problem with one or other of the RNAs. To confirm that the array data are reliable, the relative expression levels determined by array analyses and Northern blots were compared at the fifteen genes described in section 5.4.2. This time however, the comparisons were made thrice; once incorporating the data from UKY501A and UKY502A arrays; once rejecting UKY501A/UKY502A A02 data; and once rejecting the data from both UKY501A/UKY502A arrays.

At most of the fifteen genes, little difference was made by omitting the RNA A data, as is the case for *CIT2* and *HHO1* (figure 5.10a). However, the correlation at other genes, for example *YNR064C*, *HAC1* (and *MAM3*) was significantly improved (figure 5.10a). Based on this, the decision was made to exclude the data sets generated from UKY501A and UKY502A. Figure 5.10b is a bar graph depicting the UKY501/UKY502 ratio across these fifteen genes as calculated from Northern blots and microarrays, and shows that the data sets generally correlate very well.

I would mention here that excluding the UKY501A and UKY502A data sets did make a difference to the list of two-fold differentially regulated genes, but made no difference to the genes identified by the cross-referencing strategy described in section 5.5.4 below.

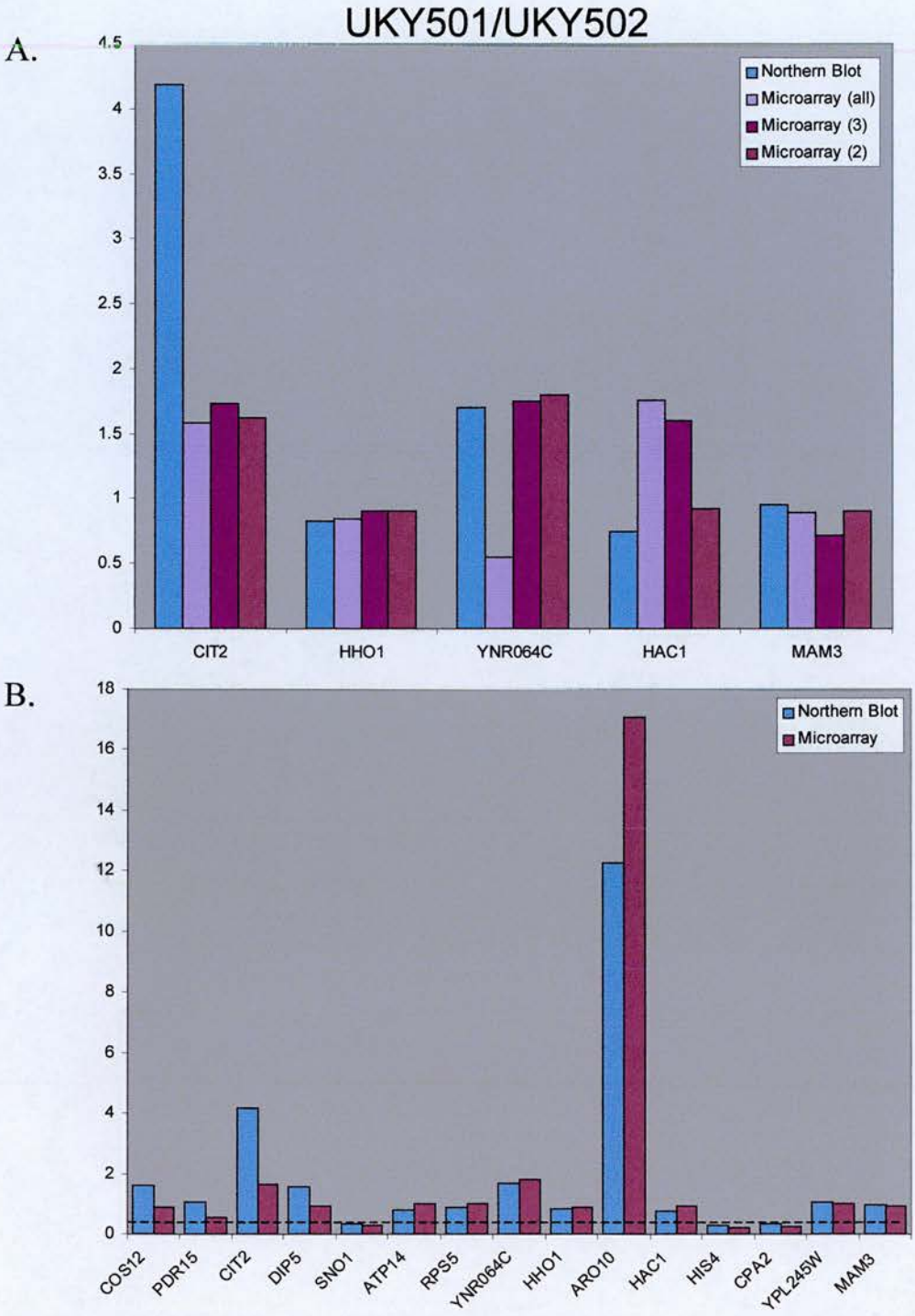

Figure 5.10 Northern blots and microarray data comparison. A) Bar graph comparing the UKY501:UKY502 mRNA expression ratio (y-axis) at 5 genes subjected to Northern blot (x-axis). Ratios calculated from Northern blots are blue; those calculated from all microarray data sets are lilac; those calculated from microarray data sets minus RNA A (A02) are purple; those calculated from microarray data sets minus both RNA A comparisons are plum. This demonstrates that the microarray data are improved at some genes by discounting data derived from the RNA A preparations. B) Bar graph depicting the UKY501:UKY502 mRNA expression ratio (y-axis) at the 15 genes subjected to Northern blot (x-axis). Ratios calculated from Northern blot data are blue, and those from microarrays (discounting RNA A data) are plum. The dashed line represents an expression ratio of 1, i.e., no difference between strains.

5.5.3 Gene Lists

Table 5.5 contains a list of all genes that are expressed to at least a two-fold lower level in UKY501 than UKY502, and the degree of down-regulation. Table 5.6 contains a list of all genes that are expressed to at least two-fold higher level in UKY501 than UKY502, and the degree of up-regulation. These lists were generated by taking mean averages across the two good data sets, for each spot in which the *p* value of the log ratio is less than 0.01 in each comparison.

Although care must be taken not to over-interpret these results, as the mutants are not being compared to WT, several points can be made. Again, the number of genes affected is small, implying that the globular domain mutations do not affect many genes in the I21V context, under these conditions. This is consistent with the effects of these mutations in the WT context. Just eight genes are down regulated by incorporation of the globular domain mutations into an I21V background, but in the cases of *ARO10* and *CLB6* this represents large 17- and 16-fold differences respectively. No mtDNA genes are represented here, indicating that UKY501 has not undergone loss of mtDNA, consistent with the undetectable loss on the Southern blot in figure 4.17.

Thirty genes are expressed to a higher level in UKY501 than UKY502, although the degree of up-regulation is fairly modest (table 5.6). These genes show enrichment of those involved in amino acid metabolism ($p<e^{-14}$), amino acid biosynthesis ($p= 7.76e^{-14}$) and amino acid transport ($p=0.005$). There is one gene in this list that is encoded

by the mitochondrial genome, *Q0297*. Presumably this is not a direct effect of the histone H4 mutations. These results are further discussed below in section 5.6.

Gene	ORF	Function	Cell. Loc.	Fold dn-reg.
ARO10	YDR380W	Phenylpyruvate decarboxylase, catalyzes decarboxylation of phenylpyruvate to phenylacetaldehyde; first specific step in the Ehrlich pathway	Cyto.	17 / 17
CLB6	YGR109C	B-typecyclin role in DNA replication during S phase	U.K.	16
YEL028W	YEL028W	Funtion unknown	U.K.	5.3
ARO9	YHR137W	Aromatic aminotransferase; first step of tryptophan, phenylalanine, and tyrosine catabolism	Nuc./ Cyto.	5.1 / 4.8
YOR387C	YOR387C	Function unknown	Sol. Frac.	2.5
YGL258W	YGL258W	Function unknown	Sol. Frac.	2.3
YGL039W	YGL039W	Oxidoreductase, catalyzes NADPH-dependent reduction of the bicyclic diketone	Cyto.	2.3
FIT2	YOR382W	Cell wall mannoprotein	Cell wall	2.3 / 2.3

Table 5.5 Genes expressed to a higher level in UKY502 than UKY501 to at least 2-fold or more, and the degree of up-regulation. Gene function and subcellular localisation (Cell. Loc) are indicated.

Gene	ORF	Function	Cell. loc.	Fold up-reg.
HIS4	YCL030C	histidine biosynthesis	Cell	4.7 / 4.6
CPA2	YJR109C	synthesis of citrulline, an arginine precursor	Cyto.	3.8 / 3.7
GDH1	YOR375C	synthesizes glutamate from ammonia and alpha-ketoglutarate	Cyto /Nuc	3.8 / 3.6
SNO1	YMR095C	Function unknown, involved in pyridoxine metabolism	Cyto.	3.7 / 3.5
Q0297	Q0297	Function unknown, dubious ORF	Mito.	3
ARG1	YOL058W	arginine biosynthesis	Cyto.	3.0 / 3.0
LYS9	YNR050C	lysine biosynthesis	Cyto.	2.9
YBR147W	YBR147W	Function unknown	U.K.	2.9
YLR162W	YLR162W	Function unknown	U.K.	2.8 / 2.6
CAR1	YPL111W	Arginine / proline degradation	Cyto.	2.8 / 2.7
LYS20	YDL182W	lysine biosynthesis	Nuc.	2.6 / 2.5
YDR326C	YDR326C	Function unknown	U.K.	2.5
OPT2	YPR194C	oligopeptide transporter activity	P.M.	2.5
ECM40	YMR062C	glutamate degradation / arginine biosynthesis	Mito.	2.5
CAR2	YLR438W	arginine catabolism	Cyto./Nuc	2.4
YGL117W	YGL117W	Function unknown	U.K.	2.6 / 2.4
PDR15	YDR406W	ATP-binding cassette (ABC) transporter activity	P.M.	2.4
LYS1	YIR034C	lysine biosynthesis	Cyto. / Perox.	2.4 / 2.2
SNZ1	YMR096W	Function unknown, involved in pyridoxine metabolism	U.K.	2.3 / 2.1
ASN1	YPR145W	asparagine biosynthesis	Cyto.	2.3
ARG4	YHR018C	arginine biosynthesis	Cyto.	2.3 / 2.2
PCL5	YHR071W	cyclin-dependent protein kinase regulator activity	CDK holo.	2.3 / 2.3
YJL200C	YJL200C	TCA cycle, aerobic respiration	Mito.	2.3 / 2.3
ADE17	YMR120C	histidine, purine, pyrimidine biosynthesis	Cyto.	2.2
AGP1	YCL025C	amino acid transport	P.M.	2.2
YOR203W	YOR203W	Function unknown	U.K.	2.3 / 2.2
PUT4	YOR348C	proline-specific permease (alanine and glycine also)	P.M.	2.1
HIS5	YIL116W	histidine biosynthesis	Cell	2.1 / 2.0
LYS21	YDL131W	lysine biosynthesis	Nuc.	2.1
YAL061W	YAL061W	putative polyol dehydrogenase	Cyto./Nuc	2

Table 5.6Genes expressed to a higher level in UKY501 than UKY502 to at least 2-fold or more, and the degree of up-regulation. Gene function and subcellular localisation (Cell. Loc) are indicated.

5.5.4 Cross Referencing of Data Sets

Cross referenced gene lists were generated as follows: average values for the degree of differential expression between strains was calculated from four and two arrays, in the case of the UKY412 (WT)/UKY500, and UKY501/UKY502 comparisons, respectively. Control spots and genes whose differential expression had a *p*-value of significance greater than 0.01 in any comparison were filtered out. The remaining average values were then filtered for: genes whose expression was at least 1.7-fold higher in UKY412 (WT) than UKY500, AND at least 1.7-fold higher in UKY502 than UKY501, and genes whose expression was at least 1.7-fold higher in UKY500 than UKY412 (WT), AND at least 1.7-fold higher in UKY501 than UKY502. A value of 1.7- rather than 2-fold was set as the significant threshold to reduce the chance of missing important genes within these fairly strict criteria.

The genes identified by this selection procedure are presented in tables 5.7a and 5.7b, which have the genes expressed to a lower level when histone H4 contains the globular domain 'humanising' mutations, and to a higher level, respectively. None of these genes have a previously identified role in the maintenance of mtDNA. Apart from mtDNA-encoded *Q0297* (which is presumably not directly affected, and whose function is not known), the genes are not directly involved in cellular respiration, although the function of *YNR064C* is not known. Nor do any of the genes encode known transcription factors, altered cellular levels of which might have downstream effects on nuclear or mitochondrially encoded genes of mitochondrial proteins.

A. Genes expressed to a higher level in UKY412 than UKY500 AND in UKY502 than UKY501

Gene	ORF	Function	Cell. Loc.	UKY412/ UKY500	UKY502/ UKY501
ARO10	YDR380W	Phenylpyruvate decarboxylase; decarboxylation of phenylpyruvate to phenylacetaldehyde; first specific step of Ehrlich pathway	Cyto.	2.4 / 2.3	17 / 16
ARO9	YHR137W	Aromatic aminotransferase; first step of tryptophan, phenylalanine, and tyrosine catabolism	Nuc./ Cyto	1.7	5.1
YNR064C	YNR064C	Function unknown	U.K.	1.8	1.8

B. Genes expressed to a higher level in UKY500 than UKY412 AND in UKY501 than UKY502

Gene	ORF	Function	Cell. Loc.	UKY500/ UKY412	UKY501/ UKY502
AQR1	YNL065W	Drug transporter	P.M.	1.9 / 1.9	1.9 / 1.8
Q0297	Q0297	Function unknown, dubious ORF	Mito.	1.9	3
PDR15	YDR406W	ATP-binding cassette (ABC) transporter activity	P.M.	3.1	2.4
SER3	YER081W	Serine and glycine bosynthesis	Cyto.	1.9 / 1.8	1.9 / 1.8
SNO1	YMR095C	Function unknown, involved in pyridoxine metabolism	Cyto.	2.1 / 2.0	3.7 / 3.5

Table 5.7 Genes identified by cross referencing. A) Genes expressed to at least a 1.7-fold higher level in UKY412(WT) than UKY500 AND in UKY502 than UKY501. Gene function, the degree of up-regulation and subcellular localisation (Cell. Loc) are indicated. B) Genes expressed to at least a 1.7-fold higher level in UKY500 than UKY412(WT) AND in UKY501 than 502. Gene function, the degree of up-regulation and subcellular localisation (Cell. Loc) are indicated.

5.5.5 Nuclease Mapping

To see whether the large differences in expression levels between strains of the genes *ARO10* and *COS12* are accompanied by any changes in nucleosome positioning, indirect end labelling mapping experiments were conducted.

5.5.5.1 ARO10

Nuclei from each of the four strains were harvested from cells grown as for the RNA preparations. After performing a time course MNase digest, purified DNA was digested to completion with *BglII*, which cuts 1375 base pairs upstream of the *ARO10* coding sequence. Gel separated fragments were blotted onto membrane, and incubated with a radiolabelled probe, which hybridizes just inside the *BglII* cut site. The phosphorimage of hybridisation is presented in figure 5.11a, which includes the approximate positions of the coding sequence and UAS_{aro} (Iraqui *et al.*, 1999).

By looking at the intensity traces in figure 5.11b, several regions within the DNA upstream of *ARO10* corresponding to the size of a nucleosome appear to be protected from MNase digestion. I have thus positioned four nucleosomes in the region, but fairly tentatively, as these regions also show some degree of protection in naked DNA. Although *ARO10* is expressed to a much higher level in UKY502 than in the other strains (figure 5.5), there appears to be no remodelling of nucleosomes associated with this increase in transcription, within the region examined. The position of UAS_{aro} indicated in figure 5.11, represents the site to which the Aro80p

transcriptional activator binds, inducing transcription in the presence of aromatic amino acids (Iraqui *et al.*, 1999). This site is at the 5' border of the first positioned nucleosome in the *ARO10* upstream region, and is not completely accessible to MNase digestion in any strain (or naked DNA). This suggests that Aro80p binds its recognition site within a partially nucleosomal context in the active gene. Because the very low level of gene expression in UKY500 is not accompanied by a shift of nucleosome positioning in this region, it can be concluded that this site is not fully protected by a nucleosome in the repressed gene either. The UKY500 band pattern shows a more regular ladder over the coding region compared to transcribing strains, where this pattern seems to be disrupted by transcriptional elongation.

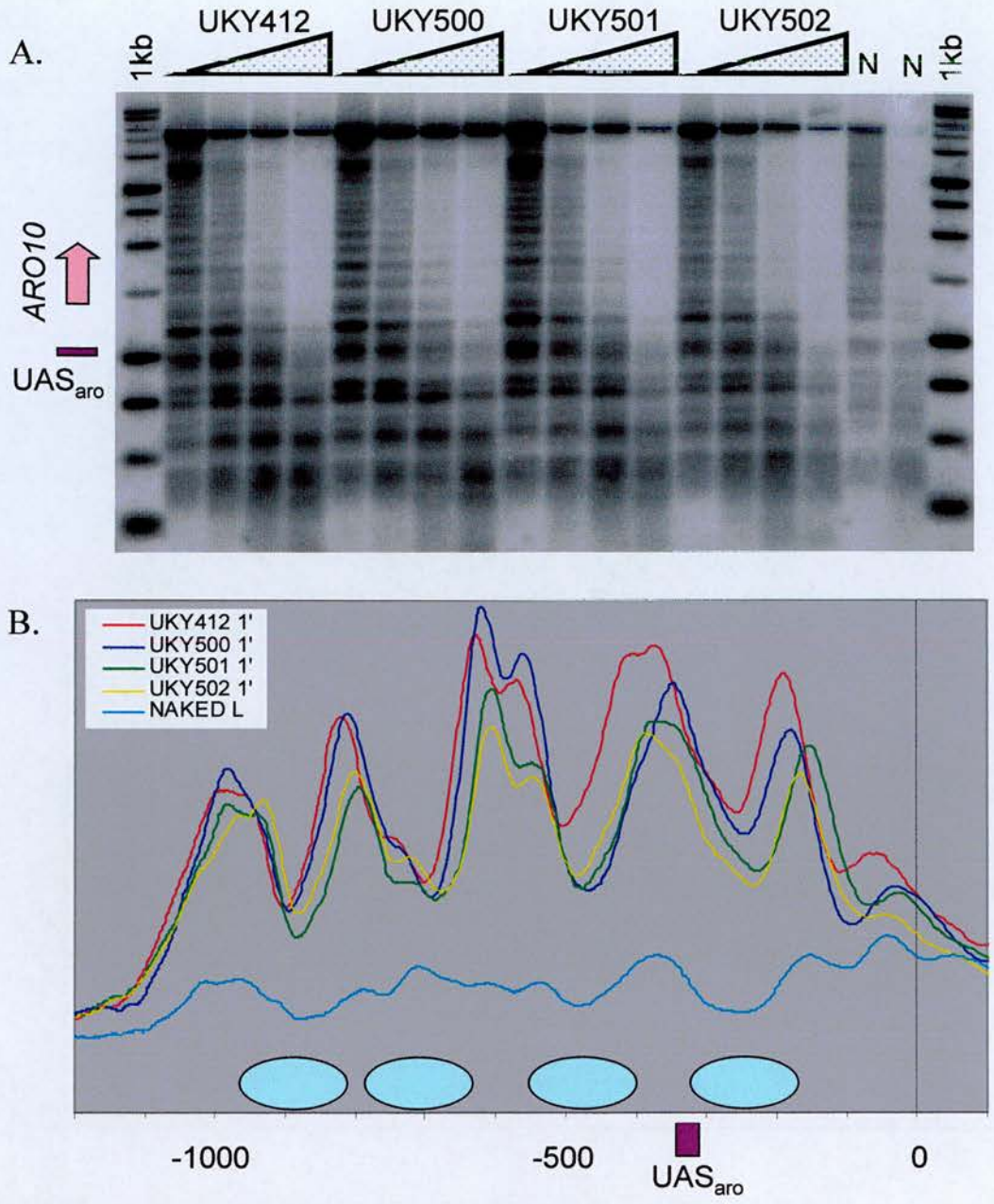

Figure 5.11 Nucleosome positions at the *ARO10* gene A) Nuclei prepared from YPD grown yeast were subjected to a time-course of partial digestion by micrococcal nuclease. Purified DNA was subsequently digested to completion by *BlgII*. Fragments were separated by agarose gel electrophoresis and transferred to nitrocellulose. Naked DNA control (N) was treated similarly, and a radiolabelled 1kb size marker was included on the gel. The blot was probed with a 436bp radiolabelled cDNA complementary to sequences inside the upstream *BlgII* site (PCR amplified from genomic DNA with primers ARO10IDELfw and ARO10IDELbk). Exposure of the blot to a phosphorescent screen generated the image shown. Positions of the *ARO10* coding sequence and upstream activation sequences UASaro are indicated. No difference in nucleosome positions are observed between strains expressing very different levels of *ARO10*. B) Intensity traces generated by quantitation of image in A. Base pairs are plotted on the x-axis and intensity on the y-axis. UKY412(WT) is red; UKY500 blue, UKY501 green; UKY502 yellow and naked DNA is turquoise. Assigned nucleosome positions are indicated by blue ovals. The position of UASaro is indicated. Position 0 on the x-axis corresponds to the beginning of the *ARO10* coding sequence.

5.5.5.2 COS12

A similar analysis was also performed at the sub-telomerically located *COS12* gene. In this instance, an *SpeI* restriction enzyme site 1165 base pairs upstream of the coding sequence was used as the reference point.

COS12 is expressed in all strains except UKY412 (WT) (figure 5.5), but again there is little difference between the position of nucleosomes on the gene in this strain compared to the others (figure 5.12). Two nucleosomes can be positioned in the coding region of the gene, and three more in the upstream region from -350 to -820. There is also a region of protection between -140 and -300 that is susceptible to digestion in naked DNA, but the protection here is not complete (indicated by the striped nucleosome). Additionally, DNA in the chromatin of this region is most accessible in UKY412 (WT) where the gene is inactive.

Little is known about the sub-telomerically encoded *COS* gene family or their protein products, but they are regulated in part by an ATF/CREB site in the upstream region, which can bind bZip transcription factors (Spode *et al.*, 2002). This element is typically located 0.8kb upstream of the *COS* gene coding sequence, but in the case of *COS12* the separation is atypically much larger, and not within the region visualized in this experiment. A longer range experiment would be needed to see if the increased accessibility of the repressed gene in UKY412 (WT) at a region near the coding sequence correlates with a decrease in accessibility at an upstream activator site, indicative of nucleosome reorganisation.

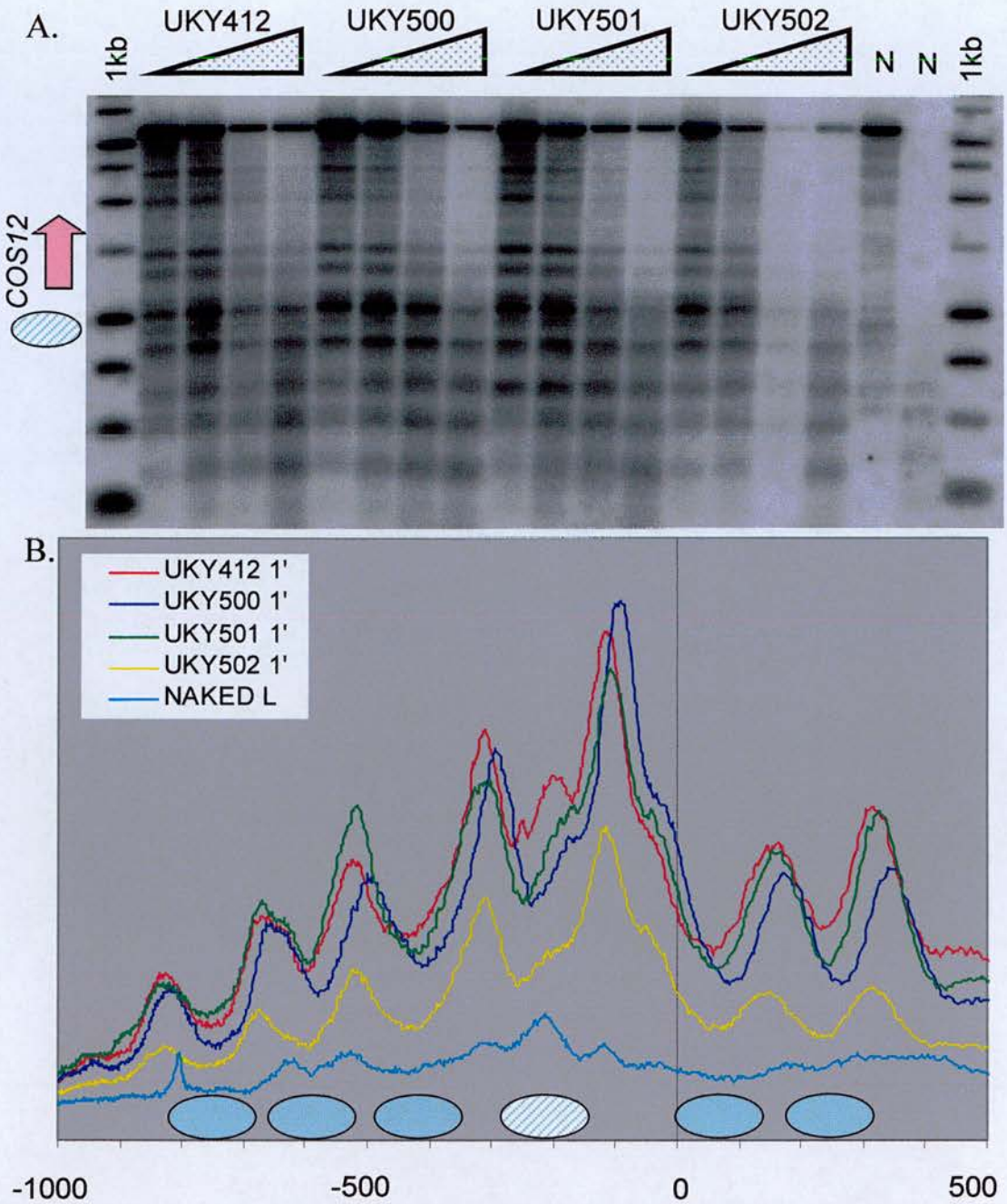

Figure 5.12 Nucleosome positions at the *COS12* gene A) Nuclei prepared from YPD grown yeast were subjected to a time-course of partial digestion by micrococcal nuclease. Purified DNA was subsequently digested to completion by *SpeI*. Fragments were separated by agarose gel electrophoresis and transferred to nitrocellulose. Naked DNA control (N) was treated similarly, and a radiolabelled 1kb size marker was included on the gel. The blot was probed with a 448bp radiolabelled cDNA complementary to sequences inside the upstream *SpeI* restriction enzyme site (PCR amplified from genomic DNA with primers COS12IDELfw and COS12IDELbk). Exposure of the blot to a phosphorescent screen generated the image shown. Positions of the *COS12* coding sequence and nucleosome which may be remodelled (striped blue oval) are shown. B) Intensity traces generated by quantitation of image in A. Base pairs are plotted on the x-axis and intensity on the y-axis. UKY412(WT) is red; UKY500 blue, UKY501 green; UKY502 yellow and naked DNA is turquoise. Unchanged nucleosome positions are by indicated solid blue ovals; potentially remodelled position is striped. Position 0 on the x-axis corresponds to the beginning of the *COS12* coding sequence.

5.6 Cross-Array Comparisons

The genes identified as having at least two-fold higher mRNA expression levels in UKY501 compared to UKY502 show significant enrichment of genes involved in amino acid metabolism, biosynthesis, and transport (table 5.6 and section 5.5.3). From these data alone it cannot be distinguished which strain is affected as compared to WT; UKY501 expression of these genes could be up-regulated, or UKY502 gene expression may be down-regulated. To distinguish between these possibilities and to determine whether there is any wide-spread pattern in comparison to WT, single-mutant data from distinct arrays need to be compared.

5.6.1 Validation

Since the Cy3 and Cy5 emissions are normalised within a single array, it is necessary to prove the validity of cross-array comparisons using Northern blot data as a frame of reference. Previous analyses used the log-ratios and associated *p*-values of significance delivered by the Feature Extraction scanning software (Agilent). Such values are not available when considering single-mutant data sets from different slides, so the Cy3 and Cy5 'processed signals' (i.e. post-normalisation emission values) were used instead. Average emission values were calculated using both Cy3 and Cy5 processed signals for each strain, on each array (an average of four values for UKY412 (WT), and two values for UKY501 and UKY502). These values were used to calculate UKY501/UKY412 (WT), and UKY502/UKY412 (WT) mRNA expression ratios. Comparison of these ratios to those calculated from Northern blots

at the fifteen genes described in section 5.4.2 demonstrates that the data correlate well, thus validating comparisons made between hybridisation signals obtained from different arrays (figure 5.13).

5.6.2 General Effect on Amino Acid Homeostasis in UKY502

Figure 5.14 is a bar chart showing mRNA expression levels of the thirty genes identified as being expressed to a significantly higher level in UKY501 than UKY502, in all four strains. Two points can be made upon examination of this graph. Firstly, all thirty genes are expressed to a lower level in UKY502 than in UKY412 (WT). In many cases the UKY501:UKY502 transcript ratio is larger than the UKY412 (WT): UKY502 transcript ratio due to an accompanying increase in UKY501 mRNA expression compared to WT. Secondly, at over half of the genes mRNA transcript levels are increased in UKY500 as compared to UKY412 (WT). These increases are not necessarily large enough to constitute biological significance, but may represent specific instances where the globular domain mutations are having similar effects in UKY500 and UKY501.

A.

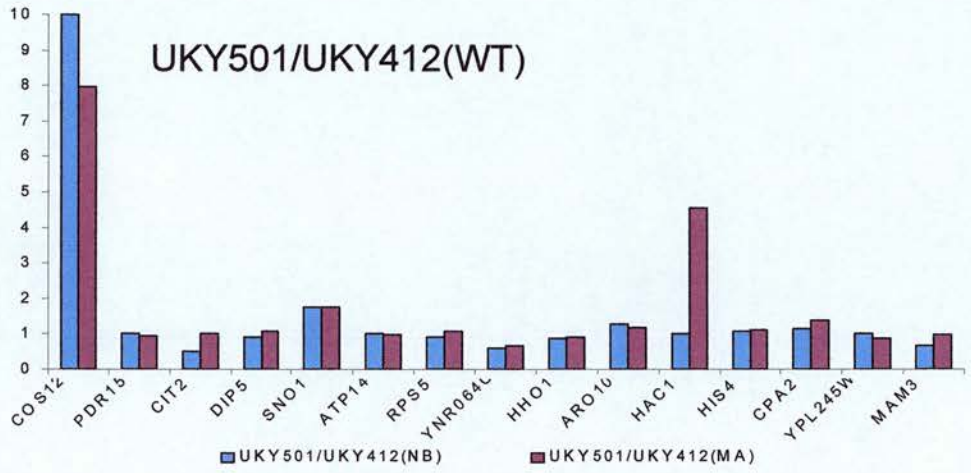

B.

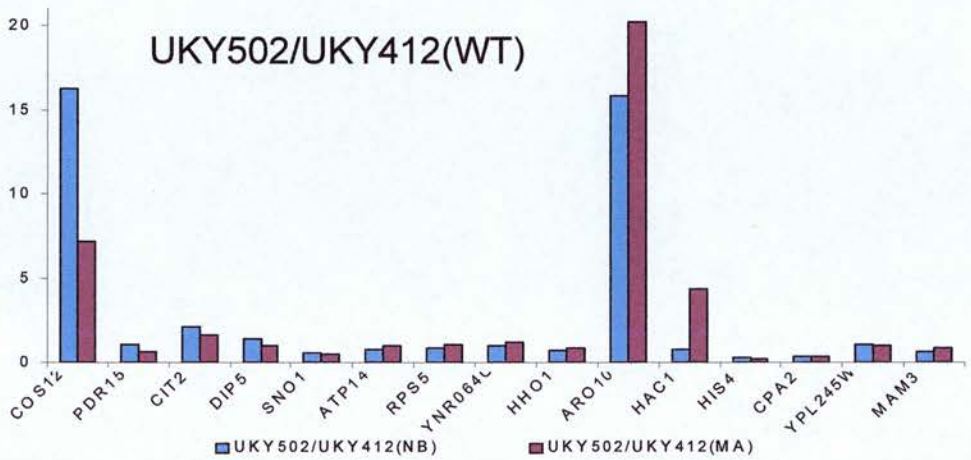

Figure 5.13 Validation of cross-array comparison. A) Bar graph comparing the UKY501:UKY412(WT) mRNA expression ratio (y-axis) at 15 genes subjected to Northern blot (x-axis). Ratios calculated from Northern blot data are blue; those calculated from microarray data are plum. B) Bar graph depicting the UKY502:UKY412 mRNA expression ratio (y-axis) at the 15 genes subjected to Northern blot (x-axis). Ratios calculated from Northern blot data are blue, and those from microarrays are plum. These charts demonstrate the validity of cross-array comparisons.

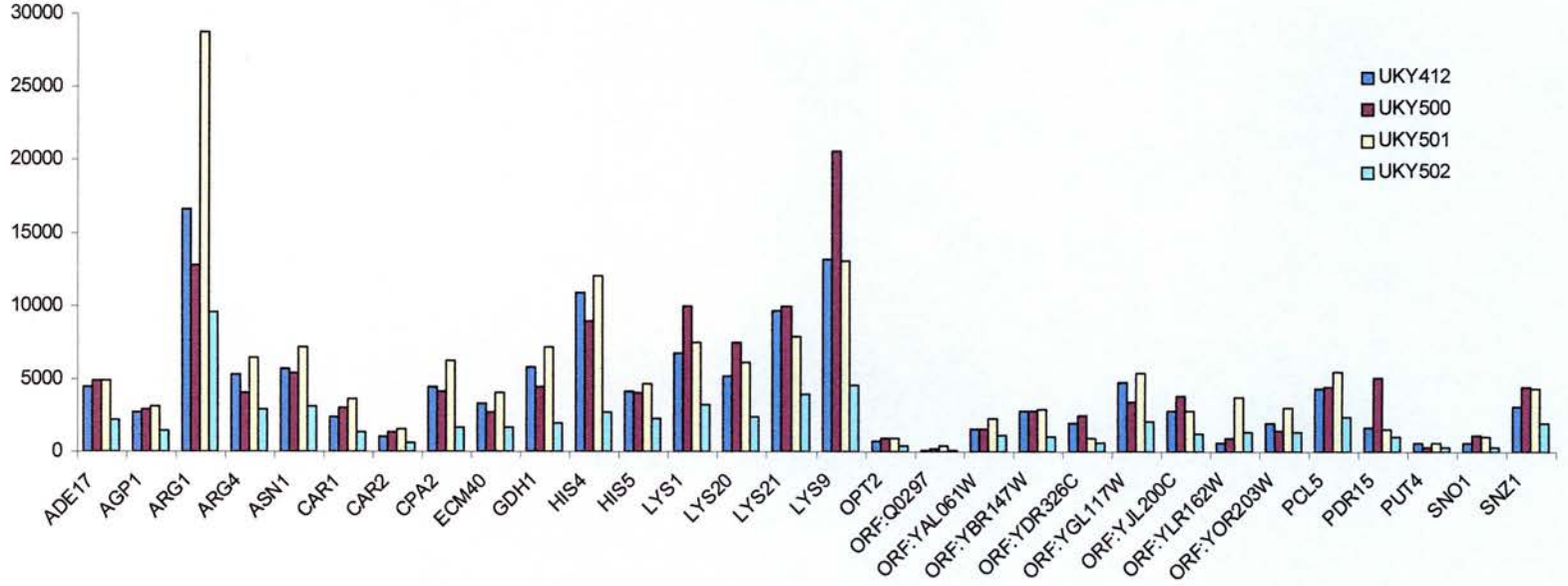

Figure 5.14 Transcript levels of the thirty genes up-regulated in UKY501 in all four strains. Intensity values are on the y-axis and gene names are on the x-axis. UKY412(WT) mRNA expression values are shown in blue; UKY500 in plum; UKY501 in yellow and UKY502 in green. In addition to being expressed to at least a 2-fold lower than in UKY501, all of the represented genes are expressed to a lower level in UKY502 than in UKY412 (WT). Accompanying increases in UKY501:UKY412(WT) further increase the UKY501:UKY502 ratio at some genes.

To see if reduced expression of genes involved in amino acid metabolism is a general feature of UKY502 compared to WT, the method of cross-array comparison was extended to the full data sets. Figure 5.15 plots the average hybridisation emission intensity for UKY412 (WT) on the x-axis, and the average hybridisation emission intensity for UKY502 on the y-axis. Positive and negative control spots have been removed. The red, dark green, yellow and light green lines represent no change, two-, three- and 10-fold changes in mRNA expression levels, respectively. Tables 5.8a and 5.8b summarise this data in terms of the number of genes up- and down-regulated between the two strains. It is worth noting that the numbers of affected genes presented in tables 5.8, and 5.9 below, may not be absolutely comparable to the numbers of affected genes detected between strains directly compared on a single array. Lack of *p*-value filtering makes the criteria less stringent and internal normalisation within a single experiment is always preferable. Thus it is likely that the number of affected genes determined when comparing across arrays represents a more generous estimate.

Of the 127 genes that have at least a two-fold greater level of mRNA transcripts in UKY412 (WT) than UKY502, only ten are increased above three-fold, and only two above 10-fold. FunSpec analysis of the two-fold higher gene list reveals enrichment of genes involved in amino acid metabolism (MIPS functional categorisation). As shown in figure 5.16, the genes identified here represent 8.3% of all the genes in the genome defined as playing a role in amino acid metabolism. Compared to 3.3% of all the genes in the genome being defined as playing a role in amino acid metabolism, this constitutes a significant enrichment ($p=6.0\text{x}10^{-7}$). The list is more specifically

enriched for genes involved in amino acid biosynthesis: 10.1% of all genes in the amino acid biosynthesis class are represented in the list, compared to 1.9% of the genome that constitutes the class (p=3.9x10^{-6}). Of the 17 genes in the group conferring a significant enrichment of genes of amino acid metabolism, 13 are concerned with import or biosynthesis of the nitrogenous side-chain amino acids lysine, histidine, arginine and proline, and one, *GDH1*, catalyses synthesis of glutamate from ammonia. This significance is not observed in the three-fold up-regulated genes.

It is clear from figure 5.15 and table 5.8 that more genes show an increase in mRNA expression in UKY502 compared to WT, than show a decrease. Of the 339 genes with mRNA expression levels at least two-fold higher in UKY502 than UKY412 (WT), 220 are yet to be assigned a name or particular function. This obviously makes statistically significant categorisation difficult, but genes *SNZ3, SNZ2* and *SNO2* constitute an enrichment of genes involved in pyridoxine metabolism (p=0.0028).

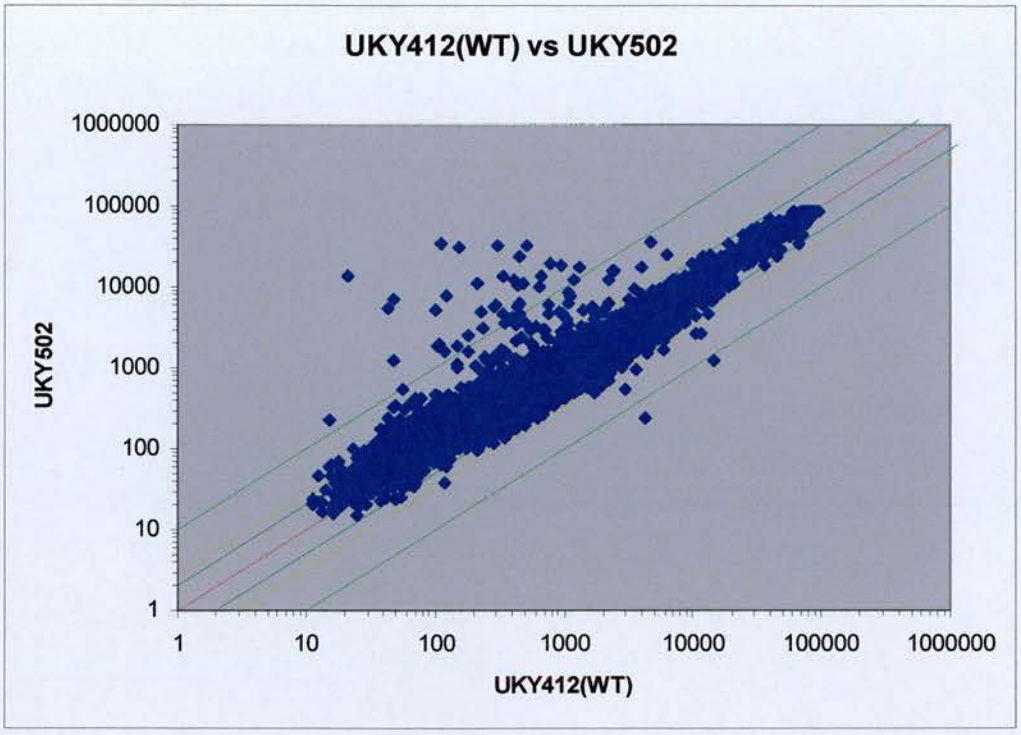

Figure 5.15 Average hybridised cDNA emission intensities for UKY412 (WT) (x-axis) and UKY502 (y-axis). Points are plotted on a logarithmic scale. Positive and negative control spots have been removed. The red line represents no change in gene expression; the dark green, yellow and light green lines represent two-, three- and 10-fold changes in gene expression levels, respectively.

A.

Number of genes with higher mRNA transcript levels in UKY412 (WT) than UKY502		
>/= 2X	>/= 3X	>/= 10X
127	10	2

B.

Number of genes with higher mRNA transcript levels in UKY502 than UKY412 (WT)		
>/= 2X	>/= 3X	>/= 10X
339	131	37

Table 5.8 Number of genes differentially expressed between UKY412(WT) and UKY502. More genes show increased transcript levels in UKY502 than a decrease. A) genes up-regulated in UKY412(WT) compared to UKY502 at 2-, 3- and 10- fold levels of significance. B) genes down--regulated in UKY412(WT) compared to UKY502 at 2-, 3- and 10- fold levels of significance.

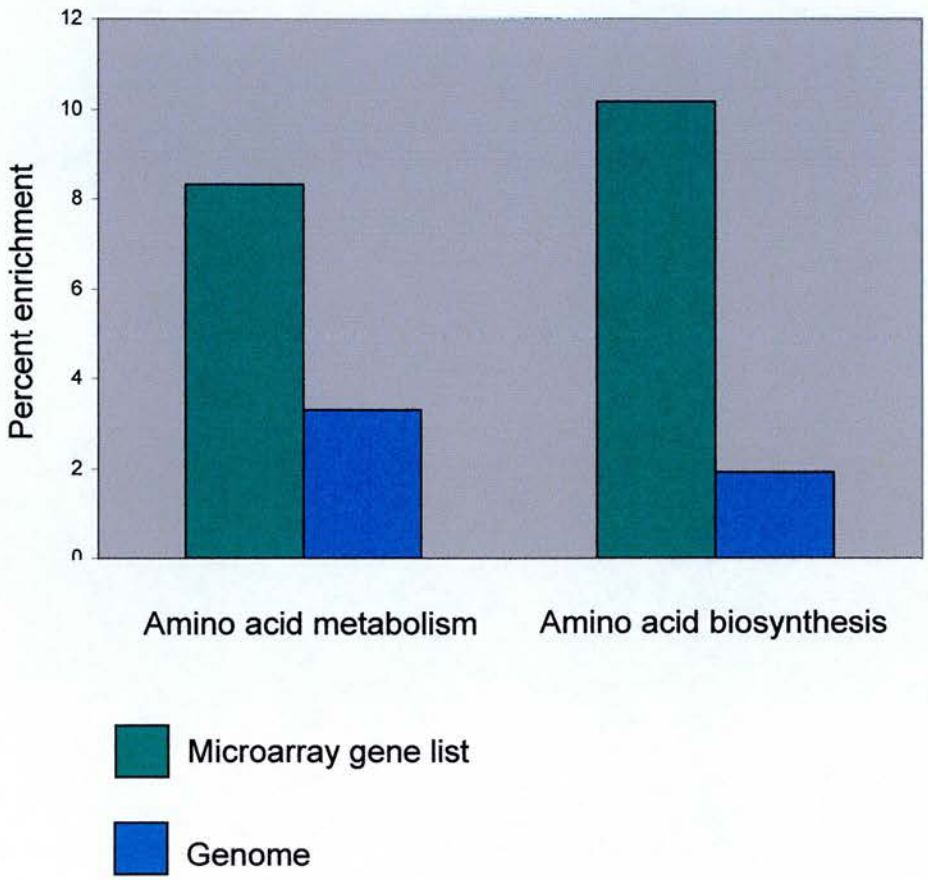

Figure 5.16 FunSpec analysis of the two-fold higher gene list reveals enrichment of genes involved in amino acid metabolism and biosynthesis compared to the genome as a whole. MIPS functional categorisation is on the x-axis, percentage enrichment is on the y-axis. Enrichment within the genes identified by microarry (green), is compared to enrichment within the genome (blue).

5.6.3 Fully 'Humanised' UKY501 is more Similar to WT than UKY502

Similar comparison of genes differentially expressed between UKY501 and UKY412 (WT) generates the scatter plot shown in figure 5.17. Visual examination of this scatter plot and the numbers of differentially expressed genes shown in tables 5.9a and 5.9b reveals an effect complementary to the observed phenotypic-rescue function of I21V recognized in chapter 4: fewer genes are affected by the combination of mutations in the globular domain of histone H4 and I21V (UKY501), than are by I21V alone (UKY502). This is further evidence for an interaction between the globular domain and tail mutations introduced into histone H4.

The 98 genes with two-fold higher transcript levels in UKY412 (WT) than UKY501 show slight enrichment of genes concerned with mRNA processing (p=0.007). 225 of the 292 genes with two-fold higher mRNA expression levels in UKY501 than UKY412 (WT) are unclassified, which precludes categorisation. Interestingly, the two genes expressed at a ten-fold higher level in WT than UKY501, namely *PAN5* and *YOR263C*, are the same as the two genes expressed to a ten-fold level in WT than UKY502. Additionally, 7 of the 8 genes with ten-fold higher transcript levels in UKY501 than WT are present in the list of genes with ten-fold higher transcript levels in UKY502 than WT. These effects are likely to be dominated by the I21V mutation, and not greatly influence by those in the globular domain.

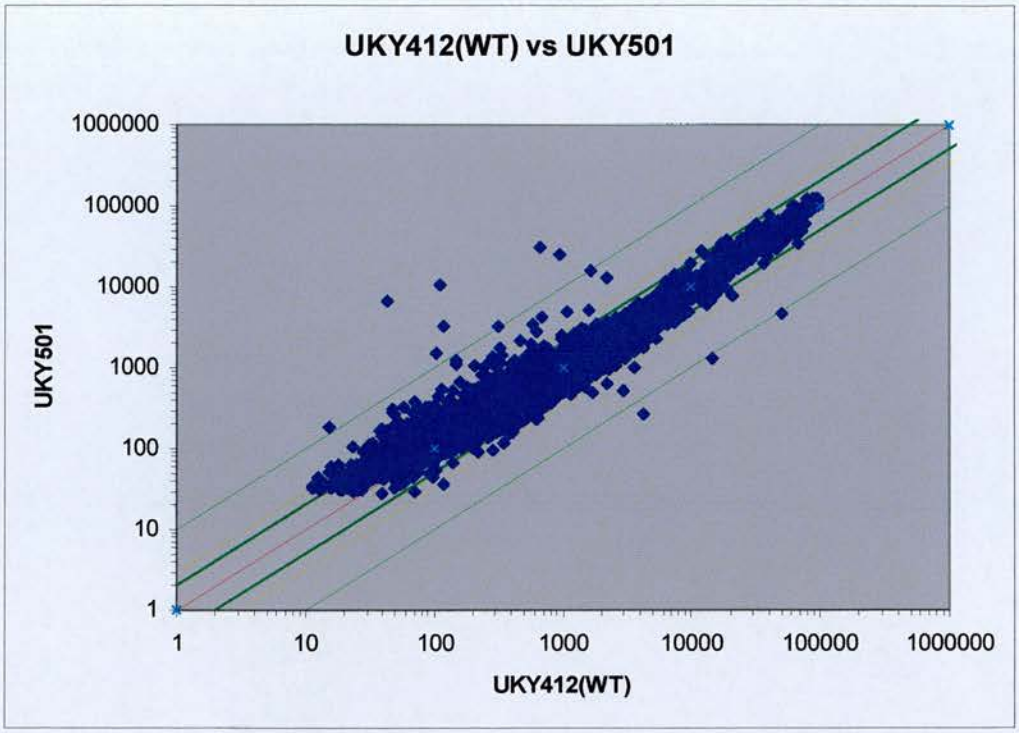

Figure 5.17 Average hybridised cDNA emission intensities for UKY412 (WT) (x-axis) and UKY501 (y-axis). Points are plotted on a logarithmic scale. Positive and negative control spots have been removed. The red line represents no change in gene expression; the dark green, yellow and light green lines represent two-, three- and 10-fold changes in gene expression levels, respectively.

A.

Number of genes with higher mRNA transcript levels in UKY412 (WT) than UKY501		
>/= 2X	>/= 3X	>/= 10X
98	7	2

B.

Number of genes with higher mRNA transcript levels in UKY501 than UKY412 (WT)		
>/= 2X	>/= 3X	>/= 10X
292	75	8

Table 5.9 Number of genes differentially expressed between UKY412(WT) and UKY501. More genes show increased transcript levels in UKY501 than a decrease. A) genes up-regulated in UKY412(WT) compared to UKY501 at 2-, 3- and 10- fold levels of significance. B) genes down--regulated in UKY412(WT) compared to UKY501 at 2-, 3- and 10- fold levels of significance.

5.7 Discussion

The microarray experiments presented in this chapter assess the impact on the yeast transcriptome of expression of mutant histone H4 proteins related to their human counterparts. The manner of pair-wise comparisons was chosen with the aim of determining why yeast strain UKY500, which expresses a partially 'humanised' form of histone H4, loses mtDNA. It was also expected that such a genome-wide analysis would reveal genes, perhaps novel ones, which are regulated at the level of chromatin.

The small number of genes with expression levels that differ by a factor of two-fold or more between UKY412 (WT) and UKY500 is surprising given the large difference between strains in levels of histone H4 acetylation, and the potential of a histone mutant to affect every gene in the nucleus. Targeted acetylation and deacetylation of histone proteins occurs in a background of constant global turnover. This flux allows for rapid removal of targeted acetylation associated with specific gene activation, and serves to keep acetylation and transcription levels down on a genome-wide scale (Vogelauer *et al.*, 2000). However, although a larger gene list might be expected on the basis of total histone H4 acetylation, it must be stressed that there is no information provided here on the relative levels of other histone modifications that have an influence on transcription, or indeed the identity of the histone H4 lysine residue(s) affected. Determination of these levels would establish whether the overall histone modification pattern in UKY500 is consistent with gene inactivation.

Strictly speaking, it could be argued that the reduced levels of histone acetylation have had an effect on overall transcription, but that such general effects are undetectable in the microarray (and Northern blot) experiments, as the normalisation procedure evens out differences in the absolute amount of mRNA that is added to the labelling reaction. However, this is not believed to be the case: firstly, cells were grown to the same density before harvesting of RNA (determined by counting cells, not measuring optical density), and comparable amounts of rRNA and *ACT1* mRNA were obtained from all strains. Additionally, to generate such similar gene expression patterns between strains, all genes would have to have been affected to the same degree by the differences in acetylation levels, and this is rather improbable.

Thirteen of the forty one genes with reduced transcript levels in UKY500 are located in mtDNA, and some or all of these presumably correspond to the portions of mtDNA that are missing in UKY500. The mitochondrial genome is not packaged in the same fashion as nuclear DNA. Rather than being complexed with nucleosomes it is associated with a high mobility group (HMG) like protein, Abf2p (Diffley and Stillman, 1991). It is therefore difficult to imagine that genes within mtDNA have been directly affected by expression of a mutant nuclear histone. A much more likely scenario is that altered expression of a nuclear gene(s) has led to mtDNA loss as a down-stream effect.

Within the nuclear genes down-regulated in UKY500 there is a huge enrichment of genes encoding mitochondrial proteins. Lesions in many genes of the mitochondrial ATP synthase complex and components of the mitochondrial transcription and

translation apparatus have been shown to cause mtDNA loss. This lends a possible explanation for loss of mtDNA by UKY500: incorporation of mutant histone H4 into nucleosomes may have reduced transcription of some mitochondrial protein genes, and the effect at one or more of these has led to loss of mtDNA. However, reduced expression of nuclear genes encoding mitochondrial proteins is a characteristic of retrograde signalling in cells with dysfunctional mitochondria. Therefore, the changes in mRNA expression levels of mitochondrial protein genes may be due to mtDNA loss, rather than the cause of it. In keeping this, twelve of the genes in this list have been previously identified as retrograde affected, as have five of the genes whose expression increases in UKY500.

That the genes down-regulated in respiratory deficient UKY500 generally correspond to genes induced on the diauxic shift is not surprising when one considers their molecular function. The bias towards TATA containing genes is also in keeping with the 'bipolar' nature of the genome proposed by Huisinga *et al.*

Most genes expressed to a lower level in UKY500 compared to UKY412 (WT), also show reduced expression in a strain bearing a histone H4 tail deletion (H4Δ2-29), implying that they are positively regulated by the H4 N-terminus. The H4Δ2-29 truncation removes all potential sites of histone H4 acetylation. Since histone hyperacetylation is associated with gene activation, removal of all acetylatable lysine residues may explain the overall decrease in transcription observed in the tail deletion mutant (Sabet *et al.*, 2003). It is intriguing that the globular domain mutations in UKY500 should have the same effect on transcript levels as the tail

deletion at these genes, but effects here are probably dominated by retrograde signalling, and genome-wide they affect less than 10% of the genes identified by Sabet *et al.*

If the global reduction of histone H4 acetylation observed in UKY500 has led to reduced expression of the represented genes, it might be expected that these same genes would show increased expression in histone deacetylase knock-out strains. In *Drosophila*, genome-wide analysis of expression patterns identified the histone deacetylase activity of Rpd3p within the SIN3 complex as a negative regulator of mitochondrial protein gene expression (Pile *et al.*, 2003), and Hda1p has been implicated in regulation of energy processes in *S. cerevisiae* (Bernstein *et al.*, 2000). However, comparison with published yeast data sets demonstrates that the mitochondrial protein genes identified here are not amongst those affected by Δ*RPD3*, Δ*SIN3* or Δ*HDA1*. This is surprising given that the genes are down-regulated in the H4Δ2-29 truncation mutant. It may imply that removal of acetylation sites is not the only factor contributing to gene inactivation, or be a reflection of the redundancy of multiple HDAC complexes. It is also unknown whether a comparison of genes induced by HDAC knock-out with those down-regulated by an observed decrease histone H4 acetylation is truly relevant. The use of HDAC inhibitors might shed some light on whether the reduced levels of histone H4 acetylation in UKY500 are responsible for the observed decreases in expression of some of the genes.

The cross-referencing strategy of microarray data sets is based on the hypothesis that the histone H4 globular domain mutations have similar effects on transcription of the

gene(s), whose altered expression leads ultimately to mtDNA loss in UKY500, in both the WT and I21V backgrounds. If true, the UKY501 versus UKY502 comparison provides an efficient way to isolate the effects of the histone H4 globular domain mutations that occur upstream of mtDNA loss. Both sets of array comparisons make another fact clear: the differences in histone H4 acetylation between strains are not due to altered expression of HAT or HDAC genes. This might suggest that the globular domain mutations affect molecular interactions between nucleosomes and a chromatin modifying activity, which in turn effects altered histone H4 acetylation levels.

Cross-referencing of data sets provides compelling evidence that most genes differentially expressed between UKY412 (WT) and UKY500 are affected downstream of mtDNA loss. Genes showing increased expression in both UKY500 and UKY501 compared to their array partners do so to only a modest degree, and it is difficult to imagine how these changes could have led to loss of mtDNA. Two of the genes down-regulated in UKY500 and UKY501 however, *ARO9* and *ARO10*, show larger differences in transcript levels. There is some circumstantial evidence that *ARO9* and *ARO10* could have been directly affected by the histone H4 mutants: they are amongst the genes whose transcript levels increase upon deletion of *RPD3* or *SIN3* (Bernstein *et al.*, 1997), and the specific transcriptional activator Aro80p binds its recognition side on partly nucleosomal DNA (section 5.5.5.1). It is possible that *ARO9* and *ARO10* (and *YNR064C*) play hitherto unidentified roles in maintenance of the mitochondrial genome (see section 5.7.1 below).

The specialised chromatin structure at telomeres made *COS12* a good candidate for observing any changes in chromatin structure that might accompany changes in gene expression induced by the mutant histone H4 proteins. Differences within the region mapped here, however, are subtle. Extended footprinting of the *COS12* upstream region might determine whether the increase in nuclease accessibility upstream of the coding sequence in the repressed strain reflects shifting of a nucleosome position. No differences in nucleosome positions are observed at the *ARO10* gene promoters of strains with very different mRNA expression levels. These results are consistent with those in previous chapters, which imply that the mutant histone H4 proteins are not exerting their effects on genes expression by interfering with the remodelling/repositioning of nucleosomes.

Extending the comparison of genome-wide mRNA expression levels to strains hybridised to different microarrays provides information on the effect of the I21V and full set of human mutations compared to WT. This reveals trends not apparent from the original pair wise comparisons. Tables 5.8 and 5.9 demonstrate that the I21V mutation in histone H4 has an overall activating effect on gene expression. In both UKY501 and UKY502, more than 2.5 and ten times as many genes are activated than are repressed at the two- and three-fold levels of significance, respectively. Many of the genes with increased expression in UKY501 and UKY502 are of unknown function, which prevents much determination of whether particular classes of genes are being co-regulated. Increased expression in UKY502 does slightly enrich for genes concerned with pyridoxine metabolism though, and amongst the genes down-regulated in UKY502 there is enrichment for genes involved in

amino acid metabolism. The effect on transcription of these genes is modest and might result from impaired recruitment of the transcriptional apparatus to the gene promoters within the context of the mutant histone, or reflect a shift in the balance of metabolites within the cell. An *in vitro* reconstitution system employing these genes and nucleosomes containing either WT or I21V histone H4 could distinguish between these possibilities.

The general activating effect of I21V seems to be tempered by the globular domain mutations in the human form of histone H4 expressed by UKY501 (figures 5.15 and 5.17). This fits well with the previously observed interaction between the globular domain mutations and I21V at the phenotypic level. On a genome-wide scale it appears that a yeast mutant expressing human histone H4 has a more similar transcriptome to WT than does a strain expressing a form of histone H4 with just one conservative mutation in its N-terminal tail. A corollary of this is that the histone H4 globular domain mutations have an overall repressive effect on gene expression. This is difficult to confirm from these data however, as alteration of gene expression patterns in UKY500 by retrograde signalling masks more direct effects of the mutations.

In addition to its general activating effect, it is likely that the I21V mutation is having particular effects at some genes, which are not greatly affected by the globular domain mutations. *PAN5* and *YOR263C* transcript levels are 12- and 18-times greater, respectively in UKY412 (WT) than UKY502. The expression levels of the same genes are similarly larger in WT than UKY501, at 11- and 16-times,

respectively. Additionally, seven of the eight genes expressed to a ten-fold greater level in UKY501 than WT are also up-regulated to a comparable extent by UKY502.

The genome-wide observation that many more genes are differentially expressed between UKY501 and UKY412(WT) than are between UKY500 and UKY412(WT) suggests that the I21V mutation in the histone H4 N-terminal tail has a greater effect on gene expression than do the mutations within the globular domain. This is perhaps to be expected from the location of these residues at solvent exposed and buried positions within the core nucleosome structure, respectively (White *et al.*, 2001). Even so, it is the globular domain mutations that ultimately precipitate loss of mtDNA.

5.7.1 A Central Role for Glutamate?

The cross-referencing strategy described above identified reduced transcription of *ARO9, ARO10* and *YNR064C* as a possible cause of mtDNA loss in UKY500. The function of *YNR064C* is unknown, but *ARO9* and *ARO10* both encode proteins that catalyse steps in the degradation of aromatic amino acids via the Ehrlich pathway. The existence of this pathway in the cytosol of *S. cerevisiae* means that yeast can survive by using tryptophan, phenlalanine or tyrosine as the sole nitrogen source.

Catabolism of phenylalanine is outlined in figure 5.18a. In the first step of the pathway phenylalanine is transaminated by either Aro9p (aromatic aminotransferase II), or Aro8p (aromatic aminotransferase I). This generates glutamate (from α-ketoglutarate), and the α-keto acid phenylpyruvate. Phenylpyruvate is decarboxylated to phenylacetaldehyde by Aro10p, which is believed to be the major activity catalysing this reaction *in vivo* (Vuralhan *et al*, 2003). The fate of phenylacetaldehyde is partly determined by the redox state of the cell: anaerobic conditions favour the reductive branch, which results in phenylethanol production, whereas in aerobic conditions phenylacetate will also be generated by oxidation.

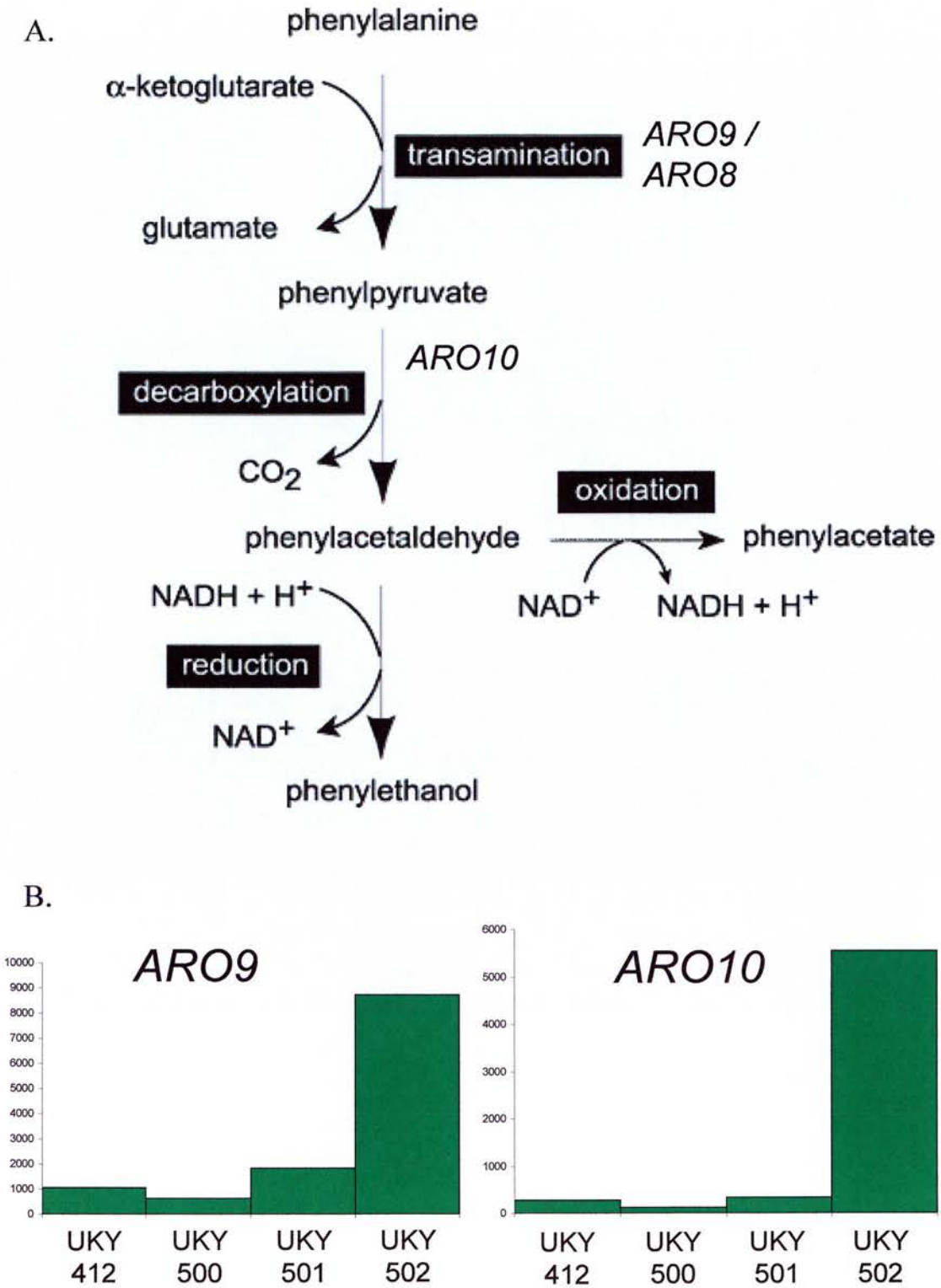

Figure 5.18 The Ehrlich pathway outlined for the catabolism of phenylalanine. A) *ARO9* and *ARO10* encode proteins capable of catalyzing the first and second steps of the pathway. B) expression levels of *ARO9* and *ARO10* as calculated from microarray. Reduced *ARO9* and *ARO10* expression in UKY500 reduces flux through the Ehrlich pathway.

Transcription of *ARO9* and *ARO10* is under two types of control. The first is general 'nitrogen-regulation' (also called the 'ammonia effect'), which parallels glucose repression as it directs use of preferred nitrogen sources (ammonia/glutamine/glutamate) when these are present. Under nitrogen-regulated conditions, transcription of genes needed to utilise secondary nitrogen sources is repressed, and the activity of permeases that import secondary nitrogen sources is down-regulated (reviewed by Magasanik and Kaiser, 2002). The second level of control is induction by aromatic amino acids, in the absence of which neither gene is transcribed. In fact, nitrogen regulation of *ARO9* and *ARO10* is mediated mainly by preventing import of the inducing aromatic amino acid (Iraqui *et al.*, 1999).

The cross-array comparisons of microarray data demonstrate that *ARO9* and *ARO10* expression is low in WT and UKY501, significantly lower in UKY500, and very high in UKY502 (figure 5.17b). Hyper-expression in UKY502 could result from either impaired nitrogen-regulation, or an effect on specific induction. Because so many genes with increased transcript levels in UKY502 compared to WT are of unknown function, it is not possible to determine whether this class is significantly enriched for genes normally repressed by nitrogen-regulation. To get an idea of whether this might be the case, all of the characterised genes with at least two-fold higher mRNA levels in UKY502 were analysed in FunSpec. This did not reveal enrichment of genes involved in metabolism of secondary nitrogen sources, suggesting that the differential expression does not result from a global defect in nitrogen-regulation in UKY502.

Specific induction of *ARO9* and *ARO10* is mediated by the zinc finger transcriptional activator Aro80p (Iraqui *et al.*, 1999). Only eight promoters in the *S. cerevisiae* genome contain an exact match to the proposed Aro80p binding site, a direct repeat of 5'-T(A/T)(A/G)CCG-3' (Iraqui *et al.*, 1999). These comprise four pairs of divergently transcribed genes, and one stand-alone. The three of these genes exhibiting phenylalanine-induced expression are *ARO9*, *ARO10* and *ESPB6* (showing increases of 6-, 30-, and 2.5-fold respectively). These all have the Aro80p binding site positioned in the forward direction, which suggests that it only functions in this orientation. The limited specificity of Aro80p control might serve to separate the pathways of phenylalanine biosynthesis and catabolism, which share the intermediate phenylpyruvate and co-exist in the cytosol (Vuralhan *et al.*, 2003). A specific effect of a histone H4 mutation on such a specific transcriptional activator could explain the identification of two co-regulated genes by the cross referencing strategy applied in this work.

Nuclease mapping reveals that the Aro80p binding site in the *ARO10* gene promoter (UAS_{aro}) is located within a region partially protected from MNase digestion by the 5' end of a positioned nucleosome. Although activation of *ARO10* is not accompanied by remodelling of a proximal nucleosome (figures 5.5 and 5.11), the semi-nucleosomal context of the Aro80p recognition site suggests that chromatin mediated regulation is important at this gene. Since import of aromatic amino acids is down-regulated in these conditions where a good nitrogen source is present, intracellular concentrations of inducer will be low: genes encoding the primary importers of aromatic amino acids for catabolism (*GAP1* and *WAP1*) are not up-

regulated by UKY502 (Iraqui et al., 1999). Hyper-expression of *ARO9* and *ARO10* in UKY502 might result from Aro80p promoting transcription more efficiently when nucleosomes contain I21V histone H4 than it does in the WT context, even with limiting amounts of inducer. The globular domain mutations in UKY501 restore expression of *ARO9* and *ARO10* to normal, suggesting that these mutations impair gene activation by Aro80p.

But how could decreased expression of *ARO9* and *ARO10* lead to a loss of mtDNA in UKY500? One possibility is that these proteins have unidentified activities that play a role in regulation of transcription. It is difficult to imagine what these might be, but Aro9p does have both a cytoplasmic and nuclear localisation (Huh *et al.*, 2003). Another possibility revolves around altered intracellular concentrations of glutamate.

Decreased Aro9p and Aro10p activity reduces flux through the Ehrlich pathway, which could reduce intracellular concentrations of glutamate. A hint that glutamate concentration is indeed significantly altered in UKY500 is provided by the increased expression of *SNO1* mRNA in this mutant. Sno1p is involved in the synthesis of pyridoxine, which is a co-factor required by transaminase enzymes. Transaminases catalyse the interconversion of amino acids by transferring the amino group from one, to the α-keto acid skeleton of another. Glutamate and α-ketoglutarate are the usual substrates/products of these reactions, and the directionality is determined by their relative intracellular concentrations (figure 5.19). Thus an increase in *SNO1*

transcription might suggest that the relative levels of glutamate and α-ketoglutarate are disrupted in UKY500 compared to WT.

Reduced levels of glutamate trigger retrograde signalling via Rtg1p and Rtg3p, which up-regulates enzymes catalysing early steps in the TCA cycle that generate glutamate (Lui and Butow 1999). In UKY500, glutamate concentration may have been lowered out of context by the specific effect of expressing a mutant histone H4 on Aro80p mediated transcription. Under these abnormal circumstances, gene expression patterns established by retrograde signalling might imbalance respiratory pathways, metabolites and redox potentials, causing mtDNA to be lost over time. Alternatively, a similar imbalance could result from an inability of Rtg1p/Rtg3p to function properly in the mutant histone H4 chromatin context. Supportive of the latter idea, a link between retrograde signalling and chromatin has been established by the interaction of Rtg proteins with SAGA (Massari *et al.*, 1999). This might explain the relatively small up-regulation of the characteristic retrograde response gene *CIT2* in UKY500, which can be as high as 40- or 50-fold.

Elevated intracellular glutamate concentrations resulting from hyper-expression of *ARO9* and *ARO10*, also fits with the patterns of gene expression observed in UKY502. With an abundant supply of glutamate, the cell can synthesise other amino acids via transamination reactions (figure 5.19). This is consistent with the observed increased transcript levels of genes required for pyridoxine synthesis. Since amino acids cannot be stored, synthesis will be diverted away from those of which the cell has plenty. This explains the decreased mRNA expression of genes which

biosynthesise arginine, lysine and proline, as these are most directly synthesised from glutamate. It also explains decreased transcription of *GDH1*: the cell has enough glutamate already, and does not need to pull it out of the TCA cycle (figure 5.1).

But whether decreased flux through the Ehrlich pathway, due to decreased expression of *ARO9* and *ARO10*, would lead to a reduction in glutamate levels *in vivo* cannot be determined from the data here alone. The hyper-expression of *ARO9* and *ARO10* by UKY502 could also be explained if *GDH1* were the directly affected gene. *GDH1* is regulated at the chromatin level by components of the SAGA and ADA complexes (Riego *et al.*, 2002). Increased *ARO9* and *ARO10* expression could represent an attempt to restore glutamate concentration reduced caused by down-regulation of *GDH1* mRNA expression in UKY502.

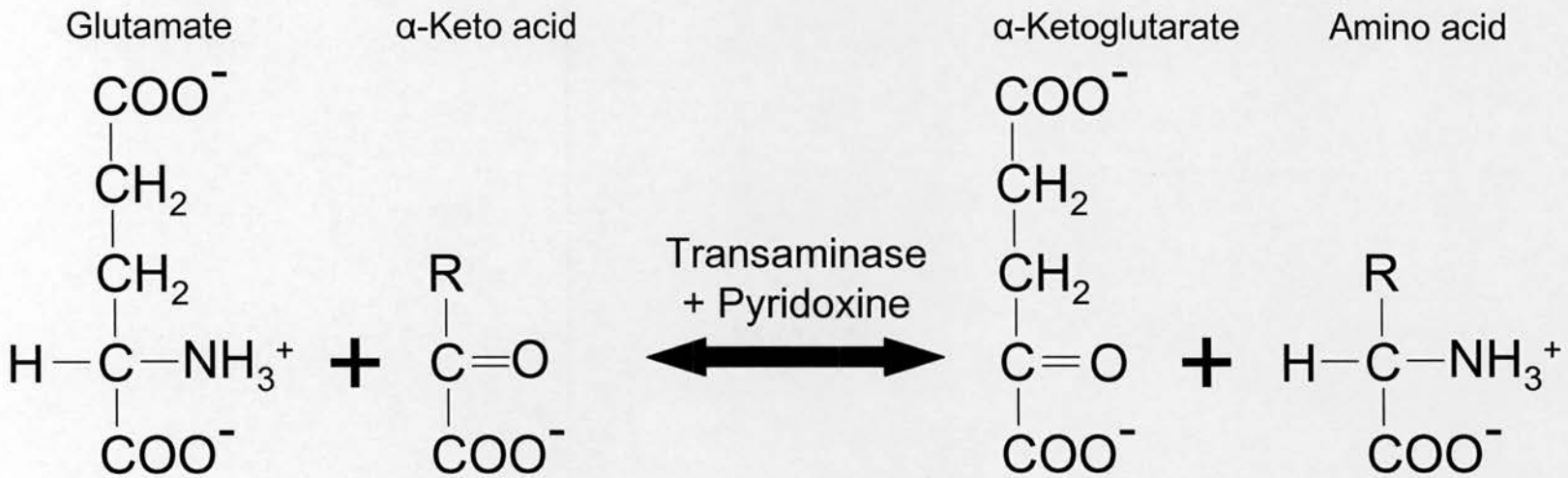

Figure 5.19 Transamination of glutamate. Transaminases catalyse the interconversion of amino acids by transferring the amino group from one to the α-keto acid skeleton of another. Pyridoxine is a co-factor required by transaminase enzymes.

5.7.2 Could Ynr064cp have a role in the Retrograde Response?

The intracellular sensor of low glutamate that induces retrograde signalling is unknown. In the microarray experiments presented here the levels of *RTG1* and *RTG3* transcripts are unaffected in UKY500. This is consistent with the primary control mechanism of these proteins being at the level of phosphorylation and subcellular location (Sekito *et al.*, 2000, Komeili *et al.*, 2000). If an improper retrograde response is indeed ultimately responsible for mtDNA loss in UKY500, there might be a role in retrograde signalling for the gene of unknown function identified by cross-referencing, *YNR064C*. A yeast two hybrid screen identified Ynr064cp as being able to interact with the bHLH transcription factor Ino4p, and this interaction was confirmed biochemically (Robinson *et al.*, 2000). The same study also demonstrated that Rtg1p and Rtg3p interact with Ino4p. Dimerisation via the amphipathic helices of their HLH domains is characteristic of bHLH transcription factors. This juxtaposes two different DNA binding domains, with both halves contributing to the DNA sequence specificity of the complex (Ma *et al.*, 1994). By heterodimerising with multiple partners, Ino4p coordinates several intracellular pathways. For instance, when complexed with Ino2p (which contains the transcriptional activation domain) it exerts control over phospholipid biosynthesis (reviewed by Greenberg and Lopes, 1996).

The fact that Rtg1p, Rtg3p and Ynr064cp can all interact with Ino4p, raises the possibility that Ynr064cp (which has homology to prokaryotic hydrolase enzymes) is a link between the retrograde and phospholipid biosynthesis pathways. In addition to

ARO9 and *ARO10*, *YNR064C* is down-regulated in UKY500 compared to UKY412(WT) and in UKY501 compared to UKY502 (table 5.7a). If glutamate concentrations are indeed lower in UKY500 and UKY501 than their array partners, down-regulation of *YNR064C* may be a characteristic of retrograde signalling. If true, this might explain the increased *PHO5* transcript levels seen in UKY500. Dimerisation of Ino4p with Rtg3p (which contains the activation domain) generates a functional transcriptional activator, which can direct expression from Ino4p responsive genes, such as *PHO5* (Robinson *et al.*, 2000). The suggestion by the authors is that a functional interaction between Ino4p and Rtg3p serves to increase phospholipid biosynthesis required for mitochondrial biogenesis when respiration is compromised. I would propose that in *petite* mutants it might support the proliferation of peroxisomes induced by retrograde signalling.

Consistent with the possible roles of Aro9p, Aro10p and Ynr064c, and also Aro80p, strains bearing deletion of these genes have a moderate growth defect on media containing lactate as the sole carbon source (SGD curated paper, unpublished). More experiments are needed to confirm if Ynr064cp does indeed have some role, perhaps a negative one, in retrograde signalling. It would be interesting to determine whether a *ΔYNR064C* strain has altered sensitivity to the non-metabolisable glutamate analogue D-aspartate in low glutamate media. Comparing the growth of a *YNR064C* over-expression strain with that of WT under conditions of glutamate starvation could also be informative.

Chapter 6: General Discussion

Yeast chromatin is often compared to the active fraction of higher eukaryotic chromatin, but its structure beyond that of the core nucleosome (White *et al.*, 2001) is not well characterised structurally. A better understanding of yeast chromatin structure would aid in interpreting the functional mechanisms involving chromatin in gene regulation. In order to highlight and learn more about the differences between yeast and human chromatin, we have substituted yeast histone H4 with its human counterpart. If it were viable, a yeast strain expressing human forms of histone proteins in place of its own might also provide an improved model of higher eukaryotic chromatin. The work presented here represents the first step in creating and understanding such a model.

This PhD thesis describes the construction and characterisation of three *S. cerevisiae* mutants that express forms of histone H4 engineered to be identical, or akin to, the human counterpart protein. In each case, the mutant histone is able to maintain yeast survival in the complete absence of the WT protein.

Under optimal conditions the 'humanised' histone H4 mutants have growth rates that are similar to WT. Only when starved of the preferred carbon source glucose, or subjected to temperature stress did phenotypic differences between mutants become apparent. The yeast strain that expresses a form of histone H4 with seven mutations within the globular domain, UKY500, moreover has a significantly altered genotype: it has lost mitochondrial DNA.

The results presented in chapter 4 demonstrate that a further isoleucine to valine substitution at position 21 (I21V) in the histone H4 N-terminus of UKY501, completing the human amino acid sequence, rescues mutant UKY500 for loss of mtDNA. Additionally, I21V partially rescues the decrease in histone H4 acetylation observed in this mutant. On the basis of these results, one might propose the model shown in figure 6.1. In WT cells, genes involved in the biogenesis or maintenance of mtDNA are expressed to normal levels. In UKY500, expression of these genes is reduced to below the threshold required to maintain a WT mitochondrial genome, perhaps as a result of a compromised histone acetyltransferase (HAT) activity in the mutant nucleosomal context. Strain UKY501 expresses a histone H4 isoform containing all of the eight amino acids substitutions that comprise the difference between the yeast and human proteins. The partially-restored levels of histone H4 acetylation in this mutant might increase expression of genes concerned with mtDNA biogenesis or maintenance to above the threshold required for its integrity. The incomplete rescue might explain why UKY501 is still compromised for growth on non-fermentable media. UKY502 contains the I21V mutation in isolation. Although this mutant exhibits enhanced growth on non-fermentable media, it has WT levels of histone H4 acetylation. An activating effect of I21V further to the influence it has on histone H4 acetylation levels could explain the growth phenotype of this mutant.

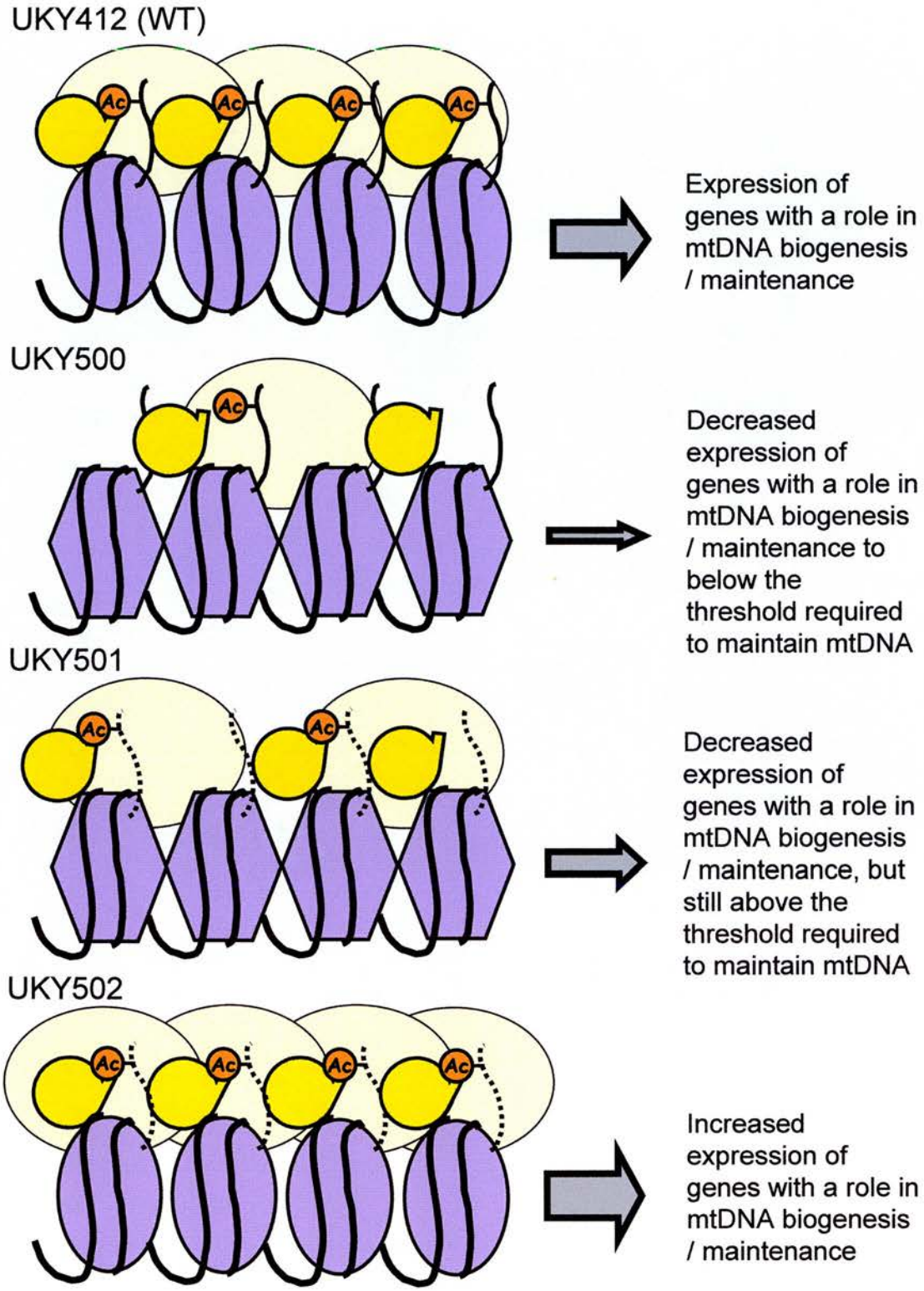

Figure 6.1 Model for mtDNA loss. Nucleosomes with WT globular domains are purple ovals; those containing 'humanising' mutations are purple hexagons. WT tails are solid black lines; those with I21V are dashed. Flesh ovals represent RNA polymerase. Yellow shapes are HATs, and acetylated lysines are indicated by orange circles. Mutations in the H4 globular domain decrease expression of genes concerned with mtDNA integrity, perhaps because HAT function is impaired. I21V increases expression of these genes, perhaps in part by restoring HAT function.

Western blots with more specific antibodies are required to determine which particular lysine residue(s) in histone H4 suffers decreased acetylation when the globular domain mutations are present. This acetylation pattern, as well as the acetylation status of other histones, could also reveal whether the mutations within the histone core have directly influenced acetylation of the tail, which is spatially distant within a single nucleosome. The microarray experiments presented in chapter 5 indicate that the different levels of histone H4 acetylation are not the result of altered HAT or HDAC transcription. Western blotting with many different antibodies would be needed to obtain a full picture of the impact of the histone H4 globular domain mutations on histone modification patterns. If a histone code does indeed exist, it is possible that the affect on histone H4 acetylation has been caused by, or leads to, an alteration in levels of other histone post-translational modifications.

It would be informative to test the relative levels of histone acetylation, and other modifications, in WT and mutant strains grown in the presence of antimycin. Antimycin inhibits electron transport, and its use would allow phenotypes resulting from decreased respiratory activity to be separated from those that are a more direct result of the histone H4 mutations. The relevance of this is apparent when one considers that NAD^+ is a co-factor for the SIR2 family of HDACs, which provides a link between chromatin regulation and metabolic status (Denu, 2003). Although the energy charge of a respiratory deficient strain is lowered, the effect on the NAD^+/NADH ratio cannot easily be predicted: both the TCA and glyoxylate cycles consume acetyl CoA and NAD^+, but whilst respiratory competent cells can regenerate NAD^+ by passage of the electrons it accepts down the electron transport

chain, respiratory deficient cells cannot. Antimycin treatment would thus permit fairer comparison of strains.

Would a similar loss of mtDNA occur if the mutant histone H4 expressed by UKY500 was incorporated into nucleosomes composed of otherwise WT, human histones? Such a question would be difficult to address in human cells for which respiration is obligatory, but since impaired mitochondrial function can cause human disease, identification of genes involved in its regulation is a valuable line of research (Steinmetz *et al.*, 2002). Genome-wide mRNA expression analyses indicate a few possible reasons for the *petite* phenotype of UKY500. The first is that an effect of the mutant histone has led to decreased expression of nuclear genes encoding components of mitochondrial electron transport, which has in turn precipitated loss of mtDNA. However, we do not think this likely due to the apparent lack of co-regulatory mechanisms of these genes under the conditions employed, and their susceptibility to retrograde response-mediated inactivation. The second possibility suggested by the microarrays is that the mutations introduced into histone H4 affect the intracellular concentrations of the important metabolite glutamate, as outlined in section 5.7.1.

The model presented in figure 6.2 is adapted from that in figure 6.1 to explain events which may be occurring in the promoter regions of *ARO9* and *ARO10*. An effect of the histone H4 mutations on the ability of the transcriptional activator Aro80p to co-ordinately recruit positive regulators of transcription to these genes, could ultimately lead to altered intracellular glutamate concentrations, as discussed in section 5.7.1.

The link between glutamate levels and respiration is provided by the TCA cycle, which is a source of both cellular energy and vital biosynthetic intermediates. Changes in glutamate concentration impose regulation upon TCA and glyoxylate cycle enzymes, which serve to readjust it. If these activities are not appropriately co-ordinated, the metabolite status and redox potentials of the cell will become imbalanced. As a non-essential component, the mitochondrial genome is inherently unstable in yeast and sensitive to a wide range of genetic and environmental factors. At the level of transcription, the alterations in gene expression patterns which occur in response to reduced glutamate concentration are initiated by retrograde signalling. Establishment of abnormal retrograde response-induced gene expression patterns in the UKY500 mutant histone H4 context could unfavourably affect cellular homeostasis, causing mtDNA to be lost over generations.

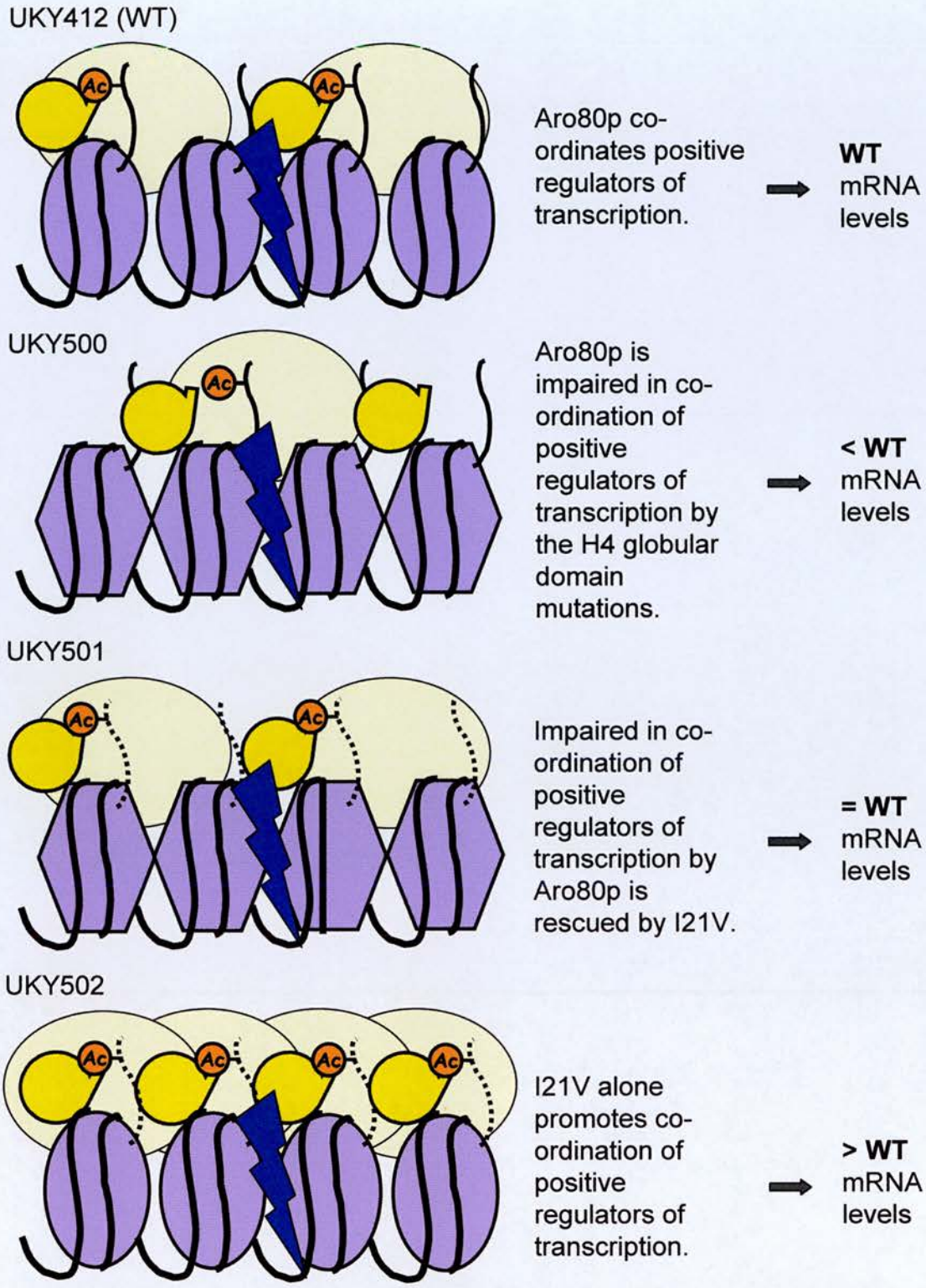

Figure 6.2 Model for events at *ARO9* and *ARO10* promoters. Nucleosomes with WT globular domains are purple ovals; those containing 'humanising' mutations are purple hexagons. WT tails are solid black lines; those with I21V are dashed. Flesh ovals represent RNA polymerase. Yellow shapes are HATs, and acetylated lysines are orange circles. The blue shape represents Aro80p. Mutations in the H4 globular domain impair recruitment of positive regulators of transcription by Aro80p at *ARO9* and *ARO10,* decreasing their expression. I21V promotes recruitment of positive regulators of transcription by Aro80p, increasing *ARO9* and *ARO10* transcription.

Comparing the transcriptomes of UKY502 and WT indicates that the I21V mutation has an overall activating effect on gene expression. This still holds true in UKY501, despite reduced levels of histone H4 acetylation in this mutant. A more complete picture of histone modification patterns is needed to understand how I21V is exerting its effect. The globular domain mutations appear to counteract this activation function to a certain degree, as the genome-wide expression patterns of fully the 'humanised' histone H4 mutant UKY501 are more similar to WT than those of UKY502. Like the original pair wise experiments, the cross-array comparisons are supportive of metabolic disruption: genes concerned with the metabolism of amino acids are affected in UKY502, and the gene *PAN5* is strongly down-regulated in both UKY501 and UKY502. *PAN5* is required for biosynthesis of pantothenate, which is a precursor to coenzyme A. Coenzyme A is an end product of the TCA cycle, whereas its acetylated adduct is both a substrate of the cycle and a donor for the reactions catalysed by HATs!

Clearly the impact of 'humanising' histone H4 mutations on yeast metabolism warrants further investigation, but properly relating observed phenotypes to effects of a chromatin mutation in the nucleus will require a combination of genetic and biochemical techniques. The sensitivity of metabolic pathways to substrate/product equilibria, as well as allosteric and feedback regulation means that effects on enzyme activity may not be visible at the level of transcription. Additionally, from transcriptome studies alone it would be difficult to distinguish the direct effects of a histone mutation from down-stream alterations in mRNA expression induced by metabolic changes.

As well as being blind to all forms of post-transcriptional regulation, microarrays provide no information on the sub-cellular localisation of proteins. A particular isoform of histone H1 has recently been shown to transmit apoptotic signals from the nucleus to mitochondria in mice (Konishi *et al.*, 2003). This involves a physical relocation of histone H1.2 from the nucleus to the cytoplasm, and results in release of pro-apoptotic factors from mitochondria. Yeast does not apoptose in the manner of mammalian cells, and is not known to have an H1.2 homologue. However, Western blotting for histone H4 in a mitochondrially derived protein preparation is needed to determine whether any mutant histone H4 protein is mis-localised here, where it could influence mitochondrial function.

Another possibility is that the primary impact of the histone H4 substitutions is not at the level of gene expression (these are secondary effects), but, for instance, they may have interfered with large-scale structure or assembly of chromatin.

When yeast grow in sub-optimal conditions, such as on a non-fermentable carbon source or at elevated temperature, they induce expression of genes to cope with the situation. If I21V has a general activating role, it might make normally repressed classes of genes easier to turn on when circumstances change. Conversely, the repressive characteristics of the globular domain mutations would make the same genes more difficult to activate. This may explain the increased growth rate of UKY502, and decreased growth rate of UKY501 on respiratory media (EtLac). Microarray experiments employing a switch from fermentable to respiratory media, in these strains and WT, would address this possibility.

The mutations introduced into the globular domain of histone H4 are in the region of a silencing domain identified on the surface of nucleosomes (Park *et al.*, 2002). About 10% of the budding yeast genome is silenced, and this requires the SIR proteins. A characteristic of SIR mediated silencing is its nucleation at specific sites, and concomitant spreading into surrounding regions. Spreading can be limited discretely by the presence of boundary elements, such as at the silent mating loci, or in a variegatable manner as in the case of sub-telomeric heterochromatin. Euchromatin is rich in epigenetic marks that are proposed to be inhibitory to the binding of SIR proteins, thus restricting the limited pools to their normal chromosomal locations (Leeuwen and Gottschling, 2002). Although genes identified by microarray do not imply an influence on silencing in UKY500 at this level of significance, it would be interesting to see if subtle effects exist.

Methylation by Dot1p of histone H3K79 affects 90% of nucleosomes, and is believed to inhibit binding of SIR proteins (Leeuwen *et al.*, 2002). Dot1p will not methylate free histone H3, implying that residues from other histones are important (Ng *et al.*, 2002). Western blotting with an antibody specific for methylated histone H3K79 would reveal whether the spatially proximal mutations in the histone H4 globular domain have affected levels of this modification. With the histone code operating *in trans*, a decrease in histone H3K79 methylation could translate into reduction of another general euchromatic mark, acetylated histone H4K16 (Robyr *et al.*, 2002). The activities of Sir2p and Sas2p limit the spread of sub-telomeric heterochromatin by their opposing affects on acetylation of histone H4K16 (Kimura *et al.*, 2002; Suka *et al.*, 2002). Reduced histone H3K79 methylation would promote

the binding of SIR proteins, and shift this balance in favour of deacetylation by Sir2p. Since SIR proteins bind more efficiently to unacetylated histone H4K16, this would lead to them binding outside of their normal domains (Hecht *et al.*, 1995). If effects at histone H4K16 are largely responsible for the decreased histone H4 acetylation observed in UKY500, it would explain the small number of affected genes indicated by the microarrays. Again, this could be determined by Western blot.

Neither the genes affected by I21V, nor their chromosomal locations imply that the general activation affect of this mutation is due to loss of silencing. However, position 21 in histone H4 has been implicated in silencing at the HM loci, where its mutation to alanine, serine or proline abrogates SIR-mediated silencing (Johnson *et al.*, 1992). The conservative isoleucine to valine substitution made here does not cause sterility however, implying that HM silencing is intact. But whilst HM silencing is extremely stable, telomeric silencing is sometimes referred to as 'semi-stable', and is more easily perturbed. I21V might have a slight de-stabilising effect on binding of SIR proteins in sub-telomeric regions.

Minor silencing defects caused by the mutations in both the globular and tail regions of histone H4 could explain why the sub-telomerically located gene *COS12* is expressed by all mutant strains. In the former case this would be due to titration of SIR proteins away from their normal location, and in the latter case because of a reduction in the strength of the interaction between SIR proteins and nucleosomes within their proper locations.

The work in this thesis demonstrates that the high degree of sequence conservation of histone H4 across species means that yeast strain UKY501 is able to survive by expressing human histone H4 in the absence of its own, WT protein. The observed interaction between the globular domain and histone H4 tail mutations highlights an important evolutionary concept: the combination of these spatially distal substitutions restores a balance that is perturbed by mutation of either region alone. The next logical step in creating a model of higher eukaryotic chromatin would be to co-express human histones H4 and H3 in yeast. Mutation of both histones might optimise interactions within the nucleosome core, as evolution has mostly likely done. By analogy with the interaction observed between globular domain mutations and I21V, this could produce a yeast strain more similar to WT than is UKY501. On the other hand, the human histone H3/H4 tetramer would represent the core of the nucleosome of the higher eukaryotic, mostly inactive chromatin structure. This, and modification of both of the N-terminal tails of histones H3 and H4 might be too severe for yeast to tolerate.

Chapter 7: Appendix

A.1 Primers used throughout this Thesis

Table A.1: Primers used in the construction of pUK plasmids, which contain site specific mutations within the *HHF2* sequence. Table includes primer name, sequence of primer when read from 5' to 3', and reference to their function.

Primer Name	Sequence (5' to 3')	Function
Hp	GTATGGCAGGACGTTCTGGG	Hybridises outside *HHF2 HindIII* site. Cloning and sequencing. Figure 3.5.
Ep	CGTATCACGAGGCCCTTTCG	Hybridises outside *HHF2 EcoRI* site. Cloning and sequencing. Figure 3.5.
Hm-H4a	ACTGCGTCCCTGATGACGTTTT CCAAGAAAACTTTCAAGACACC TCTGGTTTCTTCGTAGATCAAA	Adds site specific mutations into *HHF2* globular domain sequence. Figure 3.5.
Hm-H4c	TCCATTGCAGTAACAGTCTTT CTCTTGGCGTGTTCAGTGTAA GTAACTGCGTCCCTGATGAC	Adds site specific mutations into *HHF2* globular domain sequence. Figure 3.5.
Hm-h4b	GTTACTGCAATGGATGTTGTT TATGCTTTG	Provides overlap for SOE reaction. Figure 3.5.
I-Vfw	CGTCACAGAAAGGTTCTAAG	Adds I21V to *HHF2*. Figure 4.1-2.
I-Vbk	CTTAGAACCTTTCTGTGACG	Adds I21V to *HHF2*. Figure 4.1-2.

Table A.2: Primers used for PCR amplification of Northern blot probes in Chapters 3 and 4. Includes primer name, sequence of primer when read from 5' to 3', and the size of the PCR fragment amplified from within the coding region of the gene indicated.

Primer Name	Sequence (5' to 3')	Gene name & fragment size (bp)
NB1	tgactgaattcaaggccggt	*CYC1*; 270
NB2	aacccaccaaagccatctt	
ACT1A	gtcggtagaccaagacacc	*ACT1*; 1010
ACT1B	gtgaacgatagatggaccac	
SUC2-ielC	gatgcttttgcaagctttc	*SUC2*; 285
SUC2-ielD	cttgggagcgatagcaatg	

An *HHF2* Northern blot probe was excised from a derivative of plasmid pRS414 (ATCC) in which *HHF2* is inserted between the *NotI* and *BamH1* sites of the polylinker (pRS414.GAL.H4). This probe contains the full length *HHF2* sequence.

Table A.3: Primers used for PCR amplification of Southern blot probes used in Chapter 4. Includes primer name, sequence of primer when read from 5' to 3', and the size and position of the PCR fragment amplified from within the coding region of the gene indicated.

Primer Name	Sequence (5' to 3')	Gene name & fragment size (bp)
COXIIFWD	gcaacaccaaatcaagaaggtat	*COXII*; 256 (85-341)
COXIIBCK	gctggtgaaataacttcatcaca	
SUC2-ielC	gatgcttttgcaagctttc	*SUC2*; 285 (0-285)
SUC2-ielD	cttgggagcgatagcaatg	

Table A.4: Primers used for PCR amplification of indirect end labelling probes throughout this thesis. Includes primer name, sequence of primer when read from 5' to 3', and the size and position of the PCR fragment amplified from within the coding region of the gene indicated.

Primer Name	Sequence (5' to 3')	Size (bp)	Hybridisation position
IDEL1	catcgcgtattttgtaagct	249	1453-1204bp upstream of *CYC1*
IDEL2	gtcaagagaagcgaatacta		
CYC1Ha	gtcacgcttacattcacgcc	226	372-598bp downstream of *CYC1*
CYC1Hb	aaagccttcgagcgtcccaa		
SUC2-ielC	gatgcttttgcaagctttc	285	0-285bp downstream of *SUC2*
SUC2-ielD	cttgggagcgatagcaatg		
ARO10IDELfw	gagaggctaccattaaacaacgac	436	1347-911bp upstream of *ARO10*
ARO10IDELbk	cacaccctgaactgacgaatatac		
COS12IDELfw	tacaggcaactgtttaccaacg	448	1133-685bp upstream of *COS12*
COS12IDELbk	attaggttcatttcccaggcac		

Table A.5: Primers used for PCR amplification of Northern blot probes in Chapter 5. Includes primer name, sequence of primer when read from 5' to 3', and the size of the PCR fragment amplified from within the coding region of the gene indicated.

Primer Name	Sequence (5' to 3')	Gene name & fragment size (bp)
aro10fw	TAATGAACTGAACGCCGCTT	*ARO10*; 630
aro10bk	CCAAATCCCAGTTTTGCAGA	
atp14fw	TCAATGCTTCAGTTCTGCCA	*ATP14*; 327
atp14bk	GTTTCCTCAGCATCATCCAA	
cit2fw	ATTCAAAAGGACCTGCCCAA	*CIT2*; 577
cit2bk	TTCAAACCTGATGCAAGGGA	
cos12fw	TGCTTCTTGAGCCATTTTCC	*COS12*; 488
cos12bk	TCGTCCTCTTCGCAATTTGA	
cpa2fw	TTGCCCGTTACACCAGAATA	*CPA2*; 600
cpa2bk	TTGCGGCGGATCTTAACATA	
dip5fw	AAAACACGCGGTTGAGGAAA	*DIP5*; 639
dip5bk	ACGAAAACAGCAACGAACGA	
hac1fw	ATTCGCAATCGAACTTGGCT	*HAC1*; 536
hac1bk	CCACCGCATCAAACAAATTG	
hho1fw	AAACCACGGCAAAAAAGGAG	*HHO1*; 437
hho1bk	AGGTCAATGAAGAAGGCGAA	
his4fw	TTGGGTCGTGGCGTTTATTA	*HIS4*; 602
his4bk	CTTTTGGATTGGTCTGCTCA	
mam3fw	TCGGTGAAATTATTCCGCAG	*MAM3*; 415
mam3bk	GTTGTTTGGTTCATTGGGCA	
pdr15fw	AGCAACCATAATGCGCACAA	*PDR15*; 639
pdr15bk	GATACGATTTTGCGGCGTTT	
rps5fw	TGTTGAAGAATTCACCCCAG	*RPS5*; 539
rps5bk	TCGGCCAAAGTTTCAGCAAT	
sno1fw	TGTCCGGAAAGTCGATGAAA	*SNO1*; 499
sno1bk	AACCGCGATAGGATCAAGAA	
ynr064cfw	GATTTACGGAAACGCCAGAA	*YNR064C*; 616
ynr064cbk	AAGCGCAAAATGGCCAGTAT	
ypl245wfw	AGCACATTTGTTGGCCACTT	*YPL245W*; 414
ypl245wbk	TTTCTCCTTGATTGCCTCGT	

A.2 Addresses of Routinely used on-line Resources:

Saccharomyces Genome Database (SGD):

http://www.yeastgenome.org/

Nationol Center for Biotechnology Information (NCBI):

http://www.ncbi.nlm.nih.gov/

FunSpec (Robinson *et al.*, 2002):

http://funspec.med.utoronto.ca/

Munich Information Centre for Protein Sequences (MIPS) *Saccharomyces cerevisiae* Group:

http://mips.gsf.de/genre/proj/yeast/index.jsp

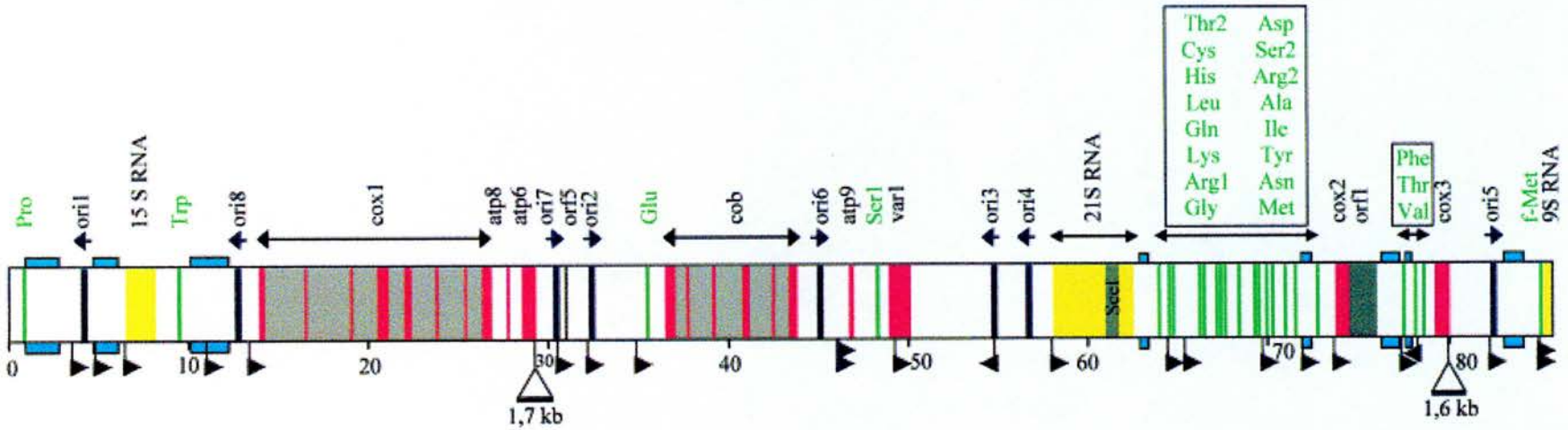

Figure A.1: Linearized map of the FY1679 mitochondrial genome (taken from Foury *et al.*, 1998). Red bars indicate exons of protein-coding genes; gray bars represent introns and intron-related ORFs. Green and yellow bars indicated tRNAs and rRNAs.; ori elements are shown in dark blue, and the light blue sections represent previous gaps in the mtDNA sequence of this strain that were filled in by this study. The two large deletions of mtDNA in this strain compared to others of the *Saccharomyces* genus are indicated by triangles. The flags indicate the transcription initiation sites and direction of the coding sequence. FY1679 is an isogenic derivative of S228C.

Chapter 8: References

Aasland, R., Stewart, A.F., Gibson, T (1996). "The SANT domain: a putative DNA-binding domain in the SWI-SNF and ADA complexes, the transcriptional co-repressor N-CoR and TFIIIB." *Trends Biochem Sci.* 21(3): 87-8.

Agatep, R., Kirkpatrick, R.D., Parchaliuk, D.L., Woods, R.A., Gietz, R.D (1998). Transformation of *Saccharomyces cerevisae* by the lithium acetate/single-stranded carrier DNA/polyethylene glycol (LiAc/ss-DNA/PEG) protocol.

Ahmad, K., and Henikoff, S (2002). "The histone variant H3.3 marks active chromatin by replication-independent nucleosome assembly." *Mol Cell* 9(6): 1191-200.

Ai, X., and Parthun, M.R (2004). "The nuclear Hat1p/Hat2p complex: a molecular link between type B histone acetyltransferases and chromatin assembly." *Mol Cell* 14(2): 195-205.

Allan, J., Hartman, P.G., Crane-Robinson, C., Aviles, F.X (1980). "The structure of histone H1 and its location in chromatin." *Nature* 288(5792): 675-9.

Allard, S., Utley, R.T., Savard, J., Clarke, A., Grant, P., Brandl, C.J., Pillus, L., Workman, J.L., Cote, J (1999). "NuA4, an essential transcription adaptor/histone H4 acetyltransferase complex containing Esa1p and the ATM-related cofactor Tra1p." *EMBO J.* 18(18): 5108-19.

Allfrey, V. G., Faulkner, R., Mirsky, A.E (1964). "Acetylation and methylation of histones and their possible role in the regulation of RNA synthesis." *Proc Natl Acad Sci U S A.* 51: 786-94.

Aravind, L., and Landsman, D (1998). "AT-hook motifs identified in a wide variety of DNA-binding proteins." *Nucleic Acids Res.* 26(19): 4413-21.

Arents, G., and Moudrianakis, E.N (1995). "The histone fold: a ubiquitous architectural motif utilized in DNA compaction and protein dimerization." *Proc Natl Acad Sci U S A.* 92(24): 11170-4.

Attardi, G., and Schatz, G (1988). "Biogenesis of mitochondria." *Annu Rev Cell Biol.* 4: 289-333.

Ausio, J., Levin, D.B., De Amorim, G.V., Bakker, S., Macleod, P.M (2003). "Syndromes of disordered chromatin remodeling." *Clin Genet.* 64(2): 83-95.

Ausubel, F. M., Brent, R., Kingston, R.E., Moore, D.D., Seidman, J.G., Smith, J.A., Struhl, K, Ed. (1998). *Current Protocols In Molecular Biology* (Volumes 1, 2, 3). Current Protocols In Molecular Biology, John Wiley and Sons, Inc.

Balasubramanian, R., Pray-Grant, M.G., Selleck, W., Grant, P.A., Tan, S (2002). "Role of the Ada2 and Ada3 transcriptional coactivators in histone acetylation." *J Biol Chem.* 277(10): 7989-95.

Basehoar, A. D., Zanton, S.J., Pugh, B.F (2004). "Identification and distinct regulation of yeast TATA box-containing genes." *Cell* 116(5): 699-709.

Baxevanis, A. D., Godfrey, J.E., Moudrianakis, E.N (1991). "Associative behavior of the histone (H3-H4)2 tetramer: dependence on ionic environment." *Biochemistry* 30(36): 8817-23.

Belotserkovskaya, R., Saunders, A., Lis, J.T., Reinberg, D (2004). "Transcription through chromatin: understanding a complex FACT." *Biochim Biophys Acta.* 1677(1-3): 87-99.

Bernstein, B. E., Tong, J.K., Schreiber, S.L (2000). "Genomewide studies of histone deacetylase function in yeast." *Proc Natl Acad Sci U S A.* 97(25): 13708-13.

Bird, A. P., and Wolffe, A.P (1999). "Methylation-induced repression--belts, braces, and chromatin." *Cell* 99(5): 451-4.

Bone, J. R., and Roth, S.Y (2001). "Recruitment of the Yeast Tup1p-Ssn6p Repressor Is Associated with Localized Decreases in Histone Acetylation." *J. Biol. Chem.* 276: 1808–1813.

Bottomley, M. J. (2004). "Structures of protein domains that create or recognize histone modifications." *EMBO Rep.* 5(5): 464-9.

Bowen, N. J., Fujita, N., Kajita, M., Wade, P.A (2004). "Mi-2/NuRD: multiple complexes for many purposes." *Biochim Biophys Acta.* 1677(1-3): 52-7.

Braunstein, M., Rose, A.B., Holmes, S.G., Allis, C.D., Broach, J.R (1993). "Transcriptional silencing in yeast is associated with reduced nucleosome acetylation." *Genes Dev.* 7(4): 592-604.

Briggs, S. D., Bryk, M., Strahl, B.D., Cheung, W.L., Davie, J.K., Dent, S.Y., Winston, F., Allis, C.D (2001). "Histone H3 lysine 4 methylation is mediated by Set1 and required for cell growth and rDNA silencing in *Saccharomyces cerevisiae*." *Genes Dev.* 15(24): 3286-95.

Brown, C. E., Howe, L., Sousa, K., Alley, S.C., Carrozza, M.J., Tan, S., Workman, J.L (2001). "Recruitment of HAT complexes by direct activator interactions with the ATM-related Tra1 subunit." *Science* 292(5525): 2333-7.

Brownell, J. E., Zhou, J., Ranalli, T., Kobayashi, R., Edmondson, D.G., Roth, S.Y., Allis, C.D (1996). "*Tetrahymena* histone acetyltransferase A: a homolog to yeast Gcn5p linking histone acetylation to gene activation." *Cell* 84(6): 843-51.

Bruno, M., Flaus, A., Stockdale, C., Rencurel, C., Ferreira, H., Owen-Hughes, T (2003). "Histone H2A/H2B dimer exchange by ATP-dependent chromatin remodeling activities." *Mol Cell Biol.* 12(6): 1599-606.

Butow, R. A., and Avadhani, N.G (2004). "Mitochondrial signaling: the retrograde response." *Mol Cell.* 14(1): 1-15.

Cairns, B. R., Kim, Y.J., Sayre, M.H., Laurent, B.C., Kornberg, R.D (1994). "A multisubunit complex containing the *SWI1/ADR6*, *SWI2/SNF2*, *SWI3*, *SNF5*, and *SNF6* gene products isolated from yeast." *Proc Natl Acad Sci U S A.* 91(5): 1950-4.

Cairns, B. R., Lorch, Y., Li, Y., Zhang, M., Lacomis, L., Erdjument-Bromage, H., Tempst, P., Du, J., Laurent, B., Kornberg, R.D (1996). "RSC, an essential, abundant chromatin-remodeling complex." *Cell* 87(7): 1249-60.

Carlson, M., Osmond, B.C., Botstein (1981). "Mutants of yeast defective in sucrose utilization." *Genetics* 98(1): 25-40.

Carlson, M., and Laurent, B.C (1994). "The SNF/SWI family of global transcriptional activators." *Curr Opin Cell Biol.* 6(3): 396-402.

Carlson, M. (1999). "Glucose represion in yeast." *Current Opinion in Microbiology* 2: 202-7.

Carmen, A. A., Milne, L., Grunstein, M (2002). "Acetylation of the yeast histone H4 N terminus regulates its binding to heterochromatin protein SIR3." *J Biol Chem.* 277(7): 4778-81.

Carrozza, M. J., Utley, R.T., Workman, J.L., Cote, J (2003). "The diverse functions of histone acetyltransferase complexes." *Trends Genet.* 19(6): 321-9.

Carruthers, L. M., Bednar, J., Woodcock, C.L., Hansen, J.C (1998). "Linker histones stabilize the intrinsic salt-dependent folding of nucleosomal arrays: mechanistic ramifications for higher-order chromatin folding." *Biochemistry* 37(42): 14776-87.

Carruthers, L. M., and Hansen, J.C (2000). "The core histone N termini function independently of linker histones during chromatin condensation." *J Biol Chem.* 275(47): 37285-90.

Chadwick, B. P., and Willard. H.F (2002). "Cell cycle-dependent localization of macroH2A in chromatin of the inactive X chromosome." *J Cell Biol.* 157(7): 1113-23.

Cherry, J. R., and Denis, C.L (1989). "Overexpression of the yeast transcriptional activator ADR1 induces mutation of the mitochondrial genome." *Curr Genet.* 15(5): 311-7.

Choe, J., Kolodrubetz, D., Grunstein, M (1982). "The two yeast histone H2A genes encode similar protein subtypes." *Proc Natl Acad Sci U S A.* 79(5): 1484-7.

Clarke, A. S., Lowell, J.E., Jacobson, S.J., Pillus, L (1999). "Esa1p is an essential histone acetyltransferase required for cell cycle progression." *Mol Biol Cell.* 19(4): 2515-26.

Collins, N., Poot, R.A., Kukimoto, I., Garcia-Jimenez, C., Dellaire, G., Varga-Weisz, P.D (2002). "An ACF1-ISWI chromatin-remodeling complex is required for DNA replication through heterochromatin." *Nat Genet.* 32(4): 627-32.

Conconi, A., Widmer, R.M., Koller, T., Sogo, J.M (1989). "Two different chromatin structures coexist in ribosomal RNA genes throughout the cell cycle." *Cell* 2(57): 753-61.

Contamine, V., and Picard, M (2000). "Maintenance and integrity of the mitochondrial genome: a plethora of nuclear genes in the budding yeast." *Microbiol Mol Biol Rev.* 64(2): 281-315.

Cosma, M. P., Tanaka, T., Nasmyth, K (1999). "Ordered recruitment of transcription and chromatin remodeling factors to a cell cycle- and developmentally regulated promoter." *Cell* 97(3): 299-311.

Cosma, M. P. (2002). "Ordered recruitment: gene-specific mechanism of transcription activation." *Mol Cell.* 10(2): 227-36.

Cross, S. L., and Smith, M.M (1988). "Comparison of the structure and cell cycle expression of mRNAs encoded by two histone H3-H4 loci in *Saccharomyces cerevisiae*." *Mol Cell Biol.* 8(2): 945-54.

Daignan-Fornier, B., Valens, M., Lemire, B.D., Bolotin-Fukuhara, M (1994). "Structure and regulation of SDH3, the yeast gene encoding the cytochrome b560 subunit of respiratory complex II." J *Biol Chem.* 269(22): 15469-72.

Davie, J. K., Edmondson, D.G., Coco, C.B., Dent, S.Y (2003). "Tup1-Ssn6 interacts with multiple class I histone deacetylases in vivo." *J Biol Chem.* 278(50): 50158-62.

de la Barre, A. E., Angelov, D., Molla, A., Dimitrov, S (2001). "The N-terminus of histone H2B, but not that of histone H3 or its phosphorylation, is essential for chromosome condensation." *EMBO J.* 20(22): 6383-93.

De Vit, M. J., Waddle, J.A., Johnston, M (1997). "Regulated nuclear translocation of the Mig1 glucose repressor." *Mol.Biol Cell.* 8(8): 1603-18.

de Winde, J. H., and Grivell, L.A (1993). "Global regulation of mitochondrial biogenesis in *Saccharomyces cerevisiae*." *Prog Nucleic Acid Res Mol Biol.* 46: 51-91.

Deckert, J., Struhl, K (2002). "Targeted recruitment of Rpd3 histone deacetylase represses transcription by inhibiting recruitment of Swi/Snf, SAGA, and TATA binding protein." *Mol Cell Biol.* 22(18): 6458-70.

DeLange, R. J., Fambrough, D.M., Smith, E.L., Bonner, J (1969). "Calf and pea histone IV. 3. Complete amino acid sequence of pea seedling histone IV; comparison with the homologous calf thymus histone." *J Biol Chem.* 244(20): 5669-79.

Denu, J. M. (2003). "Linking chromatin function with metabolic networks: Sir2 family of NAD(+)-dependent deacetylases." *Trends Biochem Sci.* 28(1): 41-8.

DeRisi, J. L., Iyer, V.R., Brown, P.O (1997). "Exploring the metabolic and genetic control of gene expression on a genomic scale." *Science* 278(5338): 680-6.

Diffley, J. F., and Stillman, B (1991). "A close relative of the nuclear, chromosomal high-mobility group protein HMG1 in yeast mitochondria." *Proc Natl Acad Sci U S A.* 88(17): 7864-8.

Dingwall, A. K., Beek, S.J., McCallum, C.M., Tamkun, J.W., Kalpana, G.V., Goff, S.P., Scott, M.P (1995). "The Drosophila snr1 and brm proteins are related to yeast SWI/SNF proteins and are components of a large protein complex." *Mol Biol Cell.* 6(7): 777-91.

Dover, J., Schneider, J., Tawiah-Boateng, M.A., Wood, A., Dean, K., Johnston, M., Shilatifard, A (2002). "Methylation of histone H3 by COMPASS requires ubiquitination of histone H2B by Rad6." *J Biol Chem.* 277(32): 28368-71.

Ducker, C. E., and Simpson, R.T (2000). "The organized chromatin domain of the repressed yeast a cell-specific gene *STE6* contains two molecules of the corepressor Tup1p per nucleosome." *EMBO J.* 19(3): 400-9.

Dujon, B. (1981). Nucleo-mitochondrial interactions. Mitochondria. J. N. Strathern, Wolf,K. and Kandewitz, F. Berlin, De Gruyter. 1.

Dumont, M. E., Cardillo, T.S., Hayes, M.K., Sherman, F (1991). "Role of cytochrome c heme lyase in mitochondrial import and accumulation of cytochrome c in Saccharomyces cerevisiae." *Mol Cell Biol.* 11(11): 5487-96.

Dutcher, S. K., and Hartwell L.H (1983). "Genes that act before conjugation to prepare the *Saccharomyces cerevisiae* nucleus for caryogamy." *Cell* 33(1): 203-10.

Ebbert, R., Birkmann, A., Schuller, H.J (1999). "The product of the SNF2/SWI2 paralogue *INO80* of *Saccharomyces cerevisiae* required for efficient expression of various yeast structural genes is part of a high-molecular-weight protein complex." Mol *Microbiol.* 32(4): 741-51.

Eberharter, A., Ferrari, S., Längst, G., Straub, T., Imhof, A., Varga-Weisz, P., Wilm, M., Becker, P.B (2001). "Acf1, the largest subunit of CHRAC, regulates ISWI-induced nucleosome remodelling." *EMBO J.* 20(14): 3781-8.

Edmondson, D. G., Smith, M.M., Roth, S.Y (1996). "Repression domain of the yeast global repressor Tup1 interacts directly with histones H3 and H4." *Genes Dev.* 10(10): 1247-59.

Eisen, J. A., Sweder, K.S., Hanawalt, P.C (1995). "Evolution of the SNF2 family of proteins: subfamilies with distinct sequences and functions." *Nucleic Acids Res.* *23*(14): 2715-23.

Elfring, L. K., Deuring, R., McCallum, C.M., Peterson, C.L., Tamkun, J.W (1994). "Identification and characterization of *Drosophila* relatives of the yeast transcriptional activator SNF2/SWI2." *Mol Cell Biol.* 14(4): 2225-34.

Epstein, C. B., Waddle, J.A., Hale, W, 4th, Dave, V., Thornton, J., Macatee, T.L., Garner, H.R., Butow, R.A (2001). "Genome-wide responses to mitochondrial dysfunction." *Mol Biol Cell.* 12(2): 297-308.

Fan, J. Y., Gordon, F., Luger, K., Hansen, J.C., Tremethick, D.J (2002). "The essential histone variant H2A.Z regulates the equilibrium between different chromatin conformational states." *Nat Struct Biol.* 9(3): 172-6.

Fatemi, M., Hermann, A., Pradhan, S., Jeltsch, A (2001). "The activity of the murine DNA methyltransferase Dnmt1 is controlled by interaction of the catalytic domain with the N-terminal part of the enzyme leading to an allosteric activation of the enzyme after binding to methylated DNA." *J Mol Biol.* 309(5): 1189-99.

Fazzio, T. G., Kooperberg, C., Goldmark, J.P., Neal, C., Basom, R., Delrow, J., Tsukiyama, T (2001). "Widespread collaboration of Isw2 and Sin3-Rpd3 chromatin remodeling complexes in transcriptional repression." *Mol Cell Biol.* 21(19): 6450-60.

Finch, J. T., and Klug, A (1976). "Solenoidal model for superstructure in chromatin." *Proc Natl Acad Sci U S A.* 73(6): 1897-901.

Fischle, W., Wang, Y., Allis, C.D (2003). "Histone and chromatin cross-talk." *Curr Opin Cell Biol. 15*(2): 172-83.

Flaus, A., and Owen-Hughes, T (2004). "Mechanisms for ATP-dependent chromatin remodelling: farewell to the tuna-can octamer?" *Curr Opin Genet Dev.* 14(2): 165-73.

Fleming, A. B., and Pennings, S (2001). "Antagonistic remodelling by Swi-Snf and Tup1-Ssn6 of an extensive chromatin region forms the background for *FLO1* gene regulation." *EMBO J.* 20(18): 5219-31.

Forsburg, S. L., and Guarente, L (1989). "Identification and characterization of HAP4: a third component of the CCAAT-bound HAP2/HAP3 heteromer." *Genes Dev.* 3(8): 1166-78.

Foury, F., Roganti, T., Lecrenier, N., Purnelle, B (1998). "The complete sequence of the mitochondrial genome of *Saccharomyces cerevisiae*." *FEBS Lett.* 440: 325–331.

Fritze, C. E., Verschueren, K., Strich, R., Easton, Esposito, R (1997). "Direct evidence for SIR2 modulation of chromatin structure in yeast rDNA." *EMBO J.* 16(21): 6495-509.

Gancedo, J. M. (1998). "Yeast carbon catabolite repression." *Microbiol Mol Biol Rev.* 62(2): 334-61.

Garcia, S. N., and Pillus, L (2002). "A unique class of conditional sir2 mutants displays distinct silencing defects in *Saccharomyces cerevisiae*." *Genetics* 162(2): 721-36.

Garcia-Ramirez, M., Rocchini, C., Ausio, J (1995). "Modulation of chromatin folding by histone acetylation." *J Biol Chem.* 270(30): 17923-8.

Garkavtsev, I., Grigorian, I.A., Ossovskaya, V.S., Chernov, M.V., Chumakov, P.M., Gudkov, A.V (1998). "The candidate tumour suppressor p33ING1 cooperates with p53 in cell growth control." *Nature* 391(6664): 295-8.

Gavin, I. M., and Simpson, R.T (1997). "Interplay of yeast global transcriptional regulators Ssn6p-Tup1p and Swi-Snf and their effect on chromatin structure." *EMBO J.* 16(20): 6263-71.

Geng, F., Cao, Y., Laurent, B.C (2001). "Essential roles of Snf5p in Snf-Swi chromatin remodeling in vivo." *Mol Cell Biol.* 21(13): 4311-20.

Georgakopoulos, T., Thireos, G (1992). "Two distinct yeast transcriptional activators require the function of the GCN5 protein to promote normal levels of transcription." *EMBO J.* 11(11): 4145-52.

Gibbons, R. J., Picketts, D.J., Villard, L., Higgs, D.R (1995). "Mutations in a putative global transcriptional regulator cause X-linked mental retardation with alpha-thalassemia (ATR-X syndrome)." *Cell.* 80(6): 837-45.

Gibbons, R. J., McDowell, T.L., Raman, S., O'Rourke, D.M., Garrick, D., Ayyub, H., Higgs, D.R (2000). "Mutations in *ATRX*, encoding a SWI/SNF-like protein, cause diverse changes in the pattern of DNA methylation." *Nat Genet.* 24(4): 368-71.

Goldmark, J. P., Fazzio, T.G., Estep, P.W., Church, G.M., Tsukiyama, T (2000). "The Isw2 chromatin remodeling complex represses early meiotic genes upon recruitment by Ume6p." *Cell* 103(3): 423-33.

Grant, P. A., Eberharter, A., John, S., Cook, R.G., Turner, B.M., Workman, J.L (1999). "Expanded lysine acetylation specificity of Gcn5 in native complexes." *J Biol Chem.* 274(9): 5895-900.

Gray, M. W. (1992). "The endosymbiont hypothesis revisited." *Int Rev Cytol.* 141: 233-357.

Graziano, V., Gerchman, S.E., Schneider, D.K., Ramakrishnan, V (1994). "Histone H1 is located in the interior of the chromatin 30-nm filament." *Nature* 368(6469): 351-4.

Greenberg, M. L., and Lopes, J.M (1996). "Genetic regulation of phospholipid biosynthesis in *Saccharomyces cerevisiae*." *Microbiol Rev.* 60(1): 1-20.

Grewal, S. I., and Moazed, D (2003). "Heterochromatin and epigenetic control of gene expression." *Science* 301(5634): 798-802.

Gromoller, A., and Lehming, N (2000). "Srb7p is a physical and physiological target of Tup1p." *EMBO J.* 19(24): 6845-52.

Gross, D. S., and Garrard, W.T (1988). "Nuclease hypersensitive sites in chromatin." *Annu Rev Biochem.* 57: 159-97.

Grunstein, M., Hecht, A., Fisher-Adams, G., Wan, J., Mann, R.K., Strahl-Bolsinger, S., Laroche, T., Gasser, S (1995). "Histone H3 and H4 N-termini interact with SIR3 and SIR4 proteins: a molecular model for the formation of heterochromatin in yeast." *Cell.* 80(4): 583-92.

Guarente, L., and Mason, T (1983). "Heme regulates transcription of the *CYC1* gene of S. cerevisiae via an upstream activation site." *Cell* 32(4): 1279-86.

Gurley, L. R., , Walters, R.A., Barham, S.S., Deaven, L.L (1978). "Heterochromatin and histone phosphorylation." *Exp Cell Res.* 111(2): 373-83.

Hake, S. B., Xiao, A., Allis, C.D (2004). "Linking the epigenetic 'language' of covalent histone modifications to cancer." *Br J Cancer.* 90(4): 761-9.

Hampsey, M., and Reinberg, D (1999). "RNA polymerase II as a control panel for multiple coactivator complexes." *Curr Opin Genet Dev.* 9(2): 132-9.

Han, M., and Grunstein, M (1988). "Nucleosome loss activates yeast downstream promoters in vivo." *Cell* 55(6): 1137-45.

Hartwell, L. H. (1973). "Synchronization of haploid yeast cell cycles, a prelude to conjugation." *Exp Cell Res.* 76(1): 111-7.

Hassan, A. H., Prochasson, P., Neely, K.E., Galasinski, S.C., Chandy, M., Carrozza, M.J., Workman, J.L (2002). "Function and selectivity of bromodomains in anchoring chromatin-modifying complexes to promoter nucleosomes." *Cell* 111(3): 369-79.

Hecht, A., Laroche, T., Strahl-Bolsinger, S., Gasser, S.M., Grunstein, M (1995). "Histone H3 and H4 N-termini interact with SIR3 and SIR4 proteins: a molecular model for the formation of heterochromatin in yeast." *Cell* 80(4): 583-92.

Henikoff, S., Furuyama, T., Ahmad, K (2004). "Histone variants, nucleosome assembly and epigenetic inheritance." *Trends Genet.* 20(7): 320-6.

Hereford, L., Fahrner, K., Woolford, J, Jr, Rosbash, M., Kaback, D.B (1979). "Isolation of yeast histone genes H2A and H2B." *Cell* 18(4): 1261-71.

Hirschhorn, J. N., Brown, S.A., Clark, C.D., Winston, F (1992). "Evidence that SNF2/SWI2 and SNF5 activate transcription in yeast by altering chromatin structure." *Genes Dev.* 6(12A): 2288-98.

Holstege, F. C., Jennings, E.G., Wyrick, J.J., Lee, T.I., Hengartner, C.J., Green, M.R., Golub, T.R., Lander, E.S., Young, R.A (1998). "Dissecting the regulatory circuitry of a eukaryotic genome." *Cell* 95(5): 717-28.

Hoppe, G. J., Tanny, J.C., Rudner, A.D., Gerber, S.A., Danaie, S., Gygi, S.P., Moazed, D (2002). "Steps in assembly of silent chromatin in yeast: Sir3-independent binding of a Sir2/Sir4 complex to silencers and role for Sir2-dependent deacetylation." *Mol Cell Biol.* 22(12): 4167-80.

Horn, P. J., and Peterson, C.L (2002). "Chromatin higher order folding--wrapping up transcription." *Science* 297(5588): 1824-7.

Horn, P. J., Crowley, K.A., Carruthers, L.M., Hansen, J.C., Peterson, C.L (2002). "The SIN domain of the histone octamer is essential for intramolecular folding of nucleosomal arrays." *Nat Struct Biol.* 9(3): 167-71.

Horton, R. M., Ho, S.N., Pullen, J.K., Hunt, H.D., Cai, Z., Pease, L.R (1993). "Gene splicing by overlap extension." *Methods Enzymol.* 217: 270-9.

Horz, W., and Zachau, H.G (1980). "Deoxyribonuclease II as a probe for chromatin structure. I. Location of cleavage sites." *J Mol Biol.* 144(3): 305-27.

Hsu, J. Y., Sun, Z.W., Li, X., Reuben, M., Tatchell, K., Bishop, D.K., Grushcow, J.M., Brame, C.J., Caldwell, J.A., Hunt, D.F., Lin, R., Smith, M.M., Allis, C.D (2000). "Mitotic phosphorylation of histone H3 is governed by Ipl1/aurora kinase and Glc7/PP1 phosphatase in budding yeast and nematodes." *Cell* 102(3): 279-91.

Huh, W. K., Falvo, J.V., Gerke, L.C., Carroll, A.S., Howson, R.W., Weissman, J.S., O'Shea, E.K (2003). "Global analysis of protein localization in budding yeast." *Nature* 425(6959): 686-91.

Huisinga, K. L., and Pugh, B.F (2004). "A genome-wide housekeeping role for TFIID and a highly regulated stress-related role for SAGA in *Saccharomyces cerevisiae*." *Mol Cell.* 13(4): 573-85.

Ikeda, K., Steger, D.J., Eberharter, A., Workman, J.L (1999). "Activation domain-specific and general transcription stimulation by native histone acetyltransferase complexes." *Mol Cell Biol.* 19(1): 855-63.

Iraqui, I., Vissers, S., Andre, B., Urrestarazu, A (1999). "Transcriptional induction by aromatic amino acids in *Saccharomyces cerevisiae*." *Mol Cell Biol.* 19(5): 3360-71.

Ito, T., Bulger, M., Pazin, M.J., Kobayashi, R., Kadonaga, J.T (1997). "ACF, an ISWI-containing and ATP-utilizing chromatin assembly and remodeling factor." *Cell* 90(1): 145-55.

Ito, T., Levenstein, M.E., Fyodorov, D.V., Kutach, A.K., Kobayashi, R., Kadonaga, J.T (1999). "ACF consists of two subunits, Acf1 and ISWI, that function cooperatively in the ATP-dependent catalysis of chromatin assembly." *Genes Dev.* 13(12): 1529-39.

Jackson, V. (1988). "Deposition of newly synthesized histones: hybrid nucleosomes are not tandemly arranged on daughter DNA strands." *Biochemistry* 27(6): 2109-20.

Jia, Y., Rothermel, B., Thornton, J., Butow, R.A (1997). "A basic helix-loop-helix-leucine zipper transcription complex in yeast functions in a signaling pathway from mitochondria to the nucleus." *Mol Cell Biol.* 17(3): 1110-7.

John, S., Howe, L., Tafrov, S.T., Grant, P.A., Sternglanz, R., Workman, J.L (2000). "The something about silencing protein, Sas3, is the catalytic subunit of NuA3, a yTAF(II)30-containing HAT complex that interacts with the Spt16 subunit of the yeast CP (Cdc68/Pob3)-FACT complex." *Genes Dev.* 14(10): 1196-208.

Johns, E. W. (1967). "The electrophoresis of histones in polyacrylamide gel and their quantitative determination." *Biochem J.* 104(1): 527-36.

Johnson, L. M., Kayne, P.S., Kahn, E.S., Grunstein, M (1990). "Genetic evidence for an interaction between SIR3 and histone H4 in the repression of the silent mating loci in *Saccharomyces cerevisiae*." *Proc Natl Acad Sci U S A.* 87(16): 6286-90.

Johnson, L. M., Fisher-Adams, G., Grunstein, M (1992). "Identification of a non-basic domain in the histone H4 N-terminus required for repression of the yeast silent mating loci." *EMBO J.* 11(6): 2201-9.

Johnston, M., and Davis, R.W (1984). "Sequences that regulate the divergent GAL1-GAL10 promoter in *Saccharomyces cerevisiae*." *Mol Cell Biol.* 4(8): 1440-8.

Johnston, M. (1987). "A model fungal gene regulatory mechanism: the GAL genes of *Saccharomyces cerevisiae*." *Microbiol Rev.* 41(4): 458-76.

Johnston, M., and Carlson, M (1992). Regulation of carbon and phosphate utilization. The Molecular and Cellular Biology of the Yeast *Saccharomyces*: Gene Expression. Broach, J.R., Pringle, J.R., Jones, E.W. NY, *Cold Spring Harbor Laboratory Press*: 193–281.

Kadosh, D., and Struhl, K (1997). "Repression by Ume6 involves recruitment of a complex containing Sin3 corepressor and Rpd3 histone deacetylase to target promoters." *Cell* 89(3): 365-71.

Kadosh, D., and Struhl, K (1998). "Targeted recruitment of the Sin3-Rpd3 histone deacetylase complex generates a highly localized domain of repressed chromatin in vivo." *Mol Cell Biol.* 18(9): 5121-7.

Kanno, T., Kanno, Y., Siegel, R.M., Jang, M.K., Lenardo, M.J., Ozato, K (2004). "Selective recognition of acetylated histones by bromodomain proteins visualized in living cells." *Mol Cell* 13(1): 33-43.

Karlberg, O., Canback, B., Kurland, C.G., Andersson, S.G (2000). "The dual origin of the yeast mitochondrial proteome." *Yeast* 17(3): 170-87.

Katan-Khaykovich, Y., and Struhl, K (2002). "Dynamics of global histone acetylation and deacetylation *in vivo*: rapid restoration of normal histone acetylation status upon removal of activators and repressors." *Genes Dev.* 16(6): 743-52.

Kayne, P. S., Kim, U.J., Han, M., Mullen, J.R., Yoshizaki, F., Grunstein, M (1988). "Extremely conserved histone H4 N terminus is dispensable for growth but essential for repressing the silent mating loci in yeast." *Cell* 55(1): 27-39.

Keleher, C. A., Passmore, S., Johnson, A.D (1989). "Yeast repressor alpha 2 binds to its operator cooperatively with yeast protein Mcm1." *Mol Cell Biol.* 9(11): 5228-30.

Keleher, C. A., Redd, M.J., Schultz, J., Carlson, M., Johnson, A.D (1992). "Ssn6-Tup1 is a general repressor of transcription in yeast." *Cell* 68(4): 709-19.

Kim, U. J., Han, M., Kayne, P., Grunstein, M (1988). "Effects of histone H4 depletion on the cell cycle and transcription of *Saccharomyces cerevisiae*." *EMBO J.* 7(7): 2211-9.

Kimura, A., Umehara, T., Horikoshi, M (2002). "Chromosomal gradient of histone acetylation established by Sas2p and Sir2p functions as a shield against gene silencing." *Nat Genet.* 32(3): 370-7.

Kireeva, M. L., Walter, W., Tchernajenko, V., Bondarenko, V., Kashlev, M., Studitsky, V.M (2002). "Nucleosome remodeling induced by RNA polymerase II: loss of the H2A/H2B dimer during transcription." *Mol Cell* 9(3): 541-52.

Kleff, S., Andrulis, E.D., Anderson, C.W., Sternglanz, R (1995). "Identification of a gene encoding a yeast histone H4 acetyltransferase." J Biol Chem. 270(42): 24674-7.

Klein, C. J., Olsson, L., Nielsen, J (1988). "Glucose control in *Saccharomyces cerevisiae*: the role of Mig1 in metabolic functions." *Microbiology* 144(1): 13-24.

Knezetic, J. A., and Luse, D.S (1986). "The presence of nucleosomes on a DNA template prevents initiation by RNA polymerase II *in vitro*." *Cell* 45(1): 95-104.

Komeili, A., Wedaman, K.P., O'Shea, E.K., Powers, T (2000). "Mechanism of metabolic control. Target of rapamycin signaling links nitrogen quality to the activity of the Rtg1 and Rtg3 transcription factors." J *Cell Biol.* 151(4): 863-78.

Konishi, A., Shimizu, S., Hirota, J., Takao, T., Fan, Y., Matsuoka, Y., Zhang, L., Yoneda, Y., Fujii, Y., Skoultchi, A.I,, Tsujimoto, Y (2003). "Involvement of histone H1.2 in apoptosis induced by DNA double-strand breaks." *Cell* 114(6): 673-88.

Kornberg, R. D., and Thomas, J.O (1974). "Chromatin structure; oligomers of the histones." *Science* 184(139): 865-8.

Krogan, N. J., Dover, J., Khorrami, S., Greenblatt, J.F., Schneider, J., Johnston, M., Shilatifard, A (2002). "COMPASS, a histone H3 (Lysine 4) methyltransferase required for telomeric silencing of gene expression." *J Biol Chem.* 277(13): 10753-5.

Krogan, N. J., Keogh, M.C., Datta, N., Sawa, C., Ryan, O.W., Ding, H., Haw, R.A., Pootoolal, J., Tong, A., Canadien, V., Richards, D.P., Wu, X., Emili, A., Hughes, T.R., Buratowski, S., Greenblatt, J.F (2003). "A Snf2 family ATPase complex required for recruitment of the histone H2A variant Htz1." *Mol Cell Biol.* 12(6): 1565-76.

Kruger, W., Peterson, C.L., Sil, A., Coburn, C., Arents, G., Moudrianakis, E.N., Herskowitz, I (1995). "Amino acid substitutions in the structured domains of histones H3 and H4 partially relieve the requirement of the yeast SWI/SNF complex for transcription." *Genes Dev.* 9(22): 2770-9.

Kukimoto, I., Elderkin, S., Grimaldi, M., Oelgeschlager, T., Varga-Weisz, P.D (2004). "The histone-fold protein complex CHRAC-15/17 enhances nucleosome sliding and assembly mediated by ACF." *Mol Cell Biol.* 13(2): 265-77.

Kumar, A., Agarwal, S., Heyman, J.A., Matson, S., Heidtman, M., Piccirillo, S., Umansky. L., Drawid, A., Jansen, R., Liu, Y., Cheung, K.H., Miller, P., Gerstein, M., Roeder, G.S., Snyder, M (2002). "Subcellular localization of the yeast proteome." *Genes Dev.* 16(6): 707-719.

Lachner, M., O'Carroll, D., Rea, S., Mechtler, K., Jenuwein, T (2001). "Methylation of histone H3 lysine 9 creates a binding site for HP1 proteins." *Nature* 410(6824): 116-20.

Längst, G., Bonte, E.J., Corona, D.F., Becker, P.B (1999). "Nucleosome movement by CHRAC and ISWI without disruption or trans-displacement of the histone octamer." *Cell* 97(7): 843-52.

Längst, G., and Becker, P.B (2001). "Nucleosome mobilization and positioning by ISWI-containing chromatin-remodeling factors." *J Cell Sci.* 114(pt 14): 2561-8.

Laurenson, P., and Rine, J (1992). "Silencers, silencing, and heritable transcriptional states." Microbiol Rev. 56(4): 543-60.

Laurent, B. C., Treitel, M.A., Carlson, M (1991). "Functional interdependence of the yeast SNF2, SNF5, and SNF6 proteins in transcriptional activation." *Proc Natl Acad Sci U S A.* 88(7): 2687-91.

Lee, D. Y., Hayes, J.J., Pruss, D., Wolffe, A.P (1993). "A positive role for histone acetylation in transcription factor access to nucleosomal DNA." *Cell* 72(1): 73-84.

Lee, K. P., Baxter, H.J., Guillemette, J.G., Lawford, H.G., Lewis, P.N (1982). "Structural studies on yeast nucleosomes." *Can J Biochem.* 60(3): 379-88.

Li, J., Moazed, D., Gygi, S.P (2002). "Association of the histone methyltransferase Set2 with RNA polymerase II plays a role in transcription elongation." *J Biol Chem.* 277(51): 49383-8.

Li, W. Z., and Sherman, F (1991). "Two types of TATA elements for the *CYC1* gene of the yeast *Saccharomyces cerevisiae*." *Mol Biol Cell.* 11(2): 666-76.

Liao, X., and Butow, R.A (1993). "*RTG1* and *RTG2*: two yeast genes required for a novel path of communication from mitochondria to the nucleus." *Cell* 72(1): 61-71.

Liao, X. S., Small, W.C., Srere, P.A., Butow, R.A (1991). "Intramitochondrial functions regulate nonmitochondrial citrate synthase (*CIT2*) expression in *Saccharomyces cerevisiae*." *Mol Cell Biol.* 11(1): 38-46.

Ling, X., Harkness, T.A., Schultz, M.C., Fisher-Adams, G., Grunstein, M (1996). " Yeast histone H3 and H4 amino termini are important for nucleosome assembly *in vivo* and *in vitro*: redundant and position-independent functions in assembly but not in gene regulation." *Genes Dev.* 10(6): 686-99.

Litt, M. D., Simpson, M., Gaszner, M., Allis, C.D., Felsenfeld, G (2001). "Correlation between histone lysine methylation and developmental changes at the chicken beta-globin locus." *Science* 293(5539): 2453-5.

Liu, Z., and Butow, R.A (1999). "A transcriptional switch in the expression of yeast tricarboxylic acid cycle genes in response to a reduction or loss of respiratory function." *Mol Cell Biol.* 19(10): 6720-8.

Lo, W. S., Trievel, R.C., Rojas, J.R., Duggan, L., Hsu, J.Y., Allis, C.D., Marmorstein, R., Berger, S.L (2000). "Phosphorylation of serine 10 in histone H3 is functionally linked *in vitro* and *in vivo* to Gcn5-mediated acetylation at lysine 14." *Mol Cell.* 5(6): 917-26.

Lowary, P. T., and Widom, J (1998). "New DNA sequence rules for high affinity binding to histone octamer and sequence-directed nucleosome positioning." *J Mol Biol.* 276(1): 19-42.

Luger, K., Mader, A.W., Richmond, R.K., Sargent, D.F., Richmond, T.J (1997). "Crystal structure of the nucleosome core particle at 2.8 A resolution." Nature 389(6648): 251-60.

Luger, K., and Richmond, T.J (1998). "DNA binding within the nucleosome core." *Curr Opin Struct Biol.* 8(1): 33-40.

Lundin, M., Nehlin, J.O., Ronne, H (1994). "Importance of a flanking AT-rich region in target site recognition by the GC box-binding zinc finger protein MIG1." *Mol Cell Biol.* 14(3): 1979-85.

Luo, K., Vega-Palas, M.A., Grunstein, M (2002). "Rap1-Sir4 binding independent of other Sir, yKu, or histone interactions initiates the assembly of telomeric heterochromatin in yeast." *Genes Dev.* 16(12): 1528-39.

Ma, P. C., Rould, M.A., Weintraub, H., Pabo, C.O (1994). "Crystal structure of MyoD bHLH domain-DNA complex: perspectives on DNA recognition and implications for transcriptional activation." *Cell* 77(3): 451-9.

Magasanik, B., and Kaiser, C.A (2002). "Nitrogen regulation in *Saccharomyces cerevisiae*." *Gene* 290(1-2): 1-18.

Maggert, K. A., and Karpen, G.H (2001). "The activation of a neocentromere in Drosophila requires proximity to an endogenous centromere." *Genetics* 158(4): 1615-28.

Makalowska, I., Ferlanti, E.S., Baxevanis, A.D., Landsman, D (1999). "Histone Sequence Database: sequences, structures, post-translational modifications and genetic loci." *Nucleic Acids Res.* 27(1): 323-4.

Martens, C., Krett, B., Laybourn, P.J (2001). "RNA polymerase II and TBP occupy the repressed *CYC1* promoter." *Mol Microbiol* 40(4): 1009-19.

Martens, J. A., and Winston, F (2002). "Evidence that Swi/Snf directly represses transcription in *S. cerevisiae*." *Genes Dev.* 16(17): 2231-6.

Massari, M. E., Grant, P.A., Pray-Grant, M.G., Berger, S.L., Workman, J.L., Murre, C (1999). "A conserved motif present in a class of helix-loop-helix proteins activates transcription by direct recruitment of the SAGA complex." *Mol Cell.* 4(1): 63-73.

McMahon, S. B., Van Buskirk, H.A., Dugan, K.A., Copeland, T.D., Cole, M.D (1998). "The novel ATM-related protein TRRAP is an essential cofactor for the c-Myc and E2F oncoproteins." *Cell* 94(3): 363-74.

McNabb, D. S., Xing, Y., Guarente, L (1995). "Cloning of yeast *HAP5*: a novel subunit of a heterotrimeric complex required for CCAAT binding." *Genes Dev.* 9(1): 47-58.

Meersseman, G., Pennings, S., Bradbury, E.M (1992). "Mobile nucleosomes--a general behavior." *EMBO J.* 11(8): 2951-9.

Meneghini, M. D., Wu, M., Madhani, H.D (2003). "Conserved histone variant H2A.Z protects euchromatin from the ectopic spread of silent heterochromatin." *Cell* 112(5): 725-36.

Mizuguchi, G., Tsukiyama, T., Wisniewski, J., Wu, C (1997). "Role of nucleosome remodeling factor NURF in transcriptional activation of chromatin." *Mol Cell.*: 141-50.

Mizuguchi, G., Shen, X., Landry, J., Wu, W.H., Sen, S., Wu, C (2004). "ATP-driven exchange of histone H2AZ variant catalyzed by SWR1 chromatin remodeling complex." *Science* 303(5656): 343-8.

Mizzen, C. A., Yang, X.J., Kokubo, T., Brownell, J.E., Bannister, A.J., Owen-Hughes, T., Workman, J., Wang, L., Berger, S.L., Kouzarides, T., Nakatani. Y., Allis, C.D (1996). "The TAF(II)250 subunit of TFIID has histone acetyltransferase activity." *Cell* 87(7): 1261-70.

Moran, L., Norris, D., Osley, M.A (1988). "A yeast H2A-H2B promoter can be regulated by changes in histone gene copy number." *Genes Dev.* 4(5): 752-63.

Myers, A. M., Pape, L.K., Tzagoloff, A (1985). "Mitochondrial protein synthesis is required for maintenance of intact mitochondrial genomes in *Saccharomyces cerevisiae*." *EMBO J.* 4(8): 2087-92.

Nasmyth, K. (1982). "Molecular analysis of a cell lineage." *Nature* 302(5910): 670-6.

Natarajan, K., Jackson, B.M., Zhou, H., Winston, F., Hinnebusch, A.G (1999). "Transcriptional activation by Gcn4p involves independent interactions with the SWI/SNF complex and the SRB/mediator." *Mol Cell Biol.* 4(4): 657-64.

Neely, K. E., Hassan, A.H., Wallberg, A.E., Steger, D.J., Cairns, B.R., Wright, A.P., Workman, J.L. (1999). "Activation domain-mediated targeting of the SWI/SNF complex to promoters stimulates transcription from nucleosome arrays." *Mol Cell Biol.* 4(4): 649-55.

Neely, K. E., and Workman, J.L (2002). "Histone acetylation and chromatin remodeling: which comes first?" *Mol Genet Metab.* 76(1): 1-5.

Nehlin, J. O., and Ronne, H (1990). "Yeast MIG1 repressor is related to the mammalian early growth response and Wilms' tumour finger proteins." *EMBO J.* 9(9): 2891-8.

Ng, H. H., Feng, Q., Wang, H., Erdjument-Bromage, H., Tempst, P., Zhang, Y., Struhl, K (2002). "Lysine methylation within the globular domain of histone H3 by Dot1 is important for telomeric silencing and Sir protein association." *Genes Dev.* 16(12): 1518-27.

Ng, H. H., Robert, F., Young, R.A., Struhl, K (2003). "Targeted recruitment of Set1 histone methylase by elongating Pol II provides a localized mark and memory of recent transcriptional activity." *Mol Cell* 11(3): 709-19.

Nishioka, K., Rice, J.C., Sarma, K., Erdjument-Bromage, H., Werner, J., Wang, Y., Chuikov, S., Valenzuela, P., Tempst, P., Steward, R., Lis, J.T., Allis, C.D., Reinberg, D (2002). "PR-Set7 is a nucleosome-specific methyltransferase that modifies lysine 20 of histone H4 and is associated with silent chromatin." *Mol Cell* 9(6): 1201-13.

Noma, K., Allis, C. D. & Grewal, S. I. (2001). "Transitions in distinct histone H3 methylation patterns at the heterochromatin domain boundaries." *Science* 293: 1150-1155.

Norris, D., Dunn, B., Osley, M.A (1988). "The effect of histone gene deletions on chromatin structure in *Saccharomyces cerevisiae*." *Science* 242(4879): 759-61.

Nourani, A., Doyon, Y., Utley, R.T., Allard, S., Lane, W.S., Cote, J (2001). "Role of an ING1 growth regulator in transcriptional activation and targeted histone acetylation by the NuA4 complex." *Mol Cell Biol.* 21(22): 7629-40.

Nowak, S. J., and Corces, V.G (2004). "Phosphorylation of histone H3: a balancing act between chromosome condensation and transcriptional activation." *Trends Genet.* 20(4): 214-20.

Oki, M., and Kamakaka, R.T (2002). "Blockers and barriers to transcription: competing activities?" *Curr Opin Cell Biol.* 14(3): 299-304.

Olesen, J. T., and Guarente, L (1990). "The HAP2 subunit of yeast CCAAT transcriptional activator contains adjacent domains for subunit association and DNA recognition: model for the HAP2/3/4 complex." *Genes Dev.* 4(10): 1714-29.

Osley, M. A., Gould, J., Kim, S., Kane, M.Y., Hereford, L (1986). "Identification of sequences in a yeast histone promoter involved in periodic transcription." *Cell* 45(4): 537-44.

Oudet, P., Gross-Bellard, M., Chambon, P (1975). "Electron microscopic and biochemical evidence that chromatin structure is a repeating unit." *Cell* 4(4): 281-300.

Owen, D. J., Ornaghi, P., Yang, J.C., Lowe, N., Evans, P.R., Ballario, P., Neuhaus, D., Filetici, P., Travers, A.A (2000). "The structural basis for the recognition of acetylated histone H4 by the bromodomain of histone acetyltransferase gcn5p." *EMBO J.* 19(22): 6141-9.

Padilla, P. A., Fuge, E.K., Crawford, M.E., Errett, A., Werner-Washburne, M (1998). "The highly conserved, coregulated *SNO* and *SNZ* gene families in *Saccharomyces cerevisiae respond* to nutrient limitation." *J Bacteriol.* 180(21): 5718-26.

Park, J. H., Cosgrove, M.S., Youngman, E., Wolberger, C., Boeke, J.D (2002). "A core nucleosome surface crucial for transcriptional silencing." *Nat Genet.* 32(2): 273-9.

Park, Y., and Kuroda, M.I (2001). "Epigenetic aspects of X-chromosome dosage compensation." *Science* 293(5532): 1083-5.

Patterton, H. G., Landel, C.C., Landsman, D., Peterson, C.L., Simpson, R.T (1998). "The biochemical and phenotypic characterization of Hho1p, the putative linker histone H1 of *Saccharomyces cerevisiae*." *J Biol Chem.* 273(13): 7268-76.

Paule, M. R., and White, R.J (2000). "Survey and summary: transcription by RNA polymerases I and III." *Nucleic Acids Res.* 28(6): 1283-98.

Pennings, S., Meersseman, G., Bradbury, E.M (1994). "Linker histones H1 and H5 prevent the mobility of positioned nucleosomes." *Proc Natl Acad Sci U S A.* 91(22): 10275-9.

Perez-Ortin, J. E., Estruch, F., Matallana, E., Franco, L (1987). "Fine analysis of the chromatin structure of the yeast *SUC2* gene and of its changes upon derepression. Comparison between the chromosomal and plasmid-inserted genes." *Nucleic Acids Res.* 15(17): 6937-56.

Peterson, C. L., and Herskowitz, I (1992). "Characterization of the yeast *SWI1*, *SWI2*, and *SWI3* genes, which encode a global activator of transcription." *Cell* 68(3): 573-83.

Peterson, C. L., Dingwall, A., Scott, M.P (1994). "Five SWI/SNF gene products are components of a large multisubunit complex required for transcriptional enhancement." *Proc Natl Acad Sci U S A.* 91(8): 2905-8.

Peterson, C. L., and Workman, J.L (2000). "Promoter targeting and chromatin remodeling by the SWI/SNF complex." *Curr Opin Genet Dev.* 10(2): 187-92.

Pfeifer, K., Kim, K.S., Kogan, S., Guarente, L (1989). "Functional dissection and sequence of yeast HAP1 activator." *Cell* 56(2): 291-301.

Pile, L. A., Spellman, P.T., Katzenberger, R.J., Wassarman, D.A (2003). "The SIN3 deacetylase complex represses genes encoding mitochondrial proteins: implications for the regulation of energy metabolism." *J Biol Chem.* 278(39): 37840-8.

Pineiro, M., Puerta, C., Palacian, E (1991). "Yeast nucleosomal particles: structural and transcriptional properties." *Biochemistry* 30(23): 5805-10.

Piskur, J. (1994). "Inheritance of the yeast mitochondrial genome." *Plasmid* 31(3): 229-41.

Piskur, J. (1997). "The transmission disadvantage of yeast mitochondrial intergenic mutants is eliminated in the mgt1 (cce1) background." *J Bacteriol.* 179(17): 5614-7.

Plath, K., Mlynarczyk-Evans, S., Nusinow, D.A., Panning, B (2002). "Xist RNA and the mechanism of X chromosome inactivation." *Annu Rev Genet.* 36: 233-78.

Prochasson, P., Neely, K.E., Hassan, A.H., Li, B., Workman, J.L (2003). "Targeting activity is required for SWI/SNF function in vivo and is accomplished through two partially redundant activator-interaction domains." *Mol Cell Biol.* 12(4): 983-90.

Quinn, J., Fyrberg, A.M., Ganster, R.W., Schmidt, M.C., Peterson, C.L (1996). "DNA-binding properties of the yeast SWI/SNF complex." *Nature* 379(6568): 844-7.

Recht, J., and Osley M.A (1999). "Mutations in both the structured domain and N-terminus of histone H2B bypass the requirement for Swi-Snf in yeast." *EMBO J.* 18(1): 229-40.

Reid, B. J., and Hartwell, L.H (1977). "Regulation of mating in the cell cycle of *Saccharomyces cerevisiae*." *J Cell Biol.* 75(2 pt 1): 355-65.

Rep, M., and Grivell, L.A (1996). "The role of protein degradation in mitochondrial function and biogenesis." *Curr Genet.* 30(5): 367-80.

Riego, L., Avendano, A., DeLuna, A., Rodriguez, E., Gonzalez, A (2002). "GDH1 expression is regulated by GLN3, GCN4, and HAP4 under respiratory growth." *Biochem Biophys Res Commun.* 293(1):79-85.

Robinson, K. A., Koepke, J.I., Kharodawala, M., Lopes, J.M (2000). "A network of yeast basic helix-loop-helix interactions." *Nucleic Acids Res.* 28(22): 4460-6.

Robinson, M. D., Grigull, J., Mohammad, N., Hughes, T.R (2002). "FunSpec: a web-based cluster interpreter for yeast." *BMC Bioinformatics.* 3(1): 35.

Robyr, D., Suka, Y., Xenarios, I., Kurdistani, S.K., Wang, A., Suka, N., Grunstein, M (2002). "Microarray deacetylation maps determine genome-wide functions for yeast histone deacetylases." *Cell* 109(4): 437-46.

Roguev, A., Schaft, D., Shevchenko, A., Aasland, R., Shevchenko, A., Stewart, A.F (2003). "High conservation of the Set1/Rad6 axis of histone 3 lysine 4 methylation in budding and fission yeasts." J *Biol Chem.* 278(10): 8487-93.

Ross-Macdonald, P., Coelho, P.S., Roemer, T., Agarwal, S., Kumar, A., Jansen, R., Cheung, K.H., Sheehan, A., Symoniatis, D., Umansky, L., Heidtman, M., Nelson, F.K., Iwasaki, H., Hager, K., Gerstein, M., Miller, P., Roeder, G.S., Snyder, M (1999). "Large-scale analysis of the yeast genome by transposon tagging and gene disruption." *Nature.* 402(6760): 413-8.

Roth, S. Y., Denu, J.M., Allis, C.D (2001). "Histone acetyltransferases." *Annu Rev Biochem.* 70: 81-120.

Rundlett, S. E., Carmen, A.A., Kobayashi, R., Bavykin, S., Turner, B.M., Grunstein, M (1996). "HDA1 and RPD3 are members of distinct yeast histone deacetylase complexes that regulate silencing and transcription." *Proc Natl Acad Sci U S A.* 93(25): 14503-8.

Rundlett, S. E., Carmen, A.A., Suka, N., Turner, B.M., Grunstein, M (1998). "Transcriptional repression by UME6 involves deacetylation of lysine 5 of histone H4 by RPD3." *Nature* 392(6678): 831-5.

Rusche, L. N., Kirchmaier, A.L., Rine, J (2002). "Ordered nucleation and spreading of silenced chromatin in *Saccharomyces cerevisiae*." *Mol Biol Cell* 13(7): 2207-22.

Sabet, N., Tong, F., Madigan, J.P., Volo, S., Smith, M.M., Morse, R.H (2003). "Global and specific transcriptional repression by the histone H3 amino terminus in yeast." *Proc Natl Acad Sci U S A.* 100(7): 4084-9.

Santisteban, M. S., Arents, G., Moudrianakis, E.N., Smith, M.M (1997). "Histone octamer function in vivo: mutations in the dimer-tetramer interfaces disrupt both gene activation and repression." *EMBO J.* 16(9): 2493-506.

Santisteban, M. S., Kalashnikova, T., Smith, M.M (2000). "Histone H2A.Z regulats transcription and is partially redundant with nucleosome remodeling complexes." *Cell* 103(3): 411-22.

Santoro, R., Li, J., Grummt, I (2002). "The nucleolar remodeling complex NoRC mediates heterochromatin formation and silencing of ribosomal gene transcription." *Nat Genet.* 32(3): 393-6.

Santos-Rosa, H., Schneider, R., Bannister, A.J., Sherriff, J., Bernstein, B.E., Emre, N.C., Schreiber, S.L., Mellor, J., Kouzarides, T (2002). "Active genes are tri-methylated at K4 of histone H3." *Nature* 419(6905): 407-11.

Santos-Rosa, H., Schneider, R., Bernstein, B.E., Karabetsou, N., Morillon, A., Weise, C., Schreiber, S.L., Mellor, J., Kouzarides, T (2003). "Methylation of histone H3 K4 mediates association of the Isw1p ATPase with chromatin." *Mol Cell* 12(5): 1325-32.

Schatz, G. (1995). "Mitochondria: beyond oxidative phosphorylation." Biochimica et *Biophysica Acta (BBA) - Molecular Basis of Disease* 1271(1): 123-126.

Schmitt, M. E., Brown, T.A., Trumpower, B.L (1990). "A rapid and simple method for preparation of RNA from *Saccharomyces cerevisiae*." *Nucleic Acids Res.* 18(10): 3091-2.

Schnitzler, G., Sif, S., Kingston, R.E (1998). "Human SWI/SNF interconverts a nucleosome between its base state and a stable remodeled state." *Cell* 94(1): 17-27.

Schwarz, P. M., and Hansen, J.C (1994). "Formation and stability of higher order chromatin structures. Contributions of the histone octamer." *J Biol Chem.* 269(23): 16284-9.

Sekito, T., Thornton, J., Butow, R.A (2000). "Mitochondria-to-nuclear signaling is regulated by the subcellular localization of the transcription factors Rtg1p and Rtg3p." *Mol Biol Cell.* 11(6): 2103-15.

Sherman, F. (1963). "Respiration-deficient mutants of yeast." *Genetics* 48: 375-85.

Shibahara, K., and Stillman, B (1999). "Replication-dependent marking of DNA by PCNA facilitates CAF-1-coupled inheritance of chromatin." *Cell* 96(4): 575-85.

Shibahara, K., Verreault, A., Stillman, B (2000). "The N-terminal domains of histones H3 and H4 are not necessary for chromatin assembly factor-1- mediated nucleosome assembly onto replicated DNA *in vitro*." *Proc Natl Acad Sci U S A.* 97(14): 7766-71.

Shiio, Y., and Eisenman, R.N (2003). "Histone sumoylation is associated with transcriptional repression." *Proc Natl Acad Sci U S A.* 100(23): 13225-30.

Simic, R., Lindstrom, D.L., Tran, H.G., Roinick, K.L., Costa, P.J., Johnson, A.D., Hartzog, G.A., Arndt, K.M (2003). "Chromatin remodeling protein Chd1 interacts with transcription elongation factors and localizes to transcribed genes." *EMBO J.* 22(8): 1846-56.

Simpson, R. T. (1978). "Structure of the chromatosome, a chromatin particle containing 160 base pairs of DNA and all the histones." *Biochemistry* 17(25): 5524-31.

Sims, R. J. r., Nishioka, K., Reinberg, D (2003). "Histone lysine methylation: a signature for chromatin function." *Trends Genet.* 19(11): 629-39.

Smith, E. R., Eisen, A., Gu, W., Sattah, M., Pannuti, A., Zhou, J., Cook, R.G., Lucchesi, J.C., Allis, C.D (1998). "ESA1 is a histone acetyltransferase that is essential for growth in yeast." *Proc Natl Acad Sci U S A.* 95(7): 3561-5.

Smith, J. S., and Boeke, J.D (1997). "An unusual form of transcriptional silencing in yeast ribosomal DNA." *Genes Dev.* 11(2): 241-54.

Smith, M. M., and Murray, K (1983). "Yeast H3 and H4 histone messenger RNAs are transcribed from two non-allelic gene sets." *J Mol Biol.* 169(3): 641-61.

Smith, M. M., and Andresson, O.S (1983). "DNA sequences of yeast H3 and H4 histone genes from two non-allelic gene sets encode identical H3 and H4 proteins." *J Mol Biol.* 169(3): 663-90.

Smith, M. M., and Stirling, V.B (1988). "Histone H3 and H4 gene deletions in *Saccharomyces cerevisiae*." *J Cell Biol.* 106(3): 557-66.

Smith, M. M. (2002). "Centromeres and variant histones: what, where, when and why?" *Curr Opin Cell Biol.* 14(3): 279-85.

Smith, S., and Stillman, B (1991). "Stepwise assembly of chromatin during DNA replication *in vitro*." *EMBO J.* 10(4): 971-80.

Sobel, R. E., Cook, R.G., Perry, C.A., Annunziato, A.T., Allis, C.D (1995). "Conservation of deposition-related acetylation sites in newly synthesized histones H3 and H4." *Proc Natl Acad Sci U S A.* 92(4): 1237-41.

Southern, E. M. (1975). "Detection of specific sequences among DNA fragments separated by gel electrophoresis." *J Mol Biol.* 98(3): 503-17.

Spode, I., Maiwald, D., Hollenberg, C.P., Suckow, M (2002). "ATF/CREB sites present in sub-telomeric regions of *Saccharomyces cerevisiae* chromosomes are part of promoters and act as UAS/URS of highly conserved *COS* genes." *J Mol Biol.* 319(2).

Steinmetz, L. M., Scharfe, C., Deutschbauer, A.M., Mokranjac, D., Herman, Z.S., Jones, T., Chu, A.M., Giaever, G., Prokisch, H., Oefner, P.J., Davis, R.W (2002). "Systematic screen for human disease genes in yeast." *Nat Genet.* 31(4): 400-4.

Stevens, B. J. (1977). "Variation in number and volume of the mitochondria in yeast accordingto growth conditions. A study based on serial sectioning and computergraphics reconstruction." *Biol. Cell.* 28(37).

Strahl, B. D., and Allis, C.D (2000). "The language of covalent histone modifications." *Nature* 403(6765): 41-5.

Strahl, B. D., Grant, P.A., Briggs, S.D., Sun, Z.W., Bone, J.R., Caldwell, J.A., Mollah, S., Cook, R.G., Shabanowitz, J., Hunt, D.F., Allis, C.D (2002). "Set2 is a nucleosomal histone H3-selective methyltransferase that mediates transcriptional repression." *Mol Cell Biol. 22*(5): 1298-306.

Straight, A. F., Shou, W., Dowd, G.J., Turck, C.W., Deshaies, R.J., Johnson, A.D., Moazed, D (1999). "Net1, a Sir2-associated nucleolar protein required for rDNA silencing and nucleolar integrity." *Cell* 97(2): 245-56.

Strathern, J. N., Klar, A.J., Hicks, J.B., Abraham, J.A., Ivy, J.M., Nasmyth, K.A., McGill, C (1982). "Homothallic switching of yeast mating type cassettes is initiated by a double-stranded cut in the *MAT* locus." *Cell* 31(1): 183-92.

Strohner, R., Nemeth, A., Nightingale, K.P., Grummt, I., Becker, P.B., Längst, G (2004). "Recruitment of the nucleolar remodeling complex NoRC establishes ribosomal DNA silencing in chromatin." *Mol Cell Biol.* 24(4): 1791-8.

Suka, N., Suka, Y., Carmen, A.A., Wu, J., Grunstein, M (2001). "Highly specific antibodies determine histone acetylation site usage in yeast heterochromatin and euchromatin." *Mol Cell.* 8(2): 473-9.

Suka, N., Luo, K., Grunstein, M (2002). "Sir2p and Sas2p opposingly regulate acetylation of yeast histone H4 lysine16 and spreading of heterochromatin." *Nat Genet.* 32(3): 378-83.

Sun, Z. W., and Allis, C.D (2002). "Ubiquitination of histone H2B regulates H3 methylation and gene silencing in yeast." *Chem Biol Interact.* 140(2): 155-68.

Suto, R. K., Clarkson, M.J., Tremethick, D.J., Luger, K (2000). "Crystal structure of a nucleosome core particle containing the variant histone H2A.Z." *Nat Struct Biol.* 7(12): 1121-4.

Svaren, J., and Horz, W (1997). "Transcription factors vs nucleosomes: regulation of the PHO5 promoter in yeast." *Trends Biochem Sci.* 22(3): 93-7.

Svejstrup, J. (2004). "The RNA polymerase II transcription cycle: cycling through chromatin." Cell 1677(1-3): 64-73.

Tamaru, H., and Selker, E.U (2001). "A histone H3 methyltransferase controls DNA methylation in *Neurospora crassa*." *Nature* 414(6861): 277-83.

Tham, W. H., and Zakian, V.A (2002). "Transcriptional silencing at *Saccharomyces* telomeres: implications for other organisms." *Oncogene* 21(4): 512-21.

Thoma, F., Koller, T., Klug, A (1979). "Involvement of histone H1 in the organization of the nucleosome and of the salt-dependent superstructures of chromatin." *J Cell Biol.* 86(2Pt1): 403-27.

Thompson, J. S., Hecht, A., Grunstein, M (1993). "Histones and the regulation of heterochromatin in yeast." *Cold Spring Harb Symp Quant Biol.* 58: 247-56.

Toyn, J. H., Gunyuzlu, P.L., White, W.H., Thompson, L.A., Hollis, G.F (2000). "A counterselection for the tryptophan pathway in yeast: 5-fluoroanthranilic acid resistance." Yeast 16(6): 553-60.

Traven, A., Wong, J.M., Xu, D., Sopta, M., Ingles, C.J (2001). "Interorganellar communication. Altered nuclear gene expression profiles in a yeast mitochondrial dna mutant." *J Biol Chem.* 276(6): 4020-7.

Treitel, M. A., Kuchin, S., Carlson, M (1995). "Repression by SSN6-TUP1 is directed by MIG1, a repressor/activator protein." *Proc Natl Acad Sci U S A.* 92(8): 3132-6.

Treitel, M. A., Kuchin, S., Carlson, M (1998). "Snf1 protein kinase regulates phosphorylation of the Mig1 repressor in *Saccharomyces cerevisiae*." *Mol Cell Biol.* 18(11): 6273-80.

Tse, C., Sera, T., Wolffe, A.P., Hansen, J.C (1998). "Disruption of higher-order folding by core histone acetylation dramatically enhances transcription of nucleosomal arrays by RNA polymerase III." *Mol Cell Biol.* 18(8): 4629-38.

Tsukiyama, T., and Wu, C (1995). "Purification and properties of an ATP-dependent nucleosome remodeling factor." *Cell.* 83(6): 1011-20.

Tsukiyama, T., Palmer, J., Landel, C.C., Shiloach, J., Wu, C (1999). "Characterization of the imitation switch subfamily of ATP-dependent chromatin-remodeling factors in *Saccharomyces cerevisiae*." *Genes Dev.* 13(6): 686-97.

Tsukiyama, T. (2002). "The in vivo functions of ATP-dependent chromatin-remodelling factors." *Nat Rev Mol Cell Biol.* 3(6): 422-9.

Tzagoloff, A. (1982). *Mitochondria.* New York, Plenium.

Tzagoloff, A., and Dieckmann, C.L (1990). "PET genes of *Saccharomyces cerevisiae*." *Microbiol Rev.* 54(3): 211-25.

Tzamarias, D., and Struhl, K (1994). "Functional dissection of the yeast Cyc8-Tup1 transcriptional co-repressor complex." *Nature* 369(6483): 758-61.

Tzamarias, D., and Struhl, K (1995). "Distinct TPR motifs of Cyc8 are involved in recruiting the Cyc8-Tup1 corepressor complex to differentially regulated promoters." *Genes Dev.* 9(7): 821-31.

Utley, R. T., Ikeda, K., Grant, P.A., Cote, J., Steger, D.J., Eberharter, A., John, S., Workman, J.L (1998). " Transcriptional activators direct histone acetyltransferase complexes to nucleosomes." *Nature* 394(6692): 498-502.

van Leeuwen, F., Gafken, P.R., Gottschling, D.E (2002). "Dot1p modulates silencing in yeast by methylation of the nucleosome core." *Cell* 109(6): 745-56.

van Leeuwen, F., and Gottschling, D.E (2002). "Genome-wide histone modifications: gaining specificity by preventing promiscuity." *Curr Opin Cell Biol.* 109(6): 745-56.

Varanasi, U. S., Klis, M., Mikesell, P.B., Trumbly, R.J (1996). "The Cyc8 (Ssn6)-Tup1 corepressor complex is composed of one Cyc8 and four Tup1 subunits." *Mol Cell Biol.* 16(12): 6707-14.

Varga-Weisz, P. D., Wilm, M., Bonte, E., Dumas, K., Mann, M., Becker, P.B (1997). "Chromatin-remodelling factor CHRAC contains the ATPases ISWI and topoisomerase II." *Nature* 388(6642): 598-602.

Varga-Weisz, P. D., and Becker, P.B (1998). "Chromatin-remodeling factors: machines that regulate?" *Curr Opin Cell Biol.* 10(3): 346-53.

Verdin, E., Dequiedt, F., Kasler, H.G (2003). "Class II histone deacetylases: versatile regulators." *Trends Genet.* 19(5): 286-93.

Vignali, M., Steger, D.J., Neely, K.E., Workman, J.L (2000). "Distribution of acetylated histones resulting from Gal4-VP16 recruitment of SAGA and NuA4 complexes." *EMBO J.* 19(11): 2629-40.

Vogelauer, M., Wu, J., Suka, N., Grunstein, M (2000). "Global histone acetylation and deacetylation in yeast." *Nature* 408(6811): 495-8.

Vuralhan, Z., Morais, M.A., Tai, S.L., Piper, M.D., Pronk, J.T (2003). "Identification and characterization of phenylpyruvate decarboxylase genes in *Saccharomyces cerevisiae.*" *Appl Environ Microbiol.* 69(8): 4534-41.

Wallis, J. W., Hereford, L., Grunstein, M (1980). "Histone H2B genes of yeast encode two different proteins." *Cell* 22(3): 799-805.

Wang, W., Xue, Y., Zhou, S., Kuo, A., Cairns, B.R., Crabtree, G.R (1996). "Diversity and specialization of mammalian SWI/SNF complexes." *Genes Dev.* 10(17): 2117-30.

Watson, A. D., Edmondson, D.G., Bone, J.R., Mukai, Y., Yu, Y., Du, W., Stillman, D.J., Roth, S.Y (2000). "Ssn6-Tup1 interacts with class I histone deacetylases required for repression." *Genes Dev.* 14(21): 2737-2744.

West, M. H., and Bonner, W.M (1980). "Histone 2A, a heteromorphous family of eight protein species." *Biochemistry* 19(14): 3238-45.

White, C. L., Suto, R.K., Luger, K (2001). "Structure of the yeast nucleosome core particle reveals fundamental changes in internucleosome interactions." *EMBO J.* 20(18): 5207-18.

Williamson, D. H. (1976). Packaging and recombination of mitochondrial DNA in vegetatively growing yeast cells. Genetics, biogenesis and bioenergetics of mitochondria. Bandlow, W.E., *et al.* Berlin, de Gruyter: 117.

Winston, F., and Allis, C.D (1999). "The bromodomain: a chromatin-targeting module?" *Nat Struct Biol.* 6(7): 601-4.

Wittschieben, B. O., Otero, G., de Bizemont, T., Fellows, J., Erdjument-Bromage, H., Ohba, R., Li, Y., Allis, C.D., Tempst, P., Svejstrup, J.Q (1999). "A novel histone acetyltransferase is an integral subunit of elongating RNA polymerase II holoenzyme." *Mol Cell* 4(1): 123-8.

Worcel, A., Han, S., Wong, M.L (1978). "Assembly of newly replicated chromatin." *Cell* 15(3): 969-77.

Wu, C. (1980). "The 5' ends of *Drosophila* heat shock genes in chromatin are hypersensitive to DNase I." *Nature* 286(5776): 854-60.

Wu, J., Suka, N., Carlson, M., Grunstein, M (2001). "TUP1 utilizes histone H3/H2B-specific HDA1 deacetylase to repress gene activity in yeast." *Mol Cell* 7(1): 117-26.

Wu, L., and Winston, F (1997). "Evidence that Snf-Swi controls chromatin structure over both the TATA and UAS regions of the *SUC2* promoter in *Saccharomyces cerevisiae*." *Nucleic Acids Res.* 25(21): 4230-4.

Xiao, T., Hall, H., Kizer, K.O., Shibata, Y., Hall, M.C., Borchers, C.H., Strahl, B.D (2003). "Phosphorylation of RNA polymerase II CTD regulates H3 methylation in yeast." *Genes Dev.* 17(5): 654-63.

Xue, Y., Wong, J., Moreno, G.T., Young, M.K., Cote, J., Wang, W (1999). "NURD, a novel complex with both ATP-dependent chromatin-remodeling and histone deacetylase activities." *Mol Cell.* 2(6): 851-61.

Yudkovsky, N., Logie, C., Hahn, S., Peterson, C.L (1999). "Recruitment of the SWI/SNF chromatin remodeling complex by transcriptional activators." *Genes Dev.* 13(18): 2369-74.

Zaman, Z., Ansari, A.Z., Koh, S.S., Young, R., Ptashne, M (2001). "Interaction of a transcriptional repressor with the RNA polymerase II holoenzyme plays a crucial role in repression." *Proc Natl Acad Sci U S A.* 98(5): 2550-4.

Zeitlin, S. G., Barber, C.M., Allis, C.D., Sullivan, K.F., Sullivan, K (2001). "Differential regulation of CENP-A and histone H3 phosphorylation in G2/M." *J Cell Sci.* 114(4): 653-61.

Zhou, Y. B., Gerchman, S.E., Ramakrishnan, V., Travers, A., Muyldermans, S (1998). "Position and orientation of the globular domain of linker histone H5 on the nucleosome." *Nature* 395(6700): 402-5.

Zitomer, R. S., Montgomery, D.L., Nichols, D.L., Hall, B.D (1979). "Transcriptional regulation of the yeast cytochrome c gene." *Proc Natl Acad Sci U S A.* 76(8): 3627-31.